REAL-TIME DATA ACQUISITION IN HUMAN PHYSIOLOGY

Real-Time Acquisition, Processing, and Interpretation—A MATLAB-Based Approach

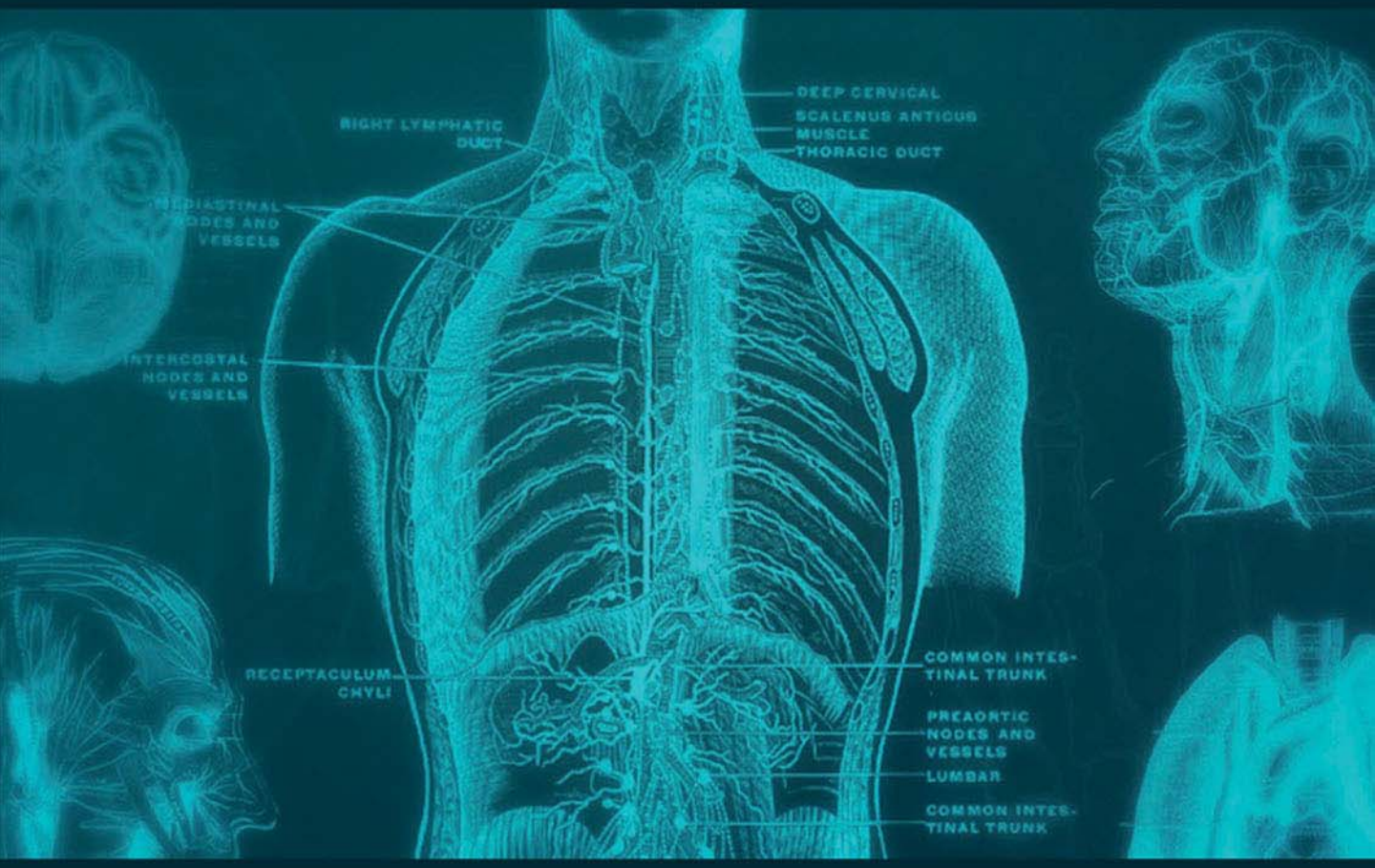

Dipali Bansal



Real-Time Data Acquisition in Human Physiology

This page intentionally left blank



Real-Time Data Acquisition in Human Physiology

Real-Time Acquisition, Processing, and Interpretation—A MATLAB-Based Approach

Dipali Bansal

Dean of Engineering, Graphic Era (Deemed to be University), Dehradun, India





ACADEMIC PRESS

An imprint of Elsevier

Academic Press is an imprint of Elsevier
125 London Wall, London EC2Y 5AS, United Kingdom
525 B Street, Suite 1650, San Diego, CA 92101, United States
50 Hampshire Street, 5th Floor, Cambridge, MA 02139, United States
The Boulevard, Langford Lane, Kidlington, Oxford OX5 1GB, United Kingdom

Copyright © 2021 Elsevier Inc. All rights reserved.

No part of this publication may be reproduced or transmitted in any form or by any means, electronic or mechanical, including photocopying, recording, or any information storage and retrieval system, without permission in writing from the publisher. Details on how to seek permission, further information about the Publisher's permissions policies and our arrangements with organizations such as the Copyright Clearance Center and the Copyright Licensing Agency, can be found at our website: www.elsevier.com/permissions.

This book and the individual contributions contained in it are protected under copyright by the Publisher (other than as may be noted herein).

MATLAB® is a trademark of The MathWorks, Inc. and is used with permission. The MathWorks does not warrant the accuracy of the text or exercises in this book. This book's use or discussion of MATLAB® software or related products does not constitute endorsement or sponsorship by The MathWorks of a particular pedagogical approach or particular use of the MATLAB® software.

Notices

Knowledge and best practice in this field are constantly changing. As new research and experience broaden our understanding, changes in research methods, professional practices, or medical treatment may become necessary.

Practitioners and researchers must always rely on their own experience and knowledge in evaluating and using any information, methods, compounds, or experiments described herein. In using such information or methods they should be mindful of their own safety and the safety of others, including parties for whom they have a professional responsibility.

To the fullest extent of the law, neither the Publisher nor the authors, contributors, or editors, assume any liability for any injury and/or damage to persons or property as a matter of products liability, negligence or otherwise, or from any use or operation of any methods, products, instructions, or ideas contained in the material herein.

British Library Cataloguing-in-Publication Data
A catalogue record for this book is available from the British Library

Library of Congress Cataloging-in-Publication Data
A catalog record for this book is available from the Library of Congress

ISBN: 978-0-12-822118-1

For Information on all Academic Press publications
visit our website at https://www.elsevier.com/books-and-journals

Publisher: Mara Conner
Acquisitions Editor: Chris Katsaropoulos
Editorial Project Manager: Chiara Giglio
Production Project Manager: Sreejith Viswanathan
Cover Designer: Vicky Pearson

Typeset by MPS Limited, Chennai, India



Contents

Preface xi
Acknowledgment xv

1. Introduction 1
1.1 Rationale 2
1.2 Technical overview 5
1.2.1 Signals 5
1.2.2 Bio-signals 7
1.2.3 Understanding biomedical data acquisition and processing system 8
1.2.4 Recent developments 12
1.2.5 Challenges in bio-signal acquisition and processing 15
1.3 Objectives 16
References 18

2. PC-based data acquisition 21
2.1 Introduction 21
2.2 Sensors and transducers 23
2.2.1 Physical sensors 24
2.2.2 Chemical sensors 32
2.2.3 Biosensors 35
2.2.4 Electropotential sensors 38
2.3 Market research and latest developments in sensor technologies 41
2.3.1 IoT sensors 42

2.3.2 RFID sensors 42
2.3.3 Wearable sensors 42
2.3.4 Pollution sensors 42
2.3.5 Optical image sensors 43
2.3.6 MEMS and NEMS sensors 43
2.3.7 Sensor materials 44
2.4 Data acquisition system hardware 45
2.4.1 Front end of data acquisition system hardware 46
2.4.2 Filtering subsystem 49
2.4.3 Interface units 51
2.5 Data acquisition system software 52
2.6 Data acquisition systems market 53
References 53

3. Detection and processing of real-time carotid pulse waves 57
3.1 Introduction 57
3.1.1 Clinical significance of carotid pulse waveform 58
3.1.2 Investigation of carotid pulse measurement 60
3.2 Experimental arrangement for detection of carotid pulse in real time 62
3.2.1 The piezoelectric sensor 63
3.2.2 The acquisition protocol and results 66
3.3 Digital filter designs 67
3.3.1 Finite impulse response filter design 68
3.3.2 Infinite impulse response filter design 70
3.4 Simulated model for real-time carotid pulse detection and processing 72
3.4.1 Filter design and analysis tool 73
3.4.2 Simulink model developed 73

3.5 Algorithm for real-time carotid pulse analysis 78
3.6 Conclusion 79
References 80

4. Real-time detection and processing of electromyography signal 83
4.1 Introduction 83
4.1.1 Application areas of electromyography signal analysis 85
4.1.2 Investigation of electromyography signal measurement 87
4.2 Signal processing the electromyography data 88
4.3 Real-time detection and processing of electromyography signal in single channel mode 93
4.3.1 Silver–silver chloride surface electrodes 93
4.3.2 Front-end amplifier and interface unit 95
4.3.3 Digital filter for online processing 96
4.3.4 The acquisition protocol and results 98
4.4 Real-time detection and processing of electromyography signal in dual channel mode 99
4.5 Standalone MATLAB code for physiological data detection and processing 103
4.6 Conclusion 105
References 105

5. Real-time detection and processing of electrocardiogram signal 111
5.1 Introduction 111
5.1.1 Interpretation of electrocardiogram waveform 111
5.1.2 Lead placement in an electrocardiogram system 114
5.1.3 Investigation of electrocardiogram signal measurement 116
5.2 Recent trends in cardiology 118

5.3 Notch filter designs for reducing power line interference in electrocardiogram signals 123
5.3.1 Computer simulation of various notch filter design topologies 125
5.4 Real-time detection and processing of electrocardiogram signal 130
5.4.1 Online algorithm for feature extraction 131
5.5 Digital signal controller-based electrocardiogram acquisition system 135
5.5.1 The acquisition protocol and results 136
5.6 Conclusion 140
References 140

6. Measurement and analysis of heart rate variability 145
6.1 Introduction 145
6.1.1 Basic block diagram for heart rate variability evaluation process 147
6.2 Heart rate variability metrics and norms 148
6.2.1 Time-domain analysis 149
6.2.2 Frequency-domain analysis 152
6.2.3 Nonlinear measurement analysis 154
6.3 QRS detection methods 156
6.3.1 Differentiation-based methods for QRS peak detection 157
6.3.2 Template matching methods for QRS peak detection 158
6.3.3 Wavelets for QRS peak detection 159
6.4 Real-time detection and analysis of heart rate variability 159
6.4.1 Dual channel system for real-time, simultaneous acquisition of ECG, and carotid pulse wave 162
6.5 Conclusion 167
References 167

7. Conclusion 175
7.1 Major contributions 175
7.1.1 Detection and analysis of carotid pulse wave 175
7.1.2 Detection and analysis of electromyogram signal 176
7.1.3 Detection and analysis of electrocardiogram signal and heart rate variability 177
7.2 Conclusion 178
7.3 Future directions 181
References 185
Index 187

This page intentionally left blank

Preface

Understanding human physiology is vital to define and design a fool-proof analytical method that encapsulates all the minor and significant signals which would lead to the correct diagnosis of a disease. Bio-signal data acquisition and their processing are a precursor for diagnostic system development. An underlying condition or disease not only needs to be diagnosed but also should be monitored and a suitable therapy needs to be provided for recovery and rehabilitation. Real-time acquisition and processing of human physiology has become indispensable as an interdisciplinary tool, which along with advancements in computational algorithms, medical science, signal processing techniques, communication engineering, and big data practices could bridge the gap and promote the universal health goals.

Existing data acquisition systems (DAQ) enable detection, processing, monitoring and analysis of human physiology, and cater to a wide range of clinical and nonclinical circumstances. Their cost-effectiveness, quality, compactness, ease of use, reduced power requirements, availability, and so on are the prime factors based on which they can be assessed objectively. A lot has been achieved in this domain; however there is still scope for improvement in terms of noise immunity, universal connectivity, real-time processing, and analysis, and also because these systems are still unaffordable and beyond the reach of common man. Modern tools and techniques that have enabled the deployment of portable computer-based DAQ can facilitate continuous monitoring of human physiology in a much simpler and affordable manner.

The book *Real-Time Data Acquisition in Human Physiology* emphasizes the strategy and deployment of a PC-based arrangement for real-time acquisition, processing, and analysis of human electrocardiogram (ECG), electromyogram (EMG), and carotid pulse waveforms. The indigenous system designed and described in this book allows easy-to-interface simple hardware arrangement for bio-signal detection. The computational functionality of MATLAB® is verified for viewing, digital filtration, and feature extraction of acquired bio-signals. This book demonstrates a method of providing a relatively cost-effective and realizable explanation to real-time monitoring, assessment, and evaluation of human physiology that can directly benefit the mass.

Key features of the book include an application-driven, interdisciplinary, and experimental approach to bio-signal processing with a focus on acquiring, processing, and understanding human ECG, EMG, carotid pulse data, and heart rate variability (HRV). It covers instrumentation and digital signal processing techniques useful for detecting and interpreting human physiology in real time, including experimental layout and methodology in an easy-to-understand manner. Detailed discussion is presented on the development of a computer-based system that offers direct connectivity with a computer via its sound card and eliminates

the requirement of proprietary DAQ and ADC subsystems. It also covers MATLAB-based algorithm for online noise reduction and feature extraction and can infer diagnostic features in real time. Proof of concept is provided for a PC-based twin channel acquisition system for recognition of multiple physiological parameters. The use of digital signal controller to enhance features of acquired human physiology has also been explained. It also presents the concept that carotid pulsation can be utilized for HRV analysis in critical circumstances using a very simple hardware/software arrangement.

This book shall be useful to undergraduate and postgraduate students of all streams who need processing of real-time data through an application-based approach. It shall serve as a reference to researchers, engineers, clinicians, and medical practitioners. The readers of this book will acquire an insight into the design and deployment of a home health care DAQ which is economic, compact, user-friendly, and has inbuilt signal processing and feature extraction algorithms. The outline is structured and covers all aspects of a computer-based real-time DAQ in human physiology.

Chapter 1, *Introduction*, of the book introduces typical bio-signal acquisition and processing techniques. Also shared are typical case studies presenting recent advancements in the domain and the challenges faced in real-time acquisition and monitoring of bio-signals. The chapter also presents the rationale behind this work and sets the objective to be achieved which is primary to gather information on human physiology through an indigenous measurement system that is portable and cost-effective, and permits to interpret and detect abnormalities through signal feature extraction algorithm designed using MATLAB, thus reducing the subjectivity involved in manual and visual diagnosis and enhance reproducibility.

Chapter 2, *PC-based data acquisition*, provides a comprehensive review of the instrumentation and signal processing techniques involved in acquiring and processing human physiological parameters. DAQ exist, which have the capability of converting analog real-world biological signals into digital domain and then utilizing the capability of a computer. These bio-signals can be visualized, stored, analyzed, and can trigger a control command. The essential components of DAQ system including sensors and transducers, data acquisition system hardware (signal conditioning unit, ADC, DAC, MUX, controllers, power management, etc.), the interface units, data acquisition system software (signal processing platforms such as MATLAB, Simulink, and LabVIEW), and computers are detailed in this chapter. Extensive review of various sensors is also covered in this chapter.

Extraction of cardiac information from the contour and parameters of carotid pulse waveform has been established and is recognized. Available technology permits noninvasive detection of carotid pulsation, yet a system requires to be evolved that is user-friendly, portable, and is affordable which can assist to pick pulse under critical situations. An easy-to-use arrangement with negligible electronic circuit complexity has been discussed in Chapter 3, *Detection and processing of real-time carotid pulse waves*, which allows real-time detection and signal processing of carotid pulse wave. Measurements in this experimentation have been done using only a piezoelectric sensor to detect the carotid pulsation of human subjects under different postures. The analog output at the piezoelectric transducer obtained

due to pulsation, when placed on the neck region, is directly fed to the sound card of a computer for visualization and further processing in real time. Virtual oscilloscopes that are freely available are used for viewing the bio-signal acquired, and digital infinite impulse response and finite impulse response filters have been designed using MATLAB and Simulink to process the signal and to draw meaningful interpretations.

EMG signal detection and analysis finds numerous clinical and nonclinical applications. Several EMG acquisition and monitoring arrangements have been developed and are still being researched to make the system compact, cost-effective, utilizing less power, with inbuilt signal processing chips to eliminate noise, having immense mathematical capability for analysis, and automated decision-making. An attempt has been made in Chapter 4, *Real-time detection and processing of electromyography signal*, to deploy an economic and user-friendly computer-based home health monitoring system that can capture human EMG signals in real time using a simple interface arrangement. The muscle contractions could be detected from different sites using an amplifier and filter hardware designed using TL-084C op-amp. The real-time acquired EMG information was further made noise interference-proof by generating digital filter algorithm in MATLAB, which has the ability to filter the bio-signal in online mode. Digital signal processing methods for feature extraction and classification of EMG signal have also been discussed in detail. The experiment is extended to explore the possibility of acquiring two bio-signals simultaneously to establish a correlation between EMG data and carotid pulsation, which can be very useful in reaching diagnostic inferences. A stand-alone executable application has also been generated using MATLAB compilers, so that the algorithm can become platform-independent.

Chapter 5, *Real-time detection and processing of electrocardiogram signal*, details the construction of an indigenous front-end amplifier system along with the 50 Hz Notch filter designs for eliminating power line interference. The system is capable of faithfully detecting the rest ECG signal in real time. Various notch filter topologies have been simulated and verified using P-spice. The simple and easy-to-interface hardware along with the analytical software developed in MATLAB is cost-effective and establishes the know-how of precisely measuring the real-time cardiac response of a human heart in a computer-based home health bio-signal detection system. The sound port interface concept is compatible with hosts of computer ports and can be extended to acquire ECG signal from multichannel 12-lead arrangement. The cost of portable ECG monitors can further be reduced by designing single-chip digital signal controller–based setup that offers detection, signal processing, and feature extraction all integrated onto one board. A stand-alone arrangement utilizing Microchip's DSC DM330011 has been established in this work to detect and process real-time ECG signal. The quality of ECG detected can be used for reaching diagnostic inferences, interpreting the PQRST waveform, and for further online processing and telemonitoring.

Tracking the well-being and fitness level of an individual has become easy and affordable with the advent of modern technologically advanced applications and wearables that require detection, collation, and interpretation of valuable health-related information. This has reached the next level of interpreting the resilience, stress, and behavioral pattern of an individual using a biomarker called the HRV. HRV gives an evaluation of the physiological

phenomenon which can be derived from the ECG and is governed by the autonomic nervous system. Various HRV metrics and norms in time and frequency domain and using nonlinear measures are required to be understood to be able to draw health-related inferences. Major element of the HRV detection and analysis arrangement is the QRS peak detection algorithm. Chapter 6, *Measurement and analysis of heart rate variability*, covers these topics in detail. There are situations when HRV calculation is not feasible using ECG signals. Under such circumstances, it may be potentially useful to use carotid pulse waves to estimate HRV parameters as they have very close indices similar to those derived from the ECG wave. The system established here presents a close link connecting HRV time domain measures, obtained from simultaneously acquired ECG signal, and carotid waves detected from the developed, real-time, dual channel, noninvasive acquisition system, and the corresponding algorithm is made in MATLAB. As detection of carotid pulse waves involves much simpler instrumentation, which is compact, less cumbersome, and requires minimum electronics in contrast to a ECG detection system, it can be deployed as an alternate to assess HRV measures.

Chapter 7, *Conclusion*, presents the major contribution and covers the continued efforts made by researchers, recent technological advancements, and modern outlook toward detecting, processing, and analyzing human physiology. It also presents the future scope of this domain that has the potential to further enhance the quality of life.

Acknowledgment

Penning my thoughts, just after finishing work on this book, gives a similar realization to a great mountain expedition. The last year was full of challenges, I changed base and needed to adjust with the challenges associated with it. The unknowns surrounding COVID were on top of the mind. Yet, truly there were many around who helped on the way.

First and foremost, I would like to thank my mother who has been a source of inspiration throughout my life in spite of her humble background. My school teachers and college professors especially Sister Ruby, S.M. Kar Sir, and late Prof. (Dr.) M.S.P. Sinha have been my guiding force who believed in me and propelled me to my present status. Special gratitude to my PhD guide Prof. (Dr.) Munna Khan, who pushed me into the world of research methodologies and provided initial exposure to the topic of "Bio-signal Processing."

I have deep felt appreciation for Prof. (Dr.) Kamal Ghanshala Ji, Chairman Graphic Era (Deemed to be University), Dehradun, who have provided continuous support during my stints with Graphic Era University, which boosted my self-belief to take up this challenge of writing another book. I would also like to thank my colleagues who during my association with them have supported me in various capacities for accomplishment of my tasks while I was caught in my efforts and thought process for this project. I would also like to thank my friends who have been a source of inspiration during rainy days.

Bundle of thanks to my publishers who gave me an opportunity to work on this project and also happy that they could adjust the manuscript submission schedules based on my requests. This undoubtedly gave me enough time to work on the details and give some thought-provoking content, which I ponder would be helpful to the readers.

Last but not the least, special thanks to my spouse, who supported me beyond expectations while I worked on the project. He has his set of challenges to surmount but did all in his limits to support this project. I would like to thank my father and my brother, who have always believed in me and have come up with suggestions and experiences from their life wherever required. I cannot forget my daughter, who is at crossroads in her career and needed undivided attention at times due to many reasons especially the uncertainties unfolded by COVID. She was extremely understanding and never complained even when I could have supported her better. I wish her loads of good things and luck in her endeavors.

There are many people who often leave an indelible impact on your life, some of them we forget without realizing that they have left an impression. I feel they are the messengers of almighty God who wants you to succeed and carry on with more in life without getting tired. I pray that the almighty always showers us with wisdom and leads our path to enlightenment.

Dipali Bansal

This page intentionally left blank

1 Introduction

Good health is indispensable for sustained social and economic development and to alleviate poverty. Universal health coverage goals of the World Health Organization (WHO) were constituted with the tenet of easy access of quality health care services at reasonable costs. The health care entails prevention, treatment, and rehabilitation and to provide palliative support. These goals can be achieved by an efficient health care system with ample finances so that medicines and equipment are accessible to the masses supported with motivated and trained health care workers.

The WHO, while recognizing the facts, closely monitors more than 1000 health-related indicators statistically through its 194 member states. The member states have been progressively working on Sustainable Development Goals (SDGs). While 17 SDGs were adopted for monitoring in 2015 by the global leadership, looking at the holistic assessment, it was enhanced to 36 health-related SDGs in 2018. The broad vision remains and relates to a "World Free of poverty, hunger, disease, and want." SDG3 is the health-related SDG signifying "Good Health and Well Being" and calls upon member countries to devise an entire ecosystem promoting universal health achievement, pre-empt health emergencies, and effectively promote robust and disease-free populations. The Millennium Development Goal (MDG) has defined certain priority areas, related to maternal and child mortality, providing nutritious food to the needy and the resolution to fight communicable and pandemic prone diseases (World Health Statistics, 2018).

However, it is a no-brainer that a qualified and equitably distributed health force, which is accessible by masses, is the bare minimum requirement to make significant progress toward the SDGs. It is a grave concern that around 75 countries globally have fewer than one physician per 1000 population. Similarly, around 87 countries have less than three nursing and midwives per 1000 population (World Health Organization, Global Health Work Force Statistics, OECD, 2019). The goal to provide basic health support still stands compromised, leave aside responding to any catastrophe and health emergency. This calls for extraordinary and out-of-the-box efforts so that the universal health goals and sustainable development can be attained.

Enhancements in medical diagnostics and better standards of living have resulted in higher life expectancy around the globe. In fact, it has shown an improvement of 5.5 years between 2000 and 2016. However, if we look across the horizon, the average span of life has gone up considerably from a mere 29 years historically to 73 years in 2019 (Global Health Observatory (GBO) Data Released by WHO).

Understanding human physiology is vital to define and design a foolproof analytical method that encapsulates all the minor and significant signals which would lead to the correct diagnosis of a disease. Biomedical signals and their processing are a precursor for

Real-Time Data Acquisition in Human Physiology. DOI: https://doi.org/10.1016/B978-0-12-822118-1.00001-1
© 2021 Elsevier Inc. All rights reserved.

diagnostic system development. Further, an underlying condition or disease not only needs to be diagnosed but also needs to be monitored and a suitable therapy needs to be provided for recovery and rehabilitation.

1.1 Rationale

Real-time bio-signal acquisition and processing of human physiology have become indispensable as an interdisciplinary tool, which along with advancements in computational algorithms, medical science, communication engineering, and big data practices could bridge the gap and promote the universal health goals.

Diagnosis, Therapy & Control and Monitoring are three pillars of bio-signal processing in clinical and nonclinical context. In case of diagnosis, pathological conditions or variations in measurements, pointing to the onset of a disease, can be identified by examining a signal information. The signal in many cases can be acquired through noninvasive sensors. The procedures involved are progressively being devised to optimize cost and make them less taxing and painful to the patients. Similarly, the acquisition and analysis of signals are becoming flexible and simpler so that the required degree of automation reaches the far-flung areas across the globe. The diagnosis can be done either at the patient site or the signal can be transmitted off-site, for analysis on a stand-alone PC or a machine within a reasonable time frame. A digital signal processor (DSP) circuit complements an onboard operating system and hardware for filtration of signal and assists large part of decision-making and diagnosis.

Therapy and control normally refers to a treatment that makes a human to feel better after an illness or injury. Digital Signal Processing has a restricted but important therapeutic role in modifying some physiological processes based on the feedback received through an algorithm in real-time or online basis. In some applications, physiological parameter monitoring is done using devices, to recognize and proactively respond to early stress symptoms. Algorithms are tailor-made to assist recovery and performance protocols, for example, in case of monitoring the performance of athletes or providing symptomatic relief to trapped individuals in calamities. For example, pacemakers are used to treat arrhythmias (irregular heart rhythms) or bradycardia where the heartbeats fall to less than 60 beats per minute (Boston Scientific – Pacemakers). These conditions impair the transport of oxygen and essential nutrients to the brain and other parts of the body. Pacemakers with leads in the right atrium and right ventricle are programmed to deliver the required electrical energy to pace the slow heartbeat as and when required. The equipment can also store or transmit information for evaluation and corrective settings later. However, the challenges exist around complex algorithms triggering response, maximum time delay acceptable for action, and low power consumption requirement for these devices, some of which as discussed above are implanted in the human body.

In case of monitoring, using Biomedical signal processing the real-time systems are connected to the patients. The systems including the sensor technologies detect the subtle

changes, say in neurological or cardiac signals on display monitors. Some of these parameters could be electrocardiogram (ECG), electromyogram (EMG), electroencephalogram (EEG), Pulse, Oxygen saturation level, Heart rate, etc. Regular monitoring is advisable both when adopting preventive and curative strategies; while the former reduces the probability of a disease advancement, the later reduces the chance of death and disability in identified patients.

Of course, the entire process of Diagnosis, Therapy & Control and Monitoring is dependent not only on the advancement in sensors and signal processing techniques but also on the human capabilities, intervention, interpretation, analysis, and timely actions.

It is quite interesting to introduce a case study involving rescue operations of Chilean miners in 2010. A remote monitoring system was deployed to rescue 33 miners who managed to survive a 69-day ordeal after getting trapped 2300 ft below earth's surface, in an unfortunate collapse of 100 years copper-gold mine located in San Jose, United States. Incidentally, the miners were lucky to have a reinforced steel shelter but barely had food to last even for 7 days. The survival was challenging as the humidity inside the mine was a steady 98% and an ambient temperature of 33°C was further complicating the matters. The miners carried a high risk of hyperthermia due to dehydration and resulting heat stroke. "Zephyr, Remote Sensing System" could be deployed; luckily 17 days after the incident, the rescue team could drill a 4.5-inch hole to reach the trapped miners. The miners were outfitted with the proprietary device to record the vital signs on daily basis but not on real-time basis. The hydration level was monitored while regular exercises were introduced to reduce the upper body weight and to increase the strength of the leg muscle. Initially, the miners worked to pump up the heart rate to 120−140 beats per minute. The entire regime was planned not only to keep them active and healthy but also to prepare them for the worst-case scenario in case of a botched-up rescue operation. One of the miners, Edison Pena, had been saved, while being critically close to hyperthermia, only because of daily monitoring (Getlen, 2014).

Subsequently in the third week, the exercises were made strenuous to push anaerobic threshold bordering 160 beats per minute. The miners were monitored for induced cardiac issues by monitoring the heart frequency, body temperature, and respiration rate. Buildup of the muscular strength of the critical body parts, lumbar region, and the abdominal region was focused upon. The training was monitored based on predictive patterns based on past experience of the team led by Dr. Jean Romagnol and Ben Morris (Romagnol). The team could diagnose the exceptions and achieve the desired results due to regular monitoring and targeted therapies. In around 5 weeks, the miners had lost 3.5−6.5 kg weight and gained stamina. They were finally rescued in a specially designed "Fenix Capsule" after 9 weeks. All, baring one miner who had a preexisting pathological condition, had heart rates as per the predictive values of 150 beats under anxiety and stress during transportation in the rescue mission. All of the miners were released within 2 days of hospitalization after rescue, although they were monitored over several weeks.

From the quoted case study, it is evident that the rapid change in technology is being endlessly tested with the requirement of providing better health care attention and

monitoring either right at medical centers or even at distant locations. The natural response of the human body under anxiety or trauma, whether on the onset of a disease or when our body is physically challenged, is echoed by the subtle deviations in physiological parameters. Accordingly, our human physiological data need to be measured repeatedly. There are plethora of applications, some of them necessitating either continuous or need-based measurement and investigation. However, the analysis may again be conducted based on the requirement or situation either at point of taking record or remotely. This flexibility opens a host of applications such as performance judgment of athletes or sportsmen, evaluating our already highly trained defense personnel posted at high altitudes, men and women in stress flying modern aircrafts or spending long periods at sea, typical applications such as people working in humid, dusty, and poorly ventilated mines below earth's crust, or simply treating the patients at health care centers or with virtual support systems. Human physiological parameters also need to be constantly measured in case of Biological feedback systems, which delivers the patients online evidence on the practical and functional position of their core systems and internal organs.

The challenges are multifold, growing populations are exerting never-ending strain on government resources coupled with better education levels and hence expectations are far higher for prompt and quality health care in closer vicinities. All this calls for continuous innovations leading to the development of reliable yet simple, low-cost, portable, and scalable methods for early detection, transmission, and measurement, with the inherent capabilities to analyze the physiological parameters leading to precise therapeutic and diagnostic decisions. Early detection of an underlying condition leading to a disease can prevent deterioration in health and hence the timeliness and methods have huge implications in prevention and patient care and recovery. The real-time acquisition and quick interpretation of physiological data improves the very sense of trust and connectedness in health care systems.

To realize this vision, many research and academic organizations and universities have started integrated efforts toward Information, Communication Technologies, and Biomedical Sciences to understand, measure, and analyze multiple biological levels in relation to human physiological parameters. Companies are expanding their research and are launching low-cost human physiological parameter detection instruments. Path-breaking developments in instrumentation evolved with the progress in better clinical measurements, enhancements in processing techniques of prevailing ones, basically boosting their content of information or validity by proper selection of Sensors, Portable Data Acquisition, Computer-based processing, wireless transmission, and feature extraction.

Looking at the overall context laid down as per the SDGs, it seems clear that if the health care systems provide quality attention with easy access at low or optimum costs, we would have gone a long way to achieve the goals. The recent advances in the process and techniques around measurement of human physiology have addressed host of technical and clinical problems. These include but are not limited to higher power capability, lesser development price, condensed physical assembly, suitable sensor setup, and algorithmic Signal Processing. The changes have brought about simplicity in continuous recording,

monitoring, and processing of human physiological parameters, feature extraction of signals, and so on; but to make these technologies affordable and to provide easy access to the public at large is still a work in progress. The identified areas of improvement include noise isolation, common connectivity, better response period, and signal-processing in real time. Gradual advancements toward portable computer-based data acquisition or DAQ software and hardware can lead to further progress in monitoring instruments. This would not only reduce the dependence on particular instruments but also be easily compatible and share costs to a large extent.

Study and investigation of bio-signals sets the base for various diagnostic, therapeutic, monitoring, and control applications as is evident from the rationale presented. Subsequent section covers the technical aspect of the study.

1.2 Technical overview

Technological developments have enabled the acquisition, processing, interpretation, and storage of vast expanses of health-related data in real-time environments be it in hospitals, at home, or even when mobile. Huge data are generated during surgical procedures, in critical care units during patient monitoring, in the form of medical images, from wearable health and wellness monitoring systems, etc. Understanding this voluminous data and extracting & interpreting information from it involves considerate evaluation of human physiology, acquisition methodologies, modern signal processing techniques, and analysis tools. Further, real-time situations and online analysis require signal processing algorithms that set gold standards to verify the outcome and are robust, reliable, exclusive to a domain of physiological analysis (e.g., when in hospitals, in high-stress situations, or on the move) and also ensure patient safety.

PC-based systems allow the acquisition and analysis of such signals and images and have become crucial for inexpensive and correct diagnostics. Computational processing on huge dataset for noise removal, long-term monitoring, etc. has been made possible due to computer-aided medical systems. It also ensures accuracy and consistency of precise and repetitive events. Investigation done by a human being is generally very subjective and qualitative. To do relative analysis w.r.t standard patterns and draw quantitative inferences from minute changes in the human physiology, it is essential to use PC-based arrangements.

The subsections shall define signals and describe typical bio-signals and their acquisition and processing techniques to understand the concept. Typical case studies presenting recent advancements in the domain and the challenges faced in real-time acquisition and monitoring of bio-signals are also shared.

1.2.1 Signals

A signal is a physical variable that transmits features of a system. Signals are either a response to a process or occur as a natural phenomenon. They could be converted and combined into alternate forms for measurement and analysis. Normally signals are useful when

they are compared or measured over a period of time or with other variables. Some examples of signals could be a sound wave; an electromagnetic wave; outputs of measuring systems such as a pH meter, voltage meter, or a thermocouple; and even the stock or commodity price changes on an exchange. Signals hence are generated in all fields of science right from biology, communications, astronomy, acoustics, seismology, telemetry, and even economics. So, we can now clearly understand that some of the signals are natural and others are responses of physical processes.

Stars emit periodic optical signals, which are interpreted by astronomers to judge their size, distance from earth, chemical composition, expected life, and energy levels. The relative platonic movement across the fault lines helps the seismologists to grade earthquake-prone regions. The location, depth, and intensity of an earthquake are also measured, so is the potency of an underground nuclear test. Similarly, the eruption of volcanoes is increasingly being predicted by measuring the strength and length of sequential minor earthquakes preceding the incident, which correspond closely to the magma movement below the earth's crust.

Cardiologists study variations in ECG to diagnose uncertain heart conditions and relate these aberrations to an evidence of myocardial infarction (heart attack) and early evidence of onset of other heart ailments. Animal echolocation or biosonar is a natural response used by many animal species such as Dolphins, Whales, Cave Birds and Shrews. Echolocation allows these animals to practically "see" the objects of desire, say food or smaller targets to be preyed, or obstructions in their path of motion, by interpreting the reflected sound wave echoes. These are some examples of natural signals.

Man-made signals include the ones originated or transmitted by say a computer, mobile or telephone, photograph, radiograph, radar systems, or other technological systems. These systems are significant as they are deployed to both measure and transmit the outputs of man-made and natural signals. The impressive advancements in communication systems have radically revolutionized the related industries dealing with human senses, that is, health care, entertainment, advertising, education, and warfare (Goleniewski, 2001). The impact of the advancements can be experienced as a huge quantum of data flows across the globe and is available for display, interaction, and analysis almost simultaneously. Signal advancements lead to effective navigation and landing systems such as CAT IIIB for planes in extremely poor visibility conditions and even the development of airborne warning systems to avoid collision between two planes in real time. Some more recent progress and latest applications are discussed further in this chapter.

It is also pertinent to understand signals as time continuous and time discrete signals. Time continuous signals are defined at every instant throughout, for example, an ECG signal originating from the heartbeats of a living being or electromagnetic (EM) waves from a distant constellation of stars. Discrete signals are defined at discrete intervals of time, for example, every second, daily, or so on. The closing or the last traded price of a stock or commodity for the day or daily is one such example. Similarly, signals could be qualified as unidimensional, that is, depending on one variable only or multidimensional, that is, depending on many variables. Temperature reading is an example of unidimensional signal.

A photograph is two-dimensional wherein the intensity of light depends on x and y coordinates, while a TV signal changes with time as content is delivered and is three-dimensional as it depends on time also.

1.2.2 Bio-signals

Living organisms develop and grow as a combined constitution of many interdependent systems. It houses the Cardiovascular or the Circulatory system, Nervous system, Digestive system, Musculoskeletal system, Respiratory system, among others. These biological systems are complex, symbiotic, and delicately connected through subsystems to carry out physiological processes. The circulatory system composing the heart pumps the blood and associated arteries carry oxygen-rich blood from the heart. The reverse cycle returns the blood with high carbon dioxide content and depleted oxygen through the veins across the body to the heart. The blood exchanges oxygen with carbon dioxide in the tiny air sacs called alveoli, in the lungs. The circulatory system transfers not only oxygen but also hormones and nutrients throughout the body. Similarly, the urinary and digestive systems collect the wastes and excess dissolved substances from the blood in the process. Endocrine systems release hormones into the bloodstream for performing many vital functions including digestion. All these systems, hence, are closely dependent on each and govern the physiological processes for streamlined working of the body.

Physiological processes exhibit complex behavior. They are associated with hormonal and nervous control or simulation, voluntary and involuntary movement of body parts, as a response to triggers or otherwise. The inputs or outputs could be a neurotransmission, physical matter movement, or even information exchange. The signals frequently associated with these are electrical, mechanical, or biochemical. Electrical signals are normally in the form of current or potential; mechanical response may be exhibited as a pressure or temperature changes, while biochemical signals lead to neurotransmission or hormonal activity. The information released by the bio-signals has to be extracted, decoded, and suitably even accentuated and cleaned before it is ready for meaningful interpretation.

Like in case of machines, deviation from routine behavior or faults is detected by abnormal signals; defects or disorders lead to alterations in physiological processes. Hence biomedical signal processing is an important indicator for complete clinical analysis and diagnosis. However, a fair knowledge of related human physiology complements the design methodology, analysis of corresponding signals, and underlying state of the system. Traditionally, biomedical signals have been extracted visually and standard outputs are obtained manually. Clearly, subjectivity creeps in during manual recordings result in the development of computer- and algorithmic-based techniques for objective quantification of output, build accuracy, and repeatability.

Physiological processes are interdependent, so are the biomedical signals that extract data deploying complex biological models requiring challenging mathematical analysis. Hence feature extraction capturing the minutest singularities of the signal is crucial for correct interpretations. Physiological signals are captured from one-dimensional time series

and two-dimensional images. The commonly known bio-signals are acoustic (ultrasound), EM waves (EEG, ECG, and MRI), radiations (X-ray, CT) or images (microscopy), etc. (Catlani et al., 2013). Many acquired signals need optimization for the removal of interference and noise originating from other physiological processes or powerlines energizing the devices. Latest biomedical instruments have been designed to detect, optimize, and measure physiological signals which are very low in amplitude like signals emanating from parts of the heart or brain. Often the sheer amount of data collected also poses a challenge as in the case of data collected in studying sleep patterns of patients. Here data size and resulting compression are not the only impediment, even making the data available for medical diagnosis over a distance via communication channels are also required to be managed correctly. In either case, while analyzing patients at patient bedside or across the Internet, signal modeling and simulation are significant for a clear and effective understanding of physiological processes.

We would discuss the basics of acquiring and processing of biomedical signals as we move ahead. Some recent advancements are also mentioned to appreciate the importance and vast applications which would motivate further work in this field (Rangayyan, 2015; Proakis and Manolakis, 1996; Oppenheim et al., 1999; Webster; Sornmo and Laguna, 2005; Cromwell et al., 1979; Bronzino, 2006; https://www.biopac.com/publication-search/; Guyton and Hall, 2000).

1.2.3 Understanding biomedical data acquisition and processing system

Classification of biomedical instrumentation is shown in Fig. 1−1. The instrumentation system can be broadly classified based on the physical quantity being measured, the principle of transduction involved, and the organ system.

Functional components of a generic medical instrumentation system are depicted in Fig. 1−2. The origin of a signal in a biomedical system is the living being or the energy applied to the living being. The Bio-signal Data Acquisition arrangement shown in Fig. 1−2

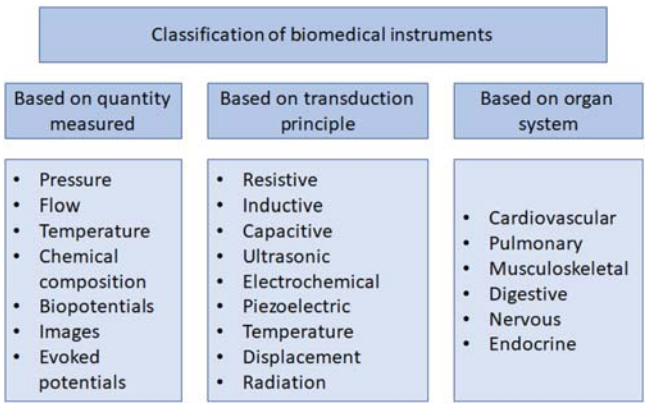

FIGURE 1–1 Classification of biomedical instruments.

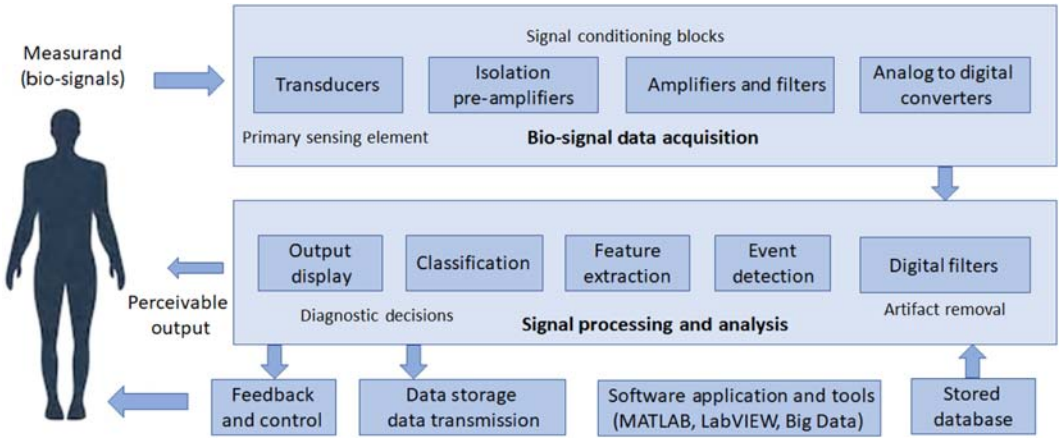

FIGURE 1–2 Bio-signal Data Acquisition and Processing arrangement.

explains the process of digitizing data acquired from the human subject so that it can be appropriately displayed, analyzed, interpreted, and stored in a computer for further monitoring, transmission, and control applications. The essential components include Transducers, Signal Conditioning unit, Analog-to-Digital Converters, Signal Processing Software, and Feedback arrangement for Control.

1.2.3.1 Measurand (bio-signals)

The physical quantity or health condition under measurement is termed as the measurand. Access to bio-signals can be from the molecular level, cell level, or organ level in the form of biopotentials from the body surface [ECG, EMG, electrooculography (EOG), EEG, etc.], blood pressure, flow, medical images, body temperature, evoked potential (auditory, visual, somatosensory, etc.), as depicted in Fig. 1−1 or in response to an external stimulation. Medical instruments are designed in such a manner that it causes minimum inconvenience to the subject and is completely safe and harmless during the measurement. Standard protocol is followed while taking measurement to ensure repeatability and consistency of the experiment. Relatively low-cost acquisition setup is used nowadays that reliably and accurately transduces, amplifies, filters, and digitizes the measurand for further processing.

1.2.3.2 Transducer

Conversion of one form of energy into another form is done using a transducer. Transducers are categorized as Sensors, Actuators or Bidirectional based on the direction of flow of information. A sensor receives the signal from a physical system and responds accordingly, whereas an actuator controls a system. The sensor has a primary sensing element (e.g., a diaphragm or a strain gage) that translates the physical quantity into an electrical output. Ideally, a sensor used in medical instruments should be sensitive, accurate, and noninvasive. It is important to understand the signal conditioning circuitry required for the chosen sensor

so that a perceivable bio-signal is recorded. PC-based systems having facilities of add-on DAQ cards are being used these days which provide an efficient and cost-effective solution to bio-signal acquisition. Such an arrangement is equipped with multiple sensors for multiple channel applications, hardware for amplification, analog filtering, insulation, and Analog-to-Digital Conversion (ADC). Advanced electronics in the form of Application Specific Integrated Circuits are used for implantable units. Design specifications to be considered while measurements using biomedical instruments include Hysteresis, Range of operation, Stability, Accuracy, Frequency Response, Signal to Noise Ratio (SNR), Sensitivity, Input Impedance, Linearity, Reliability, Power requirements, Safety, Radiation, Cost, and Compatibility.

1.2.3.3 Signal conditioning

To ensure quality measurement using the transducers, supplementary electronics called the Signal Conditioning Block is desirable between the sensing unit and the ADC. This generally includes circuits for isolation, preamplification, amplification, attenuation, filtering, linearization, calibration, etc. Modern sensors and DAQs available these days are equipped with inbuilt arrangements for signal conditioning.

1.2.3.4 Analog-to-digital converters

The fundamental component of a DAQ system is the ADC that translates real-world analog signals such as the bio-signals into its digital representation so that it can be processed and manipulated for further computation, storage, transmission, and interpretation. Sample and Hold, Quantization and Encoding are the processes carried out in the ADC. The analog signal is first sampled into discrete levels corresponding to the smallest measurable change in the measurand and then binary coded digital values are assigned to each sample. The ADC returns $2 \times N$ digital values, N denotes no of bits. More the number of bits of an ADC, more is the number of discrete levels and so, higher is the resolution of the ADC.

Aliasing would be avoided or perfect sampling of a signal can be achieved as per Nyquist Rate which states that a waveform can be perfectly reconstructed if the signal pathway provides for twice the bandwidth compared to the highest frequency component of the signal. The biopotentials recorded has a spectrum of up to 1 kHz, so the sampling rate as per Nyquist is only a few kHz. The quantization process has inherent uncertainty called the quantization error, which decides the maximum dynamic range of the ADC. ADC designed for real-world application has certain nonideal effects, quantified by AC and DC performance specifications available in the datasheets of ADCs. Speed and accuracy assist in critically analyzing the ADC performance. ADCs with 8-bit to 14-bit resolution and conversion rates below 10 M-samples per second are called the general-purpose ADCs and those with higher rates having resolution equal to or more than 16 bits are termed precision ADCs (Webster).

1.2.3.5 Data acquisition software (signal processing and analysis)

Data acquisition software is required for further signal processing and analysis and modeling of biological systems. This includes quantifying multiple channel signals, digital filter

algorithms for artifact removal, event detection, feature extraction, and classification for drawing diagnostic and predictive inferences. Artifact removal is one of the major concerns. Digital Filter Algorithms are designed to remove noise picked up from the medical instrument circuitry, the EM interference (EMI), that is, the power line interference of 50/60 Hz, grounding problems, thermal noise, and the environmental noise. The output generated is then used as feedback for control applications and system modeling. Input received for analysis can also be picked from stored standard bio-signal databases. Certain predefined data acquisition Software, such as, DAQami, programming platforms like Python, C++, DASYLab, MATLAB, and NI LabVIEW, or proprietary software can be used for analysis and interpretation and for designing customized solutions for exclusive applications.

In a computer-based system, the signal analysis may be partly performed locally using available software or DSP cards, and partly at a later stage using web-based technology. PhysioToolkit is another application software that permits detection, characterization, processing, and analysis of bio-signals. Software available on PhysioToolkit helps in extracting subtle information hidden in the detected biomedical signal to arrive at a diagnostic conclusion and even do predictive analysis.

1.2.3.6 Database

Huge and rising archive of bio-signal recordings for physiologic and related signals is easily and freely available for biomedical researchers these days on the web. The database is created using a proven experimental protocol, repeated on healthy individuals under relaxed state or when exposed to external stimuli and on patients of varying health conditions. The information is often annotated to describe the instant of occurrence of an event to assist a physician in understanding the complexity of the signal recordings. This enables them to easily comprehend human physiology to develop and analyze signal processing techniques and greatly reduces their task of data collection. It is important to test and evaluate the performance of the developed algorithm on a large dataset of signals before reaching at a conclusive decision for its application in clinical settings.

PhysioNet is one such collection of bio-signal recordings (over 75 databases) covering different clinical problems and associated open-source application software aimed to catalyze biomedical education and research. It has a wide-ranging archive called “PhysioBank” having clinical information and waveforms. The database includes information relating to cardiopulmonary, neural, gait and balance, epilepsy, sleep apnea, etc. acquired from healthy individuals, patients, and during critical care monitoring. “PhysioToolkit” is another component of PhysioNet which hosts application software for signal processing and analysis. It allows data visualization, data mining, data import/export for format conversion and creation of records, simulation and modeling, time series analysis, frequency domain analysis, and makes available software development libraries and tools. It also has WFDB Toolbox of MATLAB having a library of functions for processing physiologic signals and is a platform compatible with many operating systems.

Another most widely used database is the MIT-BIH Arrhythmia database having extracts of 2-channel ECG signal of 48 half-hour durations recorded in ambulatory conditions. The

dataset is richly annotated by cardiologists for each beat, hence the popularity. Along with this, the MIT-BIH noise-stress test database is associated, which helps in evaluating the immunity of filter algorithms under design. These databases are an adjunct to bio-signal processing and analysis (https://physionet.org/; Moody and Mark, 2001; Moody et al., 1984).

1.2.3.7 Simulation and modeling

Simulation and modeling are another valuable step used in understanding bio-signals better and thus devising robust signal processing algorithms having clinical applicability. Mathematical expressions are used to quantify and reproduce physiological signals. Simulation makes it possible to work on these imitated bio-signals under near real-time conditions, which otherwise is a tedious task. Estimated parametric values are experimented to arrive at a suitable performance measure. A biomedical model usually contains a true simulated physiological signal, which is combined with a simulated noise source to reproduce a real signal. This helps in generating bio-signals with different SNRs, which are further utilized in testing the accuracy of the algorithm developed. In certain cases, real-world noise interference is added to simulated bio-signal for performance evaluation.

1.2.3.8 Bio-signal data transmission

Ubiquitous health care requires monitoring of health status in routine at home and also when mobile. This necessitates the design of low-power, compact wireless technology for transmission of bio-signals and for monitoring the activity. Health status is also required to be transmitted from remote locations to the health centers. Modern wireless technologies such as ZigBee and GPRS can be used for Data Transmission through Wireless Personal Area Network. Wireless data transmission finds huge applications in man-machine interface and in the field of modern prosthetics. Sensors fitted with wireless technologies are implanted for prosthetic control. Embedded solution with System-on-Chip FPGA and Bluetooth are also used in smartphone applications for transmitting bio-signals. A lot is being researched in this domain to enhance the standard of living.

Case studies quoting recent developments in health care management and nonclinical applications of physiology monitoring are presented in the subsequent section.

1.2.4 Recent developments

The health care industry is under continuous evolution catering to patients looking for better and effective treatment as life expectancy has improved significantly. No doubt the latest developments in computational techniques such as Artificial Intelligence (AI) and Internet of Things (IoT) are also finding foothold in the industry. It is undeniable that IoT has developed as a breakthrough improvement in the digital health care realm, with the exponential growth of IoT medical devices, with estimated 161 million devices connected worldwide. Sensor technology advancements and the communication revolution are also making additional avenues available for patient care. We are not only talking about patient turnaround time as the only criteria for patient satisfaction in hospitals but the efficacy of treatment is playing a

bigger role. No doubt the technology upgrade is helping the doctors with objective data which assists them to resonate their clinical experience with the processed output from some of the multidimensional diagnostic frameworks. In a particular application around Epileptic seizures, cloud infrastructure coupled with cognitive abilities of IoT, process EEG signals of such patients. Other physical attributes of the Epileptic patient including gestures, movements, and facial expressions are also captured. EEG sensors and other smart sensors transmit the brain signals and other physiological inputs in real time to the cognitive framework. Clearly, these signals and data are complex and large and need human intelligence other than storage capability and sheer processing competence. The system is trained to make decision in real time on the probability of a seizure after signal processing. The system has inbuilt feature to handle the normal EEG signals which are perceptible to noise disturbance from internal and external sources. The analyzed results are made available to medical practitioners for critical patient care and were found helpful in timely intervention (Alhussein et al., 2018; Mavrogiorgou et al., 2019).

Advances in wearable technology are making significant improvements in monitoring human performance as the results are correlated with the vital signs. The role of conventional techniques in measuring bio-signals such as ECG, EMG, and EEG. are already well entrenched in clinical environments. Scientists from the Digital Health Innovation Centre have developed "Intersense," an innovative sensor-based wearable datalogger, for collating human physiological data along with environmental inputs for analysis and critical decision-making. In a specific application, using eye-tracking glasses and simultaneous data log of mobile physiological data, both the outputs are synchronized to plan product improvements and physical training modules. The application finds usage in relieving stress and fatigue, avoiding hazards, improving human performance in sports and work situations, designing ergonomic products, and so on. The special eyeglasses can be worn over the prescribed eyeglasses or as itself. The miniature cameras installed record both the scene image and the eyes themselves. Control systems inbuilt transmit the images and voice data captured via a microphone to an SD card or transmit the same wirelessly over Wi-Fi network. Heat Map, pupil diameter, eye gaze path, blinking frequency, dwell intervals, and areas of interest are captured. The physiological data including BP, ECG, EEG, EMG, EOG, Pulse, Respiratory Rate (up to 16 channels) are parallelly recorded through proprietary wearable devices and software. These outputs are suitably analyzed to arrive at important conclusions for designing safer products and avoiding mistakes and injuries (Goleta, 2020; Eye Tracking Glasses ETV; Shi and Wang, 2018).

Prematurely delivered babies often develop precarious health conditions and infections leading to respiratory distress compared to normal babies born after full-term pregnancy. Unfortunately, some of them require to be admitted to natal care ICUs, whereas many require to be just painstakingly monitored continuously for any variance in physiological parameters such as heart rate, oxygen levels, or even ECGs. A proprietary solution has been developed which could avoid unnecessary prolonged hospitalization. A specialized baby carrier has been developed for prematurely delivered babies by integrating updated sensor technology into the carrier's fabric. The arrangement tracks and analyses vital signs such as

infant's body temperature, weight, heart rate, and oxygen level. The designed sensor is miniature in size with low power requirements and transmits the physiological parameters wirelessly, thus providing mobility. The smart baby carrier detects and communicates over a web interface. This device is not only cost-effective compared to hospitalization but also maintains better connection of the infant with the parents as well (Smart Wearables: eTextile Vital Sign Sensor, 2017).

Spinal surgery is always considered tricky as intraoperative and perioperative complications can have serious consequences such as permanent nerve damage, paralysis, and loss of bladder or bowel control. Surgeons are relying on intraoperative neurophysiological monitoring in operations to cut down the associated risks and better postoperative results. An epidural electrode provides electrical simulation to the dorsal spinal cord to trigger the signal. These signals are transmitted through somatosensory network to ascertain the integrity of sensory pathways at a functional level. The integrity is checked right from the peripheral nerves to the sensory cortex vide the dorsal column. The amplitudes of motor evoked potentials and spinal motor evoked potentials are studied and ensured at lower extremities w.r.t baseline amplitudes before finalizing the procedure. This process of neurophysiological monitoring ensures least postoperative neurological complications (Proietti et al., 2013; Park and Hyun, 2015).

AI advances and latest sensor technologies have motivated technology disruptors such as Tesla to attempt autopilot cars and driverless taxies. Although the launch dates have got postponed many times, it has already prompted similar announcements from Toyota, Honda, General Motors, and Waymo (Google) to follow Tesla's Elon Musk. The success of the program depends on trust the occupants develop on the proposed autonomous system. Radar system, set of cameras, ultrasonic sensors, and an onboard powerful computer are important constituents of the system under testing with limited but progressive success. Certain applications using physiological data monitoring have been deployed on Mercedes S-class and combat helicopter crews. The car provides alerts to retain road focus or prompts a coffee breaker even suggests to pull over based on heart rate, monitoring of driver's eyes, and other physiological data. Simulated environments are being created for helicopter crews as attentiveness is a far serious matter here (Tesla.com/support/autopilot; Masters et al., 2019; Nickel et al., 2019).

Rapid industrialization and population explosion have led to increase in pollution levels and noisy traffic conditions. All these have accentuated the stress levels in individuals, and it often shows negatively in interactions. It is a normal practice to have deep green natural environments in industries that require deep eye concentration in workloads, for example, watch assembly units or electronic PCB "pick and place" requirements of various electronic components. Studies have been conducted to attempt promoting human well-being by encouraging green grassy areas among concrete spaces. Similar studies are also possible even employing virtual reality (VR) environments for humans in stressful work situations like defense force personnel deployed in remote areas or challenging roles. A proprietary data acquisition protocol and software monitors and records the conduction levels on peripheral skin to ascertain the positive impact of various VR settings on curative properties under various situations (Huang et al., 2020).

Like stress management, Disaster management also can be handled using physiological monitoring in real-time. Australia saw one of the most deadly and devastating bush fires of all times in New South Wales in January 2020. The United States has also experienced widespread forest fires in the state of California. Whether it is hurricanes on US East Coasts or other places globally, other natural disasters or incidents of terrorism, timely and effective response to emergencies is the principal aim of disaster management agencies. A network of information and communication technologies have been put in place under the Disaster Response Series of Department of Homeland Security, which proactively prepares for such contingencies of extreme magnitude. Often the information flow is severely impacted due to damage to telecommunication and power supply infrastructure during such calamities. An emergency ecosystem of communication facilitates some of the following key outcomes:

- disaster scene management leading to transfer of victims to medical centers;
- vital sign monitoring of victims—on-site and remotely;
- medical imaging;
- other decision support systems and network.

Mobile phones, tablets, walkie-talkies, mobile radios, and wearable alert and monitoring systems are some of the elements of communication and physiological monitoring used by first responders to share real-time data with on-site and off-site commanders and medical staff. Vital signs, ECG, blood oxygen levels, etc. are transmitted which enable certain critical decision-making in such challenging situations (Fant et al., 2020; Grant County – Next Generation First Responder (NGFR) Case Study).

There is a plethora of clinical and nonclinical applications of physiological data monitoring as can be gauged from case studies presented. However, there are challenges faced in real-time acquisition and processing of bio-signals.

1.2.5 Challenges in bio-signal acquisition and processing

Despite enormous technological advancements in the field of bio-signal acquisition and processing, challenges still remain to be addressed in this domain. Issues such as ease of accessibility of the measurand, dynamic nature of bio-signals, interdependency of various physiological systems, the experimental setup and protocols, noise interference, energy limitation, and safety are typical situations that require special consideration and exclusive solutions.

Our heart and brain are safely positioned in our body in shielded enclosures. Therefore access to the brain and heart signals through noninvasive procedures is sometimes inadequate for specific analysis and for drawing diagnostic inferences. However, ECG and EEG picked up using noninvasive methods serve the purpose of monitoring health condition and well-being. Invasive methods give rich and valuable information picked straight from the site but are associated with high risks. For example, a BP monitoring pressure cuff would only be indicative compared to information gathered by inserting catheters and sensors into the heart. Detecting surface EMG has its own limitations, as it is interfered by other adjoining

muscular contractions during the acquisition. More accurate EMG measurement can be assured by using needle electrodes, which may cause infection and makes the subject uncomfortable. So, it is absolutely necessary to make a trade-off between the quality of signal required against the risks that a subject can be exposed to.

Bio-signals may be periodic, quasiperiodic or stochastic in nature. Our physiological system is dynamic and nonstationary in nature. To quote an example, a normal ECG QRS wave has a rhythmic pattern and can be classified as deterministic, but the wave shape of a cardiac patient varies with time and has an element of randomness, which needs careful study. Even the surface EMG is a sum total of MUAPs of many motor units and so is stochastic in nature. Organ systems in our body are interdependent and interact with each other for proper functioning. It is therefore necessary to consider the effect of these interactions within biological systems to avoid misinterpretations. This poses a challenge in bio-signal acquisition and processing.

Sensor chosen to pick the bio-signal from the site and the entire instrumentation involved also affects the system response and may cause changes in the signal detected. As these changes are subtle in nature, it has to be analyzed with due diligence. While making measurements, involuntary movements such as breathing, heartbeat, tense muscles, coughing, and perspiration may appear as interference and disturb true detection of desired bio-signal. The experimental protocol thus essentially requires relaxed setup. The RR interval may get disturbed due to breathing itself, so it is advisable to hold the breath for few seconds during the measurement. However, for long-term monitoring, robust signal processing algorithms are used to eliminate this interference. Even, ECG of a fetus gets interfered by ECG of the mother, which can be avoided through adaptive signal processing techniques and by adopting multichannel methods only.

Bio-signals are generally in the micro- to millivolt range, so their detection demands highly sensitive instrumentation system with low noise levels. Shielding from EM waves is another major concern. External stimuli whether auditory, visual, or electrical to which a biological system is exposed to has its own safety concerns and threshold and saturation limitations. Most important of all is the safety of the patient or the subject under study. This poses a limitation on the signal quality acquired which can be catered to by signal enhancing methods and processing algorithms in a computer-aided system.

Despite all the challenges, an attempt is made through this book to develop a real-time acquisition and processing setup to comprehend human physiology and draw diagnostic inferences.

1.3 Objectives

The purpose of this book titled *Real-time data Acquisition in Human Physiology* is primarily to gather information on human physiology through an indigenous measurement system that is portable and cost-effective, cover simulation and modeling to interpret and detect abnormalities on the onset of a disease or abnormality through signal feature extraction and

artifact removal, monitor and store the health conditions in real time, and perform objective analysis through algorithm development, thus reducing the subjectivity involved in manual and visual diagnosis and enhance reproducibility. Objectives set to achieve the goal are as listed below:

- Present an application-driven, interdisciplinary and experimental approach to bio-signal processing.
- Focus on acquiring, processing, and understanding human ECG, EMG, Carotid pulse data, and Heart Rate Variability (HRV).
- Extensively cover instrumentation and digital signal processing techniques useful for detecting and interpreting human physiology.
- Cover experimental layout and methodology in an easy-to-understand manner.
- Design and discuss indigenous computer-based system developed that has the capability of easy and direct interface utilizing the sound port in PC while no proprietary DAQ or ADC units is available.
- Create MATLAB-based algorithm for noise reduction using Digital Zero Phase Band Pass Filtering techniques and feature extraction techniques in a home-based computer setup and infer diagnostic features in real-time.
- Create a simulation environment to study various 50 Hz notch filters for removal of power line interference from the acquired signal and fabricate the best-suited design for improved bio-signal detection and visualization.
- Implement a functional model in Simulink application software of MathWorks to filter and acquire real-time human physiology using its integral library.
- Use Digital Signal Controller to enhance features of acquired human physiology and establish a real-time embedded solution to biomedical instrumentation.
- Provide proof of concept of a PC-based twin channel acquisition system for recognition of multiple physiological parameters that are coherent in time for comparison and analysis.
- Derive significant inference from coherently acquired human ECG and carotid waveforms and parameterize HRV.
- Create a stand-alone, platform-independent executable file for the algorithm developed in MATLAB for deployment in future applications.
- Include recent literature and extensive bibliography.

The computer-based simple and indigenous system developed is being explained in this book. Carotid pulse wave is extracted along with the variations in the waveforms under different body postures using a piezoelectric transducer. The signal so acquired is examined on a virtual oscilloscope which is freely downloadable and simple to use. The signal is stored, loaded, and digitally filtered using MATLAB. The developed setup is verified on various human subjects. Parallelly a suitably designed Simulink model analyses the outcome of digital filtering methods on Carotid signals acquired in real time. An additional amplifier configuration is developed by means of Texas Instruments TL084C Operational Amplifier. In this case, an EMG signal is picked up under various contraction levels in bicep muscles using a standard Ag−AgCl sensor. A cascaded amplifier including DC Restoration circuit, Analog

Filters and a circuit for Right Leg Drive constitutes the front end of the acquisition process. Again, a virtual oscilloscope coupled with algorithm for digital filtration in MATLAB is deployed for this EMG Signal analysis in real time. Finally, to facilitate simultaneous and time coherent acquisition of Carotid Pulse and EMG signal under pressure change in the rectal abdominal region and related variations in Carotid waveform, a hardware channel capable to acquire dual signals is synchronized with an algorithm in MATLAB.

The work was progressed further for the acquisition and automated analysis of ECG signals. An audio processing kit developed by Microchip—dsPIC33F—Digital Signal Controller, is explored for this purpose. An additional algorithm is also made in MATLAB so that real-time automated analysis of filtered ECG signal can be realized. The twin channel arrangement explained above is utilized to acquire Carotid pulse and ECG signal simultaneously to compute parameters related to HRV in real time.

The indigenous computer-based system established allows capturing of bio-signal directly through the sound card available in a PC without the additional need of proprietary DAQ and converters for digitization. The system tested for carotid pulse wave acquisition requires only a piezoelectric sensor and no additional electronic arrangement. The amplifier system developed is successful in acquiring real-time EMG and ECG signal on a MATLAB-based oscilloscope using a versatile Ag−AgCl sensor. Hardware 50 Hz notch filter and DSC-based enhanced system gave improved ECG waveform.

MATLAB algorithm created for online parameterization allows QRS—Peak—Detection, R−R interval calculation, heart rate and Power Spectral Density evaluation of ECG waveform. HRV statistics in time domain that were analyzed are the average Heart Rate, Mean R-R Interval, SD index, etc. This algorithm is capable to run as a stand-alone executable application. The twin channel system developed depicts raised amplitude in Carotid pulse wave with increased rectus abdominis pressure and is in sync with Time Domain HRV data which is resultant from ECG data and Carotid pulse signal. The analysis clearly indicates that under critical situations, where ECG measurement is not feasible and affordable, Carotid pulse information can be a suitable alternate for HRV analysis and interpretation as there was negligible difference. The purpose is to create an indigenous, cost-effective, user-friendly solution to real-time acquisition, processing, and monitoring of human physiology which can directly benefit the common people (Bansal et al., 2009a,b,c; Bansal, 2012, 2013; Bansal and Singh, 2014).

References

Alhussein, M., Muhammad G., Hossain M.S., Amin S.U., 2018. Cognitive IoT-cloud integration for smart healthcare: case study for epileptic seizure detection and monitoring, mobile networks and applications, September.

Bansal, D., 2012. Potential of piezo-electric sensors in bio-signal acquisition. Sens. Transducers 136 (1), 147−157. ISSN 1726-5479.

Bansal, D., 2013. Design of 50 Hz notch filter circuits for better detection of online ECG. Int. J. Biomed. Eng. Technol. 13 (1), 30−48. ISSN 1752-6418 (IJBET).

Bansal, D., Khan, M., Salhan, A.K., 2009a. A computer based wireless system for online acquisition, monitoring and digital processing of ECG waveforms. Comput. Biol. Med., 39 (4), 361−367.

Bansal, D., Khan, M., Salhan, A.K., 2009b. Real time acquisition and PC to PC wireless Transmission of Human Carotid pulse Waveform. Comput. Biol. Med. 39 (10), 915–920.

Bansal, D., Khan, M., Salhan, A.K., 2009c. A real time embedded set up based on digital signal controller for detection of bio-signals using sensors. Sens. Transducers 105 (6), 26–32. June.

Bansal, D., Singh, V.R., 2014. Algorithm for online detection of HRV from coherent ECG and carotid pulse wave. Int. J. Biomed. Eng. Technol. 14 (4), 333–343.

Boston Scientific - Pacemakers: www.bostonscientific.com/en-US/about-your-device/how-pacemakers-work.

Bronzino, J.D., 2006. The Biomedical Engineering Handbook, 3rd ed CRC/Taylor & Francis.

Catlani, C., Badea, R., Chen, S.-Y., Crisan, M., 2013. Biomedical signal processing and modelling complexity of living systems 2013. Comput. Math. Methods 2013, 173469.

Cromwell, L., Weibel, F.J., Pfeiffer, E.A., 1979. Biomedical Instrumentation and Measurements. Prentice Hall.

Eye Tracking Glasses ETV, https://www.biopac.com/product/eye-tracking-etv/.

Fant, C., Adelman, D.S., Zak, C.L., Wood, L.K., 2020. Communicating data and information in disaster care. Feature: disaster response series: part 3. Nurse Practitioner 45 (2), 48–54.

Getlen, L., 2014. The untold story of how the buried Chilean miners survived, October 11, nypost.com/2014/10/11.

Global Health Observatory (GBO) data released by WHO, www.who.int/gho/en/.

Goleniewski, L., 2001. Understanding the telecommunications revolution: book chapter. In: Telecommunications Essentials: The Complete Global Source for Communications Fundamentals, Data Networking and the Internet, and Next-Generation Networks.

Goleta, Calif, Jan. 2, 2020, BIOPAC combines eye tracking with mobile data logging and physiology data collection to run experiments in the lab or in the real world. https://www.biopac.com/new-eye-tracking-glasses-bring-real-world-data-to-academic-research/.

Grant County – Next Generation First Responder (NGFR) Case Study: Physiological Monitoring. https://www.dhs.gov/publication/st-grant-county-frg-ngfr-case-study-physiological-monitoring.

Guyton, C., Hall, J.E., 2000. Textbook of Medical Physiology, 10th ed. W. B. Saunders, Philadelphia.

Huang, Q., Yang, M., Jane, H.-a, Li, S., Bauer, N., 2020. Trees, grass, or concrete? The effects of different types of environments on stress reduction. Landsc. Urban. Plan. 193 (January).

Masters, M., Donath, D., Schulte, A., 2019. An exploratory analysis of physiological data aiming to support an assistant system for helicopter crews. Intell. Hum. Syst. Integr. 744–750.

Mavrogiorgou, A., Kiourtis, A., Perakis, K., Pitsios, S., Kyriazis, D., 2019. IoT in healthcare: achieving interoperability of high-quality data acquired by IoT medical devices. Sensors (Basel) 19 (9), 1978.

Moody, G.B., Mark, R.G., 2001. The impact of the MIT-BIH arrhythmia database. History, lessons learned, and its influence on current and future databases. IEEE Eng. Med. Biol. Mag. 20, 45–50.

Moody, G.B., Muldrow, W.K., Mark R.G., 1984. A noise stress test for arrhythmia detectors. In: Proceedings of the Computers in Cardiology, pp. 381–384, IEEE Computer Society Press,.

Nickel, P., Bärenz P., Radandt S., Wichtl M., Kaufmann U., Monica L.et al., 2019. Human-system interaction design requirements to improve machinery and systems safety. In: Proceedings of the 6th International Conference on Safety Management and Human Factors at AHFE 2019, July 24–28, Washington D.C., USA

Oppenheim, V., Schafer, R.W., Buck, J.R., 1999. Discrete-Time Signal Processing, 2nd ed. Prentice-Hall, New Jersey.

Park, J.H., Hyun, S.J., 2015. Intraoperative neurophysiological monitoring in spinal surgery. World J. Clin. Cases 3 (9), 765–773. Available from: https://doi.org/10.12998/wjcc.v3.i9.765.

Proakis, J.G., Manolakis, D.G., 1996. Digital Signal Processing: Principles, Algorithms, and Applications, 3rd ed. Prentice-Hall, New Jersey.

Proietti, L., Scaramuzzo, L., Schiro, G.R., Sessa, S., Logroscino, C.A., 2013. Complications in lumbar spine surgery: a retrospective analysis. Indian. J. Orthop. 47 (4), 340−345.

Rangayyan, R.M., 2015. Biomedical Signal Analysis, Second Edition The Institute of Electrical and Electronics Engineers, Inc.

Romagnol, J., Case study: physiological status monitoring in the Chilean mine rescue operation - a doctor's view, Case-study-chilean-miners-use-zephyr-technology.pdf.

Shi, J., Wang J., 2018. Human body communication−based wearable technology for vital signal sensing, wearable technology in medicine and health care.

Smart wearables: eTextile vital sign sensor, 2017. Nijmegen, the Netherlands. https://ec.europa.eu/growth/tools-databases/dem/watify/inspiring/watify-success-stories/smart-wearables-etextile-vital-sign-sensor.

Sornmo, L., Laguna, P., 2005. Bioelectrical Signal Processing in Cardiac and Neurological Applications. Elsevier Academic Press, ISBN: 0-12-437552-9.

Webster, J.G. (Ed.), Medical Instrumentation: Application and Design. Fourth Edition, John Wiley & Sons.

World Health Organization, Global Health work force Statistics, OECD, 2019. supplemented by country data: reported by data.worldbank.org, http://www.oecd.org/els/health-systems/workforce.htm.

World Health Statistics, 2018. Monitoring health for the SDGs. https://www.who.int/gho/publications/world_health_statistics/2018/en/.

2 PC-based data acquisition

2.1 Introduction

Physiological organ systems in the human body consume energy while performing chemical, mechanical, or electrical actions, which lead to all biological activities. The resultant muscular or neural outputs or signals are transmitted as bioelectrical signals. Human body also emits bioacoustic and biooptical signals. Bioacoustic signals are largely detected using suitable microphones, such as, blood flow, lung ventilation, and digestion characteristics. Biooptical signals are generated because of the optical response of biological systems, such as, blood oxygenation level (measured based on modified IR absorption) or pulse rate monitoring (based on changes in color of the skin) (Schmidt, 2015; Cysewska-Sobusiak, 2019; Semmlow, 2012; Semmlow, 2018).

All the physiological signals are a true reflection of underlying mechanisms of various systems or variations associated with specific biological occurrences and hence are useful both for monitoring and medical diagnosis. Advanced systems for diagnosis and physiological parameter measurement were not developed in ancient times. Still there is evidence of some techniques such as "Pulse Diagnosis" or "Nadi Pariksha" both in Chinese and Indian medical systems. The examination involved feeling the pulse at three points on both the wrists by applying varying pressure using index, ring, and middle fingers. The system was supposed to proactively understand any anomalies or upcoming complications in various organs, that is, the heart, liver, kidneys, lungs, and spleen (Yoon et al., 2000; Gaddam, 2015; Selvan and Begum, 2011; Kajsa, 2008). However, acquisition and interpretation of human physiological parameters, such as, electrocardiogram (ECG) waveform got recognition in the late 19th century and early 20th century by some exemplary contributions by Nobel laureates such as Willem Einthoven and others. Initially, the laboratory instruments used were very bulky and cumbersome (Cooper, 1986). The interpretation was still very qualitative, and a lot was left to the experience of medical teams.

Intelligent methods, signal processing techniques, and computer algorithms are progressively being deployed for quantitative analysis and to arrive at informed decisions on the underlying health conditions. The basic bio-signal processing techniques have also seen major improvements (Krishnan, 2016) and could be broadly classified into:

- Time-domain analysis for event detection, for example, arrhythmia detection in ECG.
- Frequency domain analysis using Fast Fourier Transformation (FFT), for example, spectral analysis of electroencephalogram (EEG) for improved recognition of neurological ailments.
- Time-frequency approach addresses the shortcomings of time domain or frequency domain analysis. These procedures signify only the spectral properties and cannot process the dynamic nature of bio-signals, for example, analysis of sleep apnea. The next-generation techniques addressed these limitations and joint time-frequency depictions could be realized.

Real-Time Data Acquisition in Human Physiology. DOI: https://doi.org/10.1016/B978-0-12-822118-1.00002-3
© 2021 Elsevier Inc. All rights reserved.

- Nonlinear theory and neural network advancements led to automatic classification and identification of abnormality in bio-signal patterns and detection of abrupt changes, for example, wearable, embeddable, and ingestible health monitoring.
- Upgraded sensors, material science advancements, and wireless communications enabled further expansion in bio-signal monitoring.
- Endless opportunities with emerging advancements in communication and wireless technologies, for example, 5 g mobile technology, Internet of medical things and artificial intelligence (AI) enablement in medical decision assessment, VR (virtual reality), and augmented reality in health care applications.

The instrumentation involved in acquiring these bio-signals has also evolved over the years. Data Acquisition Systems (DAS or DAQ) came into existence, which had the capability of converting analog real-world physical/biological signals into the digital domain and then utilizing the capability of a computer, these bio-signals could be visualized, stored, analyzed, and could trigger a control command. The first DAQ system was developed by IBM, in the early 1960s which could record scientific data. These were bulky and expensive and required significant programming and setup expertise. A solution to this issue emerged in the form of PC-based DAQ systems. By the mid of 1980s, National Instruments Corp. (NI) devised the GPIB Data Acquisition Cards and DAQ boards which could be interfaced with low-cost PCs for the Macintosh platform. Apart from this breakthrough invention of utilizing the functionality of a personal computer for data acquisition and analysis, a proprietary application software LabVIEW offering a wide spectrum of built-in functions was also released by NI. During 1992 NI released a LabVIEW version, compatible for Windows PCs. This platform can be explored to design and develop in-house real-time DAQ. MATLAB also offers a Data Acquisition Toolbox with featured apps and functions that enable writing data to DAQ analog and digital output channels and processing the detected signals. The toolbox is compatible with a plethora of DAQ hardware, covering Universal serial bus (USB), Peripheral Component Interconnect (PCI), PXI Express devices, from NI and other vendors.

The functional components of a generic data acquisition and processing system as already introduced in Chapter 1, Introduction, are depicted in Fig. 2—1. The essential components include Sensors and Transducers, Data Acquisition System Hardware (Signal Conditioning unit, ADC, DAC, MUX, Controllers, Power Management, etc.), the Interface Units, Data Acquisition System Software (Signal Processing Platforms like MATLAB, Simulink, and LabVIEW), Computers, etc.

Generally, DAQ hardware interfaces between a PC and the analog signal. It might be packaged as modules that could be coupled with the various ports on the computer say via parallel, USB, serial port, etc., or directly to the cards in the motherboard, for example, S-100 bus, ISA, PCI, and PCI-E. An external breakout box is sometimes required to adjust many wires and limited space around the back of the PCI card. DAQ device drivers accomplish direct read and write on the hardware and provision for a standard API to facilitate the interface between user applications under diverse programming environments. DAQ software is the major element of the entire arrangement that makes large-scale data acquisition

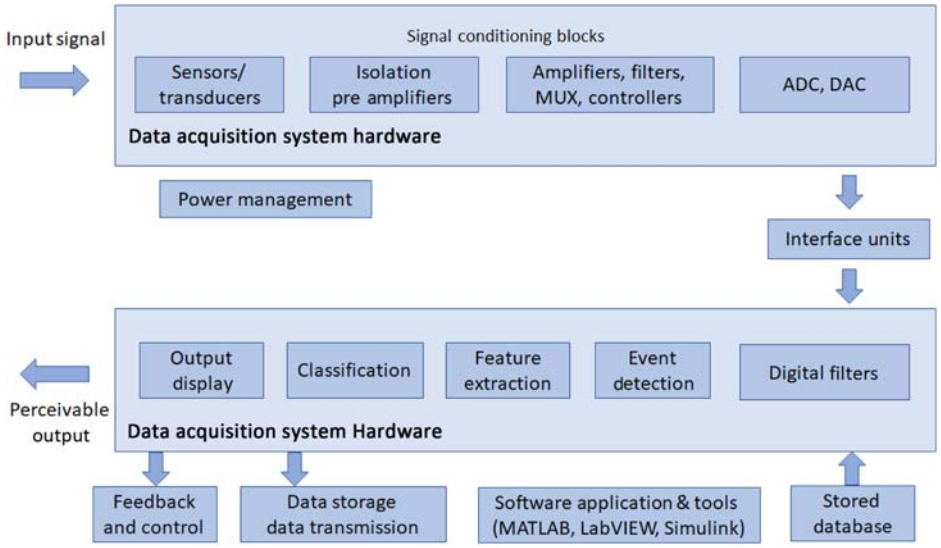

FIGURE 2–1 Depiction of a generic Data Acquisition and Processing System.

possible. The DAQ software could be written in standard languages such as C language, or proprietary software such as LabVIEW, MATLAB, and Simulink could be utilized. DAQ software offers a user-friendly platform that provides an interactive control and customization of the acquisition and analysis set up in the form of Graphical User Interface (GUI) or Text-based User Interface (TUI). GUIs are web-based application programs that offer better control compared to TUIs which are ASCII configuration files. Each component of the Bio-signal Data Acquisition arrangement is being detailed in the subsequent sections.

2.2 Sensors and transducers

Sensors are very commonly used across measurement systems in manufacturing, science, environment studies, medicine, etc. Sensors are often understood based on sensing capabilities such as mechanical, optical, electrochemical, thermal, semiconductor, or electromagnetic sensors. Biomedical sensors are designated to measure physiological and pathological parameters. Acquisition systems, techniques, and related sensors provide vital inputs to the health care professionals to not only diagnose ailments but also appreciate variations in health conditions. Biomedical sensors measure chemical, physical, and biological inputs and are also accordingly categorized as *chemical sensors, physical sensors, and biosensors*. The sensors are used both in vivo, for continuous critical monitoring (constant invasive and noninvasive measurements), and also in vitro, for diagnostic purposes. The overall emphasis of health care systems is to improve the sensor systems, drastically reduce the time for

diagnosis, move as close to the patient as possible without compromising on the quality of health outcome.

Sensors give output in the same format as per the acquired and detected input. Transducers transform the received signals from one form to another so as they could be measured, usually from a nonelectric form to electric or vice versa. In the medical field, electrodes have distinct significance. While electrodes are electric conductors, medical electrodes convert ionic potentials to electric potentials leading to quantification and diagnosis of underlying conditions. Sensors, transducers, and electrodes are the building blocks of diagnostic instrumentation. Normally, a medical instrument obtains input directly or indirectly, in the form of an analog electric signal. The heart, brain, and muscles, generate electric signals which are directly acquired by biopotential electrodes. Other physiological variables such as body temperature, blood pressure (BP) or flow characteristics, biochemical parameters, such as, ionic concentrations or gas partial pressures are nonelectrical in nature and are converted into electrical signals by transducers. Ultimately, the entire process of sensing a biological input involves sensors, transducers, and electrodes, which are sometimes grouped together and indicated as sensors.

2.2.1 Physical sensors

Physical sensors detect and monitor physical variables such as thermal, electrical, mechanical, hydraulic, and magnetic. Many physiological parameters related to BP, muscle movement, body temperature, fluid pressure (say cerebrospinal), blood flow, and rate of growth of bones have biomedical significance and are monitored by different physical sensors. Broad classification of physical sensors is discussed here.

2.2.1.1 Radiation sensors

Radiation sensors include sensors utilizing high-energy radiations such as X-rays or gamma rays for 2D/3D medical imaging and targeted treatment in many biomedical applications. These applications use ionizing radiations in the form of electromagnetic waves such as X-rays or gamma rays. X-rays are emitted in vacuum tubes by heating tungsten cathodes (A 184, Z 74) which has a very high melting point (3422°C). Electrons at high energy are released from the tungsten electrode subjected to high voltage to impinge on a metallic tungsten anode in X-ray tubes. This results in knocking off electrons from the inner orbits of the atoms, ionizing and making them unstable, leading to release of X-rays in the form of photons (1%) and balance as heat (99%) which is removed from the system. These atoms undergo chemical changes to achieve a normal state again. X-rays have higher energy than light and are directed toward the subject to be examined. They are absorbed in various proportions by soft tissues and bones because skin, muscles, and bones have different densities and atomic numbers. They find applications in diagnosing bone fractures, abnormal masses, foreign objects, pneumonia, mammography, and computed tomography scans.

Therapeutic radiation treatments using X-rays and higher energy radiations are used to annihilate tumors by focusing radiations on the diseased cells. Overexposure to X-rays can

cause change in DNA structures, which in the worst case lead to extreme results such as cancer in the long run. Clearly, the physician takes a very calculated view of the advantages and risks involved in exposure to radiations in various age groups. The patient is duly protected, and optimum strength of X-rays exposure is managed as far as possible to the target area with an X-ray film, detector, or image intensifier receiving the pass-through behind the subject. The conventional X-ray film is coated with a silver halide solution which is developed after exposure in dark rooms. The conventional system has been updated to computed radiography and digital radiography. Computed radiography cassettes have a phosphor screen that stores the latent image after exposure. The cassette when placed in a laser fed reader releases the photons as digital image is displayed. In case of digital radiography, photons from the X-rays impinge on a photoconductor layer giving positive and negative charges. Direct conversion process involves impact of X-ray photons over the photoconductor, such as amorphous Selenium(a-Se) or Cadmium telluride (Cd-Te). The photoconductors are directly mounted on a multi-microelectrode plate and convert X-rays to electronic signals for further amplification and digital output. In another method, a scintillator is used to convert X-ray photons to photons of visible light. Photodiodes with amorphous silicon convert light photons to electrical signals. This method has a relative disadvantage due to the tendency of light photons to spread, thus leading to deterioration of the final image.

Gamma rays have a higher energy level compared to X-rays. While X-rays have a wavelength of *10 to power -10m* (100−0.01 nm), Gamma rays have a wavelength of magnitude $<$ *10 to power -12m*. All naturally occurring heavy elements with $Z > 83$ are unstable with a very high energy. Such radionuclides like technetium -99m undergo radioactive decay. The nucleus attains a lower energy level by undergoing gamma decay, hence achieving comparatively lower energy levels as electromagnetic radiation or photons are released. The photons released in such a deexcitation process are called gamma rays. Radionuclides or radiopharmaceuticals or tracers are substances that are either injected intravenously or swallowed to emit controlled radiations. Measured and limited quantities of tracers have negligible pharmacologic effects on the patients. These compounds are used for brain imaging, heart imaging, detection of carcinoma in the colon or rectal regions, bone metastases, thyroid imaging, etc. The affected tissue in the body uptakes the tracer and exhibits as a "hot spot." Gamma rays released are picked up by the gamma camera or a rectilinear scanner. Positron emission tomography or PET scan uses radioactive sugar. Some commonly used radionuclides are Iodine 123, Iodine 11, Gallium 67, or Fluorine 18 fluorodeoxyglucose (administered intravenously).

Gamma camera is placed at one or many positions pointing at the organ under examination. It has a mechanism to receive and interpret gamma rays simultaneously from all cameras to create a 3D image. The gamma rays received perpendicular to the tungsten head in the camera are passed through, whereas the other oblique rays are absorbed and neglected. A collimator made of sodium iodide laced with thallium receives the rays and converts them into scintillations. These are then converted into electric signals by an array of photomultipliers reconstructing 2D or 3D picture (Zhou et al., 2015; Glenn, 2020; Radiology Cafe/Exams/FRCR Physics Notes/X-ray Imaging/Production of X-rays; Yoon, 2016; Togawa et al., 2011; Harsányi, 2000; Enderle and Bronzino, 2012; Eren and Webster, 2017; Thakor, 2015).

2.2.1.2 Mechanical sensors

Mechanical sensors include ultrasound, pressure sensors, thermal sensors, and magnetic sensors for various biomedical measurements. These sensors monitor a wide variety of physical attributes such as force, strain, mass, pressure, weight, velocity, and acceleration for giving logical outputs. The mechanical sensors account for mechanical vibrations, capacitance, piezoresistive effect, resistance, and triboelectricity. The pressure sensors, on the other hand, rely on electric potential measured by the piezoelectric material on deformation. Thermal sensors are the most commonly used sensors across industrial, environmental, and biomedical applications. Magnetic sensors detect changes in parameters related to magnetic field to give a calibrated response. Some of these sensor mechanisms pertinent for biomedical applications are discussed in brief here.

Ultrasound is the sound wave frequency larger than the upper limit of 20 kHz which can be perceived by a human ear. Bats and dolphins can emit ultrasounds. The time taken and angle of reflected waves provide them as a mean of communication and estimate on the approaching terrain, prey, and their relative location. Ultrasound waves can propagate through gases, liquids, and solids, but not through a vacuum. The speed of sound varies by the medium it travels through. The ultrasound transducer emits sound waves that are reflected off of the tissue back to the transducer. The reflected sound waves are captured and translated into electrical signals. The intensity of the reflected signal is represented by the relative brightness of the pixel on a gray-scale display. The greater the fraction of sound wave that is reflected back to the transducer, the brighter the image that is displayed. Structures with high levels of calcium or fat, such as dermoid cysts or calcified fibroids, appear bright on the gray-scale image, and muscle tissue and ovarian parenchyma appear darker.

The frequency of sound waves influences the depth of field and image resolution achieved. The transducer frequency deployed is directly related to image resolution and inversely related to the penetration achieved. This is quite important in medical ultrasound. The transducer frequency for abdominal examination is 3.5−5 MHz, pelvic imaging is done at 3.5−7.5 MHz, and so on. Lower frequencies were used earlier to ensure no deep structures and details are missed out, followed by higher levels. In ophthalmoscopy-related measurement frequencies more than 15 MHz are deployed. Higher frequency capabilities have expanded the clinical applications of ultrasound imaging.

The ultrasound probe consists of a piezoelectric crystal with metallic electrodes on either side. The electrodes on excitation based on the alternating potential applied on them produce a sound wave that is passed on to the skin or medium in contact. On the other side, the reflected return sound wave causes mechanical strain and corresponding potential at the electrodes in relation to the sound pressure. The depth of the underlying tissue is related to the time required for the return pulse, whereas the wave fraction returned determines the density or the size of the examined tissue. The beam pattern transmitted by the head corresponds to the geometry of the piezo crystal(s) and the head, and spherical waves are generated by multiple point sources in discrete bundles.

2.2.1.2.1 Doppler Sonography used measurement of blood flow

At higher frequencies, ultrasound can be scattered from RBC to ascertain blood flow velocity through veins and arteries. This technique called Doppler Sonography uses a duplex transducer, wherein the first transducer transmits ultrasound waves, whereas the other one receives the deflected waves from the blood cells in motion. The frequency shift as detected between the two piezoelectric elements is detected as the deflected angle between the incident monochromatic wave and the flow direction. This method is now being used for diagnosing conditions of poor blood flow and blood clots. Some of the well-known applications are to investigate edema in feet due to poor return blood flow or fetal heart rate monitoring, etc. (Creager et al., 2013; Breitkopf, 2009).

Pressure sensors: pressure measurement in the human body is a vital part of clinical examinations, physiological studies, and therapeutics. Cardiovascular system pressures are measured as arterial blood pressure and are often referred as important parameter of circulatory conditions.

BP measurement: BP measurement involves the measurement of systolic and diastolic pressure. The Systolic phase corresponds to mechanical movement of the heart ventricle when the aortic valve is open. The Diastolic phase refers to the arterial pressure when blood moves to the peripheral arterial system, while the aortic valve is now closed. Low BP could lead the human body into a state of shock due to inadequate flow of blood for other organs and systems. High BP on the other hand is either caused by an ailment concerning kidneys, etc. or could cause permanent damage to such organs. Hence measurement and control of BP as an important physiological parameter is always critical.

BP measurement is carried out by Indirect (noninvasive) or Direct (invasive) methods. Indirect method is normally used for routine clinical observations. The direct method may be used for continuous measurements or in emergency conditions. Auscultation and oscillometry are the two most common Indirect measurement techniques. In the auscultatory method, a cuff is placed over the upper arm and inflated above the Systolic range to block the blood flow. The cuff is then slowly deflated to measure the point at which the blood flow starts (corresponds to Systolic BP) and the point where the blood flow just becomes normal (corresponds to Diastolic BP) on the mercury column scale of the sphygmomanometer. The radial pulse palpitation intensity or the Korotkoff sounds using a stethoscope indicate the corresponding Systolic and Diastolic BP measurements. In the oscillometry method, during cuff inflation, the machine automatically detects discontinued blood flow as pulse waves stop due to increasing cuff pressure. The inflation is reversed soon after due to automatic and slow valve pressure release, recording the pressure at which the pulse pressure wave just starts and finally subsides. The machines use algorithms to convert the pressure and volume changes into BP. Oscillometry machine needs to be calibrated frequently with the Auscultation method especially with regard to different age groups and physical conditions (e.g., obesity, pregnancy) of subjects. The Auscultation method could also lead to errors due to leakages in the sphygmomanometer. These days BP monitoring at home has become very common as the technology and reliability have improved, but the BP readings often vary

based on the time of the day (early morning after sleep vs during the day) or after exercising, walking, or merely due to phobia of monitoring. Hence, monitoring by a physician is always recommended.

2.2.1.2.2 Hemodynamic invasive blood pressure sensors

Direct or invasive BP monitoring uses small silicon-based pressure sensors and is largely practiced for hospital in-patient monitoring where continuous monitoring of physiological parameters is critical for better outcomes. The pressure sensor chip is maintained in a sterilized housing and the blood through a cannula inserted in the artery is made to interact with the sensor either directly or through a separating chamber filled with silicon oil. The silicon oil chamber houses a replaceable membrane that prevents direct blood clotting on the main sensor. This method also avoids any bioelectric interference with the principal sensor chip directly and the intermediate membrane can be replaced when blood clotting takes place on its surface. Such invasive arrangement can house the signal processing module along with the pressure and temperature sensors in a single miniature circuit. Such ultraminiaturised chips are fabricated using microelectromechanical system (MEMS) technology either as piezoelectric or as fiber optic sensors. Trapped air bubbles in the catheters cause damping and degradation of the system's natural frequency. The errors could also come from long tubing, varying diameters, narrow connections, and far too many interacting components. Although the bubbles need to be avoided at the user end, many other issues are related to design of such systems.

2.2.1.3 Sensors in spirometry

Spirometry is a technique to measure respiratory flow in terms of amount and speed of air in inhalation and exhalation. Pneumotachometer or Pressure Transducer Module (PTM) measures pressure difference across an obstacle or grid as a function of flow. The flow resistance offered by the grid is predesigned and hence the flow rate is calculated from the actual pressure difference. Again, miniature silicon-based pressure sensors are deployed to measure the actual pressure difference. There are two types of Pneumotachometers—Linear Resistance and Ultrasonic PTM.

Linear resistance or the PTM consists of three parts namely resistive load (fixed), pressure sensor, and the display. As a working requirement, pressure difference and flow rate need to be linear in the working range of flow rates. The system involves an infrared detector that picks up the infrared light interruptions as the rotary blades get in motion due to passing air pressure. The infrared rays are directed across from the other end by an infrared source. The PTM is regularly calibrated w.r.t. to a standard bell spirometer connected in series.

2.2.1.4 Ultrasonic pressure transducer module

Ultrasound-based PTM's measure the transit time of a sound input through a moving medium either in direction of the sound input or against it and relate the same to the volume and flow parameters of air through the spirometer. The ultrasound transmitter and receiver set are placed at a predetermined angle or perpendicular to the airflow. The sound

either slows down or speeds up based on whether the medium is flowing in the direction of the sound or against it. Piezoelectric transducers are incorporated in the wall for flow characteristics measurement at points 1 and 2. Both these systems are used for the measurement of patient's lung function or pulmonary function testing.

Another class of spirometer known as Vortex-Shedding PTM is also used where the Reynolds number is very high. They use either ultrasonic transmission and receivers or an optical fiber arrangement for flow measurements.

Another application of Optical fiber pressure transducer is for resolving Obstructive Sleep Apnea Syndrome (OSAS), checking pressure in lungs and blood vessels, urinary bladder, digestive tract, joints, and bones. This sensing system can be used in minimally invasive mode. It has a reflective diaphragm that actually senses the pressure and two optical fibers. One optical fiber receives the light from the light source, whereas the other fiber detects the reflected light wave from the diaphragm which is incident upon a photodiode for analysis. The pressure on the reflective diaphragm bends it and changes the quantum of reflected light. The changes in the phase of light and path length are detected on the other end which are interpreted as potential difference and scaled into pressure outputs. Nontoxic materials, flexibility of optical fiber, least hazardous voltages, and negligible electromagnetic noise or interference make them an ideal choice for such applications (Avnet: Pressure Aensors).

In case of OSAS, the transducer arrangement has several transducers from the larynx right up to back of the nose. For every emitting transducer, there are two receiving transducers, while one of the transducers is catheter type and is placed in the esophagus to measure lung pressure.

2.2.1.4.1 Piezo sensors for pressure pulses

Pulse sensing has always been considered to be a convenient mode of acquiring significant physiological data regarding the circulatory or cardiovascular system. Piezo sensors are known to be sensitive and consume very low power making them suitable for many such applications. A thin-film plastic piezo sensor attached closely to the skin finds application in real-time study of the pulse pressure. The sensor is fixed on the right finger in a U-shaped housing for convenience or directly mounted onto the wrist. An electronic circuit with high-impedance FFT is used as a buffer to isolate electric interferences. Breathing waves and pulse response are separated using suitable electronic filters. Some other interesting applications include sleep apnea monitoring in babies, fetal heart rate monitoring, respiration sensors for infants, Carotid Artery Pulse wave recording, and measuring variations in joint angles (Chen et al., 1990).

2.2.1.4.2 Measurement of internal ocular pressure

Another pressure sensor application involves the usage of a silicon-based miniature mechanical sensor arrangement for the measurement of Internal Ocular Pressure (IOP) or intraocular pressure. Such investigation is mandated for the diagnosis of glaucoma, especially the disease progression. Elevated levels of IOP in opthalmoscopy are considered as a vital parameter for glaucoma risk (Goldberg, 2003). The internal pressure exerted by the spherical eyeball can be ascertained by measuring the force required to bring a portion of the sphere

to a flat position. The investigation is carried under sterile conditions wherein a glass plate is made to press against the cornea to achieve a predefined deformation. The actual force corresponding to the applanation is converted into IOP while adjusting for surface tension of the tear film and some other parameters (Stevens et al., 2012).

2.2.1.4.3 Acoustic sensors-based hearing aids

Humans have capability to appreciate sound frequency from 20 Hz to 20 kHz. Most of the conventional hearing aids and implantable sensors are designed in the essential range of 250 Hz−8 kHz. The arrangement comprises miniature microphone child parts created for this specific application. The assembly consists of microphone with preamplifier unit, signal processing section, followed by an amplifier and loudspeaker unit (Calero et al., 2018). The most commonly used microphones are electret condenser microphone based, wherein the material "electret" is permanently polarized and highly sensitive. The working principle of a microphone involves electric signal generated by a deformed diaphragm as it encounters a sound signal. The micromachined miniature mechanical elements also facilitate the provision of preamplifier in the microphone capsule itself, ensuring minimum noise aberrations in the captured signal. Various types of implantable sensors are used in acoustic aids. Capacitive sensors are usually used in subcutaneous implants, whereas the sensors implanted in the middle ear include, capacitive, electromagnetic, piezoelectric, piezoresistive, electromagnetic, and optical. Comparative studies have been conducted based on the frequency range, sensitivity, bandwidth, size, power consumption, technology, patient comfort, service life, and ease of implantation or based on specific needs which could form the basis of the selection.

2.2.1.5 Thermal sensors

Body surface and deep tissue core temperature is another important physiological parameter to establish the physical well-being of human systems. A variety of sensor devices measure temperature from the skin, oral cavities, rectum, or urinary bladder as per prevailing physical conditions and medical advice. Such thermometers use transducers, based on semiconductors, thermocouples, infrared sensors, optical fibers, quartz crystal temperature sensors, etc. Abnormal skin temperatures can be a result of irregular blood circulation or excessive heat generation in adjacent tissues. Arterial blood regulates the temperature of tissues that have high metabolic activity. Accurate observations of temperature are vital as certain targeted therapies such as thermotherapy or hyperthermia for cancer cell destruction require precise measurement of tissue temperature.

Temperature sensors are part of catheters, probes, or needles, etc. or may be used directly for measurements. *Thermistors* are metal-based sintered oxides of cobalt, iron, nickel, copper, or manganese temperature sensors having negative temperature coefficients. These sensors are extremely sensitive compared to conventional platinum probes and hence are suitable for body temperature measurement especially achieving higher resolution in small temperature range. *Thermocouples* are used for local temperature measurement in the shape of needles, catheters, and insulated wires. Typically, a thermocouple provides an

electromotive force in a closed loop having two junctions of dissimilar metals at different temperatures, often referred to as Seebeck Effect. *Diodes and transistors with p−n junction* are used as temperature sensors as a p−n junction displays good linear temperature characteristics at constant forward-bias current. *Crystal resonators* such as quartz crystal resonators are also used for temperature measurement as the frequency of resonation exhibits virtually linear temperature coefficient across a large temperature range.

Temperature measurement is carried out by both *noncontact and contact* measurement techniques based on the clinical needs and the instrument involved. Noncontact temperature measurement is achieved by utilizing the radiation heat transfer such as infrared radiation thermometers. Microwave-based radiometers can be used for deep tissue measurement and imaging. Infrared radiation thermometer detects the thermal radiation emitted by the human body or object surface corresponding to the far-infrared region. Infrared thermometers also simultaneously receive ambient radiations as reflected from the body surface. Thermal detectors and photon detectors are two types of infrared detectors. *Thermal detectors* measure temperature based on the incident strength of radiation and report it as rise of temperature. They operate at room temperature and are wavelength independent. *Photon detectors* are comparatively very sensitive and quick in output, but the sensitivity is dependent on the wavelength. These need to be cooled as incident photon excites a semiconductor for an electric output. Noncontact type *tympanic thermometer* is a very handy instrument working on the principle of capturing infrared radiation reflected by the tympanic membrane in the ear. The probe is housed as a part of the handheld thermometer which is directed slightly in the external auditory canal. The measurement process is very helpful in infants, intensive care units, and in anesthetic patients, especially as it hardly requires a few seconds for obtaining the core body temperatures. It is not a continuous process for temperature measurement and is contradicted in patients with obstructions in ears such as a foreign body, moisture, pus formation, blood, or cerebrospinal fluids.

Contact-type temperature measurement clearly requires the probe to be in physical touch with the surface or medium for measurements. Clinical *glass mercury thermometer* is the most commonly used instrument for body temperature for decades because of its simplicity, reliability, cost, and ease of handling. However, it is not suitable for continuous monitoring which is pertinent in patients during anesthesia or in duress. Some pertinent solutions for core body temperature measurements use *indwelling probes* for rectal, bladder, or esophageal measurements.

Rectal temperature probes are inserted few centimeters into the anal sphincter. These are flexible probes with a thermistor on the tip for temperature measurement. Rectal temperature measurement is considered to be gold standard in infants or noncooperative patients below the age of 4 years. It may not be suitable in infants below 2−3 months of age to avoid rectal perforation. Rectal temperatures indicate peripheral blood flow status and hence are considered to be an important parameter. It is also sometimes avoided with patients under anesthesia as the rectal temperature takes some time to stabilize and lags behind the changes in core body temperature say if measured from esophagus. *Esophageal temperature* measurements are preferred to be done close to heart levels to avoid interference from

tracheal air by inserting flexible probes through the mouth or through the nose preferably for patients under anesthesia under postoperative care. It gives a very genuine assessment of core body temperature on a continuous basis. *Bladder temperature* measurement is an automatic choice in patients who necessarily need a urinary catheter owing to problems related to irregular urine flow, enlarged prostrate requiring intervention, etc. This technique relieves the need for an additional probe to be inserted either intravenously or orally as the patient is already under severe trauma.

2.2.1.6 Magnetic sensors

Magnetic sensors have the working principle based on the measurement of changes in magnetic moment of magnetic material when exposed to magnetic fields. The magnetic materials say ferromagnetic react to temperature change or magnetoelastic materials react to a mechanical stress, in the medium with which they interact. Biomedical applications involve measurements of the changes in the vicinity of the magnetic sensors. Human body fluids including blood, organic tissues, and cerebral fluids are very compatible with iron making ferromagnetic materials an ideal choice for these sensors. Other magnetic materials such as transition metals from d-block of the periodic table are corroded by the body fluids. Overall, the sensors are made of biocompatible metals, coated metals (coating of platinum, gold, silica, etc.), or ceramics such as silicones and Teflon. The applications of magnetic sensors are in blood flow sensors and MRI (magnetic resonance imaging) systems (Rivero et al., 2012).

Physical sensors find application not only for real-time health monitoring but are also widely used in areas such as medical Robotics, Wearable commercial products, and prosthetics. Designers are on a constant rigor to develop physical sensors that are more sensitive, flexible, precise, multifunctional, stable, and optimum in their measuring capabilities. Nanomaterials, superconductors, optical fibers along with the microfabrication technique are making this possible.

2.2.2 Chemical sensors

Chemical sensors are the next major class of sensing devices that deal with the detection and measurement of chemical activities and concentration of various analytes required for the efficient functioning of the human body. Some of the vital chemical components in blood having therapeutic and diagnostic significance include dissolved oxygen, pH value, CO_2 partial pressure, O_2 partial pressure glucose concentration, and $Ca+$ concentration.

2.2.2.1 Sensors for pH and blood gases

The respiratory health and metabolic balances are represented by partial pressure of oxygen (pO_2), partial pressure of carbon dioxide (pCO_2) in the blood, and the pH value. Fall in arterial pO_2 level even briefly can cause death due to damaged brain. A spike in the pO_2 concentration due to oxygen administration could lead to permanent damage to the eyes. Fluctuations in pCO_2 levels can lead to ruptured vessels in the brain. pCO_2 levels could be elevated in chronic obstructive pulmonary disease etc., while they could be suppressed in

case of renal failure, severe diarrhea and starvation, etc. pH on the other hand signifies the health of human metabolism. pH levels could be elevated due to hyperventilation, anxiety, pain, etc. and could be lower in case of excessive use of alcohol, renal failures, liver dysfunction, etc. Above statement indicates the critical nature of these elements and need for diagnosis of underlying disease processes.

Oxygen is available in blood either in combination with hemoglobin as HbO_2 (oxyhemoglobin) or as part of the plasma. CO_2 is present in blood as carbamino compounds, dissolved and combined with plasma proteins and hemoglobin.

pH, pO_2, and pCO_2 are obtained directly by electrochemistry principles, while O_2 content and saturation, total CO_2 are calculated parameters. Over a period of time, further many methods for estimation have come up including blood gas analyses, capnography, transcutaneous technique, and pulse oximetry. The measurements differ in accuracy, continuous assessment capabilities, ease of analysis, and possibilities to acquire supplementary information. The techniques however are complementary as each one of them has unique set of applications and indications.

The pH electrode works based on the principle of the observed electrical potential measured across a thin membrane separating two solutions having different pH values. *pO_2 measurement sensor* mechanism involves an Ag/Ag−Cl electrode anode and a cathode normally made of gold or platinum. Anode annularly encloses the cathode, and the assembly is dipped in an electrolyte potassium chloride solution. A diffusion membrane separates the electrochemical cell from the blood or sample liquid. The membrane is semipermeable and allows only oxygen to pass through and prevents blood cells, proteins, ions, or water to go through. It is normally made of very thin polythene, polytetrafluoroethylene (PTFE), or polypropylene. On polarizing the electrodes with a mercury cell, after the electrolyte and sample achieve equilibrium, the proportionate partial pressure of oxygen is measured as oxygen reduction current. The pO_2 sensor was originally known as the Clark amperometric sensor. Stow-Severinghaus potentiometric electrode is classically used for pCO_2 measurement. Here, a glass pH electrode with a calomel reference electrode is used which is covered by a semipermeable membrane that allows CO_2 to pass but prevents hydrogen and bicarbonate ions to go through. A standard diluted sodium bicarbonate solution works as an electrolyte. Molecules of CO_2 diffuse through the membrane causing change in the pH value of the bicarbonate solution. The pH value corresponding to the equilibrium state is reflected by the pH meter which is calibrated for pCO_2 value (https://acutecaretesting.org/en/articles/understanding-the-principles-behind-blood-gas-sensor-technology; Yap and Aw, 2011; Huttmann et al., 2014; https://www.thoracic.org/patients/patient-resources/resources/pulse-oximetry.pdf).

Arterial blood gas analysis (ABG), Venous blood gas analysis (VBG), and Capillary blood gas analysis (CBG) are the three very commonly used invasive blood gas analysis methods for patient management in ICU. Blood gases can be secured from either arteries (for ABG), veins (for VBG), or capillaries (for CBG). Noninvasive techniques available are not suitable for pH, HCO_3, and other analyses and are not suitable for complete analyses. ABG is considered a gold standard method where the blood is drawn from radial, femoral, brachial, or umbilical (for neonates) arteries for analysis. The procedure could be painful and requires

skill to prevent air bubbles penetration in the samples. Further the blood must be stored under controlled conditions and checked within 30 min after sample is withdrawn. VBG is performed where ABG or CBG is not suitable, arterial access is not possible, indwelling catheter and repeat draw of blood samples is to be avoided. Here the sample is drawn from the central line or even from the distal port of artery catheter. VBG is suggested especially when the body is in shock or sepsis. CBG is normally very useful in children and infants. The blood sample may be taken from the fingertips or heals of the infants after arterialization. It is possible to easily train health care workers and the technique is nearly painless requiring incision only up to 1 mm in the skin. Overall experienced physicians need to understand the correlation between the observations from ABG, VBG, and CBG and to suitably decide on the best method either invasive or noninvasive for blood gas analyses.

The major challenges in invasive electrochemical sensors arise from the fact that it is not only the electrodes but the entire electrochemical cell that needs to be catheterized in case of in vivo monitoring. The other approach is to mount the electrochemical cells in the cannula dome systems to facilitate ex vivo monitoring. Miniaturized silicon-based sensors based on micromachining and microelectronics can make the task slightly easier. Another option for blood gas analyses is *a fiber optic monitoring system*. Optical sensors are known to be stable over extended periods (days) and need not be calibrated time and again unlike the electrochemical analyzers.

An optical fiber blood gas analysis consists of an instrument connected to the disposable sensor through a fiber optic cable. Light signal travels from the instrument to the sensor via the optic fiber. Suitable chemical indicator dyes are positioned at the tips of optical fiber capable of capturing and transferring the light from the instrument proportional to the analyte being measured. The chemical indicator dye is usually separated by a semipermeable membrane separated from blood or fixed in a polymer. As in case of electrochemical gas analyses, when an equilibrium is reached between the analyte concentration in the sensor and blood, an optical measurement at this instant leads to a specific wavelength signal transmission from instrument to sensor through the fiber. The sensors either use the fluorescence or adsorption characteristic of the optical dyes. In fluorescent mechanism, the dye absorbs the incident light excitation wavelength, resulting in excitation of electrons to higher energy levels. The electrons on losing this energy emit fluorescence, which is subdued in the presence of oxygen, called oxygen "quenching." This phenomenon forms the underlying principle for "optodes" or fiber optic oxygen sensors defined by Stern—Volmer equation. In case of absorbent mechanism, specific wavelengths of incident light are absorbed by the dye. The returning light intensity reflects the analyte concentration as per Beer—Lambert's law. The output in both the cases based on the light emitted by sensors is a numeric output on patient side monitors.

The electrochemical sensors are used for various applications such as measurement of pH and partial oxygen level in inner eyelids, gastric fluid pH analysis, monitoring major ion concentrations such as ionic sodium, potassium, calcium, and magnesium. Specific ion-based sensors and electrolytes are used for the desired measurements.

Noninvasive methods also form an extremely important part of clinical monitoring. Techniques such as pulse oximetry are extensively used in outdoor patient monitoring and

even self-monitoring of oxygen saturation in pandemics like Sars-Cov-2. Other methods such as Noninvasive Carbon dioxide, gas exchange monitoring, Capnometry or Capnography based on near-infrared spectroscopy, and electrical impedance tomography are also in use. Some of these methods such as monitoring of oxygenation are vital part of pediatric respiratory models. The ease of monitoring O_2 saturation has limited the usage of techniques such as gas exchange monitoring. Capnometry is widely used in ICU settings when the patient is on ventilation or general anesthesia through mainstream devices or side stream analyzers. These techniques are not based on chemical-based sensing and just a brief reference has been provided in this section (Venkatesh and Hendry, 1996; Smallwood and Walsh, 2017).

2.2.3 Biosensors

Biosensors are chemical sensing units where biological recognition achieved through precise biochemical reactions is associated or integrated with a physiochemical transducer for quantitative measurements. Hence, the major components of a biosensor include the bioreceptor, transducer, and a microelectronic unit. The receptor has specific receptivity for the analyte under measurement because of the presence of selective and active biological components. Bioreceptors could be either an enzyme, RNA or DNA, tissue or cells, and antibodies, etc. They are macromolecules that facilitate analyte or biological samples to get attached to their surface triggering a biological signal for transducer. The biorecognition is the process that entails the joining of analytes to bioreceptors resulting in the emission of heat, light, pH, or change in charge or mass, etc. The sensing effect is measured by the transducer as an optical, electrical, or thermal output through microelectronic circuits and display systems. Biosensors could be classified based on the class of receptors and transducers. Bioreceptors are generally further defined into five main categories, namely, enzymatic, antigen/antibody, nucleic acid/DNA, cell/cellular structure, or biomimetic. However, the enzyme and antibody-based bioreceptors are mostly found in many biosensor applications.

2.2.3.1 Enzymatic biosensors

Blood glucose measurement is the maiden application of enzyme-based biosensors which led to the spurt in the development of similar class of sensors. Diabetes is one of the major health issues globally today and blood glucose sensors have foremost overall share commercially. Enzymes are good bioreceptors as they have selective binding capabilities and catalytic activity. The detection and biological recognition are further amplified in a catalytic reaction compared with other binding methodologies. Enzymes are natural proteins that catalyze the target substrate particle into a product in the reaction, while not getting consumed themselves. On the other hand, it is expensive and difficult to extract enzymes in required quantities. Enzymes could also denature rapidly as they are unstable.

Glucose oxidase (God) is an enzyme recovered from certain insects and fungi (i.e., *Aspergillus niger*). The glucose biosensor in simple terms works on the principle of oxidation of glucose by the God catalyzation to give end products such as hydrogen peroxide and gluconate. The hydrogen peroxide produced is measured using suitable methods.

Next-generation glucose biosensors have been developed subsequently to improve signal accuracy and reliability. The methods such as using God enzyme for measurement of glucose have been developed further to other oxidase enzymes such as cholesterol oxidase, peroxidase enzyme, and lactate oxidase. Similarly, urease is used to change urea to ammonia leading to changed pH which can be detected optically or potentiometrically.

Affinity biosensors or immunosensors utilize antibodies as a bioreceptor to recognize specific antigens. Antigens are large protein molecules on surface of pathogens such as bacteria, viruses, or foreign objects. which evoke an immune response in the human body by producing specific antibodies. Antibodies (immunoglobins or glycoproteins) again are large plasma proteins having a Y-shaped structure with couple of heavy and light chains each.

Specific antibodies can be harvested from animals such as mice, rabbits, or even sheep as a natural defense mechanism corresponding to any target antigen. Antibody binds with specific antigen and it is possible to detect the analyte in spite of interfering foreign substances. There are five well-known classes of antibodies as per the bulky chain structure, namely, IgG, IgA, IgM, IgD, and IgE. Antibodies are also distinguished based on the receptor sites. Monoclonal antibodies have one while polyclonal antibodies have many receptor sites. Monoclonal antibodies are highly specific, whereas polyclonal ones are extremely sensitive. Immunoassays are analytic chemistry sequencing techniques used for detection of targeted objects in immune reactions. High selectivity benefits were exploited to develop path-breaking radioimmunoassay and ELISA (enzyme-linked immunosorbent assay) which are widely used in environment and medical fields for detection and target quantifications such as hormones, proteins, steroids, and tumor markers.

2.2.3.2 Aptasensors or nucleic acid bioreceptors

Aptamers or aptasensors are a class of short RNA or DNA molecules or oligomers which could bind multiple targets such as proteins, peptides, drugs, and cells. The binding leads to confirmational changes such as folding and forming double-strand structure with a small molecule. The structural changes can be detected with ease making aptamers ideal candidates as sensors as compared to antibodies and enzymes. Aptamers do not require an animal host for synthesis and can be produced in vitro at a commercial level in a pure state as “chemical antibodies.” They are also target selective and highly specific.

The biosensor mechanism encompasses DNA/RNA hybridization, for example, in case of DNA sensors used for DNA molecules recognition, single-stranded DNA segment undergoes hybridization with another DNA strand segment to form double-strand hybrid structure. The hybridization occurs between the sample DNA (target) and the known DNA molecules (probe) with a specific base sequence. Applications for such devices include local clinical testing, forensic investigation, food safety, and environment monitoring.

2.2.3.3 Living biosensors or microbial sensors

Microbial sensors employ either living tissues or microorganisms as receptors for target base selective sensing. Typically, this class of sensors is chemical sensors incorporating immobilized microorganisms such as bacteria and fungi into transducers for target detection or

understanding the "state" of surroundings. Unlike enzymatic biosensors, no purification or isolation is required in microbial biosensors, saving both cost and time. These sensors are stable at suboptimal pH and comparatively less prone to inhibition. Microorganisms house numerous enzymes and even proteins which are capable of producing a specific and selective response to the analytes. However, the reaction time is more in some cases compared to the enzyme electrodes. Some microorganisms have many enzymes and hence the selection needs to be done carefully.

The working principle of microbial biosensors around signal generation is akin to enzyme biosensors. The analytes are converted by the intracellular enzymes, consuming the other substrates and the reaction products are capable of being electrochemically measured. The resultant oxygen level, ionic composition are some parameters that indicate the metabolic state of the immobilized cell and form the basis for electrochemical determinations. Microbial biosensors have been successfully used for human hormones, DNA, and pathogen detections. They are equally good in environmental monitoring and testing of food or clinical samples.

2.2.3.4 Optical transducers

Immune systems in living things produce a wide range of antibodies in response to a variety of antigens and different enzymes present in them. This leads to numerous varieties of receptor options in nature. The right transducers hence become the limiting factor which are capable of reading and converting the signals at receptor sites. Some transducers used in biosensors are discussed in brief here.

2.2.3.4.1 Electrochemical

These transducers are very common in point-of-care instruments, simply because of portability, ease of use, reasonable costs, and disposable attributes. Various detection methods are common to electrochemical transducers. *Amperometry* measures the reduction current or the electrochemical oxidation which directly refers to the concentration from the analyte. Another electrochemical method relies on *conductometry*, which refers to the electrolytic conductivity measurement in biological membranes and enzyme reactions. *Potentiometry* is another detection method which recognizes the potential difference between a reference and an indicate electrode at equilibrium. These are widely used for pH measurements and for detecting specific ions. Finally, *modified ISFETs* (ion-sensitive field-effect transistors) measure ion concentrations by means of assigning an ion-selective membrane to ISFET, which then works as a biosensor once coupled with bioaffinity or biocatalytic layer.

2.2.3.4.2 Optical transducers

In optical biosensors, optical recognition is achieved by manipulating the interface of the biorecognition element and optical field. The objective is to generate a signal in line with the concentration of the subject of interest in the analyte. Enzymes, antigens, antibodies, nucleic acids, tissues, and cells are used as biorecognition elements. Techniques such as Surface plasmon resonance, optical waveguide interferometry, and evanescent wave fluorescence are used to detect the optic signal generated by the interaction of analyte and biorecognition

element in optical transducers. These sensors are highly sensitive, specific, cost-effective, and small in size. Evanescent field (power diminishes significantly with distance) is a common principle in biosensor transduction system. Optical transducers are detailed in the referred research article for better recognition (Damborský et al., 2016).

2.2.3.4.3 Mass-based detection methods

Piezoelectric crystals like quartz are used as mass-sensitive sensors due to their property to produce an electrical signal response to the mechanical forces and high sensitivity. Piezoelectric crystals in these sensors are enabled to vibrate at a specific frequency corresponding to the electric signal. Now, the oscillation frequency of sensor crystals matches the frequency applied. A "biocapture" layer is introduced on top of the quartz crystal having a biomolecule (normally antibodies) with specific binding capabilities to the analyte. In the presence of the sample to be checked, the antibodies and the analyte bind leading to mass change. The corresponding oscillation frequency and the related electric signal are captured and results displayed. The piezoelectric sensor and transducer mechanisms are found to be extremely sensitive for the HIV (human immunodeficiency virus) detection (Vo-Dinh and Cullum, 2000; Karunakaran et al., 2015; Togawa et al., 2011; Harsányi, 2000; Altintas, 2018; Zhou et al., 2015; Webster and Eren, 2017).

2.2.4 Electropotential sensors

Critical organs in the human body such as the heart and brain produce electrical potential which mimics their functioning. Heart signals are called ECG; similarly, brain signals are known as EEG, muscle fiber contraction, and relaxation lead to electromyogram (EMG). Even our eyes produce two types of signals, eye movement leads to electrooculogram (EOG), whereas retinal movement results in electroretinogram. Healthy organs provide known and standard electric signals, while any pathological condition can be diagnosed by the variations in these signals. Heart stress leads to arrhythmias, neurologists' study epileptic seizures, and so on, the abnormalities can be a precursor or an effect of an undesirable event. The origin of biopotential and the mechanism of transfer to the cellular level give a crucial understanding about the type and point of measurement of such signals for seamless interpretation.

The difference in ionic concentrations on either side of the semipermeable cell membranes leads to the Nernst potential or the electrochemical gradient. Predominantly Na, K, and Cl ions have the highest concentrations and play a very important part in maintaining the resting membrane potential. The sodium and potassium concentration difference is created by the active membrane transport system that pushes potassium into the cell and sodium out of it. The resultant resting potential differences are a result of higher potassium ion concentration inside and lower ionic concentration of sodium, chloride, calcium, etc. on the outside.

There are some excitable cells in the human body that respond to an electric simulation by producing an action potential triggered by rapid ionic flux across cell membranes. The excited cells generate electric current around themselves, which is detected as potentials at suitable points. In the case of the heart, the cells of sinoatrial node release an excitation that

propagates across to the ventricles from atria through defined pathways. This electric excitation leads the heart muscle into synchronous contraction. ECG is the directly linked associated biopotential as the heart contracts. EEG is related to the neuron electric excitation. The electrically excited neurons send an action potential from the axon and dendrites. EEG signal arises from cortical mantle when a host of cortical neuron cells, subcortical systems with the associated spatial dispersions, and complex delays interact. EMG signals are related to muscle fiber simulation as neural excitation is spread to the neuromuscular junction via the nerve endings. Muscle fibers have motor units, wherein each muscle fiber excitation is associated with single motor unit potential. EMG signal is the manifestation of the motor potential of a group of muscle fibers or many single motor unit potentials on the muscle or body surface. EMG signals correspond to muscle contractions or expansions. EOG is the potential associated with eye moments. It relates to the potential difference between the cornea at the front and retina at the rear end of the eye at rest and varies with the movement of the eyes. The EOG signals are not attenuated as eyes are located in sockets outside the skull structure. The electrodes are placed either on any side of the eyes or at right angles, that is, below and above the eyes to measure EOG. Each of the biopotential measurement technique and measurement is a precursor to the physiological well-being of the associated organ and related function.

It is pertinent to understand the origin of biopotentials mainly because they are of small amplitudes, low-frequency ranges, and unstable nature. Such signals are prone to noise and interference both from the skin, pickup electrodes, and the external environment (power line interference, electromagnetic waves, radio frequencies, etc.). Special electrodes are designed for biopotential measurements. Some of them are enumerated in the next section.

Biopotential electrodes are an interface between the ionic potential generated in the human body and the measurement instruments, many of which utilize electronics as basis for processing and display systems. These could be classified as either skin surface electrodes, that is, noninvasive or invasive (microelectrodes, etc.) as per the application or clinical setting. These electrodes must ensure minimum distortion to avoid motion artifacts and justify the stability and accuracy expected for biopotential analysis. Again, this class of electrodes is in positive contact with the external or internal body fluids, and hence they are constructed with nontoxic materials or coated suitably. Other design parameters that affect the selection of material for biopotential electrodes are shelf life, cost, and mechanical characteristics while addressing the issue of skin interface impedance. Skin surface electrodes are sometimes based on silver, gold, or other nonnoble materials with suitable coatings. The internal or invasive electrodes are neutral to tissue electrolytes and could include materials such as stainless steel, gold or alloys of platinum, tungsten, and iridium.

It is also very important to understand the half-cell potential or the charge distribution at the interface of the electrode and the skin. Imagine when a metal (or an electrode) is immersed in an electrolyte solution (which is ionizable), a local electric potential or charge distribution occurs at the interface (of electrolyte and metal electrode) which is called half-cell potential.

In practical situations, during biopotential measurements, a set of electrodes of same metal are used, to negate the half-cell potential for electrodes. Assuming that the half-cell

potential of the metal electrodes would be the same, a differential amplifier in the circuit connecting the electrodes amplifies the biopotential (say ECG) and cancels the half-cell potentials. In actual conditions, some difference in the half-cell potential exists due to difference in physical contact points on the body or minute differences in the material of the electrodes, which causes a resultant potential difference and flow of current, visible as superimposition on the output biopotential signals.

2.2.4.1 ECG electrodes

Commonly used ECG electrode is the Ag/Ag−Cl electrode which is available both in disposable and reusable forms. A flexible form of the electrode is made out of a polymer coated by silver powder duly prepasted with Ag−Cl gel with adhesion capabilities to the skin with an electrolyte-laden foam. The electrolyte is sodium chloride or potassium chloride, which provides better electrical contact, prevents motion artifacts, and the electrode assembly as a whole is known to provide the lowest differential half-potential and stable junction potential. The gel is sometimes applied physically in the recess provided by the electrode curvature. The electrode is coupled to the peripheral instrumentation using a Snap-On connection. There are other types of electrodes including silver discs with electrolytic AgCl coating or sintered Ag and Ag−Cl electrodes. The polymer-based reusable electrodes are a cheaper option but fail to provide the sort of adhesion to the skin as provided by the disposable electrodes with the prepasting capability.

2.2.4.2 EMG electrodes

EMG is also measured both by invasive and noninvasive variety of electrodes. EMG signals are better recorded when electrodes are placed in the vicinity of the muscle group. EMG electrodes are smaller and need to be securely attached to the skin. A recess in the electrode body provides a way for electrolytic gel. The electrodes are attached on hair-free areas suitably cleaned with alcohol and secured with a strong adhesive bandage, etc. The noninvasive ones are small circular discs of around 1 cm diameter, either made of platinum, silver/silver chloride, gold plated, or even stainless steel. The invasive electrodes record percutaneously from the nerves or the muscle fibers. These are needle-shaped electrodes with a thin metallic wire encapsulated in a hypodermic needle or a canula. Another wire-type electrode for similar application has a thin wire insulated by a Teflon layer except at the distal tip. Both these electrodes could be either bipolar or have a set of wires acting as reference and recording electrodes to complete the electric circuits. The EMG signals are of comparatively higher amplitude than ECG and EEG and hence have a slightly lesser impact of motion artifacts and noise interference.

2.2.4.3 EEG electrodes

EEG signals are associated with extremely low amplitudes and high association of noise and interference from the environment and other physiological parameters and events such as muscle noise, eye blinks, or heartbeat signals. There is a challenge around oily skin and hair around the head which impedes proper signal transduction. The noninvasive electrodes are

often cup-shaped gold-plated, platinum, or tin electrodes due to high conductivity characteristics. The cups are filled with electrolytic gel and are securely attached to the scalp with an adhesive tape. Subdermal needles are used in clinical settings to overcome the challenges explained above for better electrical conduction. As the name suggests these are inserted under the skin for EEG recordings. Some of these are made of stainless steel or platinum needle-shaped electrodes. The tips of such electrodes are so defined to penetrate the cell wall but still avoid cell damage and hence are used in controlled clinical settings.

Microfabrication techniques have enabled production of such miniature biopotential electrodes even for multichannel recordings. These microelectrodes contain integrated circuitry and are effective in neurological applications where numerous neurons are simultaneously simulated in the central nervous system. Microfabrication leads to production of highly reproducible microsensors with highly similar properties.

2.3 Market research and latest developments in sensor technologies

Sensors are an integral part of literally all equipment, gadgets, mobility solutions, communication devices, medical devices, defense applications, athletics, electronics, computers, etc. and the list of applications is just unending. Sensors are among the fastest growing markets along with mobile phones and computers. As per BBC report, the global market for sensors will top $240.3 billion in the early 2020s up from $123.5 billion in 2016, a double-digit CAGR growth. Fingerprint sensors, process variable sensors, chemical sensors, positioning and proximity sensors in particular and automotive industry, in general, are leading the growth trends in sensor technologies. Smart sensors, as they are called today, have got miniaturized with integrated electronic circuits facilitating sensing and display circuitry in the same chip. A very common example is "lab on a chip," which relies on mainly molecular biology and microfluidics as core technologies. The analytical device miniaturizes and integrates laboratory steps involved in PCR and DNA sequencing to a small single chip, leading to cost savings in space, reagents, quick diagnosis, repeated and parallel deployment with increased sensitivity and expandability (Yılmaz and Yılmaz, 2018; https://blogs.rsc.org/lc/2017/07/25/how-can-biosensors-provide-real-time-health-monitoring/?doing_wp_cron = 1610203236.9375751018524169921875; https://scitechdaily.com/tag/biosensor/).

The advantages of the new generation of sensors in real terms are flexibility, higher accuracy, and the fact that they can be easily integrated into many other distributed systems. With the advancements in communication technologies and the easy availability of high-speed Internet for data transfer, intelligent sensors can interface and interpret with or through microcontrollers. The entire ecosystem of sensor has analog and digital elements facilitating processing of data to ADC with better reliability, accuracy while maintaining the sanctity of specific functionalities. This eases out troubleshooting, which is also possible remotely in many cases.

Some of the latest sensors available across applications include Internet of things (IoT) sensors, radio frequency identification (RFID) sensors, biometric sensors, pollution sensors, image sensors, MEMS and nanoelectromechanical systems (NEMS) sensors, printed sensors, etc.

2.3.1 IoT sensors

These sensors collect data and information from the site and relay over cloud for processing and analysis. The resultant action could be triggering an alert or an action, adjustment of sensor, hence supporting in data collection, operation, or automation. They have a large field of applications including medical sensors, temperature sensors, smoke sensors, chemical sensors, RF sensors, pressure sensors, and proximity sensors. IoT sensors find diverse applicability across industries and are having maximum projected revenue share in the entire sensor universe.

2.3.2 RFID sensors

RFID sensor tags are miniature-sized set of radio transponders, radio receiver, and a transmitter. An RFID reader in the near vicinity shoots an electromagnetic pulse which is returned by the RFID tag as digital identification data to the reader. These sensors find wide range of acceptability in inventory management, precious goods monitoring, access, and attendance monitoring, toll collection, counterfeit prevention, etc.

2.3.3 Wearable sensors

Wearable sensors are integrated into accessories such as wrist bands, smartphones, eyeglasses, clothes, and headphones. They have various applications such as medical sensors, optical sensors, Global positioning system (GPS), and inertial measurement unit (IMU. Wearable sensors have been coupled with miniaturization in electronic circuits and deployed digitally in monitoring the performance of athletes and health monitoring systems. Some of the latest applications include wearable ultrasound patch, Laser powered glucose meter, breast scanner, white blood cell counter, Neural-Enabled Prosthetic Hand to name a few. The advancements in the technology are catching acceleration as more advancements in noninvasive sensing technologies are being researched. IoT sensors and wearables hold maximum potential for market expansion with the increase in numbers driving down the costs, advent of microelectronics, lower power consumption alternatives, and advancements in wireless technologies (Heikenfeld et al., 2018; Collins, 2019).

2.3.4 Pollution sensors

These sensors are used to determine the particulate matter (PM2.5 and PM10 which refer to dust particle sizes of 2.5 μm and 10 μm, respectively), carbon monoxide, ozone, nitrous oxide, and sulfur dioxide. These sensors are either Electrochemical sensors (for measurement of NO_2, SO_2, O_3, NO, CO), Photo ionization detectors (for VOC or volatile organic compounds), Optical particulate counters (for measurement of PM), Metal oxide sensors

(for measurement of NO_2, O_3, CO), and Optical sensors (used to measure CO, CO_2). Efforts are being made to drive down the cost of these sensors as more and more awareness on harmful effects of pollution are getting validated (https://ec.europa.eu/environment/air/pdf/Brochure%20lower-cost%20sensors.pdf).

2.3.5 Optical image sensors

These sensors are mostly found in digital cameras and smartphones and are a family of CMOS (Complementary Metal Oxide Semiconductor) sensors. CMOS sensors are semiconductor-based image sensors that change light input into electrical output.

2.3.6 MEMS and NEMS sensors

MEMS and NEMS are signified by the small size and typical process associated with their manufacturing. MEMS devices are fabricated by bulk machining and surface micromachining. *Bulk micromachining* involves removal of material from substrate to achieve microfeatures largely through chemical etching of silicon in desired crystallographic geometries. The etching rate is controlled by masking and doping of silicon. Methods such as ion-beam micromachining and laser machining are also used. *Surface micromachining* is the process of building the material on the base substrate to attain three-dimensional structures. The deposition processes are electroplating or chemical vapor electroplating. Masking techniques to achieve photosensitive resists are extensively deployed in the manufacturing process for creating three-dimensional structures. Other techniques such as Lithography, Abforming, and Galvano forming are used in conjunction with the above techniques to achieve notable aspect ratios. Silicon deposition is a constraint and hence bulk micromachining is only used for working on silicon. After bulk micromachining and surface micromachining, the chips are to be protected from the atmosphere. Silicon nitride-based materials or photoresistive materials are used to cover the sensing area using Low-pressure chemical vapor deposition (LPCVD) or Chemical vapor deposition (CVD) process to provide moisture protection. Sometimes if the IC is sealed in a metal or plastic resin case some sensors are also protected thermally with nichrome coating.

2.3.6.1 MEMS

Their size varies between 1 μm and 100 μm. They have integrated microelectronics coupled with various complexities of electromechanical systems and moving parts. The entire assembly of microsensors, mechanical parts, and circuit for signal conditioning is fabricated on a silicon chip. MEMS sensors generally have four major parts in a single package including mechanical microstructures, microsensors, microelectronics, and microactuators. Some applications of MEMS are accelerometers, gyroscopes, pressure sensors, magnetic field sensors, fluxgate sensors, etc. *Accelerometers* measure force of acceleration and have three underlying sensor systems piezo-resistive, silicon capacitive, and thermal accelerators. Some of the applications include shifting between modes on mobile phones, gaming joysticks, user interface control, and as step counters in gaming joysticks. *Gyroscopes* are used for appreciating the angular

rates, for example, in steering wheel sensors for stability control and rollover protection features. *Pressure sensors* are integrated with resistors and a diaphragm on microships to understand pressure, pressure changes as variation in resistance. They are widely used in medical, automotive, defense, aerospace, and industrial applications. *Magnetic field sensors* detect and quantify magnetic fields which are vital in current and speed detection, position sensing, space exploration, etc. *Fluxgate sensors* are extensively utilized in space research, industrial automation, mineral exploration, geophysics, etc. to measure low-frequency AC or DC magnetic fields.

2.3.6.2 NEMS

NEMS are similar to MEMS but are still smaller or "Nano." While MEMS are based on silicon, NEMS are preferred on Carbon materials such as diamond, graphene, and carbon nanotubes. Applications of NEMS include sensors, actuators, cantilevers, accelerometers, gears, tweezers, and other nanodevices. NEMS devices are unique as they have low mass, high resonance frequencies, more electrical strength, high surface-to-volume ratios, and hence ideal for surface sensing mechanisms.

Some of the notable sensor manufacturers include Analog Devices Inc., Custom Sensors and Technologies Inc., Delphi Automotive PLC, Infineon Technologies AG, Omron Corporation, Qualcomm Technologies, Siemens Healthcare Diagnostics, STMicroelectronics, Vishay Intertechnology Inc., Wilcoxon Research Inc. (Source: https://globalnewswire.com).

2.3.7 Sensor materials

Sensor materials have both active and passive roles. Passive materials are used for either electric connections or providing mechanical structure to the assembly. The active materials on the other hand are vital to the sensing process itself and are used in microelectronics, piezoelectric, photosensitive, chemoresistive, and magnetoresistive films. The films are also produced by LPCVD, CVD or electrodeposition process. Silicon is available in nature as silicates and oxides, is inexpensive, and is widely used as semiconducting material in crystalline form. Polysilicon structures are layered with boron etc. by ion implantation to create polycrystalline layers which are conductive. The conductivity is controlled through selective doping and also give longer stability. Other semiconductor materials used in electronic components are Gallium-arsenide (GaAs) and Indium-antimonide (InSb). Gallium-arsenide exhibits electronic properties superior to silicon but for its higher cost at present usage levels. Some advantages over silicon include faster electron mobility, higher efficiency, single-junction bandgap, moisture and heat resistance, better flexibility, and sizing. GaAs transistors operate at higher frequencies above 250 GHz and are widely preferred in satellite communications, mobile phones, and radar systems. The basic elements such as infrared LED's, IC's, solar cells, temperature sensors in optical fibers, laser diodes are also using GaAs nowadays which has led to advancements in biological detection systems. Indium-antimonide has applications in magnetic resistors and Hall Effect sensors. These magnetoresistors are finding usage as position sensors in automotive sector and for infrared imaging and thermal imaging cameras.

Some other materials as plastics and polymers are used as insulators and find applications in chemical and radiation sensors. Precious metals such as silver, gold, platinum, palladium, and rhodium are used in automotive sensors and communication devices such as mobile phones and computers. Ceramics because of the property of giving structural strength, insulation, ability to bond with other substances, thermal stability, lightweight, and neutral behavior with oxygen make them suitable candidates as sensor substrates. Overall looking at the tremendous advantages of the new age sensors, novel materials, advancement in communications is creating an entire revolution in the field of electronics, which is holding a huge promise in consumer devices, robotics, automobiles, and medical technologies (Theo, 2020).

2.4 Data acquisition system hardware

The data acquisition process entails the acquisition of signals through sensing elements and processing the output into real-world machine or human-readable formats. The data acquisition or DAQ systems acquire physical phenomena/inputs in analog format (say electric signals), process or condition the acquired signals and convert them into digital format for display, transmission, and final usage. The main elements of a DAQ system include sensors, transducers, signal conditioning arrangement (by hardware and software), and display systems.

We have discussed about the wide range of sensors in the previous Sections 2.2 and 2.3. Sensor as an element detects the input energy and exhibits a variation, which is picked up by the transducer to convert the measurand into a feasible output. The output from the sensor and transducer system could involve a subtle voltage variation, resistance change or an output current. Hence, a transducer converts one kind of energy or one physical phenomenon to another. The signal at this stage is low on amplitude, has interference from power line, environmental factors, other physiological parameters, and errors related to pickup interface. The transduced signals so acquired need to be conditioned and then processed. The conditioning involves multiplexing, amplification, filtration, conversion, digitization, power management (impedance matching, range matching), and isolation to prepare the signal for processing stage using various hardware systems. The processing stage facilitates ADC of processed signal through microcontrollers and other systems which will be covered in subsequent sections.

Amplification is carried out to adjust the signal amplitude to use the maximum dynamic range of the ADC and to ensure minimum loss of information. The concept can be understood through an illustration. If a particular ADC has an input range say of $0-5$ V and an output of 8 bit, that is, $2^8 = 256$ steps, each output step accounts for $5/256 = 19.5$ mV. Assuming the sensor gives a wave of peak-to-peak 60 mV, the wave on digitization by the ADC will use $60/19.5 \sim 3$ of the 256 output steps available. However, if the sensor is amplified to produce 5 V peak-to-peak output, almost the entire input range of ADC would be used. However, excess amplification could lead to clipping and distortion of signal. Filtering

is another conditioning operation on analog signals which removes unwanted motion artifacts, noise, or inputs from other physiological parameters from the waveform of the signal. A 50/60 Hz notch filter may be needed to remove noise of AC power lines from a system having high gain. A high-pass filter can remove low-frequency drift from a reference signal. The subsection details the frontend of the DAQ system.

2.4.1 Front end of data acquisition system hardware

The output amplitude resulting from any physiological activity is generally very small and requires amplification prior to being displayed and processed. The relevant characteristics feature that a biopotential amplifier must address are the Gain, Frequency Response, Common-Mode Rejection Ratio, Noise and Drift, Recovery Time, Input Impedance, and Electrode Polarization (Prutchi and Norris, 2004). Characteristics of the biopotential Amplifiers used as the front end of DAQ system are listed below.

2.4.1.1 Gain

The detected sensor output amplitude being of the range of few microvolts to a few millivolts requires amplification of gain X1000, measured in decibels (dB). The relation is Gain (in dB) = 20 $\log_{10}$ (linear gain).

2.4.1.2 Frequency response

Frequency Response Curves are used to understand the behavior of an Amplifier or a Filter as shown in Fig. 2−2. It gives the quantitative analysis of the output spectrum of a system/device in response to an input. It gives measure of the Magnitude (Amplitude/Gain) and Phase response w.r.t frequency. The Magnitude Response curve presents the Output−Attenuation ratio (V_{OUT}/V_{IN}) versus Logarithmic Frequency (in general). Attenuation is commonly expressed in Decibels (dB). 1 dB = 10$\log_{10}$(Power Gain).

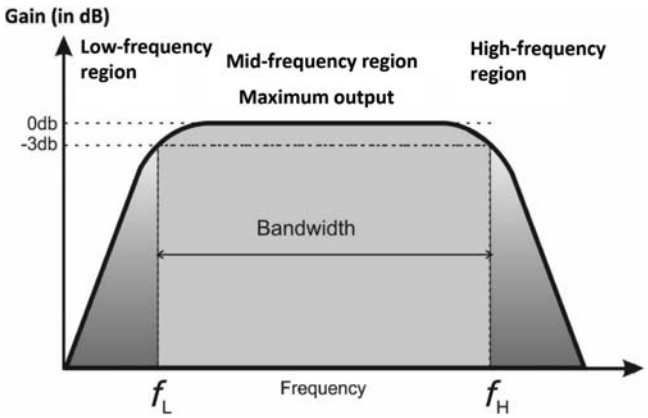

FIGURE 2–2 Frequency response curve of an amplifier/filter.

Bandwidth is defined as the frequency range permitted to pass through the filter with minimum attenuation which is mathematically equal to difference between upper and lower cutoff frequencies. The bandwidth of a band-pass filter is understood as the 3 dB bandwidth. 3 dB bandwidth is the frequency at which the power level of the signal decreases by 3 dB from its maximum value or falls to 0.707 of the gain in mid-frequency range. 3 dB decrease in power indicates that the signal power has become half of its maximum value. f_c is the cutoff frequency and f_L and f_H are the lower and upper corner frequencies, respectively. The bandwidth of an amplifier amplifies, without attenuation, all frequency components present in the bio-signal.

2.4.1.3 Common-mode rejection ratio

The human body acts as an antenna and picks up electromagnetic radiation such as 50/60 Hz power line hum and its harmonics, electronic circuits, and machines from the neighboring surroundings which adversely affect the detection of bio-signals. The common-mode rejection ratio (CMRR) of an amplifier is its capability to reject such common-mode signals interfering with the detection and is the ratio between the common-mode signal amplitude to the equivalent differential bio-signal amplitude given as CMRR (in dB) = 20 $\log_{10}$ (CMRR).

2.4.1.4 Noise and drift

Noise and drift are undesired contaminants that further interfere with the bio-signal detection process generated by the electronic circuit of the amplifier. Noise refers to the spectral components above 0.1 Hz frequencies measured in μVp-p or Volt Root Mean Square (μVRMS) and drift is the slow change that can be seen in the baseline at frequencies below 0.1 Hz measured in μVolts.

2.4.1.5 Recovery time

An amplifier may get saturated due to high amplitude input transient signals caused by electrode movement, currents, etc. The amplifier remains saturated for a finite duration known as the recovery time and then drifts back to the original baseline and operations.

2.4.1.6 Input impedance

The input impedance of an amplifier is required to be sufficiently high so that the bio-signal detected does not get attenuated significantly. The skin−electrode interface impedance has both resistive and reactive components which depend on factors such as fat, preparedness of skin, electrode surface area, and electrolyte temperature. The skin that lies between the potential source and the electrode can be simulated as a series impedance, for measurements.

2.4.1.7 Electrode polarization

Ion−electron exchange takes place between the electrode−electrolyte interface that generates the half-cell potential. The front end of an amplifier is required to deal with low amplitude bio-signals detected even in the presence of such DC potentials that can saturate the amplifier. International standards that regulate amplifier performance usually specify the electrode offsets

which for ECG measurements is 300 mV. However, situations arise where larger DC offsets can be seen like during neonatal ECG monitoring where stainless steel needle electrodes are used or when the silver plating of nondisposable electrodes wear off. Low polarization surface electrodes like Ag−AgCl electrodes are therefore recommended.

Many bio-signal amplifiers used as the frontend of a Data Acquisition System were designed using single-ended op-amp-based circuits earlier, but with the advent of economical integrated Instrumentation Amplifiers (IAs), their need has got virtually eliminated. Data Acquisition Front-end block diagram is depicted in Fig. 2−3 (Data Acquisition Handbook).

As depicted in Fig. 2−3A, the simplest DAQ system comprises a multiplexer (MUX), an IA, and the Analog-to-digital Converter (ADC). For a multiplexer to work properly, a low impedance source is desired as shown in the RC network of Fig. 2−3B. Parasitic capacitance "*C*" along with the series resistance "*R*" gets associated with the MUX and can adversely affect the accuracy of measurement. So, time constant of the RC network should be kept minimum to avoid this error. Input impedance "*Ri*" of the DAQ system and source impedance of the sensor "*Rs*" unit combine and form a voltage divider as shown in Fig. 2−3C which reduces the voltage perceived by the ADC unit *V*(ADC). The voltage read by ADC is given as

$$V(\text{ADC}) = \frac{Ri}{(Ri + Rs)} \cdot V(\text{Signal})$$

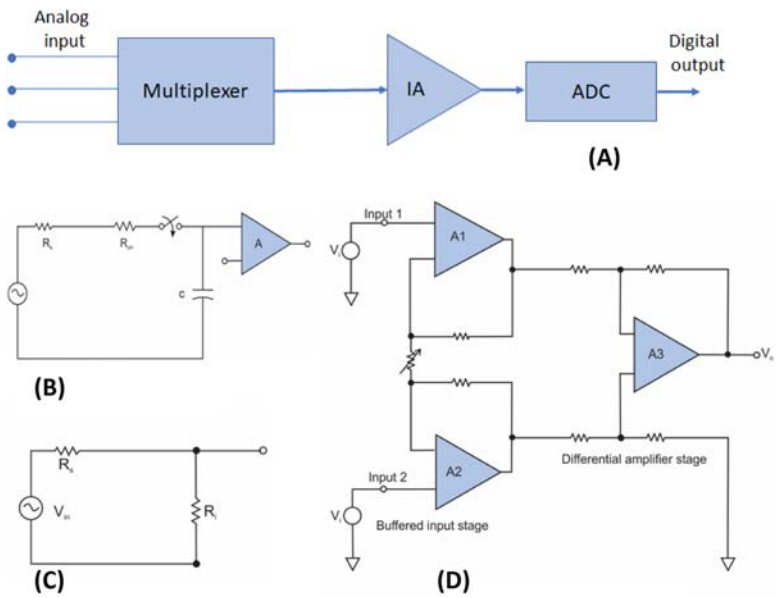

FIGURE 2–3 Depiction of Data Acquisition Front-end block. (A) DAQ front end; (B) RC time constant; (C) input and source impedance; (D) instrumentation amplifier. Source*: Data Acquisition Handbook, A Reference for DAQ and Analog and Digital Signal Conditioning, 2004−2012 by Measurement Computing Corporation.*

To have enhanced signal-to-noise ratio during measurement of signals in mV range, it is desired that *Rs* should be small enough to increase the voltage drop across *Ri*. In case of multiple channel DAQ systems, a Sample and Hold stage preceding the ADC unit is also recommended either as a subunit or as an external system. Resolution and speed of the ADC system is of prime concern in DAQ units.

Fig. 2—3D depicts the Op-Amp-Based IAs which buffers and amplifies the sensor output. IAs usually involve external resistors to set the gain of the system without affecting the high CMRR or the high input impedance requirement of the DAQ system. Input stage of the IA comprises two voltage followers having high input impedance and low output impedance to drive the ADC. The IA depicted in Fig. 2—3D offers very high impedance to the input voltages *V*1 and *V*2 and the resistor *Rm* helps in adjusting the gain. They also have precision feedback networks as part of the design and so are able to reliably detect the bio-signal even in a noisy environment.

2.4.2 Filtering subsystem

The most common filters used in designing DAQ units are the Butterworth Filter, Chebyshev Filter, and the Bessel Filter, each possessing some unique features suitable for specific applications and can be designed for low-pass, high-pass, band-pass, or band-stop frequencies. Frequency response curve of a low-pass filter is depicted in Fig. 2—4. An ideal filter possesses the following specifications:

- Passband gain should be maximum and should be flat.
- Stopband attenuation should be minimum.
- Passband to stop band roll-off (the transition band) should be steep.
- Transition width should be minimum.
- Ideally, the passband must be flat but has ripples in practical as depicted in Fig. 2—4.
- Ideal Brick wall response of Low Pass Filter (LPF) is shown in orange line in Fig. 2—4.

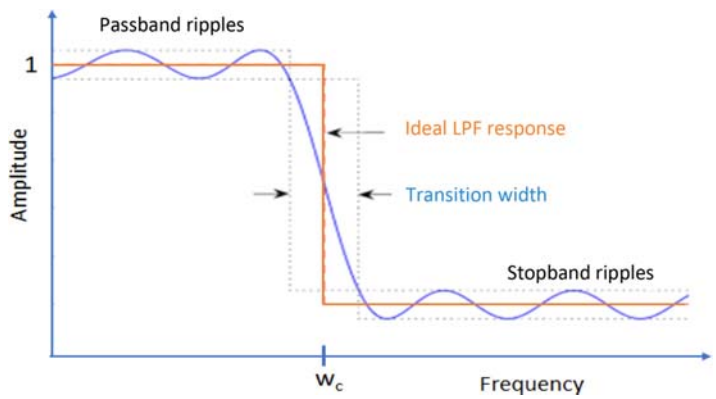

FIGURE 2–4 Low-pass filter frequency response curve.

- Band during which the filter response changes from the passband to the stopband as in Fig. 2−4 defines the transition width.
- Ideally, the stopband must be flat but has ripples in practical as in Fig. 2−4.

Therefore various mathematical approximation functions are used to design best suited transfer functions for linear analog filters. The most commonly used function is the low-pass *Butterworth Filter* design.

The filter circuits and the response curves for low-pass filters are detailed in Fig. 2−5:
The Butterworth filter has the following characteristics
The Butterworth low-pass filter has the following magnitude response

$$|H(j\Omega)| = \frac{A}{\sqrt{1 + (\Omega/\Omega_c)^{2N}}}$$

where $A =$ is the Filter Gain, $\Omega_c = 3$ dB cutoff frequency, and $N =$ Order of the Filter.

- Butterworth Filter has maximally flat passband and stopband (with no ripples).
- The higher the filter order, the more is the number of cascaded stages, and the closer it comes to the ideal "brick wall" response.
- The Transition width is very wide.
- Exhibits poor phase characteristics.
- Butterworth filter's ideal frequency response is not practical to achieve as it leads to unnecessary passband ripple.

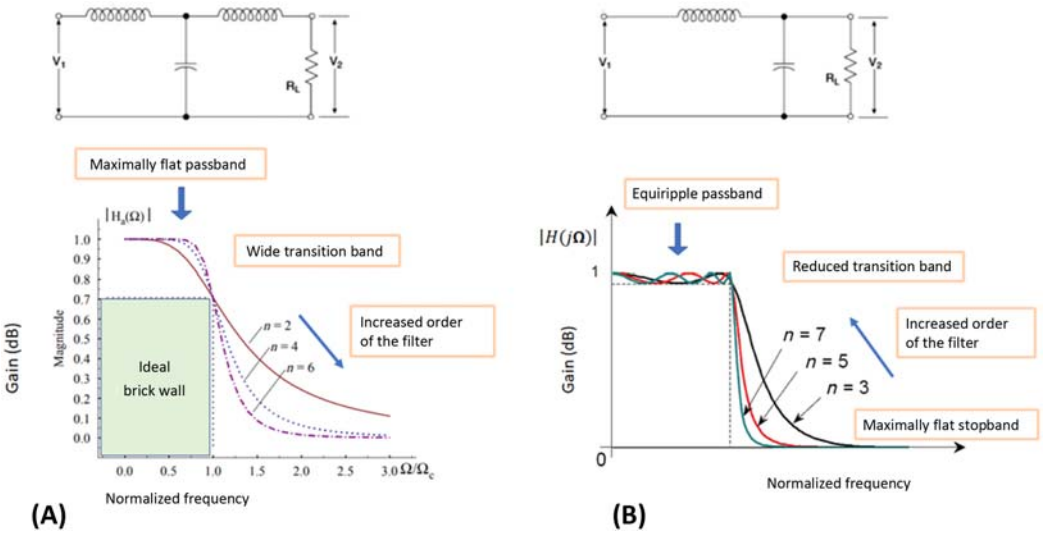

FIGURE 2–5 Low-pass filter circuits and frequency response curves of (A) Butterworth Filter and (B) Chebyshev Filter.

The Chebyshev low-pass filter has the following magnitude response

$$|H(j\Omega)| = \frac{A}{\sqrt{1 + \varepsilon^2 C_N^2(\Omega/\Omega_c)}}$$

where A = Filter Gain, $\boldsymbol{\Omega}_c$ = 3 dB cutoff frequency, N = Order of the Filter, $\varepsilon = a$ constant.

- Chebyshev Filter has Equiripple passband.
- The higher the filter order, the more it resembles the ideal response.
- The Transition width is narrow compared to Butterworth filter.
- The stopband is maximally flat.
- The phase response is more nonlinear than Butterworth filter for a particular order "*N*".

The Bessel Filter exhibits the best flat response and linear phase response but requires higher order to compensate for slow attenuation rate beyond the cutoff frequency range. Hence, a compromise is made between the filter design to be chosen depending on specific needs.

Voltage Dividers, Isolation circuits, protection subsystems etc. are further required for attenuation, isolation and protection of the DAQ units, respectively. The front-end unit interfaces with the Computer for further processing and analysis.

2.4.3 Interface units

A communication bus is an interface system, in an electronic device like computer system, to send data, power, and control signals to various components within it. The various hardware components of the computer are connected by the computer buses. For simple understanding, a bus transmits data as an interface among CPU to system memory via motherboard. The bus has multiple signal lines or wires with addresses describing the final location or retrieval site of the data. More number of wires suggest higher information or data carrying capability.

Computers could have parallel, serial, or USB connections, wired together in different topologies such as multidrop or daisy chain. They could further also be denoted as local or internal bus and expansion or external. *Internal bus* aids communication amongst internal components say between memory and video card, whereas an *external bus* facilitates communication with external components through USB, SCSI device, etc. Parallel bus transmits multiple bits at a time while serial bus transfers one bit at a time. The bus speeds are measured in bits per second or megabytes per second (MHz).

The most popular computer buses used today are the eSATA and SATA—Computer hard drives and disc drives; PCIe—Computer expansion cards and video cards; and Thunderbolt—Peripherals connected through a USB-C cable.

FireWire and USB buses are used to connect devices and transfer data to computers quickly. USB was developed to evade usage of expansion cards in PCI bus and is very commonly available in computers, cameras and other devices. FireWire, also known as High-Performance Serial Bus, handles higher data than USB but is comparatively costlier.

USB 2.0 can manage 480 Mbps data transfer rate, whereas FireWire—800 takes up to 800 Mbps. On the other hand, USB 2.0 can handle 127 devices versus 63 device capacity of FireWire 800. Both need drivers to be preinstalled for communication which then facilitate plug-and-play communication. Next-generation USB 3.0 has transfer rate up to 4.8 Gbps. FireWire connection does not need a computer and can be made directly between devices (peer-to-peer) while USB connection is host based, that is, the devices are to be connected through a computer.

2.5 Data acquisition system software

Novel methods of monitoring and analyzing human physiological parameters are based on Computer-based data acquisition systems (Emilio, 2013, MATLAB, LabVIEW). LabVIEW developed by National Instruments provides one such data acquisition and software design platform having a front panel imitating an instrument and a block diagram panel for programming that permits flexible acquisition, processing, and analysis of signals picked up from the environment. A distinct feature of LabVIEW is the huge in-built library of subroutine functions it offers and its extremely modular graphical software coding language, which is self-documented, flexible, reusable, thus enabling modification and reduced development time. LabVIEW offers "Biomedical Toolkit" with ready to implement apps, tools for customizing applications, and algorithms for physiological signal acquisition and processing and possess the following features:

- Available is a multichannel data logger for real-time acquisition, monitoring, recording, visualization, validation and analysis of bio-signals;
- Easy import, export, and conversion of physiological data formats including Biopac, MAT, and EDF;
- Permits ECG signal feature extraction, RR-interval analysis, HRV parameterization, etc.;
- Comprises Virtual Instruments library for EEG, EMG, ECG processing and analysis;
- Permits seamless integration with proprietary hardware including NI ELVIS and other NI DAQ units;
- Comprises online noise reduction set up and algorithm;
- To run the start-up kit, required is to install the LabVIEW software 8.6 run-time and NI-DAQmx 8.8.

MATLAB and Simulink along with its Data Acquisition Toolbox also provides a platform to construct and configure an interactive data acquisition system from multiple channels using standard DAQ hardware including USB, PCI, NI devices and other vendors to collect, visualize and analyze data. The Signal Analyzer app available helps in applying filtering and signal processing procedures to process the acquired signal. MATLAB codes can then be developed for automating the data acquisition process. The data detected can also be saved for postprocessing and analysis. The toolbox has several in-built functions and apps and

dynamic link libraries that allow interfacing with a particular hardware. The prime features include

- A structure for detecting real-time data into the MATLAB/Simulink workspace using PC compatible DAQ hardware;
- Provision for analog-input, analog-output, and digital Input/output subsystems;
- Support for standard hardware vendors and devices such as National Instruments boards, Microsoft Windows sound cards, Digilent Analog hardware, Analog Devices boards, and Event triggered acquisitions.

It is also possible now to have TABLET-based data acquisition systems for monitoring purposes as it offers a development environment for DAQ applications. The prime considerations are the hardware connectivity as there are very few options such as Wi-Fi and Bluetooth, the programming language that it can support, which is Android made using Java, and the driver availability.

2.6 Data acquisition systems market

The Data Acquisition Market predictive research analysis portrays that the market value had become 1.96 billion in 2019, and it is anticipated to touch 2.73 billion by 2025. The major players presently dealing with data acquisition systems are as follows:

- National Instruments: Product Range—LabVIEW software, Compact DAQ, Compact Rio.
- Keysight Technologies (Earlier Agilent Technologies): Product Range—DAQ970A, 34970A, 34972A, etc.
- Tektronix: Product Range—DAQ6510, 3700A, etc.
- Siemens: Product Range—SCADAS, Virtual Lab, TecWare software.
- Yokogawa: Product Range—DL series, SMART series, Xviewer software.

The market these DAQ units cater to range from Aerospace, Automotive, Engineering, Medical, Industrial to Power and Energy.

References

Altintas, Z. (Ed.), 2018. Biosensors and Nanotechnology, Applications in Health Care Diagnostics. Wiley. ISBN: 978-1-119-06501-2 February.

Avnet: Pressure Sensors: The design engineer's guide. < https://www.avnet.com/wps/portal/abacus/solutions/technologies/sensors/pressure-sensors/ >.

Breitkopf, D., 2009. Via Scopus – Elsevier. Imaging the uterus and uterine cavity, hysteroscopy: office evaluation and management of the uterine cavity, EID: 2-s2.0-84882551408.

Calero, D., Paul, S., Gesing, A., Alves, F., Cordioli, J.A., 2018. A technical review and evaluation of implantable sensors for hearing devices. BioMed Eng OnLine 17, 23.

Chen, Y., Wang, L., Ko, W., 1990. A piezopolymer finger pulse and breathing wave sensor. Sensors and Actuators 21–23, 879–882.

Collins, F., 2019. Giving Thanks for Biomedical Research; Posted on November 26th, 2019. < https://directorsblog.nih.gov/tag/wearable-biosensors/, https://www.electronicsforu.com/technology-trends/tech-focus/latest-sensors-applications > .

Cooper, J.K., 1986. Electrocardiography 100 years ago. Origins, pioneers, and contributors. N Engl J Med 315 (7), 461–464.

Creager, M.A., Beckman, J.A., Loscalzo, J. (Eds.), 2013. Vascular Medicine: A Companion to 'Braunwald's Heart Disease (second edition), ISBN 978-1-4377-2930-6.

Cysewska-Sobusiak, A.R., 2019. Examples of acquisition and application of biooptical signals. Phot. Lett. Pol. 11 (2), 25–28.

Damborský, P., Švitel, J., Katrlík, J., 2016. Optical biosensors. Essays Biochem. 60 (1), 91–100.

Data Acquisition Handbook, A reference for DAQ and analog & digital signal conditioning, 2004-2012 by measurement computing corporation.

Emilio, M.D.P., 2013. Data acquisition systems: from fundamentals to applied design. Available from: https://doi.org/10.1007/978-1-4614-4214-15 , © Springer Science + Business Media New York; https://in.mathworks.com/products/matlab.html, https://www.ni.com/en-in/shop/labview.html.

Enderle, J.D., Bronzino, J.D., 2012. Introduction to Biomedical Engineering, third ed. Academic Press. ISBN 978-0-12-374979-6.

Eren, H., Webster, J.G. (Eds.), 2017. Telehealth and Mobile Health. first ed. CRC Press. ISBN 9781138893498.

Gaddam, D., 2015. A survey on Nadi Pareeksha for early detection of several diseases & computational models using Nadi patterns. Int. J. Comput. Sci. Inf. Technol. 4, 3424–3425.

Glenn, S., 2020. Gamma ray. Encyclopedia Britannica, 15 May.

Goldberg, I., 2003. Relationship between intraocular pressure and preservation of visual field in glaucoma. Surv Ophthalmol 48 (Suppl 1), S3–S7.

Harsányi, G., 2000. Sensors in Biomedical Applications, Fundamentals, Technology and Applications, first ed. CRC Press.

Heikenfeld, J., Jajack, A., Rogers, J., Gutruf, P., Tian, L., Pan, T., et al., 2018. Wearable sensors: modalities, challenges, and prospects. Lab on a Chip 18 (2), 217–248.

Huttmann, S.E., Windisch, W., Storre, J.H., 2014. Techniques for the measurement and monitoring of carbon dioxide in the blood. Ann Am Thorac Soc 11 (4), 645–652.

Kajsa, L., 2008. A brief look at traditional Chinese medicine (TCM). Chapter 2, 10.1016/B978-044306899-7.50003-1.

Karunakaran, C., Bhargava, K., Benjamin, R., 2015. Biosensors and Bioelectronics, first ed. Elsevier. ISBN: 9780128031001, July.

Krishnan, S., 2016. The future of biomedical signal analysis technology. Circuit Cellar 315, 80.

Prutchi, D., Norris, M., 2004. Design and development of medical electronic instrumentation. In: A Practical Perspective of the Design, Construction, and Test of Medical Devices, John Wiley & Sons, October Print ISBN:9780471676232.

Radiology Cafe/ Exams/ FRCR physics notes/ X-ray imaging/Production of X-rays.

Rivero, G., Multigner, M., Spottorno, J., 2012. Magnetic sensors for biomedical applications, magnetic sensors - principles and applications. Kevin Kuang, IntechOpen. Available from: https://doi.org/10.5772/37285.

Schmidt, A., 2015. Biosignals in human-computer interaction. Interactions 23, 1.

Selvan, T.T., Begum, M.S., 2011. Nadi Aridhal: a pulse based automated diagnostic system. In: Proceedings of the 2011 3rd International Conference on Electronics Computer Technology, Kanyakumari, pp. 305–308.

Semmlow, J., 2012. The Big Picture: Bioengineering Signals and Systems, pp. 3–3.

Semmlow, J., 2018. The Big Picture, Circuits, Signals and Systems for Bioengineers (third ed.).

Smallwood, C.D., Walsh, B.K., 2017. Noninvasive monitoring of oxygen and ventilation. Respir Care 62 (6), 751−764.

Stevens, S., Gilbert, C., Astbury, N., 2012. How to measure intraocular pressure: applanation tonometry. Commun. Eye Health 25 (79−80), 60.

Thakor, N.V., 2015. Biopotentials and Electrophysiology Measurements, first ed. CRC Press, eBook ISBN9780429172601.

Theo S., 2020. The Latest In Sensors and Applications; November 6, 2020.

Togawa, T., Tamura, T., Åkeöberg, P., 2011. Published April 5 Biomedical Sensors and Instruments., second ed. CRC Press. ISBN 9781420090789.

Venkatesh, B., Hendry, S.P., 1996. Continuous intra-arterial blood gas monitoring. Intens. Care Med 22, 818−828.

Vo-Dinh, T., Cullum, B., 2000. Biosensors and biochips: advances in biological and medical diagnostics. Fresenius J Anal Chem 366, 540−551.

Webster, J.G., Eren, H., 2017. Jan Measurement, Instrumentation, and Sensors Handbook, Electromagnetic, Optical, Radiation, Chemical and Biomedical Measurement, second ed. CRC Press.

Yap, C.Y., Aw, T.C., 2011. Arterial blood gases. Proc. Singap. Healthc. 20 (3), 227−235.

Yılmaz, B., Yılmaz, F., 2018. Chapter 8 - Lab-on-a-Chip technology and its applications. In: Barh, D., Azevedo, V. (Eds.), Omics Technologies and Bio-Engineering. Academic Press, pp. 145−153. ISBN 9780128046593.

Yoon, J.-Y., 2016. Introduction to biosensors. From Electric Circuits to Immunosensors, Springer, ISBN 978-3-319-27413-3.

Yoon, Y.Z., Lee, M.H., Soh, K.S., 2000. Pulse type classification by varying contact pressure. IEEE Eng Med Biol Mag 19 (6), 106−110.

Zhou, G., Wang, Y., Cui, L., 2015. Biomedical sensor, device and measurement systems. Comput. Sci.

This page intentionally left blank

3

Detection and processing of real-time carotid pulse waves

3.1 Introduction

Carotid Pulse waveform is being widely analyzed by researchers and medical faculty for its shape and several attributes, as it can be related to many other physiological parameters, primarily related to the cardiac functioning of a person. The schematic depiction of a Carotid Pulse waveform is shown in Fig. 3−1. It can be observed that the common Carotid Arteries come off in pairs from the aorta and passing through the neck, it provides oxygenated blood to the head and the brain regions. It is further divided as the left and right internal and external Carotid Artery. Anatomically they are located on the left and right side of the neck. The carotid pulse is the pressure signal caused by the carotid artery which can be detected over the neck region. With every heartbeat a varying pulse signal is generated which indicates the changes in arterial blood pressure and volume. The Carotid Pulse closely resembles the signal produced at the base of the aorta due to its proximity to the heart and has a bandwidth of 0−100 Hz. The Carotid Pulse rapidly rises and reaches a peak known as the percussion wave (P), when blood ejects leading from the left ventricle, all the way up to the aorta. A secondary wave called the tidal wave (T) is generated when the reflected pulse gradually takes a return from the upper body. When the aortic valve closes, it results in a notch, termed as Dicrotic Notch. A dicrotic wave can be seen, due to the reflected pulse from the lower body. Fig. 3−1 also depicts the relation of Carotid Pulse waveform with the electrocardiogram (ECG) representing Early Systolic Peak and Late Systolic Peak that signifies the physiological implication of the Carotid Artery pulsation. The QRS complex of ECG waveform also can be related to the Dicrotic Notch of Carotid Artery pulsation. The Carotid Pulse can be effortlessly picked up using a suitable transducer placed on the neck. Patients who are in shock can be helped by the doctor by simply detecting their pulse being picked from the carotid artery pulsation (Rangayyan, 2015).

The Carotid Artery pulsation is generally inspected with the person under observation lying in the supine position, that is, with the body and chin slightly elevated, and the examiner preferably on the right side to ease palpation. While palpating the Carotid pulse, appropriate pressure is applied using the finger to realize maximum pulsation. The study of the Carotid Pulse helps in assessing heart status. The nonappearance of carotid pulsations is observed as a reduced carotid pulse amplitude. Palpation of the carotid artery usually leads to a fast-outward movement following the initial heartbeat and the pulse subsequently peaks through the systole for about one-third of the region and remains there momentarily, followed by a less rapid downstroke.

Real-Time Data Acquisition in Human Physiology. DOI: https://doi.org/10.1016/B978-0-12-822118-1.00004-7
© 2021 Elsevier Inc. All rights reserved.

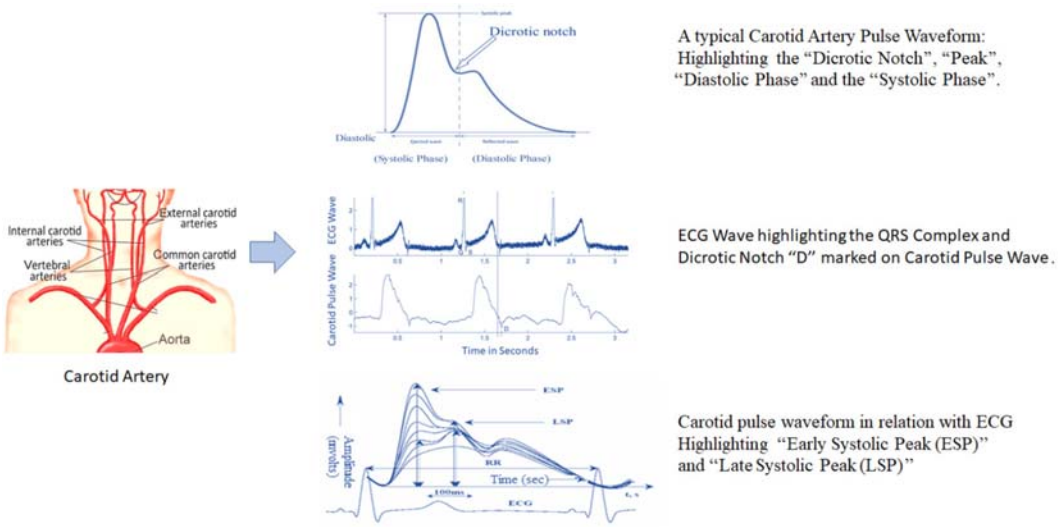

FIGURE 3–1 Schematic representation of Carotid Artery Pulse Waveform.

Anomalies in the carotid pulse could comprise of a variation in amplitude of the detected pulse peak and abnormality in upstroke or downstroke, or any other combination of such deviations. Disparities in this pattern during the upstroke or downstroke may assist in diagnosis. For example, abnormalities in carotid pulsation could be due to a premature contraction (Morris, 1990).

The deposition of plaque, owing to calcium, cholesterol, or cellular wastes, etc., on the internal side of the carotid artery, leads to constrictions. Blockage of this kind results in grave carotid artery ailments like Stenosis, leading to interrupted or less amount of oxygenated blood supply to the brain. It may also risk the patient of a stroke, which can cause everlasting disability like brain damage or even death. The factors that aggravate Carotid Artery disease are high BP, tobacco consumption, age, obesity, lethargic lifestyle, sleep apnea, etc. The initial sign of a Carotid Artery Disease is the Transient Ischemic Attack (TIA) which is due to a momentary lack of blood flow to the brain. TIA symptoms include abrupt numbness in one side of the limbs or the facial region, giddiness, distress in speaking and visibility, etc. Treatment suggested by physicians in case of mild blockage includes a change in lifestyle and medicines. However, in patients with a severe blockage, Carotid Endarterectomy is recommended where an incision is made in the front neck region for plaque removal. Carotid Angioplasty and Stenting is done to broaden the narrow passage when the blockage cannot be tackled directly (Mayo Foundation for Medical Education and Research). Evaluation and assessment of blood flow through the Carotid arteries have thus become an area of research where these pulsations are required to be critically analyzed.

3.1.1 Clinical significance of carotid pulse waveform

The carotid artery is a peripheral artery and due to its proximity to the heart, its pulse contour becomes vital to study and understand. It is also required to assess if the waveform is

present or missing, is hypokinetic (of low amplitude and volume), or hyperkinetic (exhibits brisk upstroke, high amplitude and rapid collapse). A pulse of low amplitude (hypokinetic), means low cardiac output due to shock or myocardial infarction. It could also indicate Idiopathic dilated cardiomyopathy or valvular stenosis, etc. In the case of aortic stenosis, a feeble delayed Carotid Pulse upstroke can be seen which is called pulsus parvus et tardus.

A hyperkinetic pulse is strong and has accentuated amplitude in nature and is primarily the effect of anxiety, exercise, fever, hyperthyroidism, anemia, etc. It is caused due to large left ventricular stroke volume and is indicative of normal cardiac functioning. The carotid pulse waveform of a patient with severe aortic regurgitation shows a double systolic peak pulse per cardiac cycle called a bisferiens (beating twice) pulse. Fig. 3−2 depicts the clinical significance of Carotid Artery Pulse Waveform (Chatterjee, 1997; Hajar, 2018; Walker et al., 1990). The peak of the Carotid pulse is closer to S1 (first heart sound) in general. But due to aortic stenosis, the peak gets delayed and comes closer to S2 (second heart sound). With enhanced severity of aortic stenosis, the peak further gets delayed and gets closer to S2, and its amplitude also gets reduced drastically. The abbreviation A2 represents the aortic element of the second heart sound and P2 is the pulmonary element of the second heart sound.

Other abnormal Carotid Pulse Waveforms include pulsus alternans and pulsus paradoxus. Pulsus alternans is exhibited as irregular strong and weak beats caused due to severe left ventricular failure. Pulsus paradoxus is the effect of unusually reduced left ventricular stroke volume, fall in systolic blood pressure, and decrease of pulse wave amplitude throughout

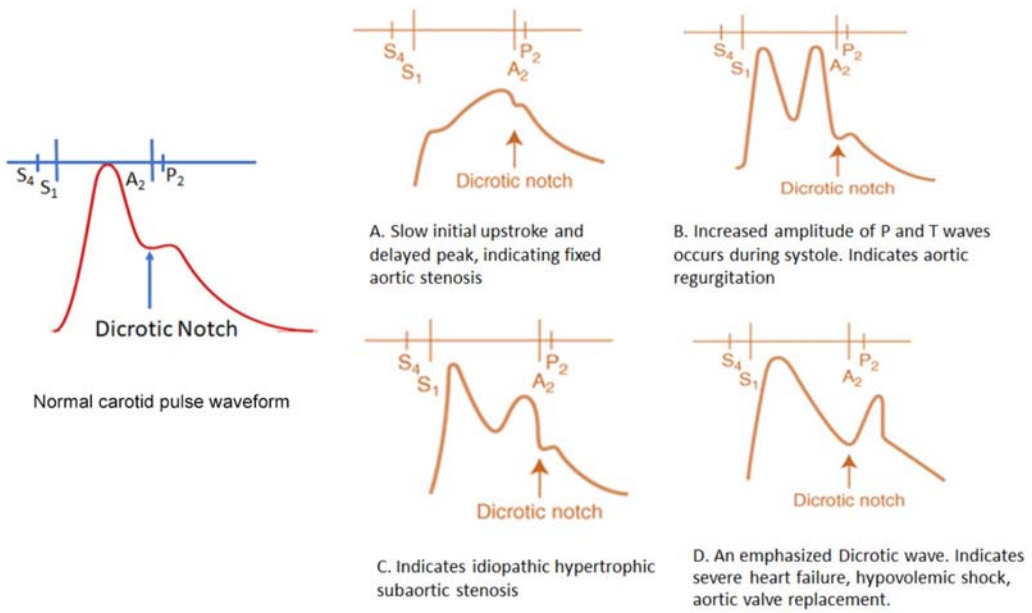

FIGURE 3–2 Clinical significance of Carotid Pulse Wave pictorially represented. *From Chatterjee, K. 1997. Bedside evaluation of the heart: the physical examination. In: Parmley, W., Chatterjee, K. (Eds.), Cardiology. JB Lippincott Co, Philadelphia, 1:13.*

inspiration. Normally systolic blood pressure falls by <10 mmHg in the inspiratory phase, but when it falls by >10 mmHg, the waveform is termed as pulsus paradoxus. It is normally an indication of acute asthma or pulmonary disease caused by chronic obstructions.

3.1.2 Investigation of carotid pulse measurement

The gold standard for acquisition and monitoring of pulse waveform is the Arterial Catheter method. However, it is an invasive procedure so the focus got shifted to a noninvasive way of detecting the Carotid Artery pulsation. Fluid volume displacement technology was one of the noninvasive method using strain gauge transducer to measure carotid artery pulse waveform. To amplify the acquired signal, a Sanborn preamplifier was used along with the sensor system. This arrangement effectively records age-related variations in the pulsation. This being a comparatively big in size arrangement, tend to pick up adjacent artifacts due to venous pulsations (Freis and Kyle, 1968).

The widely used noninvasive technologies to detect arterial pulses are the photoplethysmography, the ultrasound, and the arterial tonometry methods. The plethysmography technique is a very user-friendly method involving infrared signals to detect the blood flow volumetric pulsations, but can only pick up signals from the body extremities. The ultrasound method considered as the most accurate technique is capable of direct measurement of central artery pulsations. However, an expert hand is required for setting up the procedure. Piezoresistive pressure elements are placed over the arterial site in the applanation tonometry technique to detect the pulse. The state-of-the-art device available is the SphygmoCor, which utilizes this concept. To establish a relation between the Augmentation Index and the Pulse Wave Velocity, a ceramic-coated transducer has been used in another setup along with a SphygmoCor system to measure the carotid pulse for arterial stiffness. SphygmoCor is a clinically preferred technology used for the analysis of central arterial pressure waveform (Yasmin, 1999).

During the late 1990s, the US Preventive Services Task Force screened subjects for Carotid Artery Stenosis (CAS), but could not present evidential proof that Carotid Ultrasonography was sufficient to test asymptomatic patients for CAS. So, a team of researchers examined the pros and cons of screening asymptomatic persons having CAS with duplex ultrasonography and proposed Carotid Endarterectomy for treatment (Wolff et al., 2007). Piezoelectric sensor-based pulse detection system along with amplifiers, filters, software for artifact removal, and Data Acquisition (DAQ) units sets a very quick and easy arrangement for measurement of peripheral arterial pulse wave velocity (McLaughlin et al., 2003). In another experimentation, arterial pulse was again picked up using piezoelectric sensors. Digitization was then performed using a Digital Storage Oscilloscope interfaced with a computer followed by the Savitzky Golay filters (Winchester et al., 2007). There are emergencies of cardiac arrests where the rescue team has to manually check the carotid pulsation of the patient to assess their revival progress. A Doppler-ultrasound-based automated approach designed using Piezoelectric sensors has been taken for in vivo measurements and to monitor resuscitation progress during the cardiac arrest by a team of researchers (Yu et al., 2008). Electromechanical film sensors also allow measurement of Carotid pulsations (Alametsä et al., 2008).

Region-based methods implemented on images scanned through ultrasound have also been used to study age-related Carotid pulse variation during diastole and systole (Balasundaram and Banu, 2006). In alternative experimentation, ultrasound scanned images were used to study and filter the carotid signal for analyzing the RR interval (Reesink et al., 2007). Ultrasound scanned images processed through SphygmoCor applanation tonometry and DSP processor-based system have been further experimented to view local arterial stiffness of Carotid Pulse (Bianchini et al., 2007). To detect blockage in the Carotid Arteries, at times, a painless scan called the Carotid Duplex involving the traditional ultrasound and the Doppler ultrasound method is used. In this procedure, the Doppler probe calculates the blood flow through the artery. The carotid artery pulsation image is picked up by the B-mode sensor (St. John's Mercy Health Care). Doppler Ultrasound is a nonrisky, noninvasive method for investigation of arterial conditions, and has been preferred all along. This technique along with the Discrete Wavelet Transform method and Discrete Hidden Markov Model has been explored for classifying internal Carotid Artery pulse shape for patients with stenosis and occlusion conditions (Uğuz and Kodaz, 2010). However, the utilization of this method of ultrasound to analyze the ventriculo-arterial relationship needs further examination.

A pressure nanosensor-based device woven as a scarf allows continuous real-time monitoring of the Carotid Pulse signal. This can be very helpful in diagnosing and assisting people with weak pulse, which is difficult to detect from the radial artery but can be picked from the Carotid Artery. The scarf designed is flexible and light in weight that allows an uninhibited and comfortable arrangement for acquiring the signal. Digital filters, third party software along with the pressure sensor permits the accuracy of the acquired data (Chen et al., 2014). Fiber Bragg Grating technology is another optical fiber-based noninvasive technique used for the direct acquisition of Carotid Artery pulse waveform. This method has the inherent advantages of having a wide range of operation, electrical isolation, reduction in losses, high Signal-to-Noise ratio, and very limited susceptibility to EM Interference, an attribute much desired in biomedical devices. Leitão et al. and the team tested the feasibility and repeatability of the Fiber Bragg probe for assessment of Carotid pulsation (Leitão et al., 2013).

Nabeel et al. developed a prototype for continuously acquiring the Carotid Pulse Wave in a noninvasive manner employing a dual element photoplethysmograph probe. The arrangement effectively demonstrates real-time detection and analysis of critical variations in the Carotid Pulse Wave under normal and raised BP situations (Nabeel et al., 2017). Nabeel and his team further worked with a calibration-free, noninvasive, and direct arrangement for evaluation of local pulse pressure exhibited by regular beats transmitted from the aorta and the carotid artery. Such noninvasive assessment of local pressure difference originating between the aorta and carotid requires special attention, especially when being studied in nonspecialized routine clinical settings (Joseph et al., 2018). Arathy and the team used two microelectromechanical accelerometer sensors and a customized front end analog arrangement to develop a probe that can acquire the Carotid Artery pulsation in real-time. The mathematical models designed could effectively monitor and analyze cuff-less BP characteristics detected from Carotid Pulsation (Arathy et al., 2018).

Aging is a contemporary perception: life expectancy for human beings has multiplied almost twice, and associated with this has increased the age-related ailments, primarily the

cerebrovascular complications. Continuous pulsation of arteries causes its wear and tear and the effect is the stiffening of arteries and sustained increase in pulse pressure (PP) amplitude. This leads to brain illness like thinning of cortical gray matter, and also cognitive dysfunction. PP and brain injury are probably linked but need further investigation, so a lot is being researched to ascertain the relation among the carotid artery pulse waveform and increased flow to cerebral blood vessels and their change with age (Hirata et al., 2006; Thorin-Trescases et al., 2018).

A study performed on young adults from Australia found a correlation between the sedentary lifestyle and the stiffness of arterial walls. The study involved data analysis of Carotid pulsation picked using Ultrasound technology (Huynh et al., 2014). Further investigation revealed that physical activities improve on the arterial distensibility of the adults (Huynh et al., 2015).

Blood pressure assessment is a robust sign of cardiac health status where the enhanced systolic blood pressure reveals variations in the arterial wall stiffness and the raised pulse pressure forecasts relate aortic atherosclerosis with the arterial stiffening. BP measurement using an ultrasonic method along with image processing algorithms presents a novel noninvasive technique to detect the Carotid Artery Pulse waveform (Soleimani et al., 2017). For primary level detection of cardiac disease, a portable noncontact camera-based system has been experimented with which has the capability to precisely quantify the pulse waveform and can become the basis for developing computational techniques to analyze cardiac systolic and diastolic phases (Haji Rassouliha et al., 2019).

Diagnostic analysis of Carotid Artery diseases is being extensively researched nowadays. In certain research, authors have analyzed the relation between Carotid-femoral and Heart-femoral PWV pulsations to study community-based Atherosclerosis Risk and to assess central arterial stiffness (Stoner et al., 2020). For the primary assessment of CAS, the influence of Carotid Ultrasound is also being studied (Qin et al., 2020). Very recent statistics on death due to stroke presents, that Ischemic Stroke remains the principal cause of death, in Europe, the United States and Asian Countries, and that around 80% of them are directly related to internal Carotid Atherosclerotic Stenosis. So, it is imperative to analyze clinical data of such patients to arrive at a high-quality treatment protocol involving Carotid Angioplasty and Stent Technology. The technique is claimed to have been very effective in reducing disability and the mortality rate and also for the diagnosis of indicative internal carotid stenosis and is considered safe (Zhang et al., 2020).

From the literature presented, it is evident that measurement and analysis of Carotid Pulse Waveform are of prime importance to assess the health condition of an individual especially their cardiac status. It is also required to devise a solution that is not only affordable but is also simple, portable, sensitive and that can allow easy connectivity with a general-purpose computer for effective acquisition of the carotid waveform in real-time. The subsequent section shall detail such a setup.

3.2 Experimental arrangement for detection of carotid pulse in real time

An experimental setup for real-time detection, recording, and analysis of carotid wave contour is depicted in Fig. 3−3. The raw carotid waveform is picked up by employing a

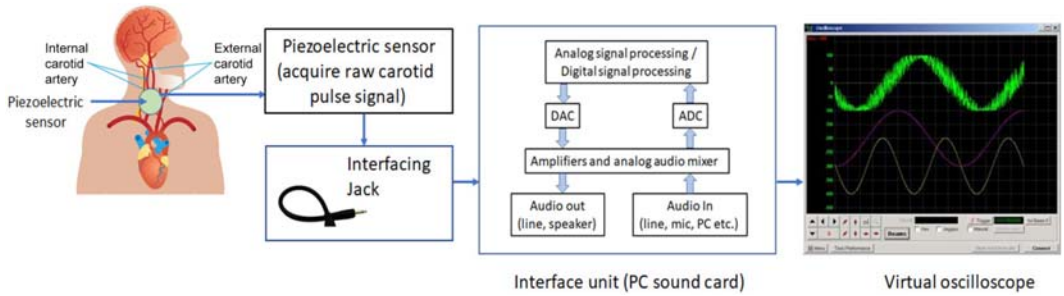

FIGURE 3–3 Block diagram representation|Detection of Carotid Pulse Wave in real time.

Piezoelectric sensor. The constructional details of the pressure sensor used include, a metal disk having a diameter of 2.0 cm with a thickness of 0.25 mm, along with a concentric ceramic layer coating having a diameter of 1.30 cm which is 0.1 mm thick. The pressure-sensitive sensor effectively detects the vibrations generated by the pulsation of the carotid artery. The detailed functioning of the Piezoelectric transducer is presented in the subsequent section.

The Carotid signal detected is interfaced with the sound port of the computer through a 3.5 mm mono jack. The sound port connects with an internal sound card of a PC which enables input and output of audio signals through the computer. This expansion card has a line-in connector to receive the analog input obtained from the sensor output and has an inbuilt amplifier and analog to digital converter (ADC) to amplify and digitize the analog input, respectively. The acquired Carotid pulse waveform is then viewed using a software virtual oscilloscope installed on the computer. The Universal Oscilloscope GUI (Real-time Plot) DLL library (https://sites.google.com/site/brnstin/) allows real-time display as data is transmitted without much delay to the oscilloscope. It is a very simple yet versatile and powerful interfacing tool.

The software oscilloscope replicates the control unit of a real oscilloscope and there is a provision for the functional attributes to be initialized. It allows easy import−export of data from MS Excel, MATLAB programs, etc. It presents a consistent and robust arrangement that allows data communication via serial port (RS232, 422, 485), sound port, USB port, Ethernet, customized DAQ cards, etc. Carotid pulse wave signals can be effectively detected using a piezoelectric sensor in real-time using this simple, portable, and cost-effective arrangement. The sound card of the PC is utilized as an interfacing unit, so the necessity of designing supplementary amplifiers, ADC, or DAQ unit is eliminated. The visualization and export of data for further analysis are done using a freely available virtual oscilloscope (Bansal et al., 2009).

3.2.1 The piezoelectric sensor

The health care sector is hugely benefitted by the innovation and integration happening in sensor technology, the microcomputers, nanotechnology, and the signal processing

algorithms. Continuous progression in research for the development of biomedical sensors has enabled the evolution of miniature, portable, user-friendly, smart sensors that can effectively translate various biological signals into measurable outputs in noninvasive mode. Piezoelectric sensors have evolved over the years as a multipurpose noninvasive means to measure pressure, acceleration, force, strain, etc., and are widely used in the auto industry, medical instruments, aerospace, nuclear devices, touchpads, etc. This section presents the potential of piezoelectric sensors to detect and examine various human physiological signals which are generally of low amplitude, are nonelectrical and quasiperiodic, and are difficult to detect and perceive otherwise. The piezoelectric sensors have the inherent benefits of being versatile, rugged, affordable, stable over temperature, linear over a wide frequency and amplitude range, immunity to electromagnetic radiation, high modulus of elasticity, and nearly insignificant deflection when compressed, etc.

Aerospace industries use sensor network arrangements made of piezoelectric material for structural health monitoring of the aircraft to identify damages if any. Piezo material is a preferred choice as it can be used both as actuators or as sensors (Qing et al., 2019). Researchers are also exploring the seamless integration of affordable nondestructive piezo sensors into industry 4.0 technologies to observe the strength of concrete beam structures (Ghosh et al., 2020). The recent development in constructional health monitoring includes a supply of green and sustainable power to piezoelectric sensor-based arrangement for IoT-based pavement (Hou et al., 2017). Research in the domain of material science, biotech, and microsystems has nurtured the development of biocompatible piezoelectric material based new age biosensors and safe and biodegradable medical implantable devices (Chorsi et al., 2019; Chen-Glasser et al., 2018). Giants like Texas Instruments are into the development of patient monitoring systems using an arrangement of pressure sensing elements, amplifier, microcontrollers, etc. [Texas Instruments]. Piezoelectric sensors are also finding increasing applications in real-time monitoring of ECG signals as the probes designed are affordable, reusable, and easily available (Ahmad, 2016). Patches made of piezoelectric substances have also been tested in vitro and in vivo to analyze bone physiology (Srivastava et al., 2017). Bluetooth-based portable device built using piezoelectric element along with signal conditioning electronics has also been designed to measure the heart rate, pulse pressure, etc. (Mokhtari and Ahmad, 2019). Very recently, piezoelectric sensors have been used to infer human vital sign information w.r.t heart and respiratory functions from the chest surface (Allataifeh and Ahmad, 2020). It is evident that Piezoelectric sensors have a plethora of applications in medical monitoring, so, the subsequent sections shall detail the principle theory behind its working and the signal conditioning techniques deployed with them.

Inspired from the Greek word “piezen” meaning push/press, has been derived the term Piezoelectric. Founded by Pierre Curie, Piezoelectric Effect is the ability of piezoelectric material to translate mechanical stress/pressure into alternating electrical force. Piezoelectricity is based on the basic principle of an electrical dipole. In the ground position, the crystal symmetry does not support the formation of an electric field as the dipoles formed by negative and positive ions cancel each other. The crystal deforms under stress losing its symmetry. This leads to a net dipole moment, which results in the formation of an electric field across the

crystal. Naturally available Piezoelectric materials are the Quartz (most preferred one), Topaz, Silk, Tendon, DNA, etc., and the synthetically generated ones include Zinc Oxide (ZnO), Lead titanate ($PbTiO_3$), Barium Titanate ($BaTiO_3$), Lead zirconate titanate (PZT), etc. Fig. 3−4 depicts the schematic symbol, pinout details, electronic equivalent circuit, and the frequency response curve of the Piezoelectric Sensor. Applying a mechanical pressure on the top of the sensor generates a voltage at the output which can be simply fed to the circuit by connecting its positive and negative terminal. Pressure and acceleration are few physical quantities that can be easily measured using the piezoelectric sensor.

The Piezoelectric sensor has large DC output impedance and its equivalent electronic circuit, as shown in Fig. 3−4, can be modeled suitably as a filter circuit and a voltage source. The Voltage "V" is directly proportional to the functional pressure, force, or effective strain. It has an internal resistance R_i due to insulation, inductance L_m is due to the inertia of the sensor and its seismic mass, the capacitance C_e is the inverse effect of the elasticity of the Piezo material used and C_0 represents the static capacitance of the sensor. When connected to a load resistance, it acts in parallel to R_i thereby affecting the cutoff frequency of the sensor. Large load and insulation resistance allows the detection of even low frequencies. The sensor has an impedance level $\leq 500\,\Omega$, operating temperature ranging from -20°C to $+60^\circ$C, requires low soldering temperature, and has a strain sensitivity of 5 V/$\mu\varepsilon$. The flat region between the high-pass cutoff frequency and the resonant peak as shown in the frequency response curve is used for various sensor applications. For optimum utilization of the sensor, signal conditioning is required (Bansal, 2012).

Of late, Piezoelectric ceramics like Lead Zirconate Titanate ($PbTiO_3 \times PbZrO_3$) and Barium Titanate ($BaTiO_3$) which are multicrystal with a high dielectric constant are in use. The electrical dipoles within these crystals are randomly oriented, so they do not exhibit the piezoelectric property initially, so they are polarized using a high DC electric field. The ceramic has robust dielectric properties, so the dipole moment remains unaffected even after the removal of the electric field applied. Thus these ceramic piezoelectric substances exhibit strong piezoelectric properties and possess the benefit of being affordable, stable and efficient with a high degree of freedom and a wide range of applications.

Lead Zirconate Titanate based ceramic piezoelectric sensor has been used in this experimentation. The ceramic disk has electrodes on its side and is laminated using adhesive to a

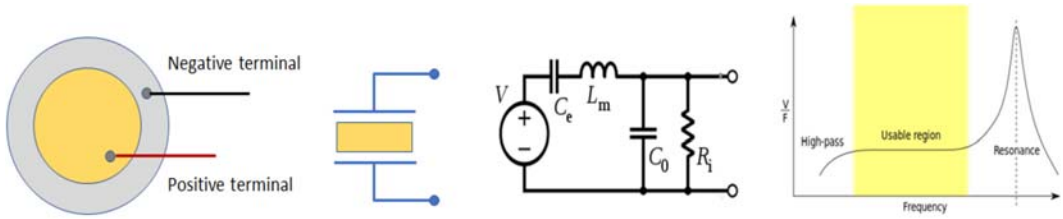

FIGURE 3–4 Electrical details of the Piezoelectric Sensor.

metal disk. The sensor used is light in weight, is compact, and is sensitive enough to pick vibrational signals of micro range without needing a bias voltage and additional signal conditioning circuitry. The detailed protocol for the acquisition of Carotid waveform in real time and the result obtained under different postures is presented in the next section.

3.2.2 The acquisition protocol and results

The subject is made to be in the supine position with the body and the chin slightly elevated and the piezoelectric sensor is gently placed over the neck region to acquire the Carotid Artery pulsation after palpating it by middle and index fingers, to capture the zone of maximum pulsation. For stable recording, the sensor is affixed on the neck using an elastic strap arrangement. This being a noninvasive procedure, causes no discomfort to the subject. The analog output of the sensor which quantifies the Carotid Artery pulsation is interfaced with the sound port of the PC using a 3.5 mm jack. The internal circuit of the sound card amplifies and digitizes the acquired input carotid signal. The result is visualized on the software oscilloscope.

The subject is then made to sit on a chair and relax and the bio-signal was recorded. Initial recordings were not considered, till the readings got stable. To avoid artifacts, the subject was advised to restrict movement. In the next stage of experimentation, the subject was made to stand up abruptly from a sitting position on the floor, and the fluctuations were noted. This was experimented on healthy volunteers, both male and female, of age group range 35−55 years, both in sitting, followed by active standing postures (with due consent). The variations in the amplitude and carotid pulse waveform periodicity were recorded was studied under various postures.

Figs. 3−5 and 3−6 show the acquired Carotid Pulsation during (A) relaxed sitting, (B) relaxed standing and (C) abrupt sitting to standing positions for different volunteers. The direct, simple, and noninvasive acquisition procedure might not present an extremely clean carotid artery waveform but is very effective in knowing the instant cardiac health status of an individual by looking at the RR interval details. As can be seen, the positive peak indicates the rise in arterial pressure resulting from ventricular contraction throughout systole. When the posture is altered, amplitude and contour also undergo changes which are the consequence of variation in heart contractions during abrupt standing.

The result in the case of the second volunteer as in Fig. 3−6 is a bit noisy as compared to the first volunteer as shown in Fig. 3−5. There could be multiple reasons behind this. The artifacts result due to muscle movement, or if the sensor is not placed properly over the arterial site and is not stable. Power line interference also causes noise to distort the detected signal. The recorded bio-signal can be filtered by designing digital filtering techniques. A model of digital filters is developed in the Simulink environment to remove these artifacts in the subsequent sections.

RR interval and Carotid pulse amplitudes for these recordings were studied by visual inspection for ten different volunteers. Table 3−1 analyzes the acquired carotid pulse waveform while sitting on the floor and during abrupt standing postures. As is evident from the tabulated data, the RR interval reduces in case of abrupt standing compared to readings taken during a relaxed position, however, an increase in amplitude is noticed after sudden standing. Reduction in the RR interval and raised pulse amplitude level during an abrupt

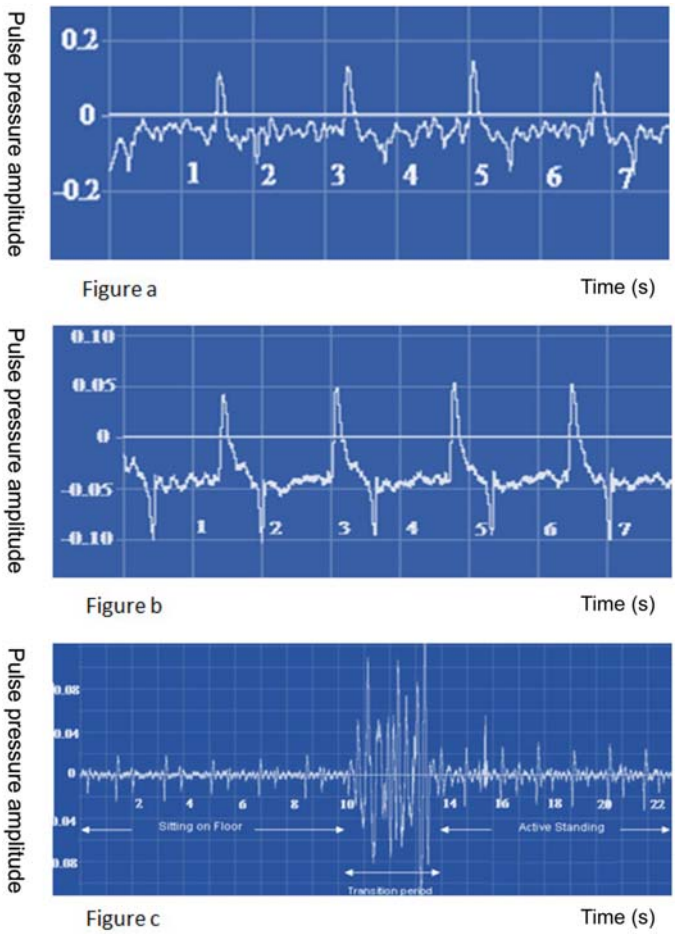

FIGURE 3–5 Volunteer 1 | Acquired Carotid Pulsation during (A) relaxed sitting, (B) relaxed standing, and (C) abrupt sitting to standing positions.

standing position is indicative of an increased heart rate. The variation in RR interval and the amplitude level also depends on their physiological status and vital statistics, that is, their BP, age, height, weight, gender, etc. This arrangement may however prove out to be very helpful in critical situations when the patient is in shock and when it becomes difficult to locate their pulse from other peripheral arteries in the human body.

3.3 Digital filter designs

The real-time raw bio-signal picked up using this simple arrangement requires signal processing algorithms for further analysis and understanding. MATLAB and Simulink are widely explored at every stage of bio-signal processing system development from preprocessing techniques to

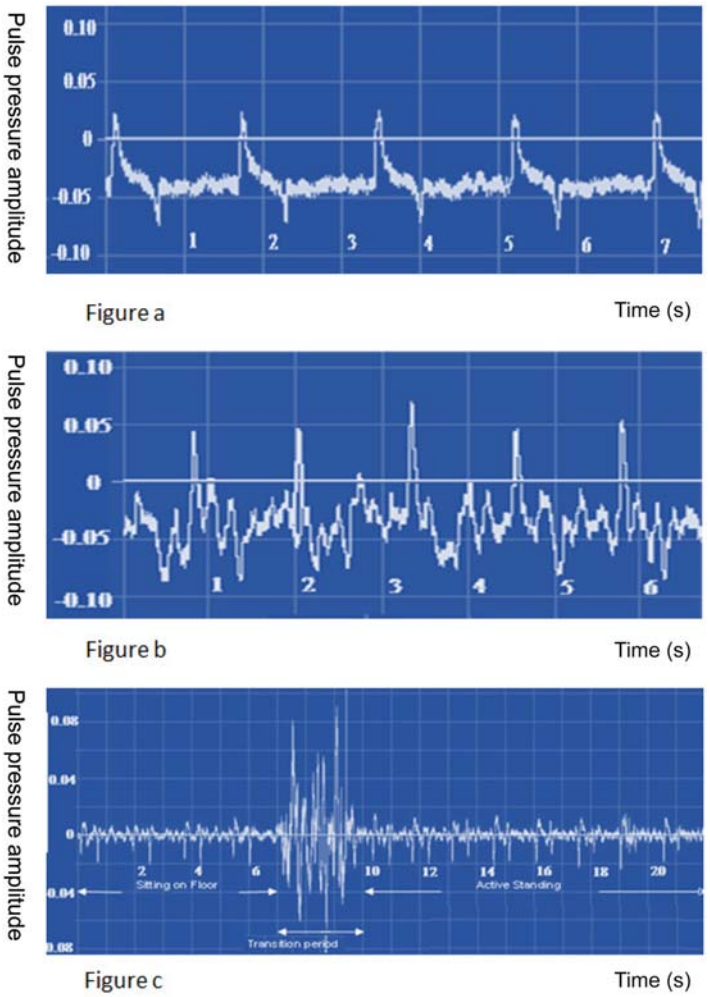

FIGURE 3–6 Volunteer 2 | Acquired Carotid Pulsation during (A) relaxed sitting, (B) relaxed standing, and (C) abrupt sitting to standing positions.

predictive models involving machine learning. Design and analysis also require the implementation of basic Digital Filters like IIR and FIR filters and adaptive and multistage Filters. This section shall briefly describe the design of FIR and IIR Digital Low Pass Filters based on their frequency response specifications using the Signal Processing Toolbox of MATLAB/Simulink.

3.3.1 Finite impulse response filter design

The frequency response curve for low-pass filter (LPF) with cutoff frequency ω_c is shown in Fig. 3—7. An ideal LPF rejects all frequency components greater than ω_c and does not change

Table 3–1 Carotid Pulse Waveform analysis under sitting and abrupt standing postures.

	RR interval (s)		Pulse amplitude (V)	
Subject	**Sitting on floor**	**Abrupt standing**	**Sitting on floor**	**Abrupt standing**
1	1.64	1.21	0.021	0.023
2	1.47	1.13	0.017	0.020
3	1.51	1.30	0.018	0.021
4	1.88	1.41	0.016	0.020
5	1.67	1.32	0.021	0.023
6	1.62	1.13	0.020	0.024
7	1.72	1.52	0.018	0.021
8	1.74	1.50	0.014	0.020
9	1.81	1.41	0.013	0.018
10	1.63	1.38	0.022	0.021

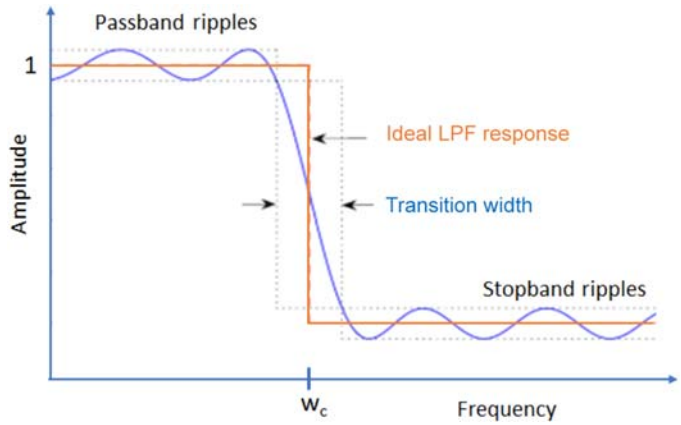

FIGURE 3–7 Frequency response curve of a Low-Pass Filter approximated with finite impulse response.

frequencies below ω_c. Designing of an ideal LPF requires an infinitely long impulse response, so having an ideal Finite Impulse Response (FIR) LPF requires approximations that lead to undesirable ripples in the passband for frequencies $\omega < \omega_c$ and also in the stopband for frequencies $\omega > \omega_c$. This also results in a transition width between the passband and the stopband.

Design specifications of a practical low-pass FIR Filter require a trade-off between the allowable transition width, the maximum permissible passband/stopband ripples along with the order of the filter. Despite underlying limitations, FIR Filters are preferred by designers as they give stable filters with linear phase response. Using the "designfilt" function of the Signal Processing Toolbox, the order of the filter may be specified. To have a minimum order low-pass FIR Filter, frequencies of stopband and passband need to be set along with

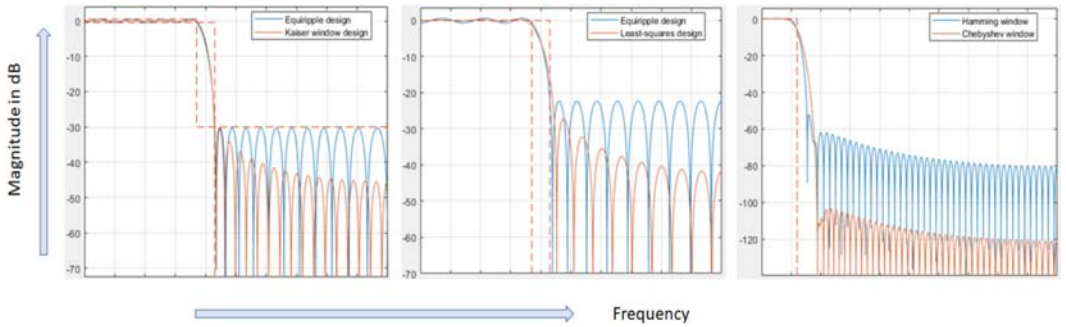

FIGURE 3–8 Design comparison for various low-pass FIR filters.

passband ripple and stopband attenuation. Linear phase Equiripple FIR Filter is the default selection using the "designfilt" function, as it gives a close approximation to the ideal response curve for a set filter order and specific tolerance limit. Kaiser window functions can also be used for designing minimum order filters as they are less expensive computationally but yield larger filter order in case of a very narrow transition width or a very large stopband attenuation design requirement. Applications that desire minimum error energy between the actual and the ideal filter for a particular frequency band, then the least-squares design is considered. Window techniques like the Hamming window and a Chebyshev window can be used for designing filters that have fixed order and a set cutoff frequency. The magnitude response curve for various low-pass FIR Filters is being compared in Fig. 3—8 (Mathworks).

3.3.2 Infinite impulse response filter design

FIR filters have the constraint of having large order structures for certain design specifications where a trade-off has to be made between the order and the permissible ripples and the transition width. However, if a recursive structure is used, smaller filter orders can be designed using Infinite Impulse Response (IIR) filters to meet the specifications. This reduces the computational complexity, but the design of a stable and causal does not have a linear phase response. The main benefit of IIR structure design over FIR structure is that, for a particular design specification of set transition width, passband/stopband attenuation, a much lower order filter can be realized, even though IIR filters show nonlinearity in phase response. This constraint can be addressed by processing the signal data within MATLAB/Simulink in "off-line" mode, that is, the complete data sequence is made available before the filtering task. The "filtfilt" function from the MATLAB library having the zero-phase band-pass filtering approach also makes it possible to design a noncausal IIR filter eliminating the effect of nonlinear phase distortion. The syntax for using the function is:

$$y = \text{filtfilt}\,(b, a, x)$$

The function processes the input data stream stored in "x" both in the forward and the reverse directions respectively, that is, after forward direction filtration, the function reverses

the sequence of filtration, by processing it back again through the filter. This results in a much-desired outcome of zero-phase distortion. The zero-phase filtering technique helps in eliminating noise from the bio-signal and also preserves the characteristics without any delay, which otherwise gets delayed in conventional filtering methods. The parameters "*a*" and "*b*" are used to set the order of the filter (mathworks.com; Gustafsson, 1996; Mitra, 2001; Oppenheim et al., 1999).

IIR Filters also have small values of group delay as compared to the FIR Filters, so the transient response is short. Various IIR Filters include the Butterworth design, which has a flat passband and stopband but a wide transition width. Chebyshev Type I filter design has reduced transition widths compared to Butterworth filter designs with the same order but has ripples in the passband. The Chebyshev Type II filters exhibit flat passbands but have equiripple stopbands. Applications where some ripples in the stopband are permissible, then small order structures work well. Another IIR Filter type is the Elliptic filter that has ripples in both the passband and the stopband. For a certain design specification, the Butterworth design has the highest order, and Elliptic design yields the smallest order. In the case of IIR Filters, apart from being conscious about the ripples and the transition width, care also needs to be taken regarding phase distortion. Study of Group Delay which should be constant ideally helps in controlling the distortion. Butterworth and Chebyshev Type II Filter designs exhibit flat Group Delay and so have the minimum distortion. Fig. 3−9 compares various IIR Filters for magnitude response and group delays (mathworks.com).

There are various applications where only one particular frequency component of the acquired signal is required to be eliminated. Mitigation of interference in the 50/60 Hz power line is a major concern in computer-based bio-signal processing and analysis system. Therefore it is of prime importance to have a Notch filter design that can remove this specific interfering frequency component. Notch filter designs using analog components are being used to remove these artifacts and can suppress the interference, but are demanding w.r.t its

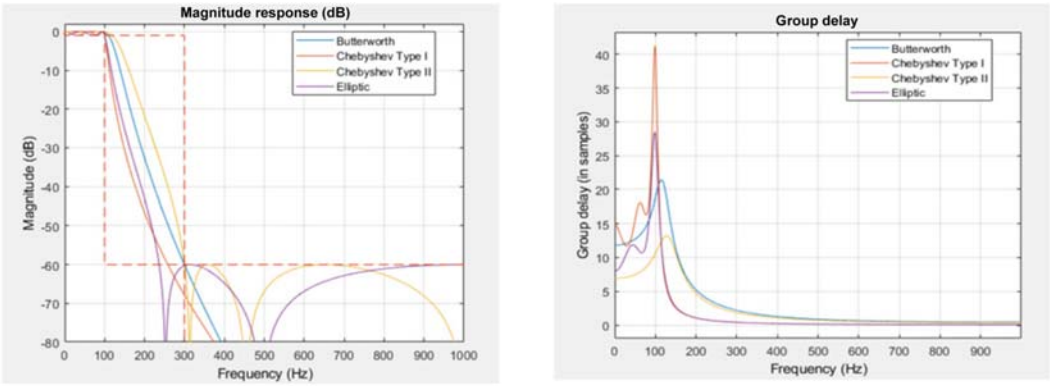

FIGURE 3–9 Various IIR Filter designs compared for magnitude response and group delays. *IIR*, Infinite impulse response.

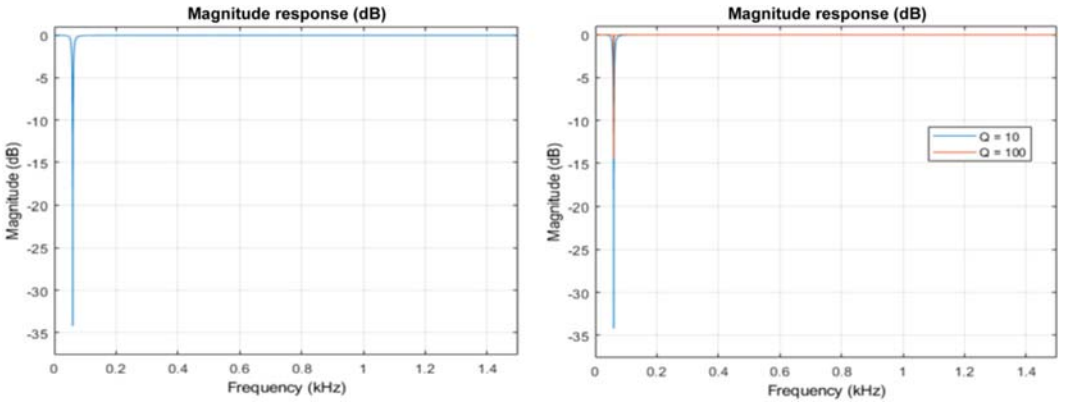

FIGURE 3–10 Magnitude response curve of a Notch Filter at different *Q*-Factors.

practical implementation. Therefore their digital counterparts are explored by researchers that are feasible and efficient in working.

Using the Bilinear Transformation technique, the analog IIR Notch filter can be converted into a digital IIR Notch filter. Notch filters are designed for the purpose by setting filter parameters, that is, the frequency to be notched, the 3-dB bandwidth, and the Quality Factor (*Q*-factor). To closely approximate the ideal characteristics, the order of the filter may be increased. The amplitude response curve of a notch filter is given in Fig. 3−10. The response at different values of the *Q*-factor is also depicted. The *Q*-factor of the notch filter gives a degree of isolation of a certain frequency from other frequency components. For a particular filter order, a high *Q*-factor is preferred by the designers.

In this experiment, Equiripple Band-Pass FIR Filters and IIR Notch filters are being used to process the real-time acquired Carotid signal. The model developed is using Simulink and is detailed in the section below.

3.4 Simulated model for real-time carotid pulse detection and processing

Simulink has been used to develop a model-based design for the bio-signal processing system using block diagrams. This simulation model allows easy acquisition, visualization, interpretation, easy verification, and code generation. Real-time live signals can also be acquired using analog-input block and can be visualized and analyzed using virtual scopes and spectrum analyzers. The Signal Processing Toolbox offers inbuilt functions for the analysis, preprocessing, and feature extraction of the acquired signals. The toolbox comprises of Filter Design and Analysis (FDA) tool as well, which helps in interpreting signal patterns, finding peaks, and parameterizing the signal in the frequency domain. The FDA tool also helps in designing, analyzing, and implementing various digital IIR and FIR Filters for their

performance and stability. The Signal Analyzer tool allows preprocessing and analysis of many signals concurrently in time, frequency, and time-frequency domains.

3.4.1 Filter design and analysis tool

The FDA Tool is recognized as a fast and great platform used to design and analyze digital IIR and FIR filters allowing import of already designed filters from the MATLAB workspace. Execution of the "fdatool" command through the MATLAB command prompt shows up the FDA Graphical User Interface (GUI) which presents a self-explanatory process for designing a filter by setting the required filter specifications. After the specifications are set, the "Design Filter" button is clicked. The code automatically generates a ".m file."

The GUI has three prime areas as detailed below:

- The region showing Current Filter Information which is at the upper left half displays the filter parameters like the structure used, its order, and its stability status.
- The region for Filter Display which is at the upper right corner gives the frequency response curve (magnitude and phase response) details, the filter coefficients, and group delay.
- The lower half has an interactive design panel area that enables us to define and set the specifications of the filter.

Multiple filter designs can be created and stored using the FDA tool and anyone can be selected depending on the application requirement. These filters can be exported to the Simulink Model as a single-input, single-output block. The "Realize Model" option allows the current filter design to be exported to the Simulink environment.

Care must be taken while setting the filter specifications. Ideally, it should be of minimum order and a stable one. The filter category can be selected as either high-pass or low-pass and band-pass. The stopband frequencies and attenuation levels are suitably selected. The filter is then tested off-line for stability and desired frequency response and then it is used for real-time applications.

FDA Tool also permits the integration of supplementary functions from other products of MathWorks viz. the Embedded Target for Texas Instruments C6000 DSP. This application generates a downloadable code for the DSP target board or assists in the generation of a synthesizable Very High-Speed Integrated Circuit Hardware Description Language (VHDL) using the Filter Design Hardware Description Language (HDL) Coder. Similarly, the Filter Design Toolbox complements innovative FIR and IIR design practices (mathworks).

3.4.2 Simulink model developed

The Simulink model developed for acquisition and signal processing of real-time carotid pulse wave is represented in Fig. 3—11. The "Analog input block" available in the "Data acquisition toolbox" allows reading input data from one or many analog-input channels and is made use of to acquire the online available bio-signal in real-time. Sound port, that is, the microphone-in line of the PC recognized as the "winsound" port in MATLAB is chosen as

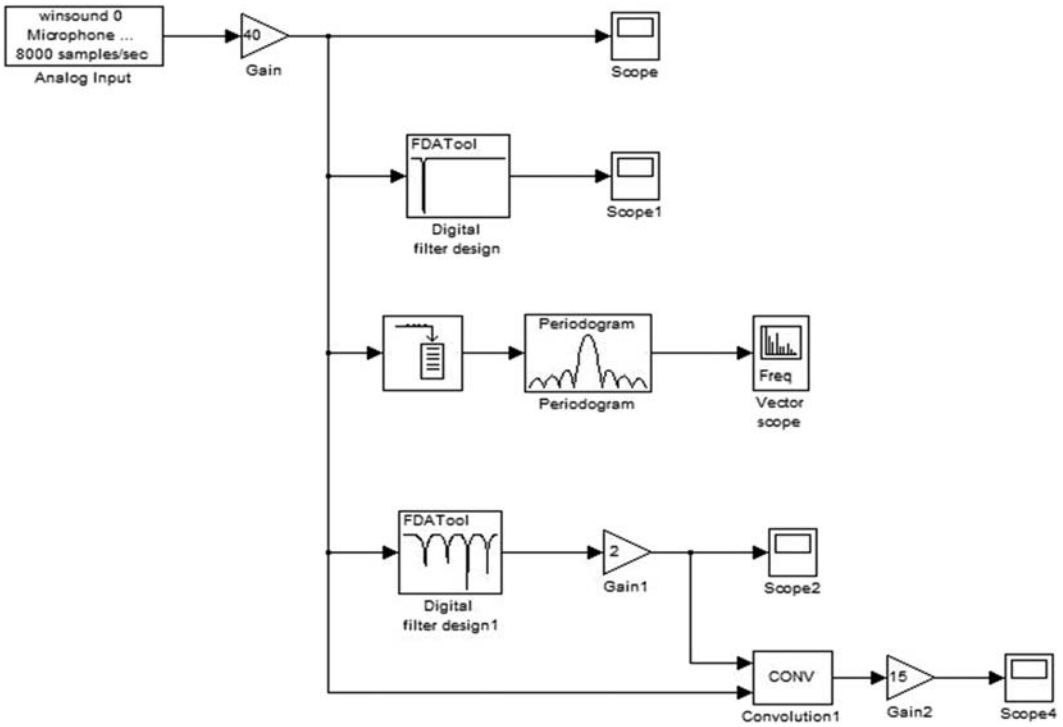

FIGURE 3–11 Simulated model for real-time acquisition and processing of Carotid Pulse wave.

the input device. The input data wave sequence is attained at a rate of 8000 samples/sec in asynchronous mode. In the asynchronous mode, the acquisition is initiated at the start of the simulation and is made to run during the acquisition process through a First In First Out (FIFO) data buffer. Although the hardware arrangement does not include an amplifier, however a gain block set to "40" is used in the model to improve the visualization of the raw data acquired. Scopes in the model help in viewing the real-time acquired bio-signal and various digital techniques modeled are added to filter the disturbance picked during acquisition to enable meaningful interpretation of carotid pulse under different postures.

In the present work, digital IIR Notch filter and Equiripple FIR BPF have been designed using the FDA tool available in the Signal processing block set of MATLAB. A stable IIR Notch filter of order "2" having Quality Factor 100 has been designed to eliminate the single frequency component of 50 Hz power line interference. The magnitude response curve for the proposed

IIR Notch filter as per Fig. 3—12. A stable Equiripple FIR band-pass filter with order 10, as per specifications enumerated below, has also been used to filter the carotid pulse wave signal.

The stopband and pass band parameter $F_{\text{stop1}} = 0.03$ Hz and $F_{\text{pass1}} = 0.05$ Hz

The stopband and pass band parameter $F_{\text{pass2}} = 150$ Hz; $F_{\text{stop2}} = 160$ Hz.

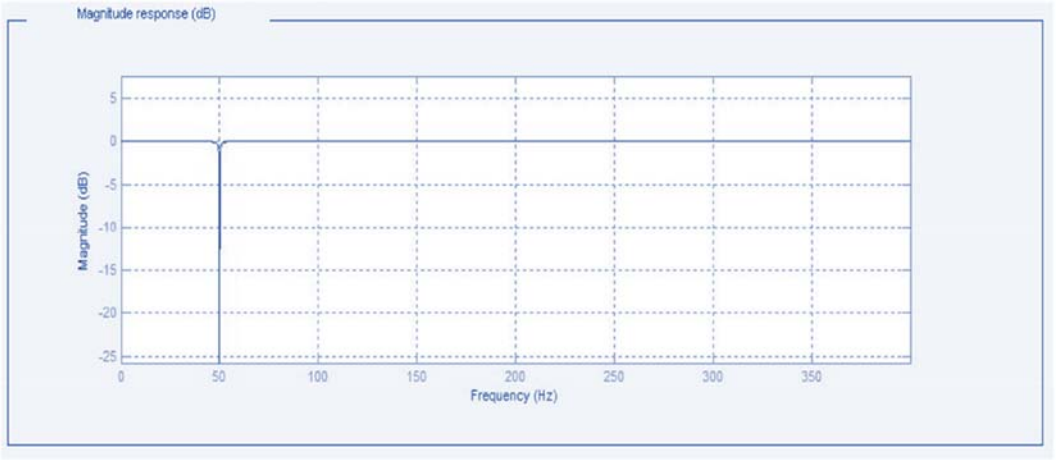

FIGURE 3–12 Magnitude response curve of 50 Hz IIR Notch Filter. *IIR*, Infinite impulse response.

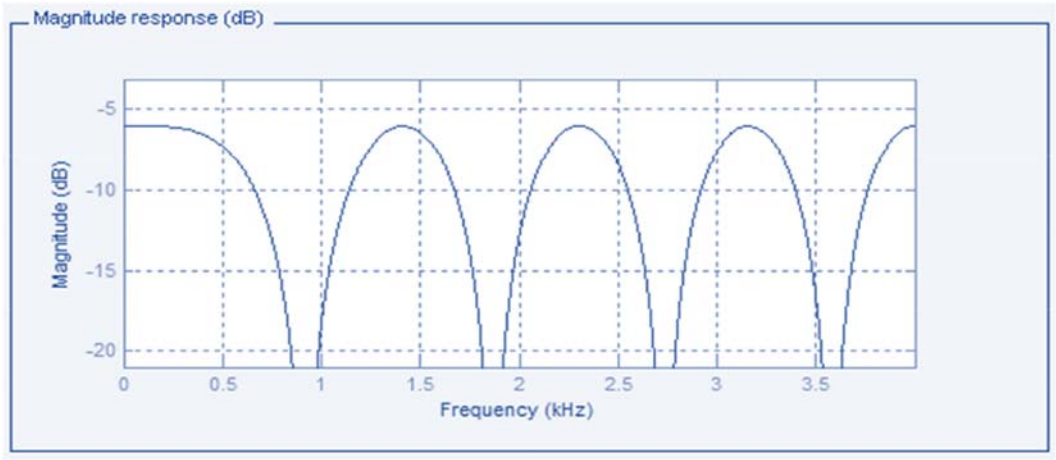

FIGURE 3–13 Magnitude response curve of equiripple FIR Band-Pass Filter. *FIR*, Finite impulse response.

The magnitude response curve of the designed Equiripple FIR BPF is as shown in Fig. 3—13.

A convolution block "conv" in Simulink from the DSP System Toolbox library is also used for filtering the acquired carotid signal. Convolution serves as the mathematical basis for filtering applications. Convolution operation finds wide application in analyzing differential equations, numerical analysis, statistics, computer vision, etc., and has developed into an

integral component for image and signal processing. While designing the FIR filter, $y[n]$ the filtered output is obtained by performing the convolution of the signal input $x[n]$ and the impulse response $h[n]$ of the filter system. The filtering operation can also be performed in MATLAB using the "conv" function, provided the signal being input is also of finite length. The Convolution block deployed in this model has two inputs, where one of them is the acquired carotid pulse wave and the other is the output obtained from the Equiripple FIR BPF block. This further filters the detected pulse wave and can be used for comparing the filtered results. For filtering the unwanted frequency components, one way is to find the Fourier Transform of input data and multiply it with a Gate having a corresponding to the desired frequency range. Inverse Fourier Transform subsequently generates the filtered output signal and is similar to the convolution operation. Convolution results in amplification or attenuation of each frequency component of the input data sequence and is independent of the other frequency components. It is also used in digital image processing algorithms for edge detection etc.

The model also deploys a spectrum analysis tool to calculate the spectral details of the acquired carotid signal. Frequency domain analysis of bio-signals is of utmost importance as it provides additional information on the characteristics of the signal being analyzed. The most significant reason is that spectrum analysis helps in perceiving small signals which go unnoticed otherwise in the influence of large signals. Power spectral density (PSD) analysis is one tool that gives the spectrum details of the signal. Parametric and nonparametric approaches can be used for the purpose where the parametric approach utilizes estimated model parameters to calculate the PSD. Yule-Walker autoregressive and the Burg method represent parametric approaches where the coefficients of the linear system are estimated first to evaluate the PSD. Their performance is more reliable when it comes to analyzing small-signal lengths as compared to the nonparametric methods. Whereas, the nonparametric approach is a conventional technique of directly evaluating the PSD. One of the methods used in this model is the "Periodogram" which is based on finding Fast Fourier Transform (FFT). For understanding the spectral resolution and to study the side lobes, a suitable window function is also required to be selected. Several window functions namely Rectangular, Hanning, Hamming, Gaussian, etc., can be used for the same. A trade-off is made w.r.t. the resolution and the side lobes while choosing the window function. Spectral analysis of bio-signals provides many instinctive interpretations about the health conditions of an individual and therefore, cautious signal preprocessing is desirable. Nonparametric spectral assessment is performed using the Periodogram block and the "Hanning window" function in this experiment. Buffer block is used to divide the signal into frames, at 128 samples per frame. Each frame is passed through the Hanning window, and then the FFT of the windowed frame is measured. FFT is analyzed for consecutive windowed frames and the result is viewed on the frequency vectorscope.

The simulated model designed, is successful in detecting the carotid pulsation in a real-time scenario. The results obtained are presented in Fig. 3−14. As is evident in the part "A" of Fig. 3−14, the raw carotid signal is heavily distorted due to interference. The prime reason is the 50 Hz power line interference in a computer-based system. When processed through a digital

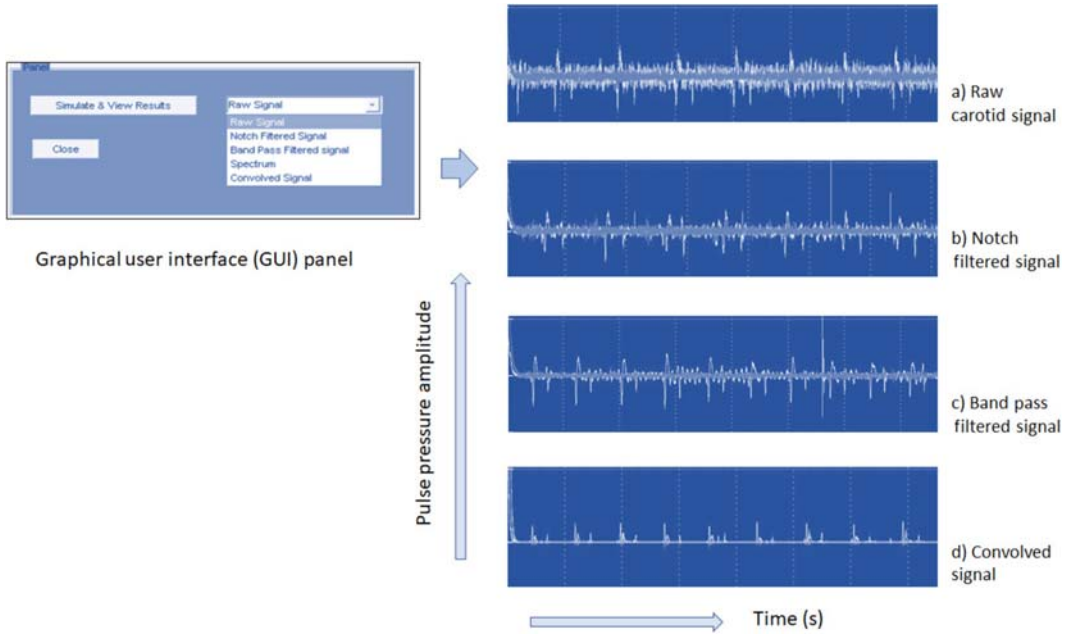

FIGURE 3–14 Carotid pulse waveform acquired in real-time viewed using the Graphical User Interface panel. (A) the raw carotid pulse signal; (B) the IIR notch filtered carotid pulse waveform; (C) the Equiripple FIR band-pass filtered output; and (D) the convolved filtered output.

IIR notch filter, the hum due to 50 Hz is greatly reduced as can be seen in Fig. 3—14B. Some unwanted spikes however appear; which could be due to nonstationary sensor-body contact. Fig. 3—14C shows the result of the filtered signal after being processed through an Equiripple FIR Band-pass filter. Fig. 3—14D represents the convolved filtered output (Bansal, 2013).

A GUI is developed to build an interactive front panel to run the simulation and view the results. GUIs also called apps in MATLAB, offer point-and-click controller for the software application designed. This eliminates the prerequisite to know and understand the syntax of the language used in the application to run the program. These GUIs can work as standalone application programs and are provided with a drop-down menu for interaction. There are various ways of creating these GUIs. One way is to convert the script into a simple app where the end-user can change or modify the variables using the control panel. Another option is to develop an interactive sophisticated app using an environment facilitating drag and drop. The third option is to program a GUI by writing codes. A simple GUI app has been generated in this example (mathworks).

The PSD evaluated using the Periodogram block and the "Hanning window" function is shown in Fig. 3—15. The 1001st frame of the spectrum scope has been captured here. This model is a simulated solution to processing the real-time acquired carotid pulse waveform. To further improve the stored carotid pulse wave after filtering, an algorithm detailed in the section below has been developed in MATLAB.

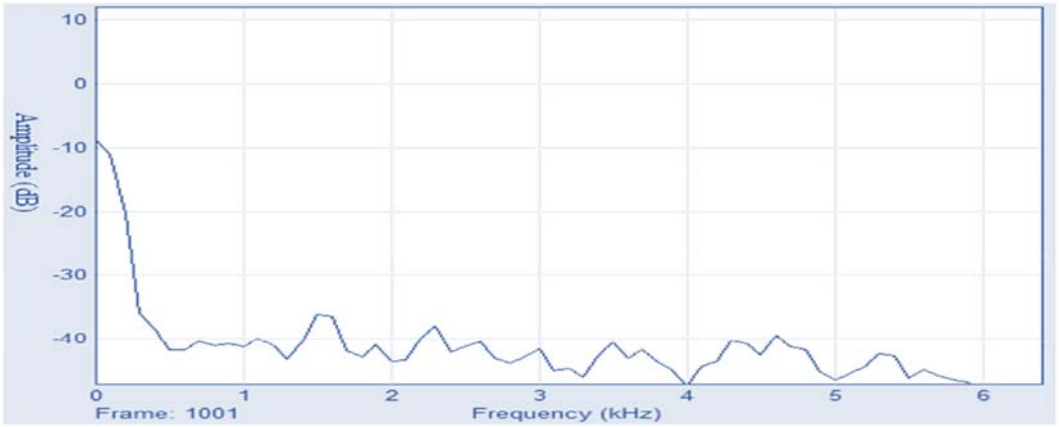

FIGURE 3–15 Power spectrum density of the real-time acquired Carotid pulse wave.

3.5 Algorithm for real-time carotid pulse analysis

MATLAB software with its enormous computational ability allows signal postprocessing for stored data sequences in off-line mode. So, digital filters can be programmed to eliminate the distortion from the logged bio-signal. Zero-phase band-pass filters have been used in this work to remove the artifacts and enhance the recorded raw carotid pulse wave detected using the simple arrangement discussed in the previous sections. The Zero-phase BPF combines LPF and HPF which performs filtering of the input data in both forward−reverse sequences. This results in no distortions in phase and thus eliminates the interference that may have been picked up along with the desired bio-signal during the acquisition.

The filter specifications set include the passband of frequency ranging from 0.05 to 50 Hz. This range sufficiently takes care of normal and elevated heart rate and is also helpful in analyzing the carotid pulse wave readings. The algorithm developed to off-line process and filter he stored carotid signal is given in the flowchart as per Fig. 3−16.

The "Load" command from MATLAB is deployed to bring the acquired and stored unprocessed raw carotid pulse data to the MATLAB workspace. A window-based digital FIR Filter having a linear phase response is implemented using the "fir1" function. The syntax is as below:

$$b = \text{fir1}(n, E_n)$$

To design a low-pass, band-pass, or multiband filter of order "n" the "fir1" filter function makes use of a Hamming window having a linear phase response. The filter design selected is subject to specifications set for W_n. In this work, the band-pass filter configuration has been used. The signal is then processed through a Zero-Phase BPF. The "filtfilt"' function as explained earlier in this chapter is used for further filtering. The results obtained for various subjects are plotted in Fig. 3−17. It is evident from the results that the disturbance

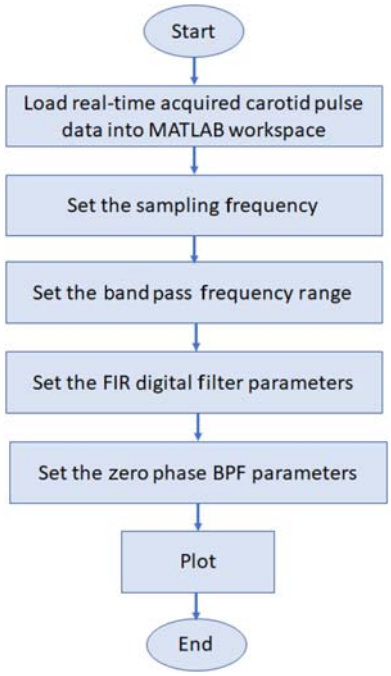

FIGURE 3–16 Algorithm for digital filtering of stored carotid pulse wave data.

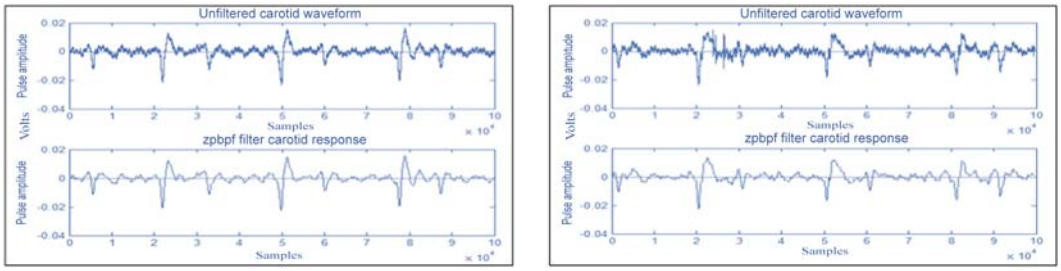

FIGURE 3–17 The raw and the digitally filtered Carotid pulse wave for different subjects.

picked up using this simple acquisition setup for detecting the human Carotid Pulse waveform is largely reduced using these digital filters. The algorithm was tested for reliability and repeatability by performing the task on multiple subjects.

3.6 Conclusion

An easy to design and implement piezoelectric sensor-based computer setup has been established that can acquire the real-time carotid pulse wave. The system is capable of efficiently

detecting the bio-signal and is user-friendly, portable, and affordable. A computer-based bio-signal detection system has the inherent advantage of providing a platform to view and analyze the picked-up signal on a software virtual oscilloscope installed on it. This capability has been made use of in this arrangement to observe and evaluate the position associated variations in the detected real-time carotid signal wave. A multipurpose and adaptable virtual software oscilloscope which is freely available has been installed for the purpose. This arrangement eliminates the need for a complex electronic circuit and therefore makes it convenient and valuable for extensive application in outpatient setups and critical circumstances. The performance being tested for reliability and efficiency can preferably be used in place of a manual pulse monitoring system.

The carotid pulse wave has been detected using an affordable piezoelectric sensor in this experiment. It is a rugged sensor, constructed using polycrystalline ceramics in place of naturally available piezoelectric materials and which is commercially available. The features of the piezoelectric may get influenced due to temperature differences which hugely depend on its manufacturing procedure and the chemical structure. The results obtained are however very encouraging.

A virtual model has been proposed in Simulink and by utilizing the familiarity with Digital Signal Processing techniques, the real-time detected Carotid pulse waveform is filtered. The simulation platform assists in digital filtering of the acquired bio-signal which is prone to noise interference when detected on a computer-based home health monitoring system. Blocks from the primary Simulink library have been used in the model and the results obtained are acceptable. This PC based arrangement poses no hardware limitations and offers a platform to acquire, view, and process bio-signals. The real-time detection system experimented is comparatively low-priced as the sound port of a computer is used as the interface thus eliminating the requirement of supplementary amplifying and filtering circuits, ADC, and DAQ units. The gaps in existing literature indicate the development of such a computer-based easy and cost-effective real-time bio-signal acquisition system.

References

Ahmad, M., 2016. Piezoelectric extraction of ECG signal. Sci. Rep. 6, 37093.

Alametsä, J., Viik, J., Alakare, J., Värri, A., Palomäki, A., 2008. Ballistocardiography in sitting and horizontal positions. Physiol. Meas. 29 (9), 1071–1087.

Allataifeh, A., Ahmad, M.A., 2020. Simultaneous piezoelectric noninvasive detection of multiple vital signs. Sci. Rep. 10, 1 416. 15 Jan.

Arathy, R., Nabeel, P.M., Joseph, J., Sivaprakasam, M., 2018. Carotid local pulse wave velocity measurement using dual-element accelerometric patch probe. Conf. Proc. IEEE Eng. Med. Biol. Soc. 2018, 4571–4574.

Balasundaram, J.K., Banu, R.S., 2006. A non-invasive study of alterations of the carotid artery with age using ultrasound images. Med. Biol. Eng. Comput. 44 (9), 767–772.

Bansal, D., 2012. Potential of piezoelectric sensors in bio-signal acquisition. Sens. Transducers 136, 147–157.

Bansal, D., 2013. Computer-based model to filter real-time acquired human carotid pulse. Signal. Process. Int. J. (SPIJ) 7 (1).

Bansal, D., Khan, M., Salhan, A., 2009. Real-time acquisition and PC to PC wireless transmission of the human carotid pulse waveform. Comput. Biol. Med. 39, 915–920. Available from: https://doi.org/10.1016/j.compbiomed.2009.07.008.

Bianchini, E., Giannarelli, C., Faita, F., Raimo, K., Gemignani, V., Ghiadoni, L., et al., 2007. The assessment of local arterial stiffness from ultrasound images. Comput. Cardiol. 34, 761–764.

Chatterjee, K., 1997. Bedside evaluation of the heart: the physical examination. In: Parmley, W., Chatterjee, K. (Eds.), Cardiology, 1. JB Lippincott Co, Philadelphia, p. 13.

Chen, D., Zhang, T., Lawo, M., Gu, Y., Zhang, Y., Chen, D., 2014. A smart scarf for pulse signal monitoring using a flexible pressure nanosensor. ISWC 14, Adjunct.

Chen-Glasser, M., Li, P., Ryu, J., Hong, S., 2018. Piezoelectric materials for medical applications, piezoelectricity—organic and inorganic materials and applications. In: Savvas, G. (Ed.) Vassiliadis and Dimitroula Matsouka, IntechOpen, 29 August 2018.

Chorsi, M.T., Curry, E.J., Chorsi, H.T., Das, R., Baroody, J., Purohit, P.K., et al., 2019. Piezoelectric biomaterials for sensors and actuators. Adv. Mater. 31 (1), Wiley online library.

Freis, E.D., Kyle, M.C., 1968. Computer analysis of carotid and brachial pulse waves. Effects of agein normal subjects. Am. J. Cardiol. 22 (5), 691–695.

Ghosh, A., Edwards, D.J., Hosseini, M.R., Al-Ameri, R., Abawajy, J., Thwala, W.D., 2020. Real-time structural health monitoring for concrete beams: a cost-effective 'Industry 4.0' solution using piezo sensors. Int. J. Build. Pathol. Adapt ahead-of-print.

Gustafsson, F., 1996. Determining the initial states in forward-backward filtering. IEEE Trans. Signal. Process. 44, 988–992. April.

Hajar, R., 2018. The pulse from ancient to modern medicine: Part 3. Heart Views 19, 117–120.

Haji Rassouliha, A., Tang, E.J.L.P., Nash, M.P., Taberner, A.J., Nielsen, P.M.F., Cakmak, Y.O., 2019. Quantifying Carotid Pulse Waveforms using subpixel image registration. In: Nielsen, P., Wittek, A., Miller, K., Doyle, B., Joldes, G., Nash, M. (Eds.), Computational Biomechanics for Medicine. Springer, Cham.

Hirata, K., Yaginuma, T., O'Rourke, M.F., Kawakami, M., 2006. Age-related changes in carotid artery flow and pressure pulses: possible implications for cerebral microvascular disease. Stroke. 37 (10), 2552–2556.

Hou, Y., Wang, L., Wang, D., Yang, H., Guo, M., Ye, Z., et al., 2017. A preliminary study on the IoT-based pavement monitoring platform based on the piezoelectric-cantilever-beam powered sensor. Adv. Mater. Sci. Eng. 2017, Article ID 4576026, 6.

Huynh, Q.L., Blizzard, C.L., Sharman, J.E., Magnussen, C.G., Dwyer, T., Venn, A.J., 2014. The cross-sectional association of sitting time with carotid artery stiffness in young adults. BMJ Open. 4 (3), e004384.

Huynh, Q., Blizzard, C., Raitakari, O., et al., 2015. Vigorous physical activity and carotid distensibility in young and mid-aged adults. Hypertens. Res. 38, 355–360.

Joseph, J., Shah, P.M.N., Sivaprakasam M, M.I., 2018. Arterial compliance probe for cuffless evaluation of carotid pulse pressure. PLoS One 13 (8), e0202480.

Leitão, C., Bilro, L., Alberto, N., Fernando Antunes, P., Lima, H.F., Andre, P.S., et al., 2013. Feasibility studies of Bragg probe for noninvasive carotid pulse waveform assessment. Portugal, J. Biomed. Opt. 18 (1), 017006.

Mayo Foundation for Medical Education and Research. https://www.mayo.edu/research/clinical-trials/diseases-conditions/carotid-artery-disease.

McLaughlin, J., McNeill, M., Braun, B., McCormack, P.D., 2003. Piezoelectric sensor determination of arterial pulse wave velocity. Physiol. Meas. 24 (3), 693–702.

Mitra, S.K., 2001. Digital Signal Processing, second ed. McGraw-Hill, New York.

Mokhtari, S., Al Ahmad, M., 2019. Portable piezoelectric cardiac abnormality detection. Alex. Eng. J. 58 (3), 1053–1061.

Morris, D.C., 1990. Chapter 20: The Carotid Pulse. NCBI Bookshelf. A service of the National Library of Medicine, National Institutes of Health. In: Walker, H.K., Hall, W.D., Hurst, J.W. (Eds.), Clinical Methods: The History, Physical, and Laboratory Examinations, third ed Butterworths, Boston, Bookshelf ID: NBK312.

Nabeel, P.M., Karthik, S., Joseph, J., Sivaprakasam, M., 2017. Measurement of carotid blood pressure and local pulse wave velocity changes during cuff induced hyperemia. Conf. Proc. IEEE Eng. Med. Biol. Soc. 2017, 1700−1703.

Oppenheim, A.V., Ronald, W.S., John, R.B., 1999. Discrete-Time Signal Processing, second ed. Prentice-Hall, Upper Saddle River, NJ.

Qin, L.W., Qin, L.H., Yu, Y., Hou, X.W., Wang, C., Weeks, C., 2020. Impact of early diagnosis of carotid artery stenosis by carotid ultrasound: a protocol of systematic review and meta-analysis. Medicine (Baltimore) 99 (22), e19709.

Qing, X., Li, W., Wang, Y., Sun, H., 2019. Piezoelectric transducer-based structural health monitoring for aircraft applications. Sensors 19, 545.

Rangayyan, R.M., 2015. ISBN: 978-0-470-91139-6 August Biomedical Signal Analysis, second ed. Wiley-IEEE Press, p. 720.

Reesink, K.D., Hermeling, E., Hoeberigs, M.C., Reneman, R.S., Hoeks, A.P.G., 2007. Carotid artery pulse wave time characteristics to quantify ventriculoarterial responses to orthostatic challenge. J. Appl. Physiol. 102, 2128−2134.

Soleimani, E., Mokhtari-Dizaji, M., Fatouraee, N., Saberi, H., 2017. Assessing the blood pressure waveform of the carotid artery using an ultrasound image processing method. Ultrasonography. 36 (2), 144−152.

Srivastava, S., Bhalla, S., Madan, A., 2017. Assessment of human bones encompassing physiological decay and damage using piezo sensors in the non-bonded configuration. J. Intell. Mater. Syst. Struct. 28 (14), 1977−1992.

St. John's Mercy Health Care, Tests & procedures, carotid artery duplex scan. <https://www.mercyhealth.com/find-a-service-or-specialty/heart-and-vascular-care/vascular/testing/carotid-duplex>.

Stoner, L., Kucharska-Newton, A., Stoner, K., Zieff, G., Dave, G., Fryer, S., et al., 2020. Associations between carotid-femoral and heart-femoral pulse wave velocity in older adults: the Atherosclerosis Risk in Communities (ARIC) study. J. Hypertens. 38 (9), 1786−1793. September 2020.

Thorin-Trescases, N., de Montgolfier, O., Pinçon, A., et al., 2018. Impact of pulse pressure on cerebrovascular events leading to age-related cognitive decline. Am. J. Physiol. Heart Circ. Physiol 314 (6), H1214−H1224.

Uğuz, H., Kodaz, H., 2010. Classification of internal carotid artery doppler signals using Hidden Markov Model and Wavelet Transform with Entropy. In: Papasratorn, B., Lavangnananda, K., Chutimaskul, W., Vanijja, V. (Eds.), Advances in Information Technology. IAIT 2010. Communications in Computer and Information Science, vol. 114. Springer, Berlin, Heidelberg.

Universal Real-time Software Oscilloscope GUI DLL Library <https://sites.google.com/site/brnstin/>.

Walker, H.K., Hall, W.D., Hurst, J.W,. (Eds.) 1990. Clinical Methods: The History, Physical, and Laboratory Examinations. Third ed. Butterworths, Boston, Copyright 1990, Butterworth Publishers, a division of Reed Publishing.

Winchester, C.C., Chou, N.Y., Winchester, L.W., 2007. Examination of pressure and volume pulse waves. Artery Res. 1 (2), 63−64.

Wolff, T., Guirguis-Blake, J., Miller, T., Gillespie, M., Harris, R., 2007. Screening for carotid artery stenosis: an update of the evidence for the U.S. Preventive Services Task Force. Ann. Intern. Med. 147 (12), 860−870.

Yasmin, Brown, M.J., 1999. Similarities and differences between augmentation index and pulse wave velocity in the assessment of arterial stiffness. QJM. 92 (10), 595−600.

Yu, A.H., Cohen-Solal, E., Raju, B.I., Ayati, S., 2008. An automated carotid pulse assessment approach using Doppler ultrasound. IEEE Trans. Biomed. Eng. 55 (3), 1072−1081.

Zhang, Y., Wang, W., Fang, Q., 2020. Clinical study of the stent forming for symptomatic internal carotid artery stenosis. Medicine. 99 (25), e20637.

4

Real-time detection and processing of electromyography signal

4.1 Introduction

Electromyography (EMG) is a diagnostic technique that gives a measure of our muscle health status and also of the nerve cells controlling them. A quantifiable and recordable electrical impulse representing neuromuscular activities is generated during muscle contraction or relaxation that gets propagated via neighboring tissues and bones. This process of muscle movement is initiated in the cerebral cortex of the brain which signals the spinal cord to trigger a muscle through the motor neurons. Beginning from the upper motor neuron, the signal is transmitted to the lower motor neuron through axons, which actually innervates the muscle and causes release of ions, and a corresponding tension is developed in the muscle which can be detected as the change in current during EMG. This current generates a transmembrane potential which is the variance in the potentials on the inside and outside of the muscle cell membrane. When muscles are not contracted, that is, when they are in quiet state, then potential of the cell membrane is polarized. During polarization, the potential difference present is termed as the resting potential. When the muscle cell is excited, depolarization occurs and is spread across. A corresponding action potential is developed which is termed as the electromyography signal. The detailed process of EMG signal generation is represented in Fig. 4−1.

Motor Unit is the smallest functional element consisting of dendrites of the motor-neuron cell body, several branches of the axon and fibers of the muscle that controls muscular contraction as shown in Fig. 4−1A. Entire muscle fibers in a motor unit behave like “one unit” during the innervation process, hence the term. At the membrane of the muscle fiber, an ionic equilibrium is maintained between the inside and the outside muscle cell during resting potential. It is around −70 mVolts during noncontraction. As depicted in Fig. 4−1B and C, an exchange of sodium (Na+) and potassium (K+) ions takes place across the membrane giving rise to an action potential. This is due to the change in the permeability of the nerve membrane. When the Na+ ion influx exceeds the threshold level (normally set to −55* (The * indicates that it is the threshold level as in the Fig, 4−1D) mVolts), depolarization occurs making the action potential to reach +30 mVolts as shown in the Fig. 4−1D.

During voluntary muscle contraction, action potentials begin to appear and on increasing the muscle contraction strength, more muscle fibers generate action potentials giving rise to a pattern that can be recorded. The summation of electrical activity of these motor units is defined as the Motor-Unit-Action-Potential (MUAP) and may be detected by placing

Real-Time Data Acquisition in Human Physiology. DOI: https://doi.org/10.1016/B978-0-12-822118-1.00005-9
© 2021 Elsevier Inc. All rights reserved.

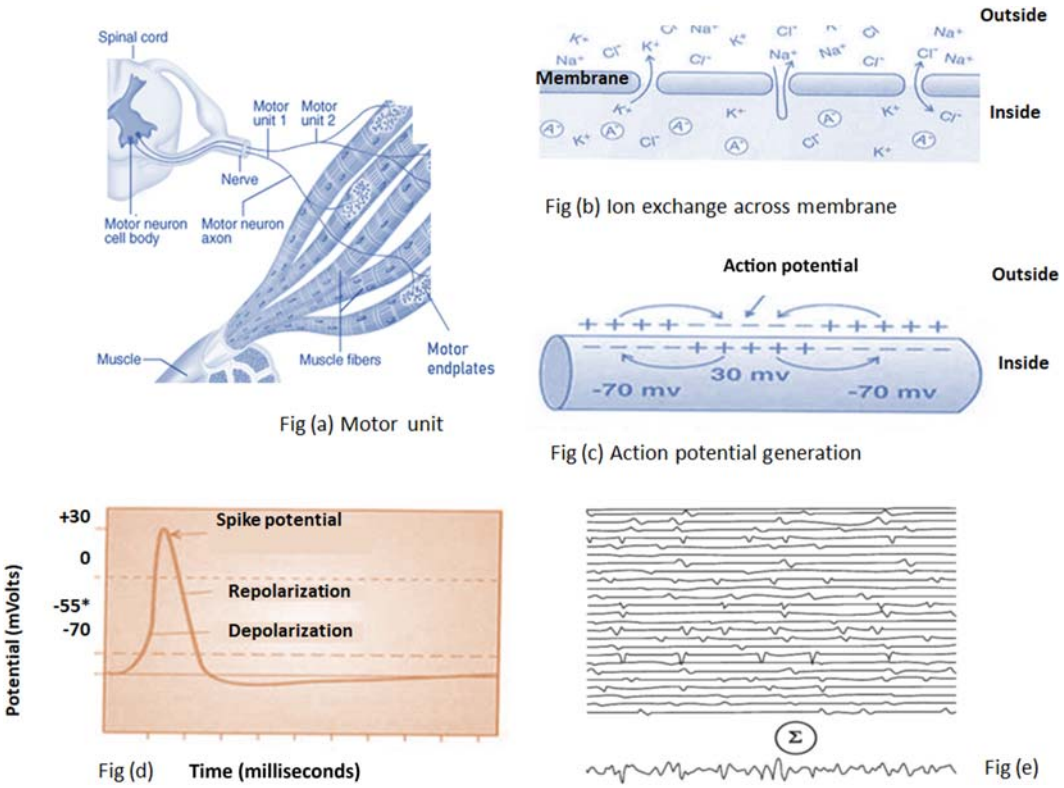

FIGURE 4–1 Representation of EMG Signal Generation Process. Photo created by *Benjamin Cummings*, Addison Wesley Longman Inc. *2001*.

electrodes on the muscles sites. Fig. 4−1E depicts the superposed EMG signal resulting by summing the MUAPs of all the active motor unit that are detected by the electrodes and is called as surface EMG. This electro-physiological action achieved from numerous motor units is studied during EMG signal analysis. Location of muscle groups to be detected decide whether EMG data is to be recorded from the surface or using fine wires that are inserted into deep muscles for intramuscular measurements.

Neuromuscular muscle activation under different movement and health conditions, tasks and training regimes can be classified into isotonic and isometric muscle contraction analysis. Whereas isotonic measurement analysis is performed for athletes and strength assessment, the isometric analysis is done during rehabilitation. A force is generated during isotonic muscle contractions due to change in muscle length because of joint movements or bicep curl, which is called concentric when the muscles shorten and is termed as eccentric contraction when they elongate. In contrast to isotonic contractions, force is generated during isometric contractions due to fluctuating tension and energy in static mode when the angle of joint or length of muscle does not vary. Isotonic and Isometric measurement analysis finds wide application in clinical

domains for classification of neuromuscular disease diagnosis, assistive control, lower limb orthosis, exoskeletons or for assessing the muscle fatigue (Subasi, 2013; Rogers and MacIsaac, 2013; Rechy-Ramirezn and Huosheng, 2015; Yan et al., 2015). Various application domains of EMG signal analysis is described in the section below.

4.1.1 Application areas of electromyography signal analysis

EMG signals (measured in microvolts) provide information on the number and amount of muscle contraction and can also reveal additional information on muscle performance or disorders, nerve dysfunction or nerve to muscle signal transmission problems. Symptoms like tingling, numbness, muscle weakness, pain, or cramps may indicate a nerve or muscle disorder [mayoclinic]. Classic benefits of EMG signal identification and investigation include decision making during pre and postsurgery, muscle training schedules, improved sports performance, biomechanics, posture control and even in detecting the muscle response in ergonomics. EMG signal identification and exploration is used in numerous clinical and non-clinical applications which includes triggering of control indication for prosthetic devices as well. Various application areas of EMG signal processing and analysis is given in Fig. 4—2 and is detailed in subsequent section.

Major applications include decision in a clinical scenario like rehabilitation post orthopedic surgery, stroke, or neurological disorder. A check on muscle status is required in such cases to monitor the motor function recovery and progress (Teasell et al., 2003). EMG recording monitoring have long been used and established in sports science and for rehabilitation of sports damages (Guissard and Hainaut, 1992; Lamontagne, 2001; Dimitrova and Dimitrov, 2003; Reaz et al., 2006; Massó et al., 2010; Maffiuletti et al., 2016). Blogger Christopher Glaeser reiterates that sports performance coaches and sports injury treatment

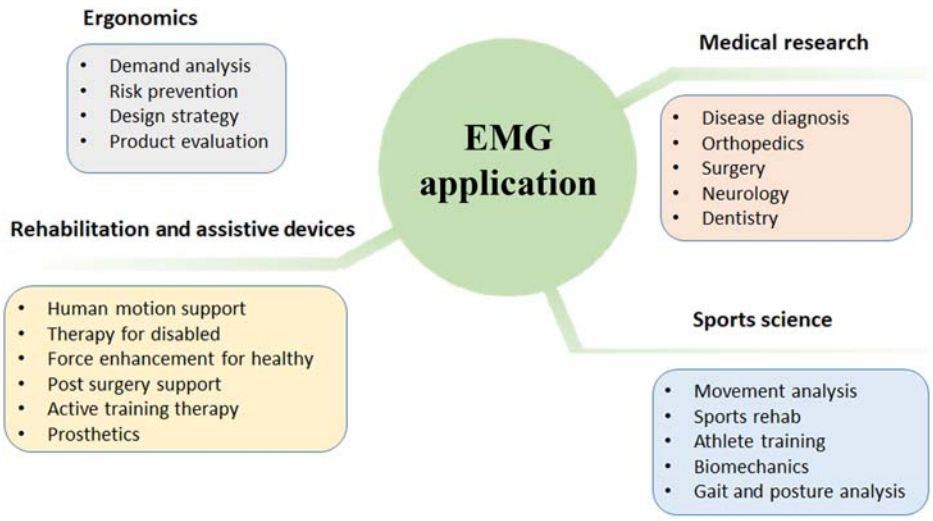

FIGURE 4–2 Application areas of electromyography (EMG).

specialists have trusted EMG signal data to offer hints and intuitions regarding muscle actions during sports events and exercises. To support the disabled in a rehab training center and also to enhance muscle strength in healthy subjects, Exoskeleton Robots are used that are mechanical extensions attached to a human body to manipulate human motion. Fleischer et al. have deployed exoskeleton in the knee joint of a patient and have also demonstrated its effective use for a human hand having 16 actuated joints to influence the finger movement (Fleischer et al., 2006). Cases of chronic pain which may be caused postsurgery or may be due to over exercise, wrong movement, improper posture or sports injury also require EMG assessment for proper diagnosis and treatment (Zech et al., 2009). Surface EMG (sEMG) recordings are used in diagnosing abnormalities, are utilized as biofeedback for rehabilitation and also finds application in physiotherapy, dentistry for sleep bruxers, fatigue evaluation and biomechanics, etc. (Amorim, 2009; Amorim and Marson, 2012, Cifrek et al., 2009). EMG recordings may also indicate cognitive behavior in a subtle manner. Correlation between the EMG and Electroencephalogram (EEG) signal features like the frequency and the phase indicate the ability of EMG data to assist monitoring of cortical information (Wu et al., 2013).

Cardiovascular diseases or blood disorders also can be addressed by EMG analysis through exercise-based cardiac rehabilitation where muscle activities and progress needs monitoring (Anderson et al., 2016). Al-Timemy et al. have investigated impact of variable force level for achieving robust control of a prosthetic limb for hand using electromyogram of the amputees (Al-Timemy et al., 2016). Control Bionics have developed a device called NeuroSwitch which is a boon for people with loss of speech and with severe disabilities like acute injury of spinal cord, motor neuron illness, or cerebral palsy. NeuroSwitch provides an advanced, easy to use and effective assistive solution to control and communicate with the surroundings making use of human EMG signals. Sensors deployed in the NeuroSwitch effectively picks even the slightest of muscle movement even if the subject is unable to see or feel the movement. The signal after amplification and filtering reaches the computer attached and allows prediction of words and has the capability to convert text to speech. This makes the user feel connected with the world (Megan Turek, 2017).

Just like EMG helps in assessing motion, fEMG is the facial EMG that is picked from face muscles which finds applications in various domains of medical research specially in rehabilitation, movement control and in diagnosing neuromuscular disorders like Parkinson's, stroke, emotions in patients with Autism, etc. Lately, fEMG has been used in market survey, web usability, augmented reality, virtual reality (AR-VR) and gaming as well due to their ability to sense subtle muscle movements (Jessica Wilson, 2018). Scano et al. have systematically reviewed application of EMG signals in a clinical setting (Scano et al., 2019). Recent studies reveal that EMG signal recordings during isometric exercises enable identifying subtle gestures based on static muscle contraction that are motionless to control prosthetic devices and also to generate control signals to trigger electronic gadgets. Flight systems are also being controlled using EMG signals based gestures to trigger the switches and the controls. Research Group at the NASA Ames Research Center at Moffett Field, have used EMG signals to actuate the joysticks and keyboards in a man−machine interface setup. Patients without

vocal cords can be assisted with a EMG based system to recognize their speech based on muscle movement pattern. Facebook in the year 2019 acquired a startup company "CTRL-Labs" which was developing a wristband that had the potential to read minds using EMG signals. Technological advancements in the field of AR-VR has truly transformed the way we are connected (Statt, Nick, 2019). Sophisticated prosthetic limbs have been developed using deep learning approach with EMG control to prove the end-to-end optimization concept (Jafarzadeh et al., 2019).

Interpretation of subject's intentions and physical status in diverse rehabilitation scenarios can be monitored using EMG. Researchers are developing multiple sensor fusion (kinetic and kinematics) based EMG pattern recognition techniques that demonstrate its ability to accurately control prosthetics and locomotion detection (Fang et al., 2020). Pain in the lower back is a very common issue caused due to strenuous ligaments, joints or muscles, poor muscle motor control or an injury. Research indicates correlation between chronic lower back pain with delayed muscle activation which makes the spine vulnerable to pain and injury which can be controlled by monitoring EMG signal patterns to restore muscle balance and control (Ullrich, 2020; Sandoval, 2010). Kobylarz, Jhonatan et al. have presented a learning method to classify gestures like thumbs up/down, using the electromyographic dataset collected using an armband so as to be connected with a machine in a nonverbal fashion (Kobylarz et al., 2020).

4.1.2 Investigation of electromyography signal measurement

The amplitude of raw EMG waveform oscillates between 0.5 and 10 m-volts and the spectral range varies between 0.05 and 500 Hz. For detection and better viewing and analysis, the raw EMG signal requires to be amplified, filtered, and digitally processed. EMG measurement is done either using electrodes that are invasive or can be picked from the muscle surface using noninvasive surface electrodes. Inherent advantages of invasive process are the precision of information gathered about muscle movement and condition, however it is unrealistic and not so popular because it requires insertion of needle electrodes inside subject's muscles. The noninvasive procedure of using surface EMG electrodes are more prone to noise and not so precise, as the MUAP taken is contaminated by bodily fat, movement of skin, motion of nearby muscles, EM noise, etc.

Upgradation in instrumentation for acquiring, processing, and transmitting noise free EMG signal are continuously being researched. Progression in DSP techniques and reduction in size of instrumentation involved has permitted the expansion of improved, cost-effective, wearable and superior EMG detection and analysis methods. Recent research has validated the deployment of a low cost and reliable EMG device well-suited for acquiring muscle information during a task or an exercise (Toro et al., 2019). Wearable technology embedded with machine learning techniques has enabled development of cost-effective 3-D printed arm bands that can capture human intent and gestures effectively (Côté-Allard et al., 2019). State of the art sensor technology with ultra-low power filtering capacity has been established for the detection of EMG signal for prosthetic control and to help an amputee with a better

quality of life (Roland et al., 2019a,b). Machine learning has become an integral part of our day to day life. Utilizing the mathematical capabilities of the technique, real-time hand gesture identification device has been developed using surface EMG (Jaramillo-Yánez et al., 2020). The hardware instrumentation blended with signal processing techniques can truly help in setting up communication between man and machine.

4.2 Signal processing the electromyography data

Being sensitive, EMG signals are vulnerable to noise and artefact contamination and so require sophisticated signal processing techniques to remove them. The cause of noise interference varies from being due to the skin electrode interference, the hardware itself, the power line hum, improper placement of electrode, or an external disturbance. The complex EMG waveform when gets influenced by noise makes it very difficult to analyze and classify them. Therefore it becomes very important to preprocess the EMG signal data for noise removal. Noise types that disturb the signal waveform may be the inherent noise present in the acquisition electronic arrangement, the ambient noise, baseline shifts or offset, artifact due to motion, Electrocardiography (ECG) interference, or crosstalk (Reaz et al., 2006; Chowdhury et al., 2013; Nazmi et al., 2016). A brief picture of typical noise kinds is presented below.

The EMG waveform is a quasi-random signal having a spectral range between 0 and 20 Hz. Influenced by the motor unit firing rate, they exhibit instability (Reaz et al., 2006; Chowdhury et al., 2013). The active motor units, firing rates and interacting behavior among the fibers of the muscle affect the information content of the EMG signals.

Electronic modules that make the EMG acquisition unit generate inherent noise that cannot be reduced completely nonetheless can be resolved using top notch electronic modules. Recordings made with Ag−AgCl electrodes render sufficient SNR and is electrically stable in nature. With large electrode size, impedance can be adjusted. So, this noise can be eliminated by using cutting edge technology in electronic circuit design.

Intelligent electronic design addresses many noise interference, but is unable to cater to the disturbance in the low frequency spectra in the range 1−10 Hz of the EMG signal, for example, the motion artifact (Reaz et al., 2006; Chowdhury et al., 2013). Activated muscles reduce in length and the skin, muscles and electrodes move with respect to each other. Thus motion artifact develops due to muscle movement beneath the skin at the interface with the electrode, causing a voltage which varies with time across the placement of electrodes. A solution to this has been proposed using a Butterworth filter design having a 20 Hz corner frequency and 12 dB/octave slope (Fratini et al., 2009; De Luca et al., 2010; Shair et al., 2017). Recessed electrodes having a layer of conductive gel amid the skin surface and the interface between electrode and electrolyte can also help in reducing the motion artifact considerably.

Auto calibration of the measurement device is done using “offset correction” function before making the recordings. This is required because a shift in the baseline can appear if the subject is not relaxed during measurement or if the electrode placement site is disturbed.

An EMG signal waveform generally returns to a base line zero in just few milliseconds and so any noticeable shift of more than 5 milliseconds indicates noise interference. The prime cause for such a disturbance is due to improper cable fixation (Konrad, 2005).

Ambient noise is caused due to 50/60 Hz power line interference as a result of EM radiation from power sources. The EMG amplifier circuit catches ground noise from the power source. To avoid this hum, all devices must be properly grounded. This becomes necessary in case of applications like treadmills, training devices, isokinetic machines, etc. that are fitted with electrical motors. Multiple plug arrangement while measurement can also lead to humming noise and must be avoided. A HPF can be designed to remove this effect, provided the interfering frequency is of the same range.

When EMG signals are to be detected from the areas close to the heart like the shoulder or trunk muscles, it can get mixed up with the ECG signals and can lead to misinterpretations. This is a result of a natural biological phenomenon that is difficult to avoid. Signal processing algorithms helps in cleaning the traces of ECG signals from the EMG signals. EMG electrode placement depends on the muscle group selected for detection and in turn decides the level to which the EMG will be corrupted by ECG. The spectral components of both the bio-signals intersect and furthermore because of their nonstationary behavior it becomes difficult to segregate the ECG artifacts from EMG signals. Recursive Least Square Adaptive Filters have been tested that can remove ECG effect in a reliable manner and maintains the EMG characteristics. Independent Component Analysis (ICA) also helps in removing the traces of ECG signal from the muscle recordings. The filtering technique is more effective when both the bio-signals are statistically independent (Butler et al., 2009; Lu et al., 2009a,b; Willigenburg et al., 2012).

A not so common noise that generally goes unnoticed while detecting EMG signals is the cross talk can lead to misinterpretations. Crosstalk may be reduced through right selection of electrode size and by maintaining gap between the interelectrodes to around 1−2 cm or to around their radius. Crosstalk can be effectively decreased by selecting electrodes having a smaller surface area.

It is very obvious that robust prior processing procedures are required to reject the effect of these interference in EMG signal so that proper interpretations and analysis can be done. To permit standard and automated classification and feature extraction of EMG signals to enable accurate and reliable solution to rehabilitation, neurophysical and assistive technologies many signal processing techniques have evolved.

Use of EMG signal for automated diagnostic analysis and interpretations, control applications or for developing assistive devices requires processing through following stages:

- Preprocessing | Segmentation of data, windows and filtration
- Feature-extraction
- Classification

Raw signal acquired is first segmented and then post filtration and rectification, a set of features are extracted for final classification and selection (Nazmi et al., 2016). For real-time applications, it is necessary to obtain small data segments of the EMG signal. Windows are designed for the purpose to optimally clip the bio-signal. Length of EMG data

and the windowing technique (both adjacent and overlapping) used are therefore of prime importance during data segmentation. EMG signals are identified to be wide-sense Gaussian random process (Hudgins et al., 1993). Researchers have identified that varied length of data segment is a performance assessment parameter for classification and if the length is less than 128 ms, it may cause high bias and variation in the extracted features, whereas if the length is in the range of 125−500 ms, the classification accuracy improves (Farina and Merletti, 2000; Englehart and Hudgins, 2003; Huang et al., 2011; Matsubara and Morimoto, 2013). Larger data segments provide supplementary facts about feature estimation and hence offer improved accuracy during real-time applications for prosthetic control (Englehart et al., 2001; Ahmad, 2009). Therefore a trade-off is suggested in the window range 150−250 ms to maintain accuracy in EMG signal classification and the delay, and a length of 100−250 ms is recommended for mechanical sensors (Long et al., 2016). Time response is also required to be fast for continuous classification purpose (Huang et al., 2008).

After the data has been segmented, it requires filtration of the noise that disturbs the EMG signal. Neuro Fuzzy systems have been implemented to design band-pass filters of cut-off frequency range 20−500 Hz to address motion artifacts for characterizing arm actions (Balbinot and Favieiro, 2013). Elimination of ECG interference from surface EMG data has been reliably and efficiently done by designing adaptive band-pass filters (Lu et al., 2009; Yeom and Yoon, 2012). Improvements in the adaptive filter technique using subtraction method presents better resuls in removing ECG traces from the EMG data (Abbaspour et al., 2014). A lot is still being explored to devise intelligent signal processing techniques to eliminate noise interference from EMG Signals. The complete process includes feature extraction and classification. Fig. 4−3 gives an outline of the EMG signal processing methods which have been developed over the years for feature extraction and classification.

Bio-signals exhibit time varying characteristics and so are nonstationary in nature. For the purpose of analyzing these biological signals, they are supposed to be stationary over a small interval of time. This however does not apply to every situation and hence techniques have been evolved to process the nonstationary signals, specifically the EMG signals. Depending on the kind of parameters being analyzed, the approch is categorized as parametric and nonparametric (Zhan et al., 2006; Korŏsec, 2000; Morren et al., 2002). The preprocessing stage eliminates inappropriate information from the signal detected and thereby enhances those features that are required to be extracted. For subsequent analysis and control, suitable biomarkers are extracted using spectral analysis methods which is a nonparametric approach. This method presents a limitation of not knowing the useful signal features to be preserved in advance during preprocessing and so the analysis begins from the spectral analysis stage and avoids preprocessing. This issue can be resolved utilizing the parametric approach that includes the preprocessing and the spectral analysis stage as well and is based on signal modeling methods like AR or ARMA model (Sakkalis et al., 2008).

The approach to spectral analysis in parametric methods involve data modeling for the output of a linear system instead of direct calculation of power spectral density (PSD). Generally, an all-pole linear system filter model having all its zeros at the origin in Z-plane is used. When the

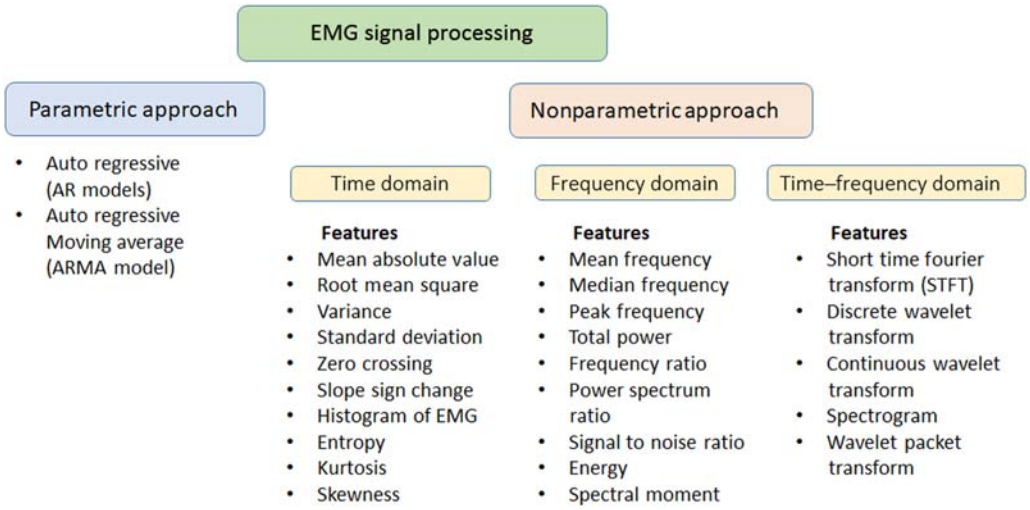

FIGURE 4–3 An outline of EMG signal feature extraction and classification methods. *EMG*, electromyography.

input to this system is a white noise, then the output obtained represents an autoregressive (AR) process and hence named as AR model. Linear set of equations are required to be solved in AR model which is a simpler task and the resolution achieved for short signal data length is higher as compared to nonparametric methods. AR models effectively assist in defining the PSD data that are large at certain frequencies and so find application in speech processing. The AR spectral estimation methods include:

- Yule-Walker method (Autocorrelation method)
- Burg method
- Covariance method
- Modified covariance method

Only Yule-Walker technique applies Windows to data. The Yule-Walker and Covariance methods minimize only the prediction error in forward direction in the least square method. The Burg and Modified version of Covariance techniques minimize prediction errors in both the directions. The Burg and Yule Walker methods always give a stable model compared to the rest [MATLAB Documentation].

The nonparametric approaches, generally includes Short-Term-Fourier-Transform (STFT), spectrogram, and wavelet transforms and do not require parameters to be known in advance for spectrum estimation. The signal analysis of the EMG signal for motion pattern recognition may be performed in time, frequency, and time−frequency domains (Hogan and Mann, 1980; Englehart et al., 1999; Oskoei and Hu, 2007; Tsai et al., 2014; Nazmi et al., 2016). The features analyzed in these domains are depicted in Fig. 4−3. The simplest of all is the Time Domain feature analysis of EMG signal, where the amplitude varying w.r.t time is analyzed for different muscle contractions and conditions. Frequency Domain features include the PSD study.

A combination of both time and frequency features are analyzed using Time−Frequency Domain which has the capability of presenting a lot of relevant information about the nonstationary data.

Time-Domain (TD) parameters that assist in extracting EMG signals for classification include Mean-Absolute-Value (MAV), Zero-Crossing (ZC), Slope-Sign-Change (SSC), Root-Mean-Square (RMS), Standard-Deviation (SD), Waveform-Length (WL), Variance (VR), etc. as depicted in Fig. 4−3 (Hudgins et al., 1993; Ahsan et al., 2011).

These TD features have been used by researchers to analyze dynamic and static arm movements of amputee, hand movements, load lifting strength, etc. (Tsai et al., 2014; Ahsan et al., 2011). RMS gives a quantitative measure of muscle movement for each channel and serves as an input to the classifier algorithm (Balbinot and Favieiro, 2013). Sophisticated TD features like Fuzzy Approximate Entropy and Maximum Voluntary Contraction are being investigated to examine the intricacies of EMG data obtained from automatic robotics supported rehab patients (Sun et al., 2014). Features like Skewness and Kurtosis have been employed for testing prosthetic hand applications (Oskoei and Hu, 2007). Use of Moving Approximate Entropy has exhibited promising results in identifying muscle contraction stages for clinical applications (Ahmad, 2009). RMS performs to be the best in comparison to other TD features like MAV, ZC, SSC, WL for electrode pair identification (Kendell et al., 2012). A lot of TD features are being explored to identify facial muscle gestures, EMG signal characteristics like periodicity, power amplitude, etc. (Hamedi et al., 2012; Al-Mulla et al., 2011).

Frequency-Domain (FD) parameters are also studied for recognizing motion patterns for assessing muscle fatigue primarily for analyzing motor-unit recruitment (Al-Mulla et al., 2011). Various FD features include Mean, Median and Peak frequencies, power, energy, frequency ratio, PSD, SNR, etc. as shown in Fig. 4−3. EMG characteristics relating to muscle contractions can be indexed using conventional FD features like PSD, Mean, Median, and Peak frequencies (Merletti, 1997). For clinical applications, such as in cases of survivors of a stroke, the neuro-muscular signals analyzed in spectral domain using Mean Power Frequency can provide great insights (Li et al., 2014). Modification to standard FD features by evaluating the mean and median of the amplitude-sprectrum instead of power-spectrum is termed as modified-mean frequency and modified-median frequency (MMNF and MMDF) that yields robust information on muscle fatigue (Phinyomark et al., 2009).

Numerous research study has been done for comparison between the TD and FD parameters for EMG signal analysis. Smaller dimensions and faster speed could be achieved with TD features, but the classification performance was not found adequate for upper limb movement pattern recognition (Tsai et al., 2014). There has been an indication of difference in TD features in case of isometric and isotonic muscle contractions which can be useful in strategizing prosthetic control applications (Lorrain et al., 2011). TD features also prove out to be more reliable compared to FD features in selecting the electrode pair combination and for long-term analysis (Phinyomark et al., 2013; Kendell et al., 2012). However, the basic assumption in TD analysis is that they adopt the bio-signal like a stationary waveform, that is incorrect for EMG signal analysis and therefore pose a limitation. The four motion EMG patterns cannot be accurately identified using TD features, but when both the domains are combined into a feature vector the results are satisfactory (Oskoei and Hu, 2006).

Time−Frequency-Domain (TFD) parameters can be of great help in our quest to improve the EMG classification precision. The features comprise STFT, Wavelets, Spectogram, etc., as summarized in Fig. 4−3. The classification error has been claimed to be reduced to 6.25% using TFD features using Wavelets in comparison to TD features at 9.25% for the upper limb classification analysis (Englehart et al., 1999). During TFD feature analysis, the energy is localized in both time and frequency domains, thus permitting precise depiction of the EMG signal characteristics (Basu et al., 2008; Guo and Kareem, 2016). Feature extraction using TFD parameters is a complex task and it leads to increased dimensions and large resolution of feature vectors (Chowdhury et al., 2013). It is therefore required to work on maintaining a balance between the dimensionality and the classification ability. Dimensionality reduction has been implemented using feature projection and selection strategies (Englehart, 1998; Ahmad, 2009; Rechy-Ramirezn and Huosheng, 2015). Feature projection approaches evaluate the finest grouping of the original features to create new feature sets whereas in the selection method, the best subset is chosen based on the application need (Oskoei and Hu, 2007; Rechy-Ramirezn and Huosheng, 2015). TFD features require additional computation time and the selection of a feature vector must to be sensibly measured.

4.3 Real-time detection and processing of electromyography signal in single channel mode

The block diagram representation of a convenient and transportable arrangement for detection of human EMG information in real-time single channel mode is sketched in Fig. 4−4. The instrumentation comprises surface electrodes (Ag−AgCl), cascaded amplifiers and filter module, mono duplication interfacing jack, 9 and 1.5 Volt battery and a computer. The silver−silver chloride (Ag−AgCl) electrodes pick the EMG signal from the bicep muscle movement and the front end section amplifies and filters the detected signal. The front-end of amplifier module has buffer amplifiers, unity-gain follower, DC-restoration circuit, right-leg drive, feedback integrator, and the power management section. Texas instrument's operational amplifier TL-084C is used to implement the front end design. The Common-Mode-Rejection-Ratio (CMRR) of the op-amp IC chip used is 86 decibels (dB) and its gain can be adjusted up to 500 times. The right leg drive circuit used as the feedback body reference further improves on the CMRR. The active integrator filter eliminates the interference picked during the acquisition process. The amplified and clean signal is acquired on a Laptop through the single channel sound port and is viewed and processed on MATLAB based virtual oscilloscope for further analysis. Details of each block is presented in subsequent sections.

4.3.1 Silver−silver chloride surface electrodes

Silver−Silver Chloride electrodes are most commonly available and are considered to be the finest performing of all the electrode types for bio-potential measurement like ECG, EMG, EEG, Electrooculography (EOG), etc. The prime advantage lays in the fact that it allows low noise level generation during signal measurement. Compared to other electrodes, specially the stainless steel ones, they offer low skin-electrode interface impedance. They are

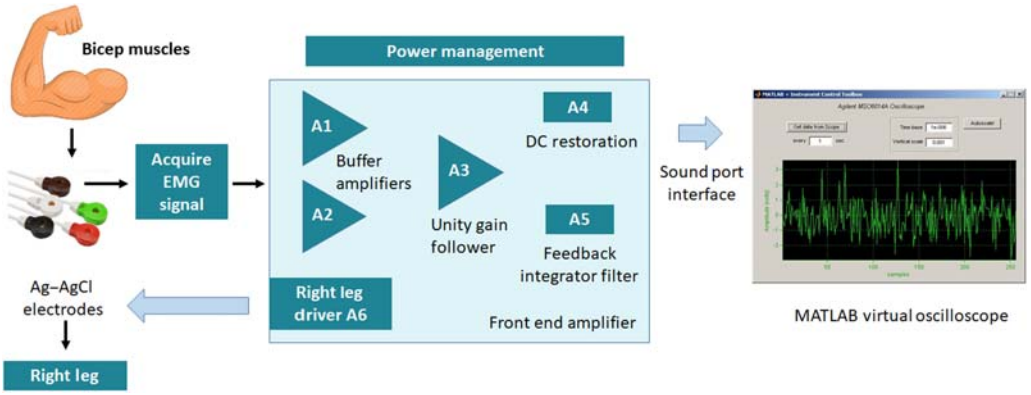

FIGURE 4–4 Block diagram representation | Real-time detection of EMG signal in single channel mode. *EMG*, electromyography.

inherently nonpolarizable electrodes; which means that the electrode−electrolyte junction does not allow charge concentration due to current flow through the electrode. This makes it a stable electrode for bio-potential recordings. The silver chloride layer between the silver layer and the electrolyte further has a stabilizing effect at the junction and helps in reducing noise. The electrodes that are sintered exhibit highest stability compared to plated ones.

BIOPAC deals with reusable Ag−AgCl electrodes for measuring bio-potentials with a series of surface or snap types. The prime features incorporated are that they are sintered, nonpolarizable, do not need chloriding, can be reused, offer high stability and minimizes artefact due to electrolyte−electrode motion. During long-term monitoring, they reduce electrolyte dissipation thus avoids drying. These electrodes are the front element of a complete data acquisition and analysis system and have been used in this arrangement.

The Silver−Silver Chloride electrolytic gel is further applied on the skin surface to decrease the skin-impedance and allows improved flow of current. These Electrodes used for sensing bioelectric potentials convert ionic-flow within the body via an electrolyte into electron-current and thus a potential can be detected. Metal is used to make these Electrodes. The Ag−AgCl electrode is electrochemically stable and consists of silver, with a jelly like electrolyte containing chloride-ions as the principle anion. This sensor is fabricated by electrolyzing a silver-plate as an anode in Sodium chloride aqueous solution to form a AgCl film on the silver surface. The reaction is given in the equation below.

$$Ag^{+} + Cl^{-} \leftrightarrow AgCl\downarrow$$

The sensor used is capable to detect low-amplitude EMG signals ranging 0.05−10 mV, has extremely high input-impedance (>5 Mega-ohms), extremely low input-leakage current (<1 micro-Amp), a frequency response that is flat in the range 0.05−150 Hz and High CMRR. The half-cell potential of Ag−AgCl electrode is around 0.22 volts higher than that of the hydrogen electrode, which is 0 volts. This half-cell potential varies based on the

conducting electrolyte type. If the electrolyte has saturated ionic concentration, then the half-cell potential reduces to about 0.20 volts and it increases to 0.27 volts with seawater. Use of two Ag−AgCl electrodes for recording, cancels the half-cell potentials and improves the measurement (https://alanmacy.com/books/the-handbook-of-human-physiological-recording/chapter-4-electrodes/; Das and Webster, 1980; Geddes and Roeder, 2001; Mcadams, 2006).

4.3.2 Front-end amplifier and interface unit

EMG signals acquired from the bicep muscles is in the amplitude ranging between 0.5 and 10 m-volts. Hence for suitable detection and analysis of the bio-signal 500 times amplification is required. If single stage DC-coupled high gain amplifiers are used to address the issue, they tend to get saturated after limited measurement. This happens due to large offset voltage of the electrode compared to low amplitude level of the EMG signal. Designs made using series capacitors and ground resistors to provide a bias path along with AC-coupling can salvage this saturation to some extent. Using resistors however degrades the CMRR. Cascade amplifier setup can help in preventing saturation of single stage amplifiers and so has been used in this experimental set up as depicted in Fig. 4−4.

The front end amplifier and filter section is designed using Texas Instrument's Operational amplifier TL-084C. The TL-08xx family of op-amps offer a wide spectrum of selection and consist of high-voltage JFET and bipolar transistors in a monolithic IC. Features include High Input Impedance, high slew rate (rate at which the op-amp changes its output with a change in the input) of 13 V/μs, lower input-bias current (30 pA), lower input-offset current (5 pA), output-short-circuit protection and lower offset-voltage temperature coefficient. The Total Harmonic Distortion is low around 0.003% which is a desired attribute in audio signal applications. Their power consumption requirement is low and they possess a wide common mode. The CMRR of the op-amp IC chip is 86 decibels (dB) and its gain can be adjusted up to 500. [TL08xx JFET-Input Operational Amplifier datasheet (Rev I)].

Blocks A1 and A2 in Fig. 4−4 representing the input stage buffer amplifier are fixed to a lower gain of multiplier 10 individually. Stages A3 and A4 are the unity gain amplifier and the dc restoration amplifier respectively. Setting the gain of dc restoration amplifier to 50 supports elimination of the dc-offset. The whole gain therefore results in 500 times amplification. The arrangement amplifies only the ac component of the detected EMG signal as desired. To prevent the amplifier output from further increasing, a −ve voltage from the active feedback integrator A5 is designed. The −ve feedback continues to influence till the output-offset at A4 becomes nil. Active integrators are utilized in the design due to the inherent advantage they possess of being linear and easy to control as compared to their passive counterpart. There are three electrodes placed on the body surface to detect the EMG signal. Two are at the bicep muscles and one is at the right leg. A right leg driver circuit A6 is also designed as depicted in the Fig. 4−4. The right-leg is fed with the amplified, summed and inverted version of the differential input at the amplifier through the right leg driver circuit. Electrodes placed on the bicep muscles, detect the EMG signal in differential mode and so by making use of right leg drive, the interference is canceled,

hence improving the CMRR. Few micro-amperes of current flows into the subject through the right leg as it acts like a ground. Noise due to common mode can be addressed and canceled by deploying ideally matched differential amplifiers (Carr and Brown, 1998; Spinelli et al., 2003). Multistage amplifiers, right leg driver and active filters facilitated in detecting the EMG signal on a virtual oscilloscope developed using MATLAB application software on a Laptop.

The EMG signal detected is the analog-output of the amplifier section developed in-house and is linked with the sound-port of the computer through a 3.5 mm dimension mono-jack. The sound port connects with an internal sound card of a PC which enables input and output of audio signals through the computer. This expansion card has a line-in connector to receive the analog input obtained from the sensor-amplifier system output and has an inbuilt amplifier and analog-to-digital converter (ADC) to further amplify and digitize the analog-input respectively. The sound-card of the PC is utilized as the linking unit, so the necessity of designing supplementary amplifiers, ADC, or Proprietary data acquisition (DAQ) unit is eliminated. The visualization and export of data for further analysis are done using a freely available virtual oscilloscope (Bansal et al., 2009, 2010).

Virtual scopes created to view and analyze the detected EMG signal are the Oscilloscope software called as the Time Scope in DSP System Toolbox of MATLAB and Simulink. This scope permits visualization, measurement, and analysis of multichannel real-time streaming bio-signals in the time domain. This eliminates the need of having traditional bulky hardware scopes for recording and analysis. The features and user interface of virtual scope is in consistence with those of a conventional hardware scope (DSP System Toolbox documentation, MATLAB).

The universally available interfacing units which connect the bio-signal amplification system with the computer-based monitoring and analysis arrangement are the parallel port, RS-232 serial port, the USB, etc. DAQ units along with the ADC section is generally made available with the commercially available bio-monitoring systems, which is autonomous in amplifying, filtering, digitizing, and interfacing to the computer for analysis and monitoring. However, they lack mathematical aptitude, and need additional driver software to provide on-line analysis. The interfacing unit implemented in this experimentation, is user-friendly, and an effective way of demonstrating the detected EMG signal that permits on-line processing and subsequent analysis. The said arrangement can be linked to any computer-based system through common communication port and eliminates the requirement of supplementary ADC unit.

The signal detected is corrupted with interference that is taken care of by designing online Digital Filters. Improved acquisition and processing of bio-signal is assured by designing software Digital Filters in MATLAB and is explained in the subsequent section.

4.3.3 Digital filter for online processing

The real-time detected EMG signals get tainted by noise primarily due to device components, motion artefacts of 20, 50 Hz power line interference and baseline wander of low frequency. Online removal of noise is achieved in the present work through digital signal processing algorithms designed using FIR digital filters in MATLAB. The Zero-Phase-Band-Pass Filter (ZPBPF) has been designed to enhance the EMG signal detected. Fig. 4—5

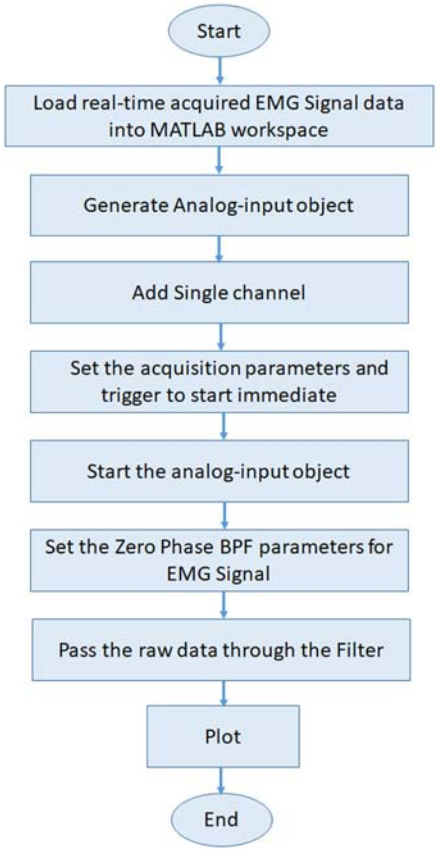

FIGURE 4–5 Algorithm flow for creating Virtual Scope and Filter to acquire EMG signal in single channel mode. *EMG*, electromyography.

presents the algorithmic flow for creating virtual scope and filters in MATLAB application environment for real-time and online detection of the EMG signal and also for eliminating noise from the acquired bio-signal in single channel mode.

An oscilloscope window gets generated with the program created in MATLAB which efficiently displays the acquired EMG signal in real-time. An analog input object is created to link with the acquisition device, which is the window's sound card in this experiment. The "Addchannel" command is used to add a single channel to it. The input arguments of this function specifies the object to which the channel has been added to and also tells about the hardware being added. MATLAB recognizes "winsound" as the sound card connector's name. The syntax used for creation of the analog input object "ai," for communicating with the sound card and for adding channels to the object are:

```
analoginput('winsound')
get(ai, `channel')
```

To initiate the analog-input object, attainment parametric considerations viz. sample rate and samples/trigger are established as per the requirement. After setting the parameters, the analog-input object is initiated using 'start (ai) function and information is recorded using the "getdata" function for subsequent plotting using the "plot" function. Once the requisite EMG signal data length is recorded, "stop" function is made use of to end the analog-input object from running and is then deleted to save space using the function "delete."

Once the EMG signal is detected and recorded in real-time, online digital filter algorithms are programmed to eliminate interference from the bio-signal and thus improve the quality of the physiological parameter. The syntax used to achieve the purpose is as under:

Function fir1(N, Wn, 'bandpass'): Generates a Nth order digital FIR band-pass filter
Function filtfilt: Does zero-phase-band-pass filtering. ZPBPF is an arrangement of a LPF and a HPF and has been explained in previous chapter. The frequency band is selected to cover the complete spectrum of EMG signals.

4.3.4 The acquisition protocol and results

Two Ag−AgCl reusable surface eledctrodes are positioned on the bicep muscles to detect the muscle movements. One electrode is positioned on the right-leg as reference to obtain the EMG signal. Ag−AgCl conductive gel is put on skin surface for effective acquisition. To avoid motion artifacts, the subject is asked to be in a relaxed state. To make recordings for various bicep muscle activation levels, the subject is made to contract and relax the bicep muscles. The EMG signal acquired noninvasively is amplified using the cascade amplifier set to a gain of 500 times for further viewing and analysis. The amplifier's analog voltage output is connected to the sound-port of the computer. The signal appearing at the sound card is identified by the virtual oscilloscope programmed after digital filtering in MATLAB.

Surface EMG detected post filtering for varied levels of contractions in Bicep Muscles are depicted in Fig. 4−6A−C. The amplitude levels clearly indicate the corresponding muscle contraction strengths. Surface EMG detected post filtering for two simultaneous yet different levels of contractions in bicep muscles is depicted in Fig. 4−7. The virtual software oscilloscope and the band-pass zero-phase filter designed in MATLAB successfully detects the EMG signal took from the sound-port of the Laptop. The detected EMG signal is of low strength of small mVolts and is in the spectral range 0.05−500 Hz. Criticality of the spectrum makes it essential to test the algorithm for digital filter with different cut-off frequency range. Sampling rate fixed for acquisition is 8000 samples/sec, so, the horizontal-axis identifies only 10 sec of data in the effects shown. The vertical-axis represents amplitude of the acquired EMG data.

Better-quality result and hardware effectiveness can be attained by appropriate selection of electrodes, its location and proper skin preparation. Ag−AgCl electrodes were chosen for EMG signal acquisition as they are effortlessly obtainable and possess negligible half-cell-potential leading to minimum offset. However, some noise is also acquired using these electrodes, hence development of electrodes with inbuilt processing arrangement can be a potential area of research. The Instrumentation Amplifier designed using TL-084C provides adequate

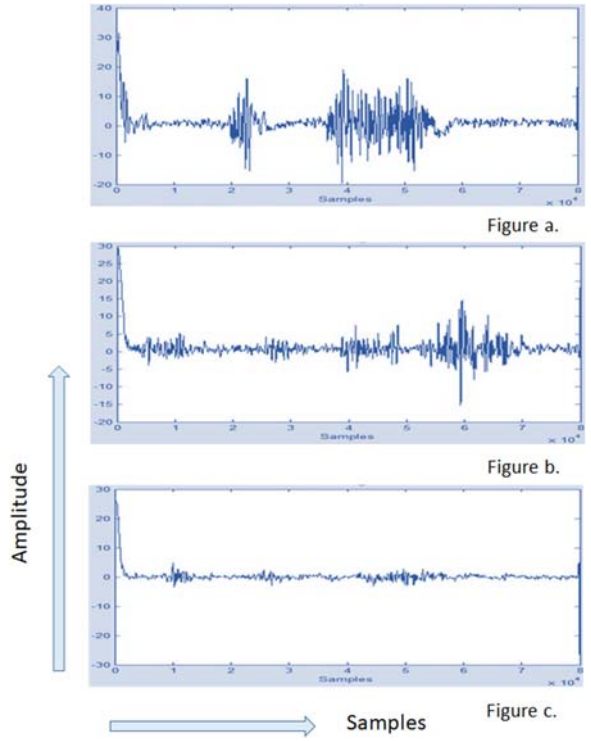

FIGURE 4–6 Surface EMG detected post filtering for varied levels of contractions in Bicep Muscles. *EMG*, electromyography.

amplification and has a CMRR of 86 dB, hence effectively discards the power line hum and the harmonics generated. This has the adverse effect of amplifying the noise as well. Digital filters that can notch these frequency components can be a feasible explanation to this issue. Reduction in consumption of power, size, etc., are other potential areas of research in bio-signal processing.

4.4 Real-time detection and processing of electromyography signal in dual channel mode

The experiment has been extended to acquire two bio-signals simultaneously using a dual channel mode data acquisition system. The arrangement concurrently detected muscle contractions of Rectus Abdomen and the Carotid pulsation. Functional block representation of computer-based dual-channel mode is depicted in Fig. 4−8.

The instrumentation set up comprises the EMG acquisition arrangement detailed in sections above along with the sensor to pick the carotid pulse waveform. Muscle contractions have been picked from the rectal abdomen and the carotid pulse is detected by placing the piezoelectric sensor on the neck region. A stereo input jack is used to interface the analog

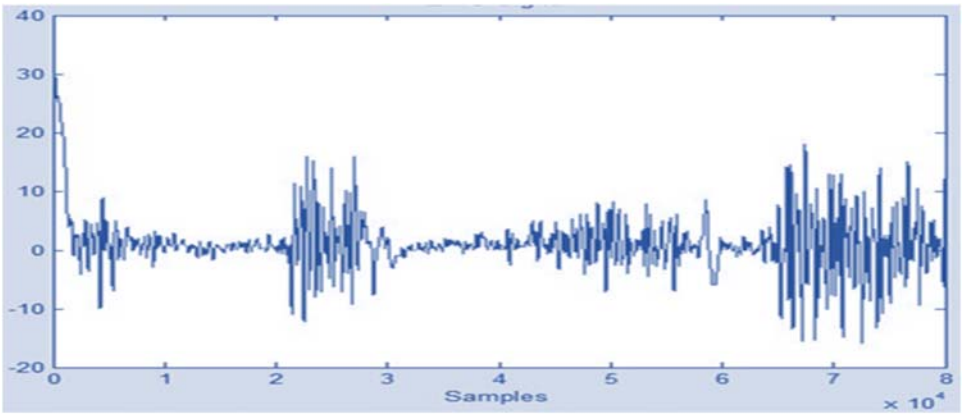

FIGURE 4–7 Surface EMG detected post filtering for two simultaneous yet varied levels of contractions in Bicep Muscles. *EMG*, electromyography.

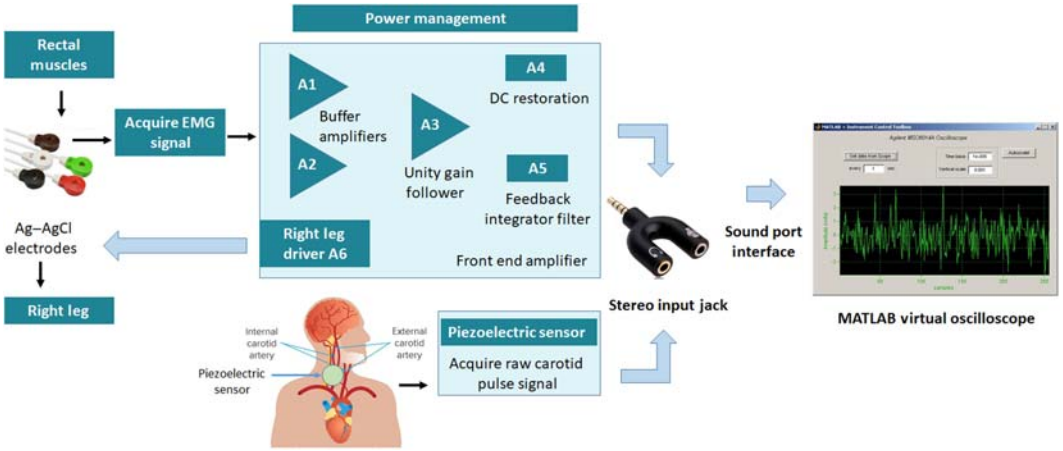

FIGURE 4–8 Block diagram representation | Real-time acquisition of EMG data and Carotid pulsation using dual channel mode. *EMG*, electromyography.

output obtained for both the bio-signals, that is, the muscle contractions and the carotid pulse to the sound-port of the computer. Digital filtration algorithm and virtual oscilloscopes programmed in MATLAB effectively detected both the bio-signals simultaneously in real-time. The algorithmic flow for dual channel mode detection and filtration of EMG data and Carotid pulse waveform is depicted in Fig. 4–9.

The algorithm requires creation of the analog-input object where two channels are made available to simultaneously detect both the EMG signal and the Carotid pulsation appearing at the interfacing junction which is the sound port. The band pass frequency of the FIR filter

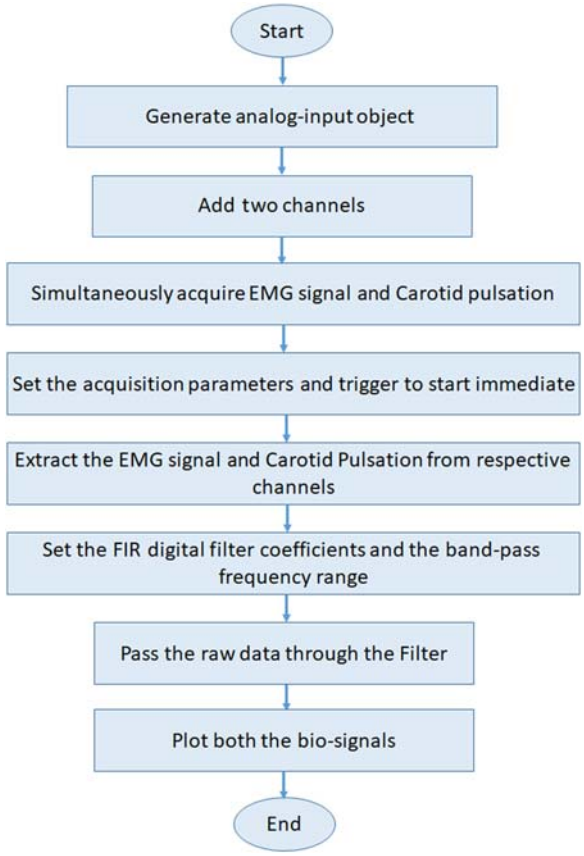

FIGURE 4–9 Algorithm flow for creating virtual oscilloscope and digital filter in MATLAB to concurrently acquire EMG data and Carotid pulse waveform in dual channel mode. *EMG*, electromyography.

is fixed to 0.05−50 Hz for filtering the Carotid pulsation and the range is between 1 and 200 Hz for filtering of the EMG data.

EMG data generated due to rectus abdominal muscle contraction appears at channel one and the simultaneously detected Carotid pulsation appears at channel two. Results were recorded. Drift in base line occurs as seen in Fig. 4−10 may be because the subject was not in a relaxed state during measurement or because the electrode placement site got disturbed. Taking proper care, the subsequent recordings were made. Figs. 4−11 and 4−12 could be recorded without any base line drifts. It can be clearly noticed in these results that increase in pressure during the abdominal muscle contractions leads to a hind pressure resulting in corresponding raised amplitude level of the Carotid pulsation. This is an unmistakable indication of a correlation among the contraction in abdominal rectus muscle and the Carotid pulse waveform. The algorithm developed in MATLAB effectively detects and filters two

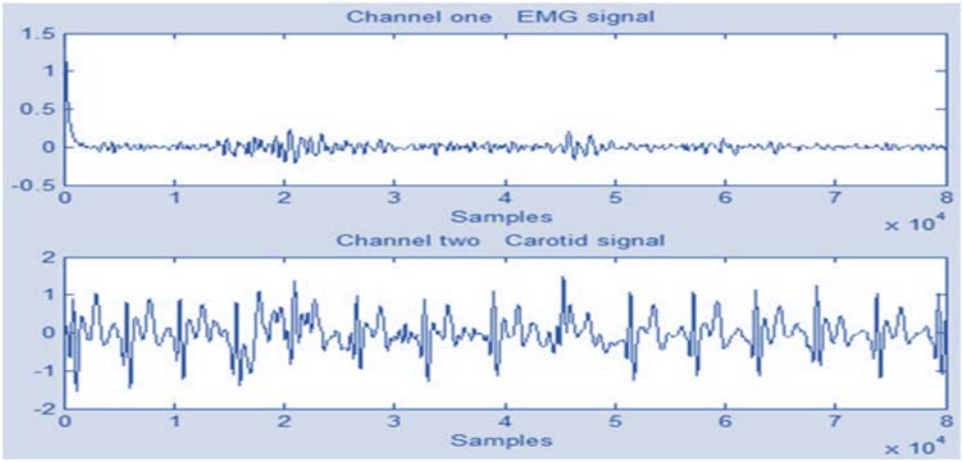

FIGURE 4–10 Base line drift | Simultaneously acquired EMG due to rectus-abdomen muscle contractions and Carotid pulse waveform. *EMG*, electromyography.

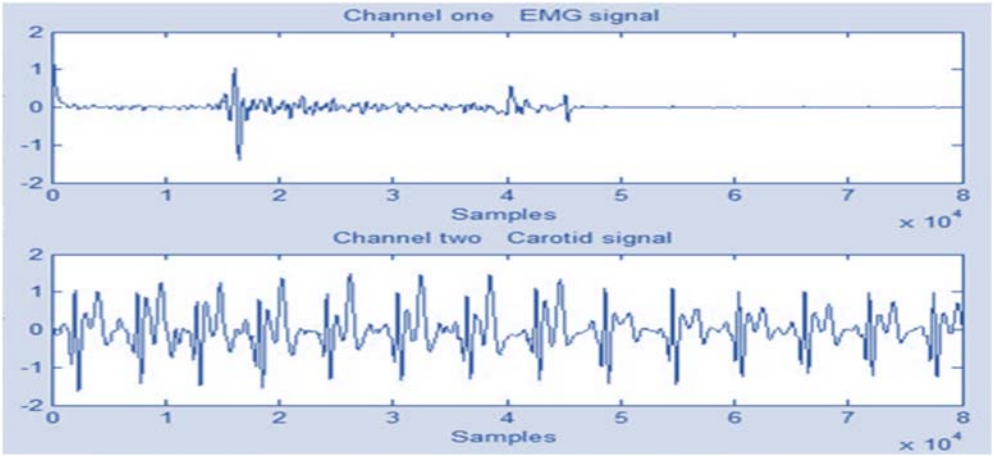

FIGURE 4–11 Subject 1 | Filtered result of concurrently detected rectus-abdomen muscle contractions and Carotid pulse waveform (with no base line drift).

bio-signals simultaneously in real-time which can be of great clinical advantage to reach diagnostic decisions.

The graphical user interface developed through MATLAB platform permits on-line filtration. A derived advantage of on-line digital filtering processing is that the information content of the acquired bio-signal can be sent for further analysis with reduced noise interference. The dual channel experimentation deployed in this work can further be expanded to acquire multiple signals simultaneously. The FIR filters designed have

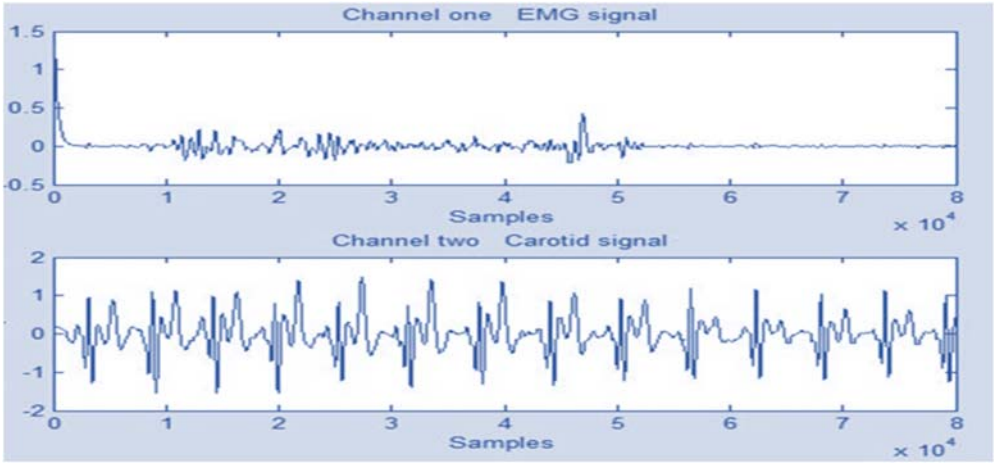

FIGURE 4–12 Subject 2 | Filtered result of concurrently detected rectus-abdomen muscle contractions and Carotid pulse waveform (with no base line drift).

the inherent desirable characteristics of being stable, having linear phase characteristics in the pass-band and practically realizable. Linear phase characteristics enable distortion free acquisition of detected bio-signal. The concluding form of the algorithm generated in this work, can be further assembled to develop an independent app incorporating a compiler in MATLAB, thereby making it self-regulating and reducing the cost of the system. The process to develop a stand-alone system is explained in the subsequent section.

4.5 Standalone MATLAB code for physiological data detection and processing

MATLAB is a user-friendly, exclusive, multiple paradigm software design environment, and numerical computing tool established by MathWorks. It allows manipulations on matrix, creation of functions and data plots, algorithmic implementations, formation of user interfaces, and is compatible with other language algorithms. It provides an Editor to generate executable script and function files using codes and in-built functions. The program is stored with a ".m" extension and can be run from the command prompt of MATLAB. However, there is a provision to mask the ".m" file and create a standalone executable application program to make it platform independent.

MATLAB supports Windows, Linux and macOS platforms for generating standalone apps. Prewritten functions can be packaged using MATLAB Compilers and the generated executable file can be made to run without having licensed version of MATLAB on the target system. Various options presented below are available to create standalone apps:

- Application Compiler app can be used to install the standalone application and also to install requisite dependences of the system targeted.
- The function compiler.build.standalone can also be used to develop a executable standalone file which does not contain MATLAB Runtime or installer. Function compiler.package.installer is used for packaging.
- The "mcc" command can also be used. This also does not include the MATLAB Runtime or the installer and is required to be packaged separately.

These Standalone executable files combine the abilities of MATLAB tools to create a custom-made app for the end-users. The process adopted in this work to develop a stand-alone app for bio-signal detection and filtering in MATLAB is depicted in Fig. 4—13.

Steps for generating the standalone app:

- Invoke the MATLAB compiler: use "m-build" at the command prompt.
- The Interpreter recognizes the command and permits selection of requisite Compiler.
- Select Lcc C version 2.4. to be the compiler for the selected version of MATLAB used.

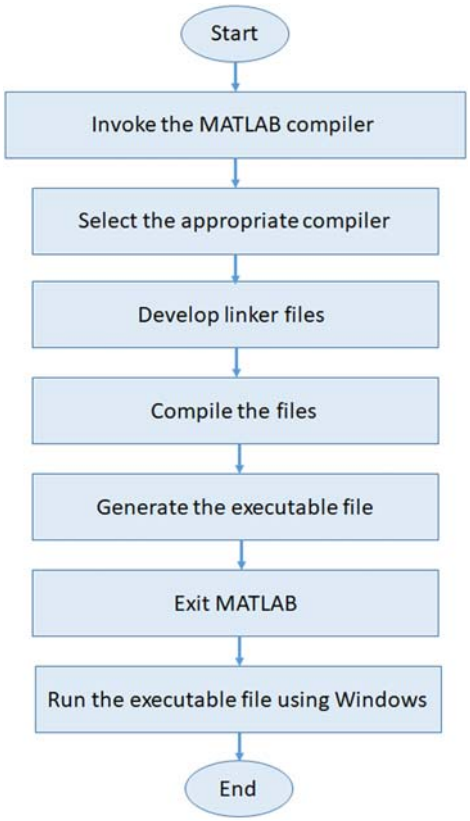

FIGURE 4–13 Algorithm for generating MATLAB stand-alone executable file.

- Generate the linker files and the .dll files.
- Configure the Compiler.
- Compile the program source code: Use the command "mcc −m (filename)."
- Complete the compilation and create the standalone executable file.
- "Windows" attaches the .exe extension of the executable file with the file name.
- Run the .exe file from the "Windows" dos prompt.
- The command line window opens and the plot is generated.

The user thus, does not require to load MATLAB application software for running the bio-signal acquisition and processing app. This leads to the successful generation of an independent on-line program with the ability to simultaneously acquire two real-time bio-signals that can be viewed, processed, digitally filtered and analyzed on a virtual oscilloscope.

4.6 Conclusion

EMG signal detection and analysis finds numerous clinical and nonclinical applications. Characteristic advantages include decision making during pre and postsurgery, muscle training schedules, improved sports performance, biomechanics, posture control, generation of control signal for prosthetic tools and even in detecting the muscle response in ergonomics. Several EMG acquisition and monitoring arrangements have been developed, and are still being researched to make the system compact, cost-effective, utilizing less power, with inbuilt signal processing chips to eliminate noise, having immense mathematical capability for analysis and automated decision making. An attempt has been made in this work to deploy an economic and user-friendly computer-based home health monitoring system that can capture human EMG signals in real-time. The muscle contractions could be detected from different sites including the bicep muscles and the rectus abdominal muscles using an amplifier and filter hardware designed using TL-084C op-amp. The real-time acquired EMG information was further made noise interference proof by generating digital filter algorithm in MATLAB, which has the ability to filter the bio-signal in on-line mode. The experiment is extended to explore the possibility of acquiring two bio-signals simultaneously to establish a correlation between EMG data and Carotid pulsation, which can be very useful in reaching diagnostic inferences. The dual channel arrangement was effective in capturing both the bio-signals concurrently using easy interface arrangement between the amplifier section and the computer-based system installed with the MATLAB application software. A standalone executable app has also been generated using MATLAB compilers, so that the algorithm can become platform independent and can be made to run even using Windows. This makes the entire set-up very cost-effective.

References

Abbaspour, S., Fallah, A., Removing, E.C.G., 2014. Artifact from the surface EMG signal using adaptive subtraction technique. J. Biomed. Phys. Eng. 4, 33−38.

Ahmad, S.A., 2009. Moving approximate Entropy and its Application to the Electromyographic Control of an Artificial Hand (PhD thesis), University of Southamptom, Southampton, UK.

Ahsan, M.R., Ibrahimy, M., Khalifa, O., 2011. Neural Network Classifier for Hand Motion Detection from EMG Signal. Springer, Berlin, Heidelberg; Kuala Lumpur, Malaysia, pp. 536–541.

Al-Mulla, M.R., Sepu, F., Co, M., 2011. A review of non-invasive techniques to detect and predict localised muscle fatigue. Sensors 11, 3545–3594.

Al-Timemy, A.H., Khushaba, R.N., Bugmann, G., Escudero, J., 2016. Improving the performance against force variation of EMG controlled multifunctional upper-limb prostheses for transradial amputees. IEEE Trans. Neural Syst. Rehabil. Eng. 24 (6), 650–661.

Amorim, C.F., Hirata, T., 2009. Behavior analysis of electromyographic activity of the masseter muscle in sleep bruxers. J. Bodyw. Mov. Ther. 14 (3), 234–238.

Amorim, Ć.F, Marson, R.A., 2012. Application of surface electromyography in the dynamics of human movement, computational intelligence in electromyography analysis—a perspective on current applications and future challenges, Naik, G.R. (Ed.), IntechOpen.

Anderson, L., Oldridge, N., Thompson, D.R., Zwisler, A.-D., Rees, K., Martin, N., et al., 2016. Exercise-based cardiac rehabilitation for coronary heart disease: cochrane systematic review and meta-analysis. J. Am. Coll. Cardiol. 67, 1–12.

Balbinot, A., Favieiro, G., 2013. A neuro-fuzzy system for characterization of arm movements. Sensors 13, 2613–2630.

Bansal, D., Khan, M., Salhan, A.K., 2009. A computer based wireless system for online acquisition, monitoring and digital processing of ECG waveforms. Comput. Biol. Med., Elsevier, Science Direct 39 (4), 361–367.

Bansal, D., Khan, M., Salhan, A.K., 2010. Wireless transmission of EMG signal and analysis of its correlation with simultaneously acquired Carotid pulse wave using dual channel system, IEEE digital library, eHealth, Telemedicine, and Social Medicine. In: ETELEMED '10. Second International Conference, pp. 125–129.

Basu, B., Nagarajaiah, S., Chakraborty, A., 2008. Online identification of linear time-varying stiffness of structural systems by wavelet analysis. Struct. Health Monit. 7, 21–36.

Butler, H.L., Newell, R., Hubley-Kozey, C.L., Kozey, J.W., 2009. The interpretation of abdominal wallmuscle recruitment strategies change when the electrocardiogram (ECG) is removed from the electromyogram (EMG). J. Electromyogr. Kinesiol. 19 (2), e102–e113.

Carr, J.J., Brown, J.M., 1998. Introduction to Biomedical Equipment Technology, fourth ed Prentice Hall, Inc, Eaglewood Cliffs, NJ.

Chowdhury, R.H., Reaz, M.B.I., Ali, M.A.M., 2013. Surface electromyography signal processing and classification techniques. Sensors 13, 12431–12466.

Cifrek, M., Medved, V., Tonković, S., Ostojić, S., 2009. Surface EMG based muscle fatigue evaluation in biomechanics. Clin. Biomech. 24 (4), 327–340.

Côté-Allard, U., Gagnon-Turcotte, G., Laviolette, F., Gosselin., B., 2019. A low-cost, wireless, 3-D-printed custom armband for sEMG hand gesture recognition. Sensors 19 (12), 2811.

Das, D.P., Webster, J.G., 1980. Defibrillation recovery curves for different electrode materials. IEEE Trans. Biomed. Eng. 230–233. BME-27.

De Luca, C.J., Donald Gilmore, L., Kuznetsov, M., Roy, S.H., 2010. Filtering the surface EMG signal: movement artifact and baseline noise contamination. J. Biomech. 43 (8), 1573–1579.

Dimitrova, N.A., Dimitrov, G.V., 2003. Interpretation of EMG changes with fatigue: facts, pitfalls, and fallacies. J. Electromyogr. Kinesiol. 13 (1), 13–36.

DSP System Toolbox documentation, MATLAB. Design and simulate streaming signal processing systems. <https://in.mathworks.com/products/dsp-system.html>.

Englehart, K., 1998. Signal Representation for Classification of the Transient Myoelectric Signal (PhD thesis), University of New Brunswick, Saint John, NB, Canada.

Englehart, K., Hudgins, B., 2003. A robust, real-time control scheme for multifunction myoelectric control. IEEE Trans. Biomed. Eng. 50, 848–854.

Englehart, K., Hudgins, B., Parker, P.A., Stevenson, M., 1999. Classification of the myelectric signal using time–frequency based representations. Med. Eng. Phys. 21, 431–438.

Englehart, K., Hudgin, B., Parker, P.A., 2001. A wavelet-based continuous classification scheme for multifunction myoelectric control. IEEE Trans. Biomed. Eng. 48, 302–311.

Fang, C., He, B., Wang, Y., Cao, J., Gao, S., 2020. EMG-centered multisensory based technologies for pattern recognition in rehabilitation: state of the art and challenges. Biosensors 10, 85.

Farina, D., Merletti, R., 2000. Comparison of algorithms for estimation of EMG variables during voluntary isometric contractions. J. Electromyogr. Kinesiol. 10, 337–349.

Fleischer, C., Wege, A., Kondak, K., Hommel, G., 2006. Application of EMG signals for controlling exoskeleton robots. Biomed. Tech. (Berl.) 51 (5–6), 314–319.

Fratini, A., Cesarelli, M., Bifulco, P., Romano, M., 2009. Relevance of motion artifact in electromyography recordings during vibration treatment. J. Electromyogr. Kinesiol. 19 (4), 710–718.

Geddes, L.A., Roeder, R., 2001. Measurement of the direct-current (Faradic) resistance of the electrode–electrolyte interface for commonly used electrode materials. Ann. Biomed. Eng. 29, 181–186.

Guissard, N., Hainaut, K., 1992. EMG and mechanical changes during sprint start at different front block obliquities. Med. Sci. Sports Exerc. 24, 1257–1263.

Guo, Y., Kareem, A., 2016. Non-stationary frequency domain system identifi cation using time–frequency representations. Mech. Syst. Signal. Process. 72/73, 712–726.

Hamedi, M., Salleh, S.H., Noor, A.M., Swee, T.T., Afizam, I.K., 2012. Comparison of different time-domain feature extraction methods on facial gestures' EMGs. Prog. Electromagn. Res. Symp. Proc. 12, 1897–1900.

Hogan, N., Mann, R.W., 1980. Myoelectric signal processing: optimal estimation applied to electromyography—part I: derivation of the optimal myoprocessor. IEEE Trans. Biomed. Eng. 27, 382–395.

Huang, H., Kuiken, T.A., Lipschutz, R.D., 2008. A strategy for identifying locomotion modes using surface electromyography. IEEE Trans. Biomed. Eng. 56, 65–73.

Huang, H., Zhang, F., Hargrove, L.J., Dou, Z., Rogers, D.R., Englehart, K.B., 2011. Continuous locomotion-mode identification for prosthetic legs based on neuromuscular–mechanical fusion. IEEE Trans. Biomed. Eng. 58, 2867–2875.

Hudgins, B., Parker, P., Scott, R.N., 1993. A new strategy for multifunction myoelectric control. IEEE Trans. Biomed. Eng. 40 (1), 82–94.

Jafarzadeh, M., Hussey, D.C., Tadesse, Y., 2019. Deep learning approach to control of prosthetic hands with electromyography signals. 2019 IEEE International Symposium on Measurement and Control in Robotics (ISMCR). IEEE, pp. A1–4.

Jaramillo-Yánez, A., Benalcázar, M.E., Mena-Maldonado, E., 2020. Real-time hand gesture recognition using surface electromyography and machine learning: a systematic literature review. Sensors 20 (9), 2467.

Kendell, C., Lemaire, E.D., Losier, Y., Chan, A., Hudgins, B., 2012. A novel approach to surface electromyography: an exploratory study of electrode-pair selection based on signal characteristics. J. Neuroeng. Rehabil. 9.

Kobylarz, J., Bird, J.J., Faria, D.R., Ribeiro, E.P., Ekárt, A., 2020. Thumbs up, thumbs down: non-verbal human-robot interaction through real-time EMG classification via inductive and supervised transductive transfer learning. J. Ambient Intell. Humaniz. Comput. Springer Science and Business Media LLC.

Konard P., 2005. The ABC of EMG: A Practical Introduction to Kinesiological Electromyography. Noraxon Inc. USA, version 1.0 April 2005.

Korŏsec, D., 2000. Parametric estimation of the continuous non-stationary spectrum and its dynamics in surface EMG studies. Int. J. Med. Inform. 58–59, 59–69.

Lamontagne, M., 2001. Application of electromyography in sport medicine. In: Puddu, G., Giombini, A., Selvanetti, A. (Eds.), Rehabilitation of Sports Injuries. Springer, Berlin, Heidelberg.

Li, X., Shin, H., Zhou, P., Niu, X., Liu, J., Rymer, W.Z., 2014. Power spectral analysis of surface electromyography (EMG) at matched contraction levels of the first dorsal interosseous muscle in stroke survivors. Clin. Neurophysiol. 125, 988–994.

Long, Y., Du, Z.-J., Wang, W.-D., Zhao, G.-Y., Xu, G.-Q., He, L., et al., 2016. PSO-SVM-based online locomotion mode identification for rehabilitation robotic exoskeletons. Sensors 16, 1408.

Lorrain, T., Jiang, N., Farina, D., 2011. Influence of the training set on the accuracy of surface EMG classification in dynamic contractions for the control of multifunction prostheses. J. Neuroeng. Rehabil. 11, 8–25.

Lu, G., Brittain, J.-S., Holland, P., et al., 2009a. Removing ECG noise from surface EMG signals using adaptive filtering. Neurosci. Lett. 462 (1), 14–19.

Lu, G., Brittain, J.S., Holland, P., Yianni, J., Green, A.L., Stein, J.F., et al., 2009b. Noise from surface EMG signals using adaptive filtering. Neurosci. Lett. 462, 14–19.

Maffiuletti, N.A., Aagaard, P., Blazevich, A.J., Folland, J., Tillin, N., Duchateau, J., 2016. Rate of force development: Physiological and methodological considerations. Eur. J. Appl. Physiol 116, 1091–1116.

Massó, N., Rey, F., Romero, D., Gual, G., Costa, L., 2010. Surface electromyography applications in the sport. Apunt. Med. Esport. 45 (165), 121–130.

Matsubara, T., Morimoto, J., 2013. Bilinear modeling of EMG signals to extract user-independent features for multiuser myoelectric interface. IEEE Trans. Biomed. Eng. 6, 2205–2213.

Mcadams, E., 2006. Bioelectrodes, Encyclopedia of Medical Devices and Instrumentation, vol. 1. Wiley-Interscience, Hoboken, NJ, USA, pp. 120–166, 17.

Merletti, L.C., 1997. Surface EMG signal processing during isometric con- tractions. J. Electromyogr. Kinesiol. 7, 241–250.

Morren, G., Van Huffel, S., Helon, I., et al., 2002. Effects of non-nutritive sucking on heart rate, respiration and oxygenation: a model-based signal processing approach. Comp. Bio-chem. Physiol. A Mol. Integr. Physiol. 132 (1), 97–106.

Nazmi, N., Rahman, M.A.A., Yamamoto, S.-I., Ahmad, S.A., Zamzuri, H., Mazlan, S.A., 2016. A review of classification techniques of EMG signals during isotonic and isometric contractions. Sensors 16, 1304.

Oskoei, M., Hu, H., 2006. GA-based feature subset selection for myoelectric classification. IEEE Int. Conf. Robot. Biomim. 1465–1470.

Oskoei, M.A., Hu, H., 2007. Myoelectric control systems—a survey. Biomed. Signal. Process. Control. 2, 275–294.

Phinyomark, A., Limsakul, C., Phukpattaranont, P., 2009. Novel feature extraction for robust EMG pattern recognition. J. Comput. 1, 71–80.

Phinyomark, A., Qu, F., Chrbonnier, S., Serviere, C., Tarpin-Benard, F., Laurillau, Y., 2013. EMG feature evaluation for improving myoelectric pattern recognition robustness. Expert. Syst. Appl. 40, 4832–4840.

Reaz, M.B.I., Hussain, M.S., Mohd-Yasin, F., 2006. Techniques of EMG signal analysis: Detection, processing, classification and applications, Biological Procedures Online., 8. Springer-Verlag, London, UK, p. 163.

Rechy-Ramirezn, E.J., Huosheng, H., 2015. Bio-signal based control in assistive robots: a survey. Digit. Commun. Netw. 1, 85–101.

Rogers, D.R., MacIsaac, D.T., 2013. A comparison of EMG-based muscle fatigue assessments during dynamic contractions. J. Electromyogr. Kinesiol. 23, 1004–1011.

Roland, T., Amsuess, S., Russold, M.F., Baumgartner, W., 2019a. Ultra-Low-Power Digital filtering for insulated EMG sensing. Sensors 19 (4), 959.

Roland, T., Wimberger, K., Amsuess, S., Russold, M.F., Baumgartner, W., 2019b. An insulated flexible sensor for stable electromyography detection: application to prosthesis control. Sensors 19 (4), 961.

Sakkalis, V., Cassar, T., Zervakis, M., Camilleri, K.P., Fabri, S.G., Bigan, C., et al., 2008. Parametric and nonparametric EEG analysis for the evaluation of EEG activity in young children with controlled epilepsy. Hindawi Publishing Corporation, Computational Intelligence and Neuroscience, vol. 2008, Article ID 462593, p. 15.

Sandoval, A.E., 2010. Electrodiagnostics for low back pain. Phys. Med. Rehabil. Clin. N. Am 21 (4), 767–776.

Scano, A., Zanoletti, M., Pirovano, I., Spinelli, L., Contini, D., Torricelli, A., et al., 2019. NIRS-EMG for clinical applications: a systematic review. Appl. Sci 9, 2952.

Shair, E.F., Ahmad, S.A., Marhaban, M.H., Mohd Tamrin, S.B., Abdullah, A.R., 2017. EMG processing based measures of fatigue assessment during manual lifting. Biomed. Res. Int. 2017, Article ID 3937254, 12 pages.

Spinelli, E.M., Pallàs-Areny, R., Mayosky, M.A., 2003. AC-coupled front-end biopotential measurements. IEEE Trans. Biomed. Eng. 50 (3), 391–395.

Statt, N., 2019. Facebook acquires neural interface startup CTRL-Labs for its mind-reading wristband. The Verge.

Subasi, A., 2013. Classification of EMG signals using PSO optimized SVM for diagnosis of neuromuscular disorders. Comput. Biol. Med. 43, 576–586. <https://www.mayoclinic.org/tests-procedures/emg/about/pac-20393913>.

Sun, R., Song, R., Tong, K.Y., 2014. Complexity analysis of EMG signals for patients after stroke during robot-aided rehabilitation training using fuzzy approximate entropy. IEEE Trans. Neural Syst. Rehabil. Eng. 22, 1013–1019.

Teasell, R.W., Foley, N.C., Bhogal, S.K., Speechley, M.R., 2003. An evidence-based review of stroke rehabilitation. Top. Stroke Rehabil. 10, 29–58.

TL08xx JFET-Input Operational Amplifier datasheet (Rev I). <http://wiki.amperka.ru/_media/products:troyka-ph-sensor:tl081bcd-datasheet.pdf>.

Toro, S. F. del, Wei, Y., Olmeda, E., Ren, L., Guowu, W., Díaz, V., 2019. Validation of a low-cost electromyography (EMG) system via a commercial and accurate EMG device: pilot study. Sensors 19 (23), 5214.

Tsai, A.C., Hsieh, T.H., Luh, J.J., Lin, T.T., 2014. A comparison of upper-limb motion pattern recognition using EMG signals during dynamic and isometric muscle contractions. Biomed. Signal. Process. Control. 11, 17–26.

Turek, M., 2017. <https://www.closingthegap.com/a-new-way-of-communication-for-persons-living-with-paralysis-and-loss-of-speech/>.

Ullrich, P., 2020. Electromyography (EMG). <https://www.spine-health.com/treatment/diagnostic-tests/electromyography-emg>.

Willigenburg, N.W., Daffertshofer, A., Kingma, I., van Dieën, J.H., 2012. Removing ECG contamination from EMG recordings: a comparison of ICA-based and other filtering procedures. J. Electromyogr. Kinesiol. 22 (3), 485–493.

Wilson, J., 2018. <https://imotions.com/blog/facial-electromyography/>.

Wu, Y., Martínez, M.Á.M., Balaguer, P.O., 2013. Overview of the application of EMG recording in the diagnosis and approach of neurological disorders. Electrodiagnosis in New Frontiers of Clinical Research, Hande Turker. IntechOpen.

Yan, T., Cempini, M., Oddo, C.M., Vitiello, N., 2015. Review of assistive strategies in powered lower-limb orthoses and exoskeletons. Robot. Auton. Syst. 64, 120–136.

Yeom, H., Yoon, U., 2012. ECG Artifact removal from surface EMG using adaptive filter algorithm. Int. J. Multimed. Ubiquitous Eng. 1, 533–538.

Zech, A., Hübscher, M., Vogt, L., Banzer, W., Hänsel, F., Pfeifer, K., 2009. Neuromuscular training for rehabilitation of sports injuries: a systematic review. Med. Sci. Sports Exerc. 41, 1831–1841.

Zhan, Y., Halliday, D., Jiang, P., Liu, X., Feng, J., 2006. Detecting time-dependent coherence between non-stationary electrophysiological signals—a combined statistical and time–frequency approach. J. Neurosci. Methods 156 (1-2), 322–332.

This page intentionally left blank

5 Real-time detection and processing of electrocardiogram signal

5.1 Introduction

The Electrocardiogram (ECG) is an ever expanding application domain. Conventionally, ECG is required to be measured in the hospitals for monitoring patients, but with the growing demand of enhancing quality of life, it is trending to have mobile, compact and wearable ECG monitors for continuously checking the health status. Even subtle deviations in the physiological signs can be noticed through these wearable health monitoring units, which can be further transmitted to a physician and gives a sense of connectedness with them and early clinical decisions can be arrived at.

The ECG is the electrical measurement of the heart activity. Our heart maintains adequacy of blood flow throughout our body and delivers oxygen and nutrients to the brain and other vital organs. It receives deoxygenated blood and waste from the body, and pumps it to the lungs for getting oxygenated. After oxygenation, blood returns to the heart and is pumped back to the body. Fig. 5—1 below depicts the human heart and the corresponding classical ECG waveform. Lot of meaningful information relating to human physiology can be derived from the PQRST wave of ECG.

Cardiac cycle gets initiated at the Sinoatrial (SA) Node. The SA node placed near the superior vena cava in the right atrium has the ability to depolarize spontaneously at a rate 70 times/min, without any stimulus, generating an action potential and hence is termed as the natural pacemaker of heart. Action potential generated at the SA node moves through the atria via the Atrioventricular (AV) Node in the form of an electrical pulse, to the Ventricles. The Atrioventricular node links the atria and the ventricles. On receiving the atrial impulse, the AV node delays it on purpose, so that the atria get plenty of time to fill blood into the ventricles before commencement of ventricular contraction. The action potential includes activation, that is, depolarization and recovery, that is, repolarization giving rise to electrical currents and in turn the ECG waveform is generated. The P-wave generated is the result of atrial initiation and the QRS-complex results from the ventricular initiation. The T wave appears due to repolarization of the ventricular myocardium.

5.1.1 Interpretation of electrocardiogram waveform

Interpretation of ECG comprises analysis of the morphology of its standard waveform and the various associated intervals. The analysis begins from the onset of the P-wave. Expanse between the beginning of the P wave and the beginning of the QRS-complex is termed as the

Real-Time Data Acquisition in Human Physiology. DOI: https://doi.org/10.1016/B978-0-12-822118-1.00003-5
© 2021 Elsevier Inc. All rights reserved.

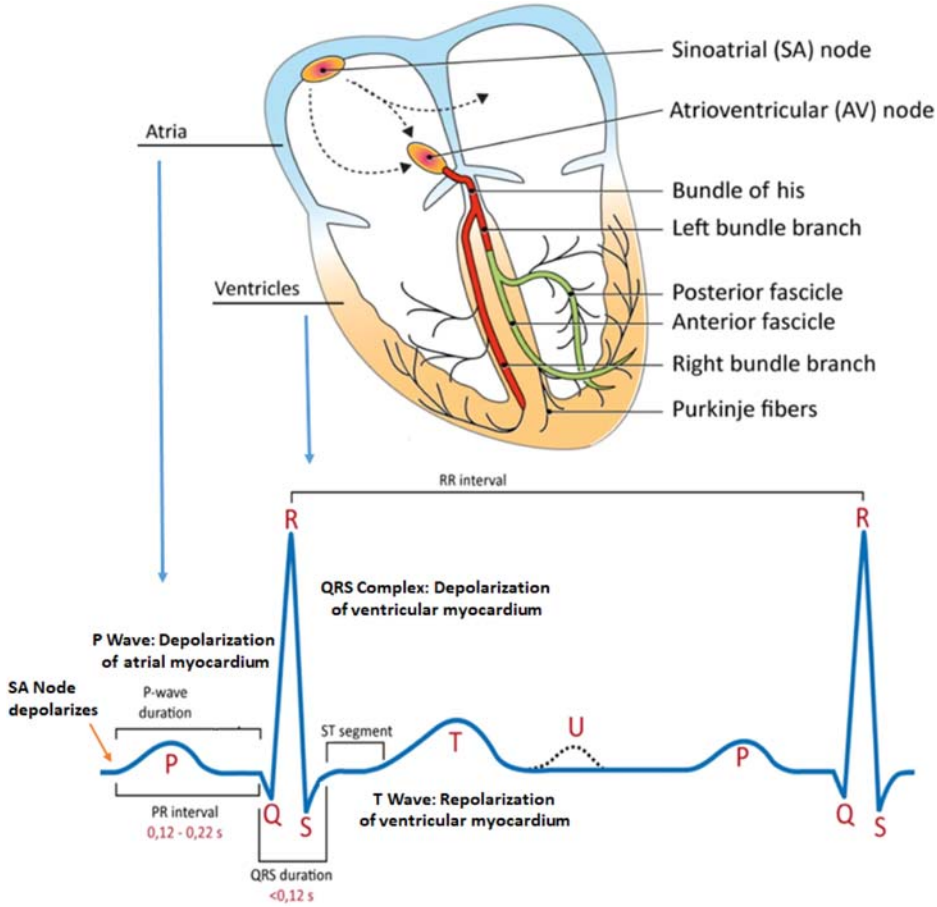

FIGURE 5–1 Depiction of the human heart and the corresponding ECG waveform (https://ecgwaves.com/topic/systematic-clinical-ecg-interpretation-review-guide). *ECG*, electrocardiogram.

PR-interval (0.12−0.22 s) and is used to find if the conduction of electrical impulse is normal or not in traveling from the atria till the ventricles. The straight line amid the end of P wave and onset of QRS-complex serves as the baseline of the ECG waveform and is a reflection of slow transmission of electrical impulse at the AV-node. The QRS complex can be seen as the result of left ventricular depolarization, as left ventricles generate much more electrical impulse compared to the right ventricles. A short duration of QRS complex (generally <0.12 s) is appropriate as it is an indication of proper conduction and rapid depolarization of the ventricles. Interpretation of the ST segment can indicate many underlying conditions, for example, acute myocardial ischemia may deviate the ST segment. In case of difficulty in discerning the base line using PR interval, then interval between T and P points can be referred as the baseline. Deviation in the T wave can be misleading in clinical practices, so it requires proper interpretation. There should be a smooth transition from ST segment to the T wave. Sometimes,

the U wave may occur in subjects having slow heart rates which is still an elusive domain. The periodicity of these segments help in analyzing the heart rate and each segment in the cardiac cycle may correspond to a health condition, which can be used by cardiologists to reach diagnostic inferences. Let us discuss each interval in detail.

Enlargement of Atria causes deviation in the P wave contour. In case of pulmonary valve stenosis or if the pulmonary arterial pressure is high, the right atrium gets enlarged and enhanced amplitude of P wave can be noticed. In case of mitral valve stenosis, the left atrium gets enlarged and the corresponding region of P wave gets amplified. The rhythm generated by the SA node is normal and is termed as sinus rhythm. If a beat results due to action potential generated outside the SA node, it is called as the ectopic beat. The appearance of P wave gets affected due to ectopic beats. If the ectopic beat source is nearby the AV node, then an inverted P wave is seen. Ideally the P wave should have a duration less than equal to 0.12 s and its amplitude should be less than 2.5 mm in the limb leads.

Transmission of impulse through the AV node can be normal paced, slow or even bypassed. This has an effect on the duration of the PR interval. If the interval is prolonged and exceeds 0.22 s, it is a manifestation of AV block. The primary cause could be age-related degenerative fibrosis, myocardial infarction or the effect of medication etc. Although AV node is the lone linkage between the atria and the ventricle, there could be an alternate pathway which bypasses the atrial impulse directly and causes premature depolarization. This leads to a condition called preexcitation having reduced PR interval less than 0.12 s.

Wide QRS complex (interval greater or equal to 0.12 s) also has its own implications. Prolonged QRS interval indicates that ventricular depolarization is slower than expected. Clinicians generally face difficulties in deciphering the QRS complex durations. Raised amplitude level of QRS complex may be due to enlarged ventricles. Electrode placement and an individual's physique also impact the amplitude level. Patients with chronic obstructive pulmonary disease also have reduced amplitude level. Ideally R wave should be less than 20 mm in limb leads (https://ecgwaves.com/topic/systematic-clinical-ecg-interpretation-review-guide). It is very important to interpret the ECG in a systematic manner else it may prove out to be detrimental.

Automated ECG devices with in-built signal processing modules present an instant analysis and interpretations related to the ECG waveform for their intervals and amplitudes, and are also equipped to compare them with the standard or previous recordings to draw inferences. Computerized bio-signal analysis and processing units take account of signal digitization, filtering, feature extraction, and classification, so require sufficient understanding of ECG characteristic features w.r.t the signal frequency to be able to design filters and, suitable lead placement.

The most noticeable waveform in an ECG signal is the QRS complex having a base frequency of approximately 10 Hz measurable at the body surface. The frequency ranges between 1 and 2 Hz in T waves. To derive diagnostic information, the spectrum analysis of QRS complex may vary in adults and in infants. In adults, information is contained mostly below 100 Hz, and in infants it can be noticed at 250 Hz or even at 500 Hz frequencies. Filters that are designed to remove artefacts are set to a band-pass range of 1−30 Hz,

however they do not serve the purpose of recording the bio-signal information because this range may distort the high- and low-frequency component of the ECG waveform. High frequencies if not adequately present can lead to improper evaluation of the signal QRS peak and may disturb smoothening of the notches and the Q waves. Likewise, if certain low-frequency components are missing, it can distort the repolarization. So, design of transfer functions for the filtering algorithm requires a thoughtful approach. Computer-based diagnostics and analysis of ECG waveform therefore must take care of interference in low-frequency range arising due to baseline wander, movement, and respiration and also cater to disturbances in higher frequency range generated due to muscle movement, power-line interference, etc. (Kligfield et al., 2007).

The lower bound of frequency in the ECG signal theoretically is 0.5 Hz corresponding to a heart-rate of 30 beats per min (bpm) but practically it is not possible to go lower than 0.67 Hz corresponding to 40 bpm. The 1975 American Heart Association endorsements suggested a lower cut-off frequency of 0.05-Hz for drawing diagnostic inferences from the ECG, thus taking care of repolarization, but could not prove itself in removing the baseline-wander. Elimination of baseline-wander is prerequisite during ECG analysis to align the recordings with the templates. Design of a zero-phase shift filter having a flat step response is effective in removal of the baseline wander without affecting the low-frequency range suggested. Analog filters designed with lower bounds around 0.5 Hz tend to introduce distortions in the ST segment because of nonlinear phase, but the bidirectional digital filter designs permit this range without introducing phase distortions. So, to eliminate distortions in the ST segment, the AHA in 1990 acclaimed the cut-off for low-frequencies should be equal to 0.05 Hz for general filters and 0.67 Hz for linear-phase digital filters (Kligfield et al., 2007).

Upper frequency bound in the ECG signals depend on the sampling rate which is set as per the Nyquist theorem to around twice the rate of the chosen high-frequency cut-off. Inappropriate high-frequency setting during ECG analysis may decrease the QRS peak and would fail to notice the subtle variations. The European CSE group recommended that ECG waves must have a high-frequency cut-off of 150 Hz so that the amplitude is around 20 Micro V with a period of 6 ms to get noticed. A sampling rate of 500 samples/sec permits a cut-off value of 150-Hz in grownups and around 250 Hz in infants. A 2001 Dutch article also, demonstrated that to have reduced amplitude errors, a bandwidth up to 250 Hz is required in children and around 150 Hz for young people. The 1975 American Heart Association however has limited the high-frequency range to 100 Hz to sustain the diagnostic precision of ECG. These recommendations prove out to be in-effect in eliminating interference from the ECG acquisition system for continuous monitoring and analysis (Kligfield et al., 2007).

5.1.2 Lead placement in an electrocardiogram system

For further reducing the effect of noise interference and for improving the quality of ECG signal acquired, it is essential to properly prepare the skin and appropriately place the electrodes. Fig. 5−2 depicts the details of lead placement arrangement in an ECG system, the

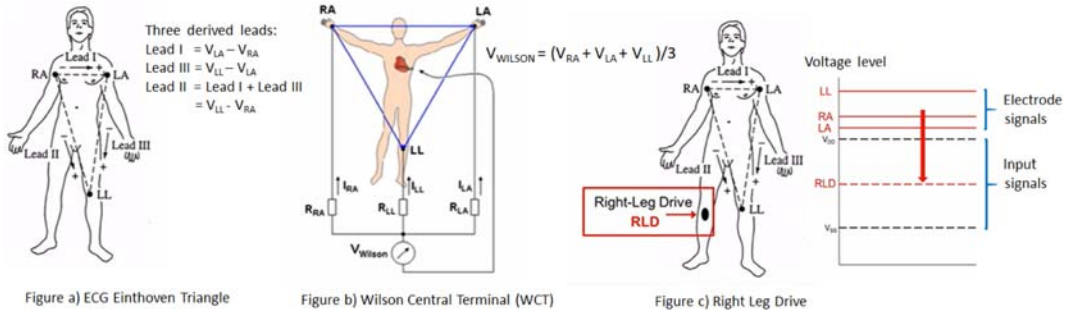

Figure a) ECG Einthoven Triangle

Figure b) Wilson Central Terminal (WCT)

Figure c) Right Leg Drive

FIGURE 5–2 Depiction of lead placement in an ECG system (A) ECG Einthoven Triangle, (B) Wilson Central Terminal (WCT), (C) Right leg drive and its effect. (https://training.ti.com/how-measure-ecg-introduction-what-ecg). *ECG*, electrocardiogram.

typical leads used for measurement and also illustrates how some leads can be derived from others.

In an ECG system, a lead is the difference in voltage measured by an electrode at two points on the body. The total leads may vary generally in an ECG measurement system, where simple portable ones used commercially require not more than two or three primary leads. Whereas, complex high quality ECG diagnostic systems may go up to 12 or more lead arrangement. More the number of leads, more is the angle that can be viewed and so more is the information gathered on the heart health status.

The potential at the electrode can be evaluated as the weighted average of the potentials from electrodes placed at two or further body positions. The three primary limb-leads can be obtained using the Einthoven's triangle, as shown in Fig. 5—2A. The three primary measuring electrodes are positioned on the left-arm (LA), right-arm (RA), and the left-leg (LL). The three main limb leads Lead-I, Lead-II, Lead-III can be derived using these electrode potentials as below:

$$\text{Lead I} = \text{Difference in potential } (V_{\text{LA}} - V_{\text{RA}})$$

$$\text{Lead III} = \text{Difference in potential } (V_{\text{LL}} - V_{\text{LA}})$$

$$\text{And Lead II (as per Einthoven's law)} = \text{Lead I} + \text{Lead III} = V_{\text{LL}} - V_{\text{RA}}$$

An additional electrode placement at the right leg termed as the right leg driver (RLD) as shown in Fig. 5—2C is recommended for DC coupled ECG monitoring system for a specific task due to its inherent advantages. The common mode voltage present in the human body floats w.r.t the ECG measurement unit and if it is not addressed, the voltage picked up by the electrodes fall outside the detectable range as shown in Fig. 5—2C. The RLD circuit drives a voltage into the subject causing the DC level of other measuring electrodes detectable.

Fig. 5—2B presents the Wilson Central Terminal (WCT) based chest lead arrangement. Unlike the primary leads placed on the limbs which are based on differential measurements, the chest leads measurements are made w.r.t reference voltage at the center of the

Einthoven triangle termed as WCT as shown in the figure. The WCT reference terminal is evaluated as the average of RA, LA, and LL electrode potential. Potential difference between WCT and RA is termed as the frontal plane limb lead VR, between WCT and LA is VL, and with LL it is VF. These leads have comparatively low amplitudes which was modified by Goldberger who developed the "augmented unipolar" limb leads, which gave 50% larger amplitude in comparison to the WCT. These augmented leads named aVR, aVL and aVF give improved information on the ECG signal. Each of the augmented leads makes use of the primary electrodes and the average of other two for measurement.

$$\text{For example: } aVR = RA - (LA + LL)/2.$$

The standard ECG measurement system uses the 12-lead arrangement involving three limb-leads (I, II, and III), three augmented-limb leads that are modified version of the WCT (aVR, aVL, and aVF), and 6 precordial leads (V1 to V6). The limb-lead electrodes are positioned on the wrists and the ankles, and the subject lies in the supine position. Proper electrode placement can modify the ECG signal, and can be very helpful in making clinical decisions. The section below details the norms followed and the hardware required to design the ECG acquisition system.

5.1.3 Investigation of electrocardiogram signal measurement

The most commonly used ECG measurement system is as depicted in Fig. 5−3 consisting of the three electrodes (RA, LA, and RLD) single-lead arrangement. As shown, every electrode is followed by a protection circuit, which isolates the subject from the faulty currents and also protects the Analog to Digital Converter (ADC) unit from over voltage situations. Also added is a unit for the detection of lead-off to monitor and ensure that the electrodes are connected properly. This is followed by the Instrumentation Amplifier (INA) stage to provide gain. Key features of the front end of INA stage are the low input bias current (less than few nano-amperes), high-input impedance, low-input current noise and input voltage noise, and high DC/AC CMRR. The final stage is the ADC connected to the control unit through an interfacing arrangement. The 3-lead system are much more complicated than the single-lead arrangement shown, as two ADC channels are required and for a 12-lead system an extra block is required to set-up the WCT voltage of Wilson Central Terminal to measure the chest leads.

As shown in the Fig. 5−3 subsection; the components prior to the front end of INA include the current limiting series resistors to avoid the situation of short circuit with power supply voltage, a common-mode and an antialiasing filter. For patient protection, the resistance value ranges from 10 K to 20 K. The antialiasing filters are the Low Pass Filter (LPFs) designed to eliminate the high frequencies. As shown in the circuit, the pull-frequency of the antialiasing filter is made by resistance in series for each signal input and, the differential capacitor C-diff which is much larger (10 times) than the common mode capacitor C-cm. A diode circuit is also put in place to clamp the input voltage (kV range) and avoid shocks

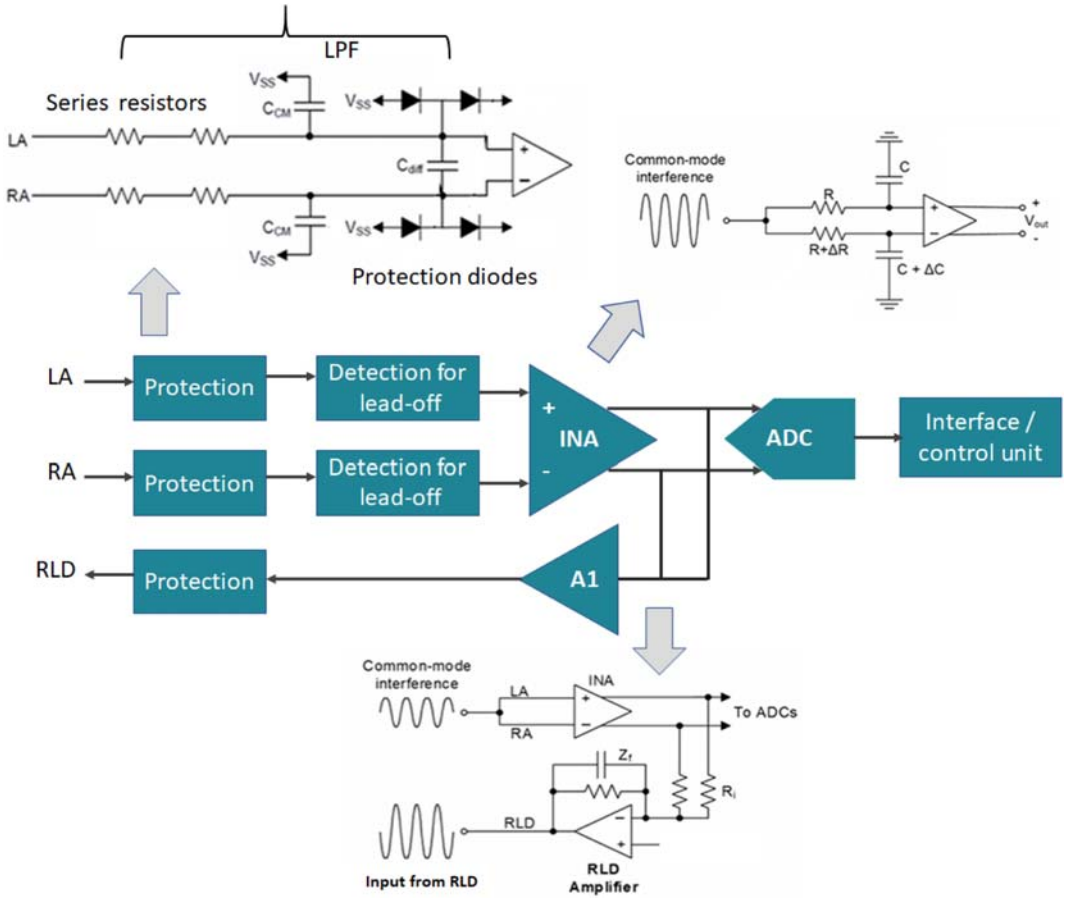

FIGURE 5–3 Depiction of three electrodes single-lead ECG acquisition system. (https://training.ti.com/how-measure-ecg-introduction-what-ecg). *ECG*, electrocardiogram.

from the defibrillator. The lead-off section send an alert to the physician through the measurement of impedance, if the electrodes are not placed properly.

Another subsection in Fig. 5−3 depicts a common-mode signal applied at both the inputs of an INA having a good Common Mode Rejection Ratio (CMRR). One of the most challenging tasks in ECG signal acquisition is the rejection of common-mode interference arising due to the PLI. This chapter shall discuss in detail the design of notch filters for the removal of PLI. Two common mode RC filters are designed to reduce the interference, but are not very effective, as there exists a component mismatch of ΔR and ΔC due to the tolerance limits of these passive elements. The CMRR worsens and gives poor rejection due to this and its value at a frequency "*f*" and filter cut-off frequency f_c becomes:

$$\mathrm{CMRR} = 20\log_{10}\left(\Delta R/R + \Delta C/C\right) + 20\log_{10}\left(f/f_c\right)$$

A solution to this problem is found by designing the RLD circuits. The RLD provides DC bias and supresses the common mode AC signals. As depicted in the figure, the common-mode signal is derived from the output stage of the differential INA, both connected at the inverting-input junction point of the RLD amplifier A1, thus forming a large negative feedback loop for the common mode signals.

$$\text{Output at the RLD amplifier} = -Z_f/R_i(\text{RA} + \text{LA})$$

ADC generally is the last stage of the front end ECG acquisition system before it is interfaced with the control and display section. Novel ADC units with high resolution are being designed which exhibit the property of DC coupling with the INA inputs and can measure ECG signals of even small amplitudes despite large DC offsets.

The preceding sections have detailed the clinical significance of the ECG signal, interpretations that can be derived from the PQRST waveform, ideal lead placement and the basic instrumentation involved in acquiring the bio-signal, and the section below presents the latest trends in cardiology.

5.2 Recent trends in cardiology

Cardiovascular disease (CVD) causes 17 million deaths or 31% fatalities globally today which will rise to 23 million by 2030 as per WHO data. The scope of technology innovation and intervention is immense with technology spends likely to top $40 billion in the same period which is only a part of estimated $500 billion setback to economy annually in USA alone. Point-of-care diagnostics and remote patient monitoring have developed over the years with introduction of wearables, molecular diagnostics, lab-on-a-chip, lateral flow assays, etc. but major success has not been achieved. Heart pacemakers were introduced as long back as 50 years for cardiac arrhythmia management but further advancements are required in cardia tissue engineering through bio-printing etc. to provide quantum leap in care and recovery (News, Cardiac Diagnostics, 2019).

Holter ECG machines were introduced in 1940s followed by the ambulatory version in 1950s. The later version or the need for continuous monitoring of heart related physiological parameters is relevant in patients requiring long-term monitoring as the arrhythmic events in some cases do not surface out in days but in weeks. Diagnostic yields are positively impacted as the patient uses a wearable device as compared to traditional Holter's which monitors them for merely 24 or 48 h. Hence in such cases wearable devices with single leads or newer Band-Aid type devices are relatively successful and comfortable with patients as well. Machines with multiple leads cannot be used while performing daily chores and also loose contact in some lead can hamper the entire monitoring protocol spread over weeks. Some of the smarter versions approved by USFDA include Patch Holter by ScottCare novi +, Cardea SOLO by Cardiac Insight, Bioflux by Biotricity, PocketECG by Medicalgorithmics, and Zio patch by iRhythm Zio patch. Furthermore, some cardiologists also differentiate the requirements based on the physical conditions of the patients, for example, premature

ventricular contractions may require a multichannel monitoring only. But the preference can be zeroed down only if the technology enables products tailored to the specific requirements and patient needs. Single channel or stand-alone wearable patches need to be referred back to the diagnostic centers for analysis of captured data, while some recent versions capture data locally in computers, which can be shared with the physicians. Overall, these wearables are patient-friendly and relatively cost-effective (SPONSORED CONTENT, FEATURE, ECG, FEBRUARY 19, 2020).

Fascinating innovative trends in cardiac technologies will play a major role in clinical practice in the coming future. To quote a few:

- *Artificial Intelligence* (*AI*) *in Cardiology*: AI and ML have already occupied space in this domain and is augmenting the cardiologists to speed up the diagnostic assessment. Finest of cardiac monitoring systems are integrating AI for identifying the anatomy, segmenting, labeling, automating measurements and report generation. ECG wearable units and smart phone based apps like "Apple Watch", "Kardia Alivecor," etc. also use AI for automatic detection of arrhythmia and sends an alert when a risk is detected. AI and ML techniques have prompted global AI leaders in cardiology diagnostics, "Cardiologs" to offer an exceptional solution for EKG recording for analyzing ambulatory signals for diagnosis of cardiac arrythmia based on cloud-based architecture. This enables clinicians to access the patient records remotely and provide timely, accurate and cost-effective solutions as compared to other solutions in the market. It seems the solution has found recognition with physicians and scores of patients in USA since 2018 (NEWS, ECG, DECEMBER 12, 2019a).
- *Trans-catheter Aortic Valve Replacement* (*TAVR*): TAVR is emerging as a new standard of cardiac care in place of surgical valve replacement. It is predicted that by 2025, 75% of aortic valves will be replaced using TAVR. Big names like Medtronic, Abbott and Boston Scientific, etc. are investing in this concept.
- *Wearable Solutions*: 24X7 tracking of health status has become possible due to the inventions made in the wearable devices. Wearable units are increasingly replacing the Holter monitors and are becoming a part of remote monitoring systems, cardiac rehabilitation and for patients with heart disorders.
- *Virtual Reality* (*VR*) *and Augmented Realty* (*AR*) *in Cardiology*: AR-VR technology has enabled virtual proctoring of knowledge transfer and offers a 360-degree view to understand the procedural navigation of device implant, permits 3D simulation of lesions in the arteries, makes possible a virtual tour to cath lab, can even virtually preplan the surgical procedure by marking the skin for incisions etc.
- *Big Data*: Clinical decision support system has become a need in the hospitals for data mining their medical records. Data analytics software are being used for automated and efficient pulling of patient's records, managing staff, tracking procedural details, identifying patients at risk for heart failure and other critical diseases, patient care, etc. and reduce workflow bottlenecks. This enables preventive health care system in place of the earlier system of reactive approach for treatment.

- *Holographic Navigation through the Cath Lab*: Holograms are making it possible to view live images of heart in the cath lab using a special screen, enabling 3-D reconstruction of image for visualization and for deployment of device.
- *Robotics in Cardiology*: Although an expensive arrangement, Robots in the cath lab permit precise catheter manipulation using a remote control arrangement. Siemens and a French-based company Robocath is planning to expand its product line in this domain (Dave Fornell, 2020)

Some proprietary software, for example, Cardiac Insight, have developed very robust ECG algorithms with platforms which are extremely interactive facilitating minute views and deep analysis of practically every heartbeat and associated events. The detailed data interpretation leaves the clinicians with sufficient opportunities for deriving a professional diagnosis without compromising on the sensitivity involved around patient health information and being at peace about such information being processed at third party sources. The patient satisfaction as compared to when the patient was using bulky Holter machines is extremely positive. Present day medical care ecosystem has many important and inevitable stakeholders including insurance companies. The clean diagnosis from such platforms not only leaves the patients satisfied, clinicians efficient, but offers transparency to insurance companies while processing claims (Smithsonian National Museum of American History, 2011; Kennedy, 2013; Health Quality Ontario, 2017; SPONSORED CONTENT, FEATURE, ECG, SEPTEMBER 27, 2018).

Another versatile set of ECG devices from Bittium deserves attention to comprehend the technological progress and prowess in present times. Water proof miniature product, Faros, is suited both for Outpatient Department (OPD) and IPD patients requiring limited stay in health care centers. The instrument captures ECG, allied cardiac events, mobile telemetry and assessment of physiological parameters related to autonomic nervous system. Built-in algorithms for arrhythmia detection and event recording leads to faster diagnosis and discharge of patients. The allied product "Cardiac Navigator" can analyze longer records of ECG records running into days, presenting intuitive results and accurate final diagnosis. Bittium also has a web-based solution for monitoring cardiac events called "HolterPlus." The analysis based on the smart inputs leads to faster diagnosis and the findings are uploaded for records and further refining patient care (NEWS, ECG, JANUARY 22, 2020).

Many existing standard ECG techniques require the patients to be at a clinical station with fingers of both hands being involved in analyzing and calling out the results of the investigations. Mobile applications also detect atrial fibrillation and can prevent fatal incidences of strokes and permanent damage to heart muscles. A novel approach utilized signals from left ear lobe instead of the right hand to acquire ECG output. The results as noted over 32 volunteers were the same as compared to the standard method, wherein the index and middle fingers of both hands were involved. This approach frees up the left right hand, making the method to be an excellent option even for self-monitoring for athletes, military personnel and drivers, etc. while in motion (FEATURE, ECG, MAY 03, 2019, SANKET SOLANKI).

AI coupled with EKG studies have resulted in a boon for patients suffering or with left ventricular dysfunction (LVDD). Many times, such conditions are asymptomatic and may

not present any prewarning to an impending heart failure. The incidence is prevalent in large percentage of population and significantly reduces quality of life and expectancy. The condition can be treated on diagnosis, but the diagnosis entails costly investigations like MRI, CT scans and ECG, etc., or some painful blood tests. Mayo Clinic has stored and analyzed data of 625,326 (and running) patients, both transthoracic ECG and EKG acquired in pairs. The researchers have carefully studied, created and tested a trained neural network, based on AI, which compares the EKG recording of patient under observation to reliably distinguish asymptomatic LVDD. The model also has capability to point out very early stage, minute EKG variations, which could later prognosticate into LVDD. This opens the door for various other similar investigations for early indicative diagnosis of critical diseases and vulnerabilities (Vasan et al., 2018; NEWS, ECG, JANUARY 08, 2019b). In a similar fashion, another exclusive device MyoVista from HeartSciences, have presented results on early LVDD detection. The study lays emphasis on the fact that abnormal relaxation is a distinguishing precursor to LVDD and other heart ailments (Kitzman et al., 2012; NEWS, ECG, APRIL 27, 2018).

The overall trends and advancements in ECG monitoring are prompting many Biomedical equipment manufacturers to embrace data management elements into the existing offerings. The renewed focus of health care providers and governments to centralise the electronic medical records so as the investigations, diagnosis, therapeutics and outcomes for individual patients are recorded and made available at a single place is another meaningful objective to adopt and present processed information. The approach would make quantum improvements in patient care and satisfaction, while cutting down significant duplicity of efforts and ensuring continuity of treatment. It is a clear outcome that the technology will continuously evolve to reach higher levels and cater to customer expectations and governing landscape (FEATURE, SEPTEMBER 17, 2009).

Clinical studies are indicating clear association among COVID-19 and cardiovascular ailments. The prognosis is even worse for patients with preexisting cardiovascular vulnerabilities. Patients with COVID-19 are under increased risk of acquiring viral myocarditis, coronary syndromes, arrhythmia, and venous thromboembolism. Clinicians across China, India, Italy, USA, etc. have found layers of complicacies in treatments of such patients. ECG and ultrasound were increasingly used by health professionals in China to preempt such cases with suspected cases of myocarditis in China. In Italy strain imaging coupled with ultrasound was used to understand the physical condition of heart in COVID surviving patients. American Heart Association, after studies, indicated strange mechanism of heart cell death in heart muscles. In case of critical patients, prioritizing clinical studies becomes more of a challenge for physicians and hence performing rapid ECG's at the initial stage is vital. Handheld, point-of-care ultrasound machines capable of giving AI based intelligent results to essential parameters like ejection fraction can make a huge difference to saving lives. Better technologies which assist in faster and efficient clinical diagnosis will always help in similar emergency situations (Anders Wold, 2020; Nishiga, et al., 2020).

Another notable application for rapid detection of myocarditis using noncontact method was developed for COVID-19 by Mesuron Inc., USA. The application considers magnetometers for *superconducting quantum interference device* (*SQUID*) for monitoring events

related to such patients. The technology proposed is most sensitive to detection of changes in T-waves, which are vital in monitoring such patients and as per studies ECG as a monitoring tool, fails to detects such changes in at least 50% of such cases. SQUID has many advantages as it is almost instant, noninvasive, sensitive, no contact and no radiation diagnostic tool indicating myocardial abnormalities including ischemia. The results can indicate segregation of low-risk and high-risk cardiac patients (NEWS, CARDIAC DIAGNOSTICS, 2020; Rajpal et al., 2020).

As it is evident from the review of recent trends in cardiology, the progression made in developing the ECG acquisition and monitoring devices. The range is broad going from modest and convenient Holter units to trendy and expensive implantable devices. However, there are still clinical and technical limitations that need to be resolved. Some of the monitors available only collate data in ambulatory patients and do not provide online processing and analysis. There are arrangements like EPI-MEDIC having an array of sensors involving numerous wires connecting between these sensors and the device, making it cumbersome and thus limiting the comfort level and movement of the subject (Zheng et al., 2007). Some of the monitoring devices also lack universal connectivity with the display and analysis section through the commonly available communication ports and are restricted by the proprietary units. The hospitals mostly make use of Wilson Central Terminal set up of 3-lead arrangement which can damage the overall amplifier characteristics. The Implantable Cardioverter Defibrillator offers a costly and intrusive procedure to acquire the bio-signal and is therefore recommended only for those who are at a high risk of cardiac arrest (Thakor, n.d.). MOLEC monitors are an expensive embedded solution to real-time ECG detection, processing, analysis and for notification of abnormalities (Rodríguez et al., 2005). Certain available data analytics algorithms are complex, and are unable to implement obvious decisions. So it is evident that, there is still a possibility for improvement in ECG monitoring devices predominantly in the domain of their vulnerability to interference, PLI, nonexistence of widespread connectivity, high cost, and processing in off-line mode. The subsequent section covers various notch filter circuit simulated and implemented for elimination of PLI from the ECG acquired using a computer-based indigenous system.

Apart from this, the real-time embedded arrangements developed using Digital Signal Processors (DSP) also play a major role in designing a compact solution and analyzing and processing multichannel information. The reduction in cost of this technology has made it popular and so is easily and commercially available to produce high in speed, compact, accurate, noise immune, low power consuming, and easily programmable devices. The limitation however is the inability to do online processing and analysis and the use of ADC and Data Acquisition (DAQ) units as an essential element of the bio-signal detection system. An attempt is also presented here in this chapter that explains the design and implementation of a low-cost, smart general purpose dsPIC digital signal controller (DSC) based scheme for uninterrupted monitoring, signal processing, eliminating the requirement of additional DAQ and ADC units and automated analysis of ECG signal that can lead to computer-generated diagnostic inferences. The drive for this initiative comes from the urge to understand how modern ECG monitors can assist in comprehending and presenting ECG signals with precision and utility in practice.

5.3 Notch filter designs for reducing power line interference in electrocardiogram signals

In India, the power line frequency is 50 Hz, that generates a fluctuating magnetic field through induction, and if a human body is in close vicinity to the power buses, they get capacitively coupled through the stray capacity developed. In a 3-electrode ECG system, capacitive-coupling exists between the power-line, the human body and the electrodes used for measurement as is depicted in Fig. 5—4. "C" represents the capacitive coupling between the power line and the body, "C1" and "C2" are the capacitive coupling between the electrodes and the power line.

The capacitance generated can be evaluated using the expression:

$$C = \varepsilon_0 \frac{A}{d}$$

where "A" represents the area in sq.m, "d" is the distance between the plates, measured in meters and the constant $\varepsilon_0 = 8.85 \times 10^{-12}$ F/m. Now, for understanding the effect, if we assume that one square-meter of the human body which is one meter away gets coupled with the power lines, the stray capacitance calculated comes equal to 8.85 pF. This stray capacitance coupled with 50 Hz power line frequency exceeds the amplitude level of the ECG signal which is of the order of 1 mV and poses a problem.

The power line interference (PLI) appears as a common-mode signal at both the input measuring electrodes of the amplifier system, because of the capacitive coupling due to power line and the earth ground. This interference is not the same as between the human body and the isolated-ground of the power supply, thus giving rise to a leakage current which introduces a 50 Hz interfering signal seen on both electrode inputs of the amplifier as well. Apart from this, if the cables used have different capacitive-coupling to the power mains and to the ground, it may cause interference. Therefore even if a small current as low as 0.1 μA flows, and the input electrodes have an impedance of 5 kΩ, then also the differential 50 Hz signal will be equal to 1 mV at the amplifier input, interfering with ECG signal.

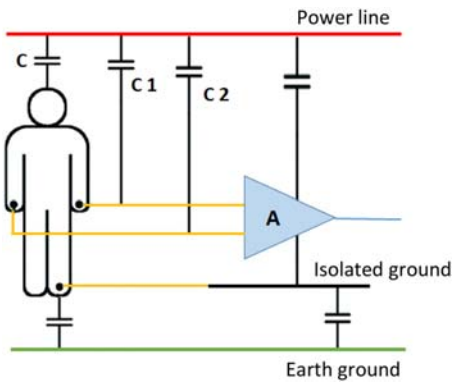

FIGURE 5–4 Depiction of power line interference (PLI) in the 3-electrode ECG system. *ECG*, electrocardiogram.

The fact that the common-mode signal appears equally at both the input terminals of the differential amplifier, helps in eliminating the interfering effect of power line voltage. Yet, because balancing may not be as proper in the differential amplifier in real-time applications, a common mode signal interferes with the acquired and amplified bio-signal. It is therefore of prime importance that the CMRR, which is the figure-of-merit of an amplifier and the rejection of interference deciding factor should be high.

Present biomedical INAs possess a very high CMRR but are still tainted by the remaining PLI primarily due to electrode impedance differences and the stray currents passing through the human body and the electrode cables. So, even a very high CMRR is unable to eliminate the interfering effects and the issue gets aggravated if the amplifier system has a floating input for ensuring safety of the subject. Many hardware solutions like shielding of cables, RLDs, etc. are proposed to improve the CMRR, which have the potential to reduce the impact of stray currents through the body. They are however, still not very efficient in reducing the PLI.

Filters can be deployed to eliminate the 50 Hz frequency from the bio-signal. An ECG signal is characterized from its PQRST wave shape, hence the filter type designed is of prime importance. This is because, filters attenuate the unwanted frequencies, but at the same time they affect the desired frequencies containing information pertaining to ECG signal as well, thus altering the basic shape of the QRS complex. So, to eliminate a particular frequency of 50 Hz noise (in India), a distinctive filter called the “notch filter” can be designed. Spectral analysis of ECG waveform reveals that it has meaningful information both above and below the 50 Hz frequency. The P-wave and T-wave have much lower than 50 Hz frequency components and the R-wave also lies below 50 Hz range. Some information is present in frequencies beyond 50 Hz. So a filter that can notch exactly the 50 Hz component is a viable solution to this issue.

For retrieval of true ECG signal, so that precise information can be extracted for further processing and analysis, it is essential to cancel the PLI. This domain has always attracted researchers and is still drawing a lot of attention and numerous innovative signal processing methods are being reported in the literature (Pei and Tseng, 1995; Chandrakar and Kowar, 2012; Sharma and Pachori, 2018). Notch filters designed based on Fourier techniques and Infinite Impulse Response (IIR) and FIR filters are being used for the purpose. Designs involving multiple-notch filters exhibiting enhanced transient response have been implemented to subdue the harmonics of PLI (Piskorowski, 2012). Tunable notch filter algorithm that are adaptable and that can preserve the selectivity and can attenuate the frequency to be notched have also been tested for precise assessment of ECG signal (Verma Singh, 2015). ECG signal improvement has been achieved using adaptive approaches involving spectro-temporal filters (Tobón and Falk, 2018). Adaptive IIR notch filtering has also been verified for many identical bandwidths to reduce the effect of PLI (Wang et al., 2017). Suchetha and team have addressed the issue of eliminating PLI using empirical mode decomposition based filters and have also presented a comparative analysis (Suchetha and Kumaravel, 2013; Suchetha et al., 2017). Digital notch filter designs are also explored to subdue the PLI in ECG signals. They however, may suffer from momentary interferences and the ringing-effect, due to improper sampling period selection during digitization. Researchers have addressed this issue by developing a sharp resolution adaptive notch filter (Chen et al., 2019). So, hardware notch filters are also required to be implemented.

Numerous hardware 50 Hz notch-filter design topologies utilizing minimum quantity of high-precision components have therefore been developed in the subsequent section using P-Spice. Add-on notch filter circuits have been implemented based on the simulated outcomes and when attached with the indigenous bio-signal acquisition system produces the ECG signal providing supreme clinical inputs post further processing.

5.3.1 Computer simulation of various notch filter design topologies

Designing, verifying and fabricating hardware circuits is a computationally intensive, tedious, and a time consuming process. Gaining understanding of an electrical circuit becomes simpler, if software simulating tools are used to analyze the components and the connections of the circuit before actually building the circuit. This enables efficient design process which is cost-effective, faster and provides improved alternatives to circuit components. The software platform allows voltage and current analysis, generates time and frequency response curves, and helps to comprehend the functioning of various elements of the circuit at different test points. It generates virtual circuits that can be accessed at any node for debugging and lets you try components that are physically not available. Many manufacturers are providing filter design simulation platform, some of which are stand-alone solutions that can be installed on a computer and few run on proprietary websites. Active and passive, both kind of filters can be designed using these software tools. Few available circuit simulation programs are:

- LTSpice | circuit design has to be predecided [en.wikipedia.org/wiki/LTspice]
- PSpice by ORCAD | for analog and mixed signal circuits

  [https://www.orcad.com/products/orcad-pspice-designer]

- FilterLab by Microchip for active circuits
  [microchip.com/developmenttools/ProductDetails/filterlabdesignsoftware]
- WEBENCH Filter Designer for active designs
  [ti.com/design-tools/signal-chain-design/webench-filters.html]
- Filter Design Tool for active filters [https://www.ti.com/design-resources/design-tools-simulation/filter-designer.html].
- Filter Wizard for active filter designs
  [www.analog.com/designtools/en/filterwizard]
- ELSIE for passive circuit design [www.tonnesoftware.com]
- Filter Design and Analysis for both active and passive designs [sim.okawa-denshi.jp/en/Fkeisan.htm]
- FilterPro Active Filter Design Software
  [https://filterpro.software.informer.com/3.0]
  The filter design tool enables design, optimization, and simulation of complete multistage active/passive filters within no time. There is a provision to select the optimum filter design based on response, settling time, pass-band and stop-band ripples and attenuation. Making a trade-off between parameters like cost, gain-bandwidth product and design topologies like Sallen-Key, multiple feedback, etc., best suited

operational amplifier can be chosen. The circuit built can then be analyzed for step response, frequency response, etc. using Monte-Carlo and Corner analysis tools. It facilitates selection of flat pass-band, sharp transition band, linear phase delay and frequency band from 0.1 Hz to 10 MHz. Schematics can be easily generated for print, reducing time to market. To ease and speed up the process of active filter design, some companies deal with free of cost filter design software like FilterCAD developed by Linear Technology and FilterPro designed by Burr-Brown. OrCAD PSpice has been made use of in this work for simulating and verifying the filter circuit as it provides a high-performance platform and the flexibility to choose circuit components, and parameters before finalizing the layout for fabrication.

Design of active notch filters to eliminate 50 Hz PLI is very common. They however pose design concerns regarding repeatability, stability and tuning of notch filter's center frequency f_0. So, various notch-filter design topologies with following desired goals have been verified:

- A filter that notches exactly the 50 Hz frequency component instead of rejecting a band of frequency
- A circuit design with minimum number of operational amplifiers
- A circuit that can operate with single supply source
- A design that permits independent tuning of center frequency f_0 and the Q factor
- A circuit with reduced number of high-precision components required for tuning
- A filter design with a sharp and good notch depth

The most common notch filter design is the twin T-network also known as parallel T configuration. Twin T-network consists of passive R-C branches consisting of two T-shaped sections in parallel. One T-network is made up of 2-R and 1-C forming the LPF while the other is made of 2-C and 1-R forming the HPF. The frequency offering maximum attenuation is termed as the notch frequency f_0 and is given by the expression:

$$f_0 = \frac{1}{2\pi RC}.$$

To have a narrow notch and a high attenuation level, op-amp is used in the design. The circuit diagram of design 1 is shown below in Fig. 5—5. with two op-amps, where R5 is 1/2 of R1 and R2. R3 is calculated based on R1 and R2 combination. Likewise, C4 and C5 are 1/2 of C3 calculated by parallel combining C4 and C5. The frequency response shows a good notch-depth at 50 Hz with sharp cut-off and as expected, the response is almost flat over the usable range.

The problem with twin T design is the relatively low figure of merit "Q" which disturbs the filter selectivity. This can be enhanced by incorporating a voltage follower in the circuit, with feedback at the R/2 and 2 C junction point. The Capacitance C is preferred to be less than 1 microfarad and then R is considered for having a notch at 50 Hz. An emitter follower can also be used in the design, instead of the voltage follower. However, the inherent advantage of using a voltage follower is the high input resistance which gives output voltage equal to the input magnitude and phase as it behaves as a buffer. The twin "T" configuration made

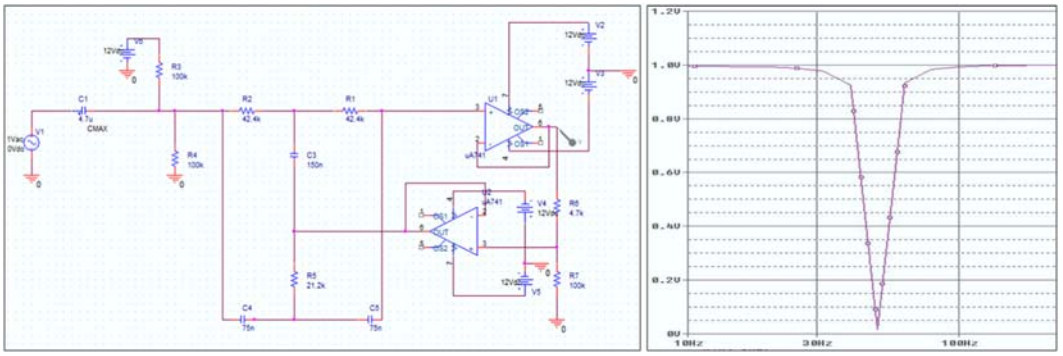

FIGURE 5–5 Design 1: 50 Hz notch filter circuit and its frequency response curve.

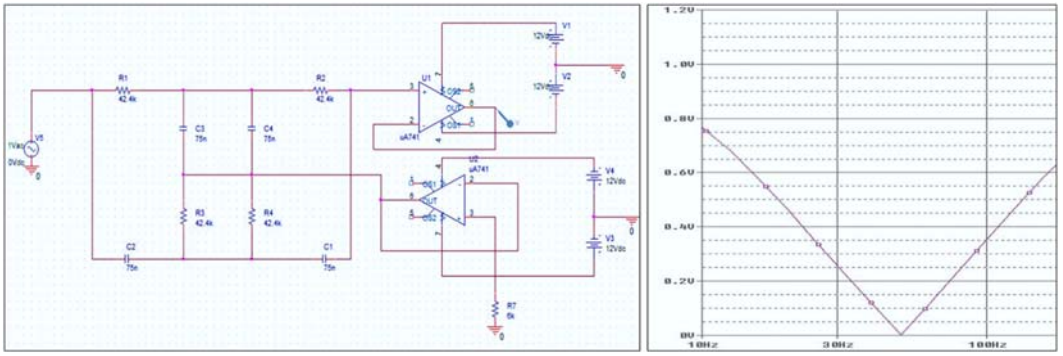

FIGURE 5–6 Design 2: 50 Hz notch filter circuit and its frequency response curve.

with op-amps combined with a voltage follower offers high *Q* factor and a fairly deep notch. The op-amps used offer high input impedance permitting large R and low C values in the design topology that finds application in low-frequency situations.

Design 2 circuit shown in Fig. 5—6 again has two op-amps, however, more number of high precision components are used. The response curve clearly shows that high depth of notch is achievable, but sharp drop-offs is not possible and the response curve is not flat.

Simple notch filter design 3 as in Fig. 5—7 uses single op-amp and minimum number of R and C components. The response curve as seen has high depth of notch, but sharp drop-offs is not achievable and the response curve is not flat.

Design 4 of Fig. 5—8 below, is bootstrapped at the junction of R2 and C1 to the voltage follower output. It is also a single op-amp filter circuit with least number of passive components. Bootstrapping increases the Q in accordance with the signal that is fed-back to R2 and C1. The frequency response obtained shows sharp cut-off notch with flat response, but the notch-depth is not as desired.

Design 5 as in Fig. 5—9 is obtained by modifying circuit in design 4 by using two voltage followers in the new design. The second follower further stabilizes the *Q* factor and permits elimination over a widespread range of input frequencies by feeding back a portion of the

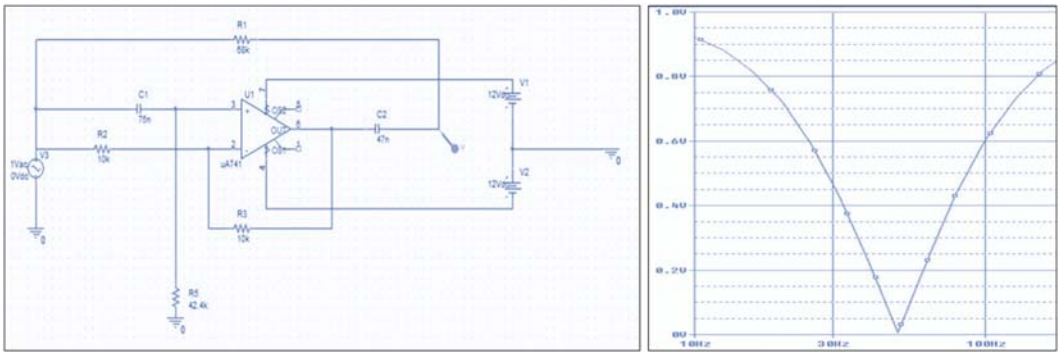

FIGURE 5–7 Design 3: 50 Hz notch filter circuit and its frequency response curve.

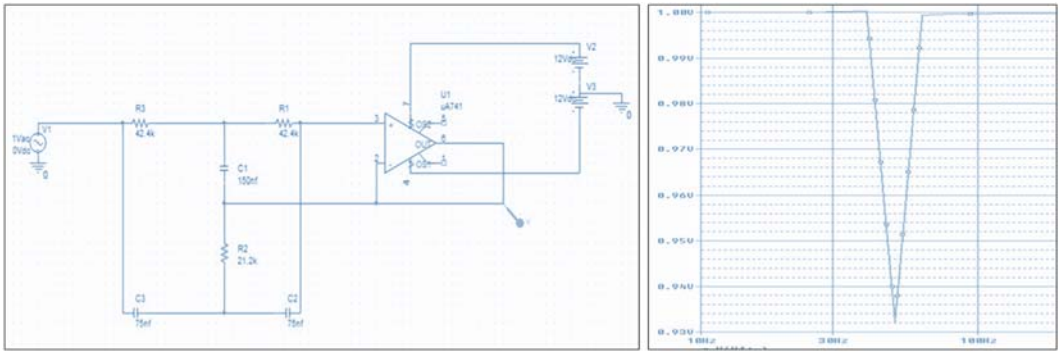

FIGURE 5–8 Design 4: 50 Hz notch filter circuit and its frequency response curve.

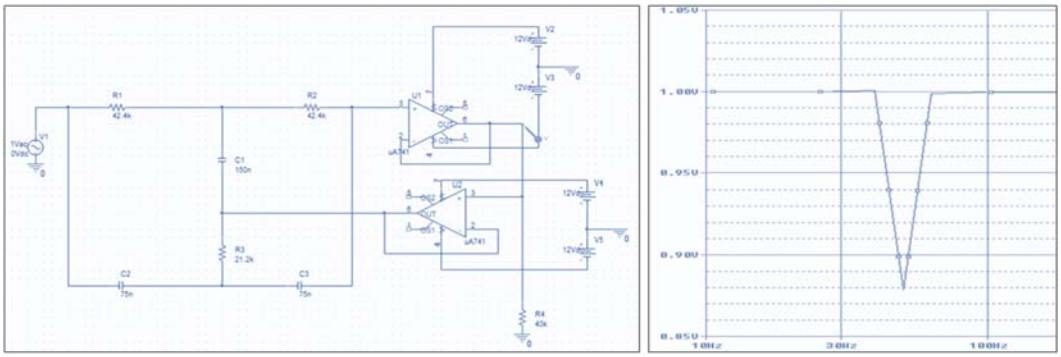

FIGURE 5–9 Design 5: 50 Hz notch filter circuit and its frequency response curve.

output to the intersection at R3 and C1. The signal fed-back decides the notch Q. The response curve obtained has sharp cut off, but the notch-depth is not as desired.

Fig. 5—10 is the 50 Hz notch-filter design 6, having a single op-amp is not very flexible, but still offers a desirable notch depth in comparison to other single op-amp notch circuit

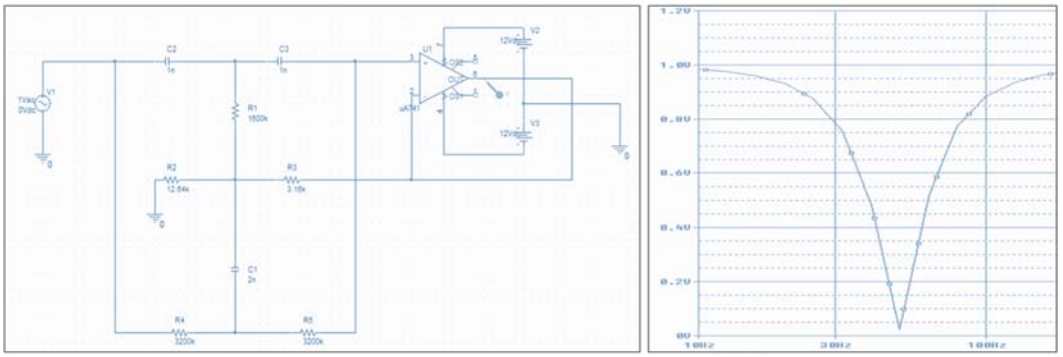

FIGURE 5–10 Design 6: 50 Hz notch filter circuit and its frequency response curve.

Table 5–1 Comparison of component values for various 50 Hz notch-filter circuits simulated in PSpice.

Circuit designs	op-amps required	Tuning capacitors required	Tuning resistor required	Center-frequency evaluation		
				R	***C***	f_0
Design 1	2	3	3	42.4 K	75 n	50.02
Design 2	2	4	4	42.4 K	75 n	50.02
Design 3	1	2	3	42.4 K	75 n	50.02
Design 4	1	3	3	42.4 K	75 n	50.02
Design 5	2	3	3	42.4 K	75 n	50.02
Design 6	1	3	5	3.2 M	1.0 n	49.72

designs simulated earlier. It does not allow easy trimming of the center frequency as this involves modifications of R1, R4 and R5. The circuit is made of 6 high-precision constituents that are required for tuning, out of which two are the ratios of others. The resistors R2 and R3 are required to be lesser as matched to R4 and R5, thus increasing the extent of resistor values. This adversely disturbs the notch-filter depth and the center-frequency. Sharp drop-offs are not achievable as can be seen in the response curve, but notch depth achieved is good.

Standard R and C components and UA741 Operational Amplifier have been used to design and simulate the notch filter circuit. Detailed component values and center frequency value f_0 for each design is figured in Table 5−1. The R and C components selected produce a notch at the center-frequency of 50.02 Hz for nearly all the circuits simulated.

Theoretical results of simulation in terms of the notch depth achieved are not possible in real-time, because of tolerance variation in passive components used in the design. Component tolerances have the effect of altering the response and, so, high-quality circuit parts are used for accurate, high-quality notch filter circuit. Metal film resistors with 1% tolerance and carbon film types with 5% tolerance are commonly used. Small capacitors below 100 pF, as used in this work, require NPO ceramic capacitors. Large ceramic disks and Al-electrolytic capacitors have wide tolerance range and so are not advised as this leads to instability with temperature and the applied voltage.

Circuit design 1 gave the desirable frequency response with strong attenuation, sharp drop-off, flat usable range and very good notch depth at 50 Hz frequency. This design was fabricated to be used as an add-on 50 Hz analog notch filter with the ECG front end amplifier to reduce the effect of PLI acquired during ECG detection and is detailed in the subsequent section.

5.4 Real-time detection and processing of electrocardiogram signal

The functional block diagram representation of the indigenous system established for real-time acquisition and processing of ECG signal is drawn in Fig. 5−11. The front end amplifier detailed in Chapter 4, that was developed for acquiring the EMG signal in real time, is added with a notch filter circuit designed in-house for detecting the ECG waveform. The reusable Ag−AgCl electrodes are placed on the right-arm and the left-arm and as a reference on the right leg for acquiring the ECG signal. For better detection of the bio-signal, electrolytic gel is applied on the skin surface prior to acquisition. The detailed circuit diagram for acquiring the ECG signal is shown in Fig. 5−12.

Literature reports various circuits to detect ECG signal from a 3-electrode system and a few of them were tried during the experimentation. This circuit diagram deployed using the op-amp TL-084C, gave the best results. It comprises of Buffer Amplifiers, Unity gain follower, DC restoration circuit, an integrator filter in feedback and a driver circuit for the reference right leg electrode. Additional notch filter circuit to eliminate the 50 Hz hum has also been designed using standard R and C components and an op-amp UA741. The simple interface concept deployed and the software oscilloscope designed, as has been explained in chapter 4, proves out to be efficient in acquiring and processing the ECG signal as well.

The ECG signal picked up using this arrangement has an amplitude of the order of 1 mV peak to peak. Therefore the cascade amplifier designed, provides an amplification of 500 times, in order to enable the bio-signal perceivable and useful for further processing, without getting saturated. The set-up also gives enhanced CMRR. Deployment of such a large gain amplifier circuit for detection of ECG signal poses practical challenges as, even the adjacent noise gets equally amplified. As can be noticed, it is imperative to eliminate the power-line

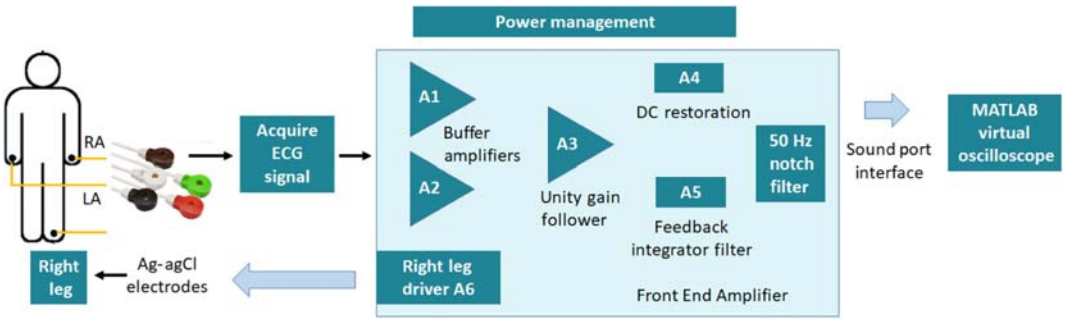

FIGURE 5–11 Block diagram representation | Real-time detection of ECG signal. *ECG*, electrocardiogram.

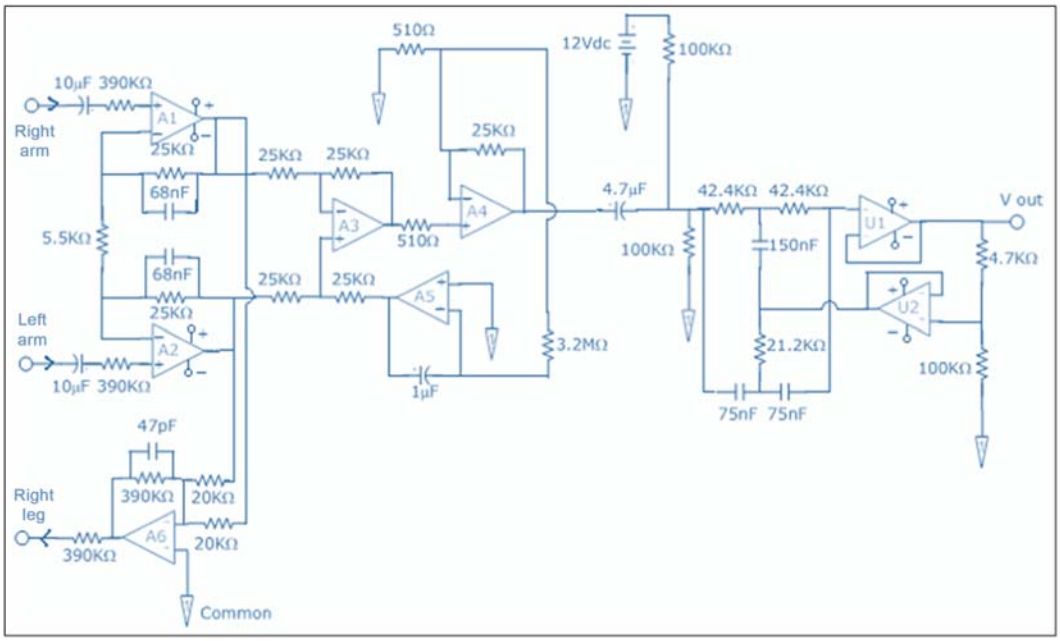

FIGURE 5–12 Detailed circuit diagram for real-time detection of ECG signal. *ECG*, electrocardiogram.

hum. Fifty Hz hardware notch filters designed and fabricated in the previous section helps in removing the power-line hum. Further digital filtering and processing is also done in on-line mode using zero-phase BPF as was done in capturing and analyzing EMG signal, with frequency range set as per ECG signals.

Fig. 5−13 displays the captured rest ECG signal with notch filter (Fig. 5−13B) and without notch filter (Fig. 5−13A) circuit. On the *X*-axis are the detected samples of ECG signal in time and on the *Y*-axis is the amplitude of the signal. A sampling rate of 8000 samples/second is set for acquiring the bio-signal and therefore, 80,000 samples are captured in 10 s, as is seen. On comparing Fig. 5−13A and B, it is clear that the 50 Hz notch filtered output has improved. The detected ECG signal is further processed for feature extraction and for drawing diagnostic inferences.

5.4.1 Online algorithm for feature extraction

Characteristic features of ECG signals are an illustration of the electrical action of the blood flowing through the heart and can be extracted from the PQRST waveform. The ventricular depolarization can be analyzed from the QRS-complex which is the utmost significant feature. Atrial depolarization is characterized from the P-wave and the T wave portrays the repolarization of the ventricles. The resting state is reflected in the consequent period of in-activity.

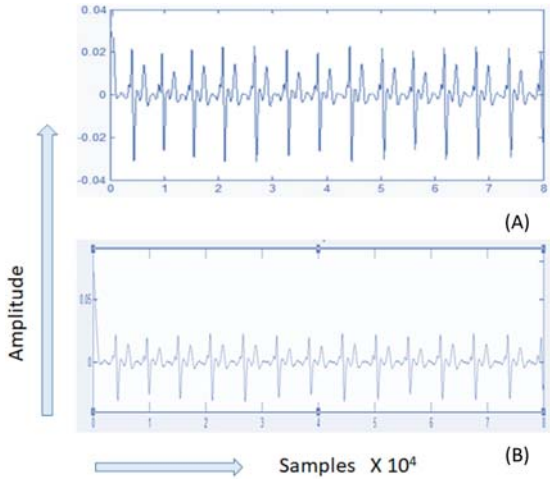

FIGURE 5–13 Rest ECG signal captured (A) without notch Filter (B) with notch filter circuit. *ECG*, electrocardiogram.

Automated and reliable detection of QRS peaks in the ECG waveform can lead to improved diagnostic inferences, and so a lot is being researched to devise an algorithm with higher performance. To quote a few recent developments in this area; the basic algorithm proposed by Pan-Tompkins is being modified using optimized band-pass filters and tried on MIT-BIH arrhythmia data-base so as to eliminate false detection of QRS peaks (Sathyapriya et al., 2014). The peak detection algorithms are generally limited by the nonstationary behavior of the QRS waveform and the interfering noise. A novel approach which exhibits effortlessness and robustness is the peak finder designed using the Hilbert transform and the MA filter (Manikandan and Soman, 2012). Postfiltration, the ECG signal is passed through a Differentiator, to enhance the ECG signal and then improved adaptive threshold technique is explored for effective identification of QRS complex (Ehab and Ali, 2019). Deep Recursive Long Short-Term Memory (LSTM) approach has also been verified for characterizing the ECG signals (Qi et al., 2019). LSTMs, have lately emerged as the most extensively used recurrent neural network type design, a concept of deep learning along with wavelets for classifying ECG signals. (Yildirim, 2018). Convolutional Neural Network and Radial Basis Probability Neural Network have been combined to devise a novel approach for feature extraction and classification of multichannel 12-lead ECG signals (Wu et al., 2020). Wavelets have been extensively used for automated QRS-complex detection and classification of heartbeat in the ECG Signal (Bouny et al., 2020a,b).

Most of the proposed algorithm are tested on stored database and perform off-line analysis on costly platforms with no time constraints. There is a need to work online in real-time for characterizing the bio-signal. For real-time analysis, a hardware friendly approach deploying exponential transform technique to reduce the amplitude difference of the ECG wave peaks along with the PD-control based adaptive threshold methodology has been tested and implemented (Chen et al., 2020). Still, there is a lot to be tried to offer a

portable and wearable cost-effective solution catering to the time limiting and computational load constraints of an online analysis system (Zalabarria et al., 2020).

An attempt has been detailed here, that has the ability of online analyzing the real-time acquired ECG signals using the hardware set-up developed indigenously. Algorithm has been designed using the functionality of MATLAB software to identify peaks of the QRS complex. Fig. 5−14 gives the flow for online extracting features of the real-time acquired ECG signal and also presents the method adopted for spectral analysis of the bio-signal. Analysis in frequency domain provides added facts about the human physiological parameter. The algorithm established effectively recognizes the QRS peak of the ECG waveform and also computes its power spectral density (PSD). An Analog input object is created in MATLAB to acquire the single channel ECG signal in real-time. The sound port of the Laptop is used as the interface to detect the output of the front end amplifier system and the notch filter. Acquisition parameters are set to suit the detection of ECG signals. The Analog object

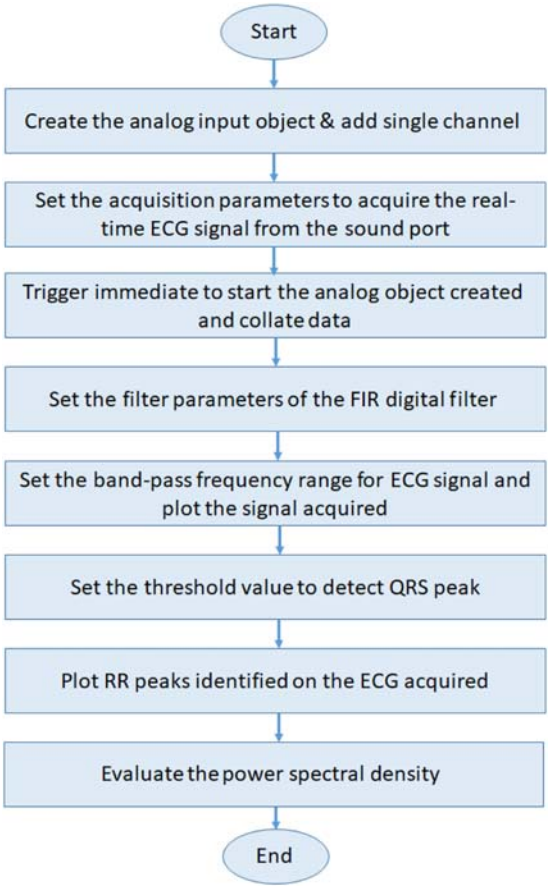

FIGURE 5–14 Algorithm flow for online spectral analysis and feature extraction in real-time acquired notch filtered ECG signal. *ECG*, electrocardiogram.

created is triggered and ECG information is collated. The ZPBPF digital filter parameters are set and the frequency range is fixed as per the bio-signal. RR Peaks are detected in the ECG waveform by setting the threshold to a certain level for identifying the QRS complex. Spectral analysis is done by evaluating the PSD.

MATLAB oscilloscope window displays the ECG signal with RR-peaks distinctly identified for different subjects as shown in Fig. 5−15. The spectrum of ECG signals falls in 0.05−100 Hz range, so digital-filter programmed is verified with different lower/upper cut-off band-pass boundaries. As we know, spectral analysis helps in further arriving at inferences,

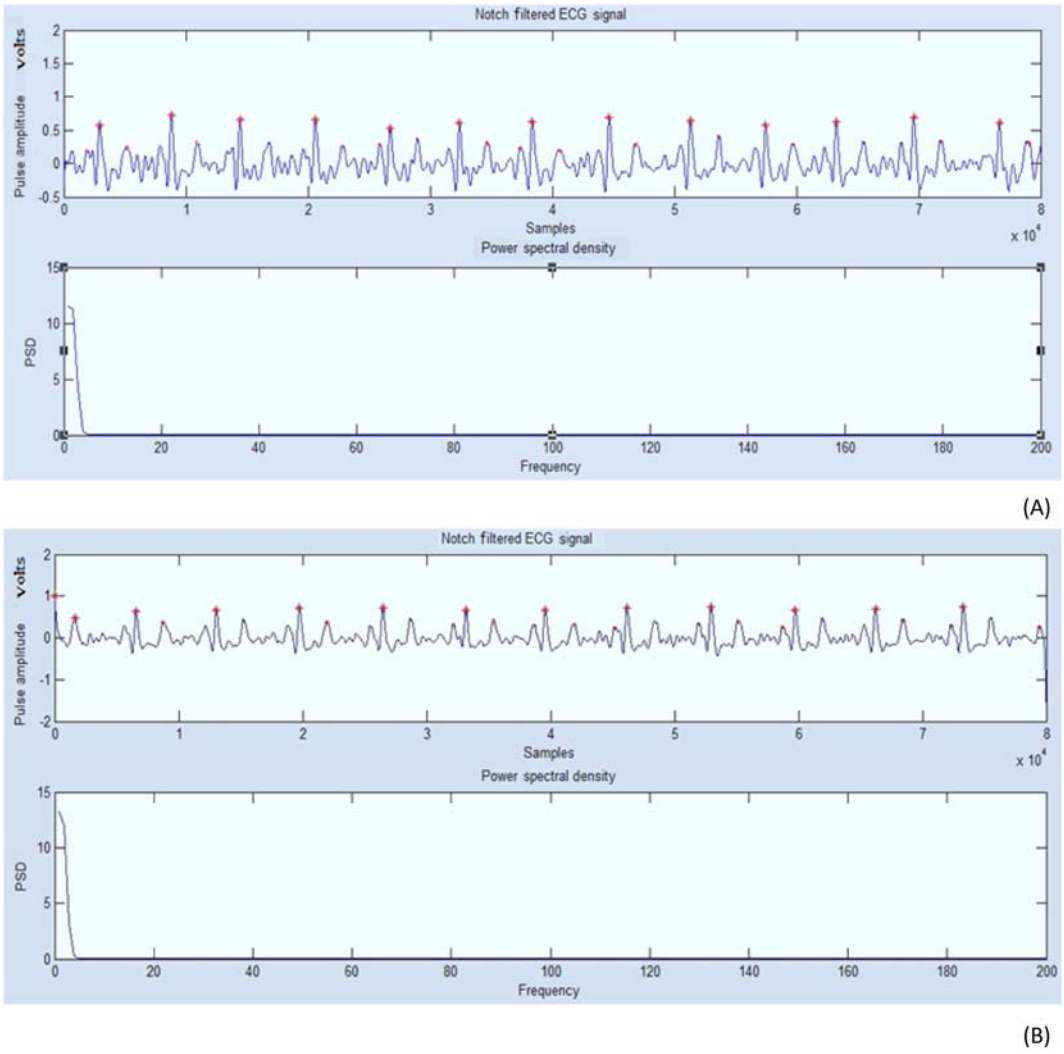

FIGURE 5–15 Results showing RR-peak and PSD of notch filtered real-time acquired ECG signal. (A) Subject 1, (B) Subject 2. *ECG*, electrocardiogram.

so PSD is also evaluated as shown in Fig. 5−15. which may vary depending on the individual. Much more feature identification functions can be included in the existing algorithm for classification of Heart abnormalities, HRV analysis, generation of alert signal, etc.

Increasing popularity of ECG devices to monitor and timely detect cardiovascular irregularity is continuously challenging researchers to devise solutions that can deliver with high speed and precision a good quality real-time ECG signals. Combining the excellent control ability of Microcontrollers with the processing abilities of DSP, DSC systems are being developed and extensively studied to provide a complete system-on-chip solution to real-time acquisition and processing of ECG signal having fast computational capabilities, high sampling rate, multichannel synchronization capability for real-time detection, digital filtering algorithms, data storing options, mobile app and automated feature extraction, classification and analysis programs. The section below details a DSC based system implemented for real-time ECG acquisition and characterization.

5.5 Digital signal controller-based electrocardiogram acquisition system

Biological signal measurement, processing and analysis in real-time involves handling of huge data size, interpretation of complex signal waveforms, adequate sampling speed, etc. which tends to limit the performance of the Microcontrollers used, the analog circuits designed and also the computational ability of the computer. DSCs are a hybrid solution to this issue, offering computational and processing capability of DSP processors and the hardware capacity of Microcontroller units (MCUs). DSP processors allow a computerized methodology for easy acquisition and analysis of human physiological parameters, time−frequency analysis, pattern recognition, filter algorithms, etc. at improved speeds, and can handle huge data size (Ressler et al., 2007). In the year 2018, Microchip Technology Inc. introduced a novel set of 16-bit DSCs with two in-built cores, suitable for mobile apps, like ECG monitoring units, which enabled collection and processing of bio-signal information in real time. They also implemented an IIR filter to reduce interference picked up from the surroundings during acquisition (Ngoc Thang Bui et al., 2020). MCUs enable fast interrupt times, peripheral control, general purpose Input−Output, etc.

DSCs manufactured by Texas Instruments (TIs) offer an on-chip way out to real time detection, processing, and characterization of ECG signals. Heart-rate units compatible to the RS232 computer port have been designed using TIs MSP430FG439 MCUs that gives digitalized result displayed on a LCD (Murugavel Raju, 2007). DSP processor TMS 320F206 and a MCU 89C55 is also implemented to acquire real-time ECG from a 12-lead synchronized multichannel system at high sampling rate of 1000 Hz with 12-bit precision that can automatically compute the ECG parameters viz. heart rate, P-R interval and Q-T interval (Yang et al., 2002). Researchers have established a real-time RR interval evaluation system based upon the correlation technique implemented on a cost-effective DSP processor (TMS320C31) where the bio-signal can be acquired at a 1 KHz sampling rate (Buttfield and Bolton, 2005). Real-time assessment of fetal ECG has been verified using an embedded framework of dual-core OMAP-L137

low-power processors where the general purpose MCUs presents a GUI and the 300 MHz floating point TMS320C6713 DSP processors permit modified signal processing algorithms to be implemented (Pani et al., 2013). Algorithm for de-noising and characterizing the ECG signals acquired using a single lead system, using wavelets has been verified for routine clinical application, using the codec input of DSP starter kit (TI TMS320C67) (Balasubramaniam and Nedumaran, 2009). A compact real-time ECG monitoring and wireless transmission unit has been designed using the ATmega328P MCU and the ZigBee interface module where the bio-signal can be viewed and analyzed on GUIs designed on LabVIEW and MATLAB configurations (Ehnesh et al., 2020). TMS320C25 DSP processor has been explored over the years to develop an enhanced ECG acquisition and processing system (Sahambi et al., 2000; Mohammad et al., 2003). Vendors like Hyperstone, Motorola, STMicroelectronics have also entered the space for development of DSP processors and development boards, that allow fast processing of algorithm to detect and analyze the bio-signals to enable patient monitoring (Kondra et al., 2005; Chang et al., 2004; Khatib et al., 2006).

In this experimentation, Microchip's dsPIC DSC based economical real-time arrangement for acquisition, processing and analysis of ECG signal has been detailed. The hardware circuit developed for front-end amplifier and the notch filter designed remains the same as presented earlier. The software developed in MATLAB environment for digital filtering and peak detection also is the same. To initiate the development process, a vast range of DSP processors commercialized by vendors like Texas Instruments, Analog Devices, FreeScale (Motorola) and MicroChip were reviewed for their flexibility, programming ability and quality (BDTI's Pocket Guide, www.BDTI.com/benchmarks; Microchip. MPLAB Starter kit, www.microchip.com; Processor Comparison, www.pentek.com) These processors ranged from being in fixed point/floating point formats and 8/16/32/40-bit data size.

Once the selection of DSP processors is finalized, add-on development boards of the DSP kit are analyzed for features relating to the peripherals available and the interfaces suiting the application. The development process comprises utilizing the functional capability of the Integrated Development Environment (IDE), the debugger and the GUI available in IDE for fast project design execution and for fixing the issues. After finalizing the DSC, a suitable sensor, amplifier, analog filter, notch filter arrangement is chosen to detect the bio-signal. Further processing and feature extraction algorithms along with the control section are then verified on a suitable software application platform that can allow on-line analysis. The subsection below explains the process adopted for acquisition and the results obtained.

5.5.1 The acquisition protocol and results

The complete block diagram representation of a DSC based real time solution for detection and analysis of ECG Signal is depicted in Fig. 5−16. The acquisition and processing system comprises Ag−AgCl electrodes to sense the electrical activity of human heart using a three electrode set-up, the front end amplifier system with cascaded arrangement and feedback integrator, the RLD as reference, 50 Hz hardware notch filter circuit to eliminate PLI, DSC with inbuilt amplifiers, ADC and antialiasing filters for fast processing and for supporting

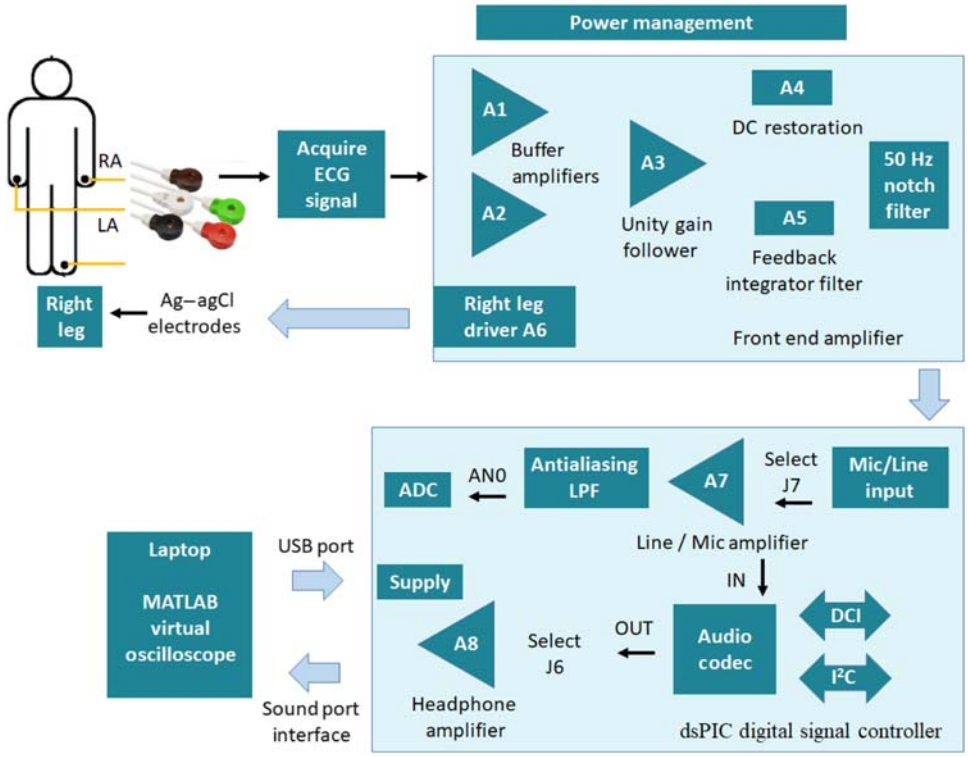

FIGURE 5–16 Block diagram representation | Real-time detection of ECG signal using digital signal controller. *ECG*, electrocardiogram.

real-time detection and MATLAB application software for display, further filtering, processing and parameterization of ECG signal.

An intelligent and fast processing design solution is proposed for ECG detection and continuous monitoring based on Microchip's MPLAB dsPIC DSC board with part number DM-330011. Power supply to the board is managed through the USB port of a computer. Features of the dsPIC DSC board includes:

- Features similar to the general purpose fixed point DSC dsPIC 33FJ 256 GP 506.
- A debugger and programming circuit for on-board programming of applications.
- An arrangement to input audio (analog) signals from line-in or an external microphone.
- An ADC module for conversion of analog signal (ECG system output) to digital signal.
- Audio/Codec Unit and Amplifiers.
- An on-board module for digital filter software processing.
- Compatible interfacing possibilities with PIC24 MCUs and dsPIC30F DSCs.
- The DSC has 256-KB Flash and a RAM of 16-KB.
- The DSC is of 16/24/32-bit with 48-kHz max-frequency.
- CPU has the speed of 40 MIPS.

- Operating temperature ranges -40°C to 85°C.
- The operating voltage ranges from 3 V to 3.6 V.
- A 6th order Sallen-Key LPF with a cut-off frequency of 3300 Hz suitable for bio-medical uses.
- Digital-Communication Peripheral available: 2-UART, 2-SPI, 2-I^2C.
- Analog-Peripheral comprise: 1 ADC 18x12-bit at 500 kbps.

The dsPIC33F DSC board with the in-built functionality mentioned, along with the cascaded amplifier and filter system faithfully acquires the bio-signal. The proof of concept for the front end amplifier using TL-084C differential amplifier has already been verified and established. The notch filter circuit design uses 741 op-amps as has been detailed in the previous sections. For detection of ECG signal, analog signal acquired from the front-end amplifier and filter circuit is sent to the 12-bit inbuilt ADC module of the DSC kit post amplification by a noninverting Line/Microphone Amplifier and post filtering through an antialiasing filter. This is done by routing the ECG signal through the line-in socket point J7 (as shown in Fig. 5—16) for obtaining its digitized version. This eliminates the additional requirement of an ADC unit, thereby making the arrangement less cumbersome, cost-effective and compact. Filtered output from the antialiasing filter is linked to the input node AN0 of the ADC module as shown in the block diagram.

The DSC unit allows saving the acquired ECG signal through its serial Flash memory for further processing and analysis. The recording protocol includes the following steps:

- The switch S1 on the board is pushed to turn off the Red LED and turn on the Yellow LED (this is done to erase the serial Flash memory).
- Switch S2 is pushed to re-play and visualize the saved ECG signal. This turns on the Green LED.
- The step of pushing switch S1 can be performed again to erase the prior data and to set the Flash memory ready for new recordings.

The dsPIC33F board features an application program for recording and playing back the detected information. This application program modifies the incoming signal by compressing it to 8-bits from 16-bits using the G.711 μ-law encoding algorithm. These encoded bits are then stored on the serial flash memory. The G.711 μ-law decoding algorithm is then utilized for playing back the recordings in the memory using the Audio Codec module. Taking commands from the application program, operating parameters like sampling rate, filter settings, communication protocol etc. of the Codec unit are controlled. This information is transferred through the Inter-Integrated Circuit (I^2C) unit featured on board. Codec does conversion of analog ECG signal into digital signal for the Digital Converter Interface (DCI) unit and then converts it back into analog form after processing through the two-way communication DCI module. Output from the codec unit, is analog in nature which is interfaced to the output amplifier through the socket point S6 as depicted in Fig. 5—16. The amplified output is interfaced directly with the MATLAB virtual oscilloscope window through the sound port of the computer. Programs developed in MATLAB further filter the detected ECG signal and identifies RR-peak for characterizing the bio-signal. The software tool available with the DSC kit is tested and verified for the ZPBPF and peak detection algorithm developed earlier.

The DSC DM330011 based improved system developed, faithfully acquires, filters, displays, records and digitally processes real-time ECG Signal as shown in Fig. 5—17. The algorithm designed for peak detection clearly marks the RR-peak in the acquired ECG signal, which can prove to be very useful in drawing diagnostic inferences related to heart.

DSC possess inherent advantages over conventional microcontrollers in terms of the architecture used. DSC modules make use of Harvard design taking distinct memories for data and instructions while conventional MCUs use the Von-Neumann design that have a particular memory to contain both data and instructions. As information can be fetched at the same time in Harvard architecture, it provides higher speed. DSP processors make use of fixed point and floating point formats, each with certain merits and demerits. In fixed point format, numbers are represented with minimum 16-bits, are low in cost and power requirements whereas, floating point DSP processors use a minimum of 32-bits for storing data and allow faster implementation suited for custom applications. The DSP processors TS 20x manufactured by Analog Devices exhibit improved floating and fixed point operations. (Processor Comparison, pentek.com). The development tools offered by the manufacturers along with DSC kits also show a major part in planning the design of ECG monitoring units. Tool offered by Texas Instruments is the Code Composer Studio that provides an environment for fast implementation using high-level C-callable functions, and runs on Windows. Microchip's DSC boards also deliver a comprehensive user friendly IDE environment and can work on Windows. The dsPIC DSC DM 330011 board used for developing an automated acquisition system has on-board ADC and so reduces the complexity of the ECG monitor. This arrangement of integrating DSCs with the commonly used hardware/software arrangement for acquisition, processing, analysis and continuous monitoring of ECG signals in real-time helps in reducing the constraint of making a compromise between the efficiency, cost, size, power requirements, etc. The experiment established

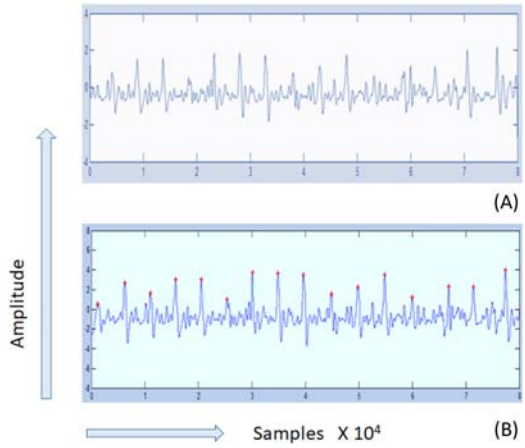

FIGURE 5–17 Results showing (A) Filtered ECG signal detected using digital signal controller and (B) Peak detected ECG signal using digital signal controller. *ECG*, electrocardiogram.

confirms refined real-time assessment of ECG signals by means of Microchip's DSC boards that needs less power, is compacted and is economical.

5.6 Conclusion

The indigenous front end amplifier system along with the fifty hertz notch filter designed for eliminating PLI is capable of faithfully detecting the rest ECG signal. Various notch filter topologies were simulated and verified using P-spice. One of the design circuits has strong attenuation capability, exhibits good notch depth and reasonably sharp drop-offs, so it's hardware was created and implemented along with the amplifier section for ECG detection. The notch filtered ECG clearly indicates the removal of 50 Hz hum from the detected bio-signal (Bansal et al., 2008).

The simple and easy to interface hardware along with the analytical software developed in MATLAB is capable of acquiring and processing bio-signals like ECG, EMG, EEG by simply adjusting the gain requirements and the filter bandwidth settings (Bansal et al., 2009a,b). The arrangement detailed is economic and establishes the know-how of precisely measuring the real-time cardiac response of a human heart in a computer-based home health bio-signal detection system. This can be further explored to be wirelessly transmitted in real-time to health care enablers for quick assistance and advise even when in remote situations. The sound port interface concept is compatible with hosts of computer ports and cost-effective and can be extended to acquire ECG signal from multichannel 12-lead arrangement. The cost of portable ECG monitors can further be reduced by designing single-chip DSC based set-up that offers detection, signal processing and feature extraction all integrated onto it. A similar stand-alone arrangement utilizing Microchip's DSC DM330011 has been established in this work to detect and process real-time ECG signal (Bansal et al., 2009a,b). The quality of ECG detected can be used for reaching diagnostic inferences and for further online processing and distant tele-monitoring. Such a concept can take tele-medicine and remote health monitoring to greater heights and to a practically achievable level and support health care in far flung areas and during distress. There is still a lot that requires to be explored, before the ultimate objective of a cost-effective and compact, easily available home health care solution for on line monitoring and automated diagnostic system can be accomplished.

References

Anders, W., 2020. Heart Disease and COVID-19: An Epidemic Within a Pandemic Creates a Cardiac Conundrum, Blog, Aug 17, 2020.

Balasubramaniam, D., Nedumaran, D., 2009. Implementation of ECG signal processing and analysis techniques in digital signal processor based system, IEEE International Workshop on Medical Measurements and Applications, Cetraro, pp. 60–63.

Bansal, D., Khan, M., Salhan, A.K., 2008. Simulation of various fifty hertz notch filters for ECG devices. In: proceedings of International Conference on Digital Factory, ICDF 2008, C.I.T, Coimbatore, August 2008, pp. 1007–1011.

Bansal, D., Khan, M., Salhan, A.K., 2009a. A computer based wireless system for online acquisition, monitoring and digital processing of ECG waveforms. Comput. Biol. Med. 39 (4), 361–367. Elsevier.

Bansal, D., Khan, M., Salhan, A.K., 2009b. A real time embedded set up based on digital signal controller for detection of bio-signals using sensors. Int. J. Sensors Transducers 105 (6), 26–32. ISSN 1726-5479.

BDTI's Pocket Guide to Processing Engines for Embedded Applications. http://www.BDTI.com/benchmarks.html.

Bouny, L.E., Khalil, M., Adib, A., 2020a. A wavelet denoising and teager energy operator-based method for automatic QRS complex detection in ECG signal. Circuits Syst. Signal. Process. 39 (10), 4943–4979.

Bouny, L.E., Khalil, M., Adib, A., 2020b. ECG heartbeat classification based on multi-scale wavelet convolutional neural networks. ICASSP 3212–3216.

Bui, N.T., Phan, D.T., Nguyen, T.P., Hoang, G., Choi, J., Bui, Q.C., et al., 2020. Real-time filtering and ECG signal processing based on dual-core digital signal controller system. IEEE Sens. J. 3.073. Available from: https://doi.org/10.1109/jsen.2020.2975006.

Buttfield, A.C., Bolton, M.P., 2005. Real time measurement of RR intervals using a digital signal processor. J. Med. Eng. Technol. 29 (1), 8–13.

Chandrakar, C., Kowar, M.K., 2012. Denoising ECG signals using adaptive filter algorithm. Int. J. Soft Comput. Eng. 2 (1), 120–123.

Chang, M.C., Lin, Z.X., Chang, C.W., Chan, H.L., Feng, W.S., 2004. Design of a System-on-Chip for ECG signal processing, 2004 IEEE Asia-Pacific Conference on Circuits and Systems, December 6–9, pp. 441–444.

Chen, B., Li, Y., Cao, X., Sun, W., He, W., 2019. Removal of power line interference from ECG signals using adaptive notch filters of sharp resolution. IEEE Access. 7, 150667–150676.

Chen, A., Zhang, Y., Zhang, M., Liu, W., Chang, S., Wang, H., et al., 2020. A real time QRS detection algorithm based on ET and PD controlled threshold strategy. Sensors 20, 4003.

Dave Fornell, D.A.I.C. (Ed.), 2020. Cardiovascular Technologies to Watch in 2020, Blog. 24 January 2020.

Ehab, A.R.H., Ali, S.H., 2019. Hilal Al-Libawy detection of electrocardiogram QRS complex based on modified adaptive threshold. Int. J. Electr. Comput. Eng. 9, 3512–3521.

Ehnesh, M., Abatis, P., Schlindwein, F.S., 2020. A portable electrocardiogram for real-time monitoring of cardiac signals. SN Appl. Sci. 2, 1419.

Feature, ECG, May 03, 2019, Sanket Solanki, ECG Industry blooms with innovative devices and new methods.

Feature, September 17, 2009, Ravindra Sharma, Senior Analyst, Millenium Research Group.

Kennedy, H.L., 2013. The evolution of ambulatory ECG monitoring. Prog. Cardiovasc. Dis. 56 (2), 127–132. Available from: https://doi.org/10.1016/j.pcad.2013.08.005. Epub 2013 Sep 11.

Kitzman, D.W., et al., 2012. LV Diastolic Dysfunction and Prognosis. Circulation 125 (6), 743–745. Available from: https://doi.org/10.1161/CIRCULATIONAHA.111.086843. 2012 February 14.

Health Quality Ontario, 2017. Long-term continuous ambulatory ECG monitors and external cardiac loop recorders for cardiac arrhythmia: a health technology assessment. Ont. Health Technol. Assess. Ser. 17 (1), 1–56. Published online 2017 Jan 31.

Khatib, I.A., Poletti, F., Bertozzi, D., Benini, L. et al. (2006), A Multiprocessor System-on-Chip for Real-Time Biomedical Monitoring and Analysis: Architectural Design Space Exploration, 43rd Design Automation Conference (DAC 06).

Kligfield, P., Gettes, L.S., Bailey, J.J., Childers, R., Deal, B.J., Hancock, E.W., et al., 2007. Recommendations for the standardization and interpretation of the electrocardiogram, part I: the electrocardiogram and its technology a scientific statement from the American Heart Association Electrocardiography and Arrhythmias Committee, Council on Clinical Cardiology; the American College of Cardiology Foundation; and the Heart Rhythm Society. Circulation 115, 1306–1324.

Kondra, S., Yew, C., Ahmad, F., Hofmann, U.G., 2005. Prototype of a Patient Monitoring Device based on an embedded RISC/DSP system, ICMP 2005/BMT Conference, Nuremberg, Germany, September 2005.

Manikandan, M., Soman, K., 2012. A novel method for detecting R-peaks in electrocardiogram (ECG) signal. Biomed. Signal. Process. Control. 7, 118–128.

Microchip. MPLAB Starter kit for dsPIC Digital Signal Controllers. User's Guide. <www.microchip.com>.

Mohammad, S., Lim, Z., Lin, Y., Sani, A., Zanjani, K., Paracha, M., et al., 2003. Real-time ECG analysis using a TI TMSC54x Digital Signal Processing Chip. Comput. Cardiol. 30, 541–544.

News, Cardiac DIAGNOSTICS | DECEMBER 18, 2019, The Cardiovascular Disease Technology Market Will Exceed $40 Billion by 2030; IDTechEx Research outlines upcoming developments in CVD in its "Cardiovascular Disease 2020–2030: Trends, Technologies & Outlook" Report.

NEWS, CARDIAC DIAGNOSTICS, OCTOBER 06, 2020, Rapid Heart Function Analysis by Avalon-H90 Device May Identify Myocarditis In COVID-19 Patients.

NEWS, ECG, APRIL 27, 2018; HeartSciences MyoVista ECG Device Shows Promise in Detecting Abnormal Cardiac Function.

NEWS, ECG, DECEMBER 12, 2019a, Cardiologs Earns Frost & Sullivan's New Product Innovation Award.

NEWS, ECG, JANUARY 08, 2019b, EKG With Artificial Intelligence Reliably Detects Heart Failure Precursor.

NEWS, ECG, JANUARY 22, 2020, Bittium Exhibits ECG Solutions for Cardiology at Arab Health.

Nishiga, M., Wang, D.W., Han, Y., et al., 2020. COVID-19 and cardiovascular disease: from basic mechanisms to clinical perspectives. Nat. Rev. Cardiol. 17, 543–558.

Pani, D., Barabino, G., Raffo, L., 2013. NInFEA: an embedded framework for the real-time evaluation of fetal ECG extraction algorithms. Biomed. Tech. (Berl.) 58 (1), 13–26.

Pei, S.-C., Tseng, C.-C., 1995. Elimination of AC interference in electrocardiogram using IIR notch filter with transient suppression. IEEE Trans. Biomed. Eng. 42 (11), 1128–1132.

Piskorowski, J., 2012. Suppressing harmonic powerline interference using multiple-notch filtering methods with improved transient behavior. Measurement 45 (6), 1350–1361.

Processor Comparison: Texas Instruments C6000 DSP and Motorola G4 PowerPC, <www.pentek.com>.

Qi, J., Shi, P., Hu, L., Zhang, T., Xie, S., 2019. ECG Characteristic Wave Detection Based on Deep Recursive Long Short-Term Memory. J. Med. Imaging Health Inf. 9, 1920–1924.

Rajpal, S., Tong, M.S., Borchers, J., et al., 2020. Cardiovascular Magnetic Resonance Findings in Competitive Athletes Recovering From COVID-19 Infection. JAMA Cardiol. Published online 11 September 2020.

Raju, M., 2007. Heart-Rate and EKG Monitor Using the MSP430FG439, Texas Instruments Application Report, SLAA280A–Revised September 2007.

Ressler, J., Dirscherl, A., Grothe, H., Wolf, B., 2007. The use of digital signal processors (DSPs) in real-time processing of multi-parametric bioelectronic signals. Biomed. Tech. (Berl.) 52 (1), 143–148.

Rodríguez, J., Goñi, A., Illarramendi, A., 2005. Real-time classification of ECGs on a PDA. IEEE Trans. Inf. Technol. Biomed. 9 (1), 23–34.

Sahambi, J.S., Tandon, S.N., Bhatt, R.K.P., 2000. An automated approach to beat by beat QT- interval. analysis, IEEE Eng. Med. Biol. 97–101.

Sathyapriya, L., Murali, L., Manigandan, T., 2014. Analysis and detection R-peak detection using Modified Pan-Tompkins algorithm. 2014 IEEE International Conference on Advanced Communications, Control and Computing Technologies, Ramanathapuram, pp. 483–487.

Sharma, R.R., Pachori, R.B., 2018. Baseline wander and power line interference removal from ECG signals using eigenvalue decomposition. Biomed. Signal. Process. Control. 45, 33–49. Aug.

Smithsonian National Museum of American History. At the Heart of the Invention: The development of the Holter Monitor. Published online Nov. 16, 2011.

SPONSORED CONTENT, FEATURE, ECG, SEPTEMBER 27, 2018; How Advances in Wearable Cardiac Monitors Improve the Patient and Clinician Experience.

SPONSORED CONTENT, FEATURE, ECG, FEBRUARY 19, 2020; Moving Beyond Holter ECG: The Rise in Next Generation Technology.

Suchetha, M., Kumaravel, N., 2013. Empirical mode decomposition based filtering techniques for power line interference reduction in electrocardiogram using various adaptive structures and subtraction methods. Biomed. Signal. Process. Control. 8, 575−585. Nov.

Suchetha, M., Kumaravel, N., Jagannath, M., Jaganathan, S.K., 2017. A comparative analysis of EMD based filtering methods for 50 Hz noise cancellation in ECG signal. Inform. Med. Unlocked 8, 54−59.

Thakor, N.V. n.d. Therapeutic/Prosthetic Devices − Pacemakers & Defibrillators. Lectures on Biomedical Instrumentation, JHU Applied Physics Lab. biomedical engineering and neurology at the Johns Hopkins University School of Medicine.

Tobón, D.P., Falk, T.H., 2018. Adaptive spectro-temporal filtering for electrocardiogram signal enhancement. IEEE J. Biomed. Health Inf. 22 (2), 421−428.

Vasan, R.S., Xanthakis, V., Lyass, A., Andersson, C., Tsao, C., Cheng, S., et al., 2018. Epidemiology of left ventricular systolic dysfunction and heart failure in the Framingham Study: an echocardiographic study over 3 decades. JACC Cardiovasc. Imaging. 11 (1), 1−11.

Verma, A.R., Singh, Y., 2015. Adaptive tunable notch filter for ECG signal enhancement. Procedia Comput. Sci. 57, 332−337.

Wang, Q., Gua, X., Lin, J., 2017. Adaptive notch filter design under multiple identical bandwidths. AEU-Int. J. Electron. Commun. 82, 202−210. Dec.

Wu, L., Wang, Y., Xu, S., Liu, K., Li, X., 2020. A CNN-RBPNN Model with feature knowledge embedding and its application to time-varying signal classification. IEEE Access. 8, 108503−108513.

Yang, Y., Yin, D., Freyer, R., 2002. Development of a digital signal processor-based new 12-lead synchronization electrocardiogram automatic analysis system. Comput. Methods Prog. Biomed. 69 (1), 57−63.

Yildirim, Ö., 2018. A novel wavelet sequence based on deep bidirectional LSTM network model for ECG signal classification. Comput. Biol. Med. 96, 189−202.

Zalabarria, U., Irigoyen, E., Martinez, R., Lowe, A., 2020. Online robust R-peaks detection in noisy electrocardiograms using a novel iterative smart processing algorithm. Appl. Math. Comput. 369, 124839.

Zheng, J.W., Zhang, Z.B., Wu, T.H., Zhang, Y., 2007. A wearable mobihealth care system supporting real-time diagnosis and alarm. Med. Biol. Eng. Comput. 45, 877−885.

This page intentionally left blank

6 Measurement and analysis of heart rate variability

6.1 Introduction

Tracking the well-being and fitness level of an individual has become easy and affordable with the advent of modern technologically advanced apps and wearables that require detection, collation, and interpretation of valued health−related information such as BP, heart rate, blood sugar level, number of steps, calorie intake, etc. This has reached the next level of interpreting the resilience, stress, and behavioral pattern of an individual using a biomarker called the heart rate variability (HRV) (Marcelo Campos, 2019; https://medi-core.com/en/technology/hrv.html; https://elitehrv.com/heart-rate-variability-vs-heart-rate).

We are aware that heart rate is denoted by, number of times the heart beats in 1 min (bpm), which is generally in the range 60−80 bpm as the resting heart rate of a healthy human being in a relaxed state. This rhythmic heart beat pattern is not regular, and a variation occurs in between the time gap of every beat. This moment-to-moment variation in the beat pattern goes unnoticed during heart rate measurements. HRV gives a measurement of this physiological phenomenon that can be derived from the ECG signal and is defined as the deviation between the time interval of every heartbeat and is governed through the autonomic nervous system (ANS). Larger the variability among the beats, healthier is considered the functioning of the human body. The ANS is categorized as the parasympathetic nervous system (PSNS) and the sympathetic nervous system (SNS). The ANS continuously regulates the involuntary body processes such as breathing, blood pressure, heart rate, proper functioning of arteries, etc. Fig. 6−1 depicts the ANS along with the HRV pattern generated thereby.

Heart beat rhythm is triggered at the sinoatrial (SA) node. The SA node is situated in the right-atrium of the heart and is recognized as the natural pacemaker. The sympathetic and para-sympathetic components of the ANS impact the generation of impulse at the SA node. These impulses are also influenced by the hormones and immunity level present in the blood stream. As also depicted in Fig. 6−1, PSNS symbolizes the resting, digesting, and the relaxed state, that can think, repair and rebuild stimulation of the immune system, the digestive system, and other organs. PSNS activities indicate a healthy functioning of body, facilitates a quick response (0.2−0.6 s), and lead to reduced heart rate and increased HRV (Berntson et al., 1997a,b). The SNS on the other hand gets dominated when we are in the survival mode, that is, when our fight or flight mode is activated thereby releasing sympathetic hormones generated by the adrenal glands. During SNS activation the response is slow, the heart rate goes high, the BP shoots, there is reduced flow of blood to the vital

Real-Time Data Acquisition in Human Physiology. DOI: https://doi.org/10.1016/B978-0-12-822118-1.00009-6
© 2021 Elsevier Inc. All rights reserved.

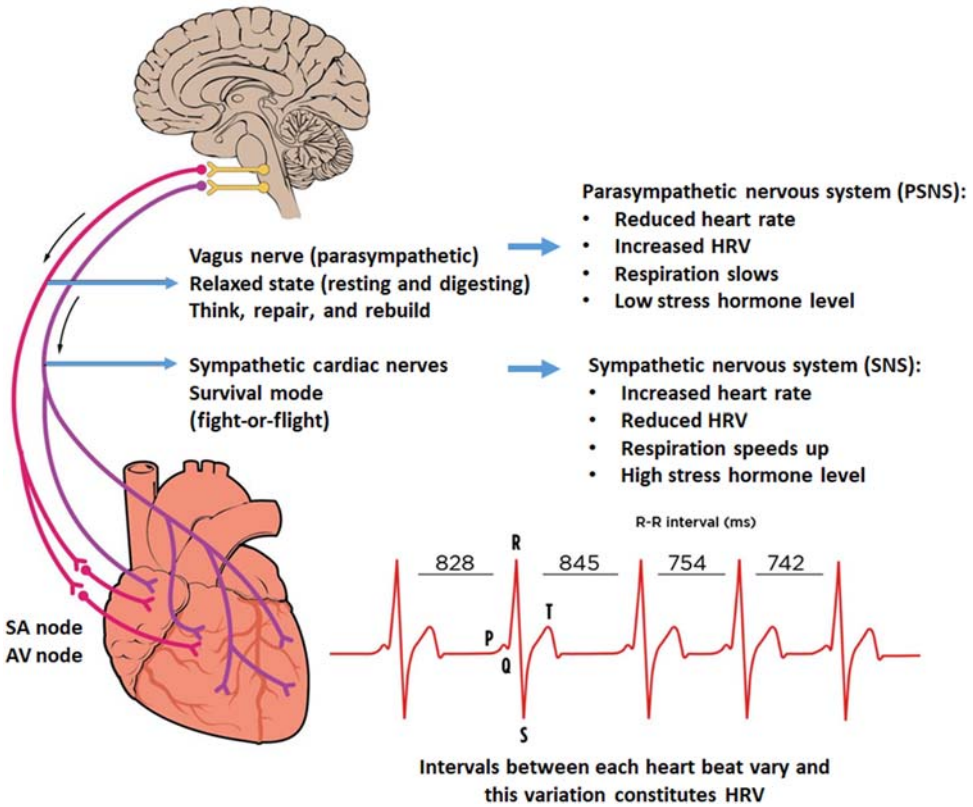

FIGURE 6–1 Depiction of ANS and HRV. *ANS*, autonomic nervous system; *HRV*, heart rate variability.

organs and the digestive system and the HRV decreases. The PSNS input to the heart is through the vagus-nerve and the SNS input is through the postganglionic fibers from the sympathetic trunk which innervate the SA node and the atrioventricular (AV) node. So, it is the neural communication channels that interact between the heart and the brain causing generation of HRV. A balance is always maintained between both the ANS activities, where one may be more dominant than the other at one point of time. SNS gets priority at a given time because it signifies immediate survival. Factors that can influence these activities and in turn the HRV are the mental stress level, sleep cycle, illness, infections, improper nutrition, lack of physical activities, isolation, happiness, excitement, age, gender, etc. HRV analysis is an exciting way to noninvasively monitor the ANS imbalance and research in the past few years has established the relational connect between low HRV level and deteriorated depression and anxiety level and is also indicative of cardiovascular illness and the risk of even death. High HRV indicates a healthy heart and lifestyle, resilience to stress, and emotional strength. When in resting state, high HRV is favorable but during exercise or during active state a relatively lower HRV is favored. The gold standard to measure and analyze the HRV is using the long length of ECG data.

The bottom line is that HRV tracking can motivate the way one lives and thinks and can provide great insights into the behavioral impact on the nervous system and the functions of vital organs and body parts (Buccelletti et al., 2009; The Framingham Heart Study, 1994; Berntson et al., 1997a,b; Braune and Geisendörfer, 1995).

6.1.1 Basic block diagram for heart rate variability evaluation process

It is evident that HRV analysis provides great insights into the functioning of the heart and many cardiopathological inferences can be drawn based on the inputs. The functional block diagram for HRV evaluation process is represented in Fig. 6–2.

The HRV analysis process flow begins with the acquisition of ECG signals in real time or can also be performed on ECG data acquired from MIT-BIH database. The major modules for HRV analysis include the preprocessing block, the learning module, the detection and classification block, and the HRV analysis module. These stages ensure selection of reasonably noise-free ECG data segments and automated detection and classification of ECG features for further analysis.

The first stage of data preprocessing module comprises of signal amplification, band-pass filtering, artifact removal, and digitization of the signal. The learning module does initialization of a threshold value for QRS peak detection based on averaging concept and also initializes the parameters required for the classification of ECG data. The *RR* intervals are also averaged for final calculation. After the learning phase is over, the algorithm designed for detection based on the QRS detector concept by Pan-Tompkins is utilized to find the locations of the peak QRS and then the classification of the ECG waveform is performed as normal or abnormal heartbeat. Classification is based on the rhythmic behavior of heart and the amplitudes related to the QRS peak. Standard *RR* interval is evaluated by the interval in between QRS peaks of normal beats. *RR* interval calculation has its implication in analyzing the HRV. HRV analysis is accomplished using linear or nonlinear techniques. Linear methods

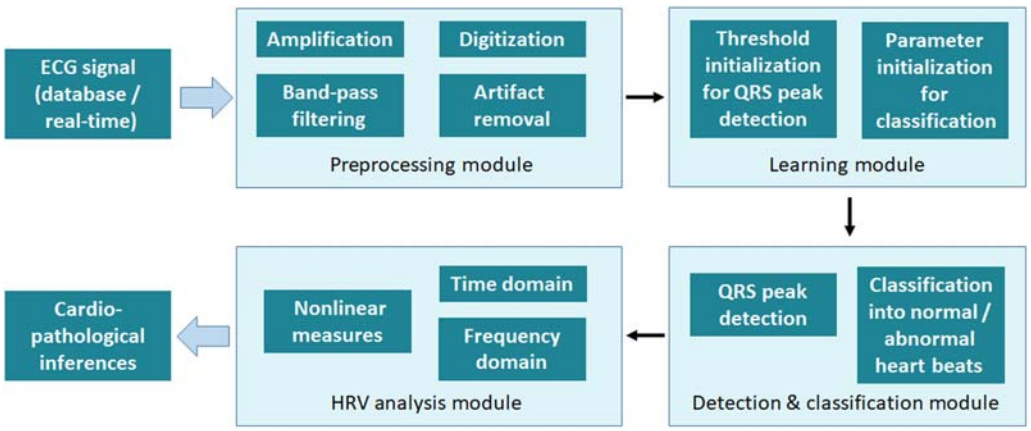

FIGURE 6–2 Functional block diagram depicting heart rate variability analysis process.

include analysis both in time and in frequency domain. Cardiopathological and diagnostic inferences can be drawn from HRV analysis. Various HRV metrics and norms are presented in the subsequent section.

6.2 Heart rate variability metrics and norms

HRV analysis for short-term ECG sequences of ~5 min length, ultrashort-term length of less than 5 min, and 24-h long segment can be carried out in time and frequency domains, and also using nonlinear techniques. The HRV time domain metrics compute the extent of variability in measuring the interbeat interval (IBI), between consecutive heartbeats. The most frequently known time domain parameters along with their short description and unit of measures are summarized in Table 6–1. As per a consensus reached in 1996 between the European Society of Cardiology (ESC) and the North American Society of Pacing and Electrophysiology (NASPE), the main parameters related to heart rate rhythms in frequency domain could be divided into four bands. The frequency domain estimation can be performed for the absolute or the relative power and the details are summarized in Table 6–2. The, nonlinear measurements as detailed in Table 6–3 helps us to understand and measure the randomness of the time series (Shaffer and Ginsberg, 2017; Martínez et al., 2017; Malik et al., 1996; Li et al., 2019; Singh et al., 2018a,b;

Table 6–1 Time domain HRV measures.

Parameter	Unit	Description
Time domain measures		
NN 50 count	Count	No. of successive *RR* intervals that differ by more than 50 ms
pNN 50	%	NN 50 count divided by total number of *RR* intervals
MAX–MIN	ms	Difference between shortest and longest *RR* interval
Statistical measures		
SDNN	ms	Standard deviation of *RR* intervals
$\overline{RR}$	ms	Mean of *RR* intervals
$\overline{HR}$	ms	Mean heart rate
SDNN index	ms	Mean of the standard deviations of *RR* intervals for each 5 min segments in 24 h recording
SDANN	ms	Standard deviation of averages of *RR* intervals for each 5 min segments in 24 h recording
RMSSD	ms	Root mean square of the difference of consecutive *RR* intervals
SDSD	ms	Standard deviation of differences between successive *RR* intervals
Geometric measures		
HRV index	Count	Total number of *RR* intervals divided by height of histogram of *RR* interval
Differential index	ms	Difference between widths of histograms between successive *RR* intervals
TINN	ms	Baseline width of *RR* interval histogram

HRV, heart rate variability.

Table 6–2 Frequency domain HRV measures.

Measures	Unit	Description	Frequency
Absolute measures			
Peak frequency	Hz	VLF, LF, HF band frequencies	–
Total power	ms^2	Sum of the energy in the frequency bands	$\sim \leq 0.4$ Hz
ULF	ms^2	Power | ultralow frequency range	≤ 0.003 Hz
VLF	ms^2	Power | very low frequency range	0.003–0.04 Hz
LF	ms^2	Power | low frequency range	0.04–0.15 Hz
HF	ms^2	Power | high frequency range	0.15–0.4 Hz
Relative measures			
LF-norm	%	Normalized low frequency power	LF/(Total power − VLF) × 100
HF-norm	%	Normalized high frequency power	HF/(Total power − VLF) × 100
LF/HF	%	Ratio of low and high frequency power	–

HRV, heart rate variability; *HF*, high frequency; *LF*, low frequency; *VLF*, very low frequency.

Table 6–3 Nonlinear HRV measures.

Measures	Unit	Description
S	ms	Total HRV represented by area under the ellipse
SD1	ms	Poincaré plot standard deviation, perpendicular to the line of identity
SD2	ms	Poincaré plot standard deviation, along the line of identity
SD1/SD2	%	Ratio
SampEn		Sample entropy analyzing the time series
ApEn		Approximate entropy analyzing the time series
DFA 1		Detrended fluctuation analysis|short-term fluctuation
DFA 2		Detrended fluctuation analysis|long-term fluctuation

HRV, heart rate variability.

Tarvainen and Niskanen, 2012; Task force of the European society of cardiology and the North American society of pacing and electrophysiology, 1996; Acharya et al., 2006).

6.2.1 Time-domain analysis

The time domain parameters provide the simplest method of estimating HRV as they can be applied straight on to the sequence of consecutive *RR* intervals. The obvious and acceptable index is the *RR* interval mean values ($\overline{RR}$) and the resultant mean heart rate (HR). ($\overline{RR}$) can be found using the following formula:

$$\overline{RR} = \frac{1}{N}\sum_{i=1}^{N} RR_i$$

where N denotes the total quantity of successive *RR* intervals, RR_i is the ith component for *RR* interval.

Many other such indices relating to *RR* series variants are defined. HRV time domain parameters are analyzed by observing the data length of less than 1 min to 24 h. Formerly, HRV was evaluated from the $\overline{RR}$ values and its standard deviation calculated by observing the short-term 5 min ECG data sequence. These time domain measures include pNN 50, NN 50 count, MAX-MIN, HRV-index, differential index, TINN or the triangular-interpolation of the NN-interval histogram, etc. summarized in Table 6−1.

Heart Rates observed and noted over longer lengths of 24 h duration, assist in evaluating more intricate statistical HRV time domain parameters like SDNN, SDNN index, SDANN, RMSSD, SDSD, etc. These may be the resultant of direct *RR* interval measurements or the difference between them or could be derived from the instantaneous heart rate. As indicated in Table 6−1, these measures may be analyzed from the total length of ECG data or may be derived by means of smaller sections of the recordings. This permits HRV analysis to be done during various modes, for example, sleep, rest, etc. The standard time domain statistical measure that helps in interpretation is SDNN or the standard deviation of the NN interval. We can also call it as the standard deviation of IBI for the normal sinus beats without the ectopic beat, which mathematically is the square root of variance. We are aware that variance represents the total power, so the SDNN index reveals entire cyclic components liable for variability in the recordings. SDNN is measured in milliseconds and is represented as per the following formula:

$$\text{SDNN} = \sqrt{\frac{1}{N-1}\sum_{i=1}^{N}(RR_i - \overline{RR})^2}$$

where N denotes the overall number of successive *RR* intervals, RR_i represents the ith component of *RR* interval. *SDNN* reflects both, short-term (5 min) and long-term variability, and is capable of predicting both illness and mortality. SDNN measured over 24 h sequence is considered the gold standard for identifying and developing effective treatments for cardiac patients (Task force of the European society of cardiology and the North American society of pacing and electrophysiology, 1996). Both SNS and PSNS activities influence the SDNN and finds correlation with ultralow frequency (ULF) power, VLF power, LF power, and also total power (Umetani et al., 1998). During 24 h recordings, LF power predominantly contributes to SDNN (Kuusela, 2013). Longer sequences offer wider range of data interpretations for different stimulations, work load, sleep cycles, etc. The 24 h recordings indicate the SNS impact on HRV metrics (Grant et al., 2011). Individuals can be categorized as unhealthy if their SDNN value falls below 50 ms, are advised to take care of their health if it falls in the range 50−100 ms and are found to be healthy and at a lower risk of cardiac issues if it is beyond 100 ms (Kleiger et al., 1987).

Another statistical metric SDSD represents only the short-term variability (Kuusela, 2013) and gives the standard deviation of successive differences in *RR* intervals as follows:

$$SDSD = \sqrt{E\{\Delta RR_i^2\} - \{E\Delta RR_i\}^2}$$

In the concept of probability, the "Expected Value'" for a random variable "Y" is symbolized by $E[Y]$ which denotes the weighted average, also understood as the arithmetic mean of large quantity of independent random variables.

SDANN metric gives the standard deviation for the means, for every 5 min segments in milliseconds, extracted from a 24 h recordings. SDANN cannot be considered as a replacement for SDNN because it is calculated using smaller fragments of 5 min duration instead of the complete 24 h long data sequence (Kuusela, 2013; Shaffer et al., 2014). The formula for SDANN is as follows:

$$\text{SDANN} = \sqrt{\frac{1}{m-1}\sum_{s=1}^{m}\overline{RR}_s - \overline{\overline{RR}_{all}})^2}$$

where "m" denotes the total quantity of small segments studied from the 24 h long sequence and "s" is all the fragments of 5 min duration. $\overline{RR}_s$ denotes the mean of the *RR* interval in fragment "s" and $\overline{\overline{RR}_{all}}$) is the mean value of all the segments.

SDNN index signifies the mean of standard deviation for all the small 5 min segments in milliseconds, extracted from a 24 h HRV recordings correlating to the VLF power range and reflecting the autonomic influence on HRV (Shaffer et al., 2014). This is mathematically evaluated as follows:

$$\text{SDNN} - \text{Index} = \frac{1}{m}\sum_{s=1}^{m} SDNN_s$$

RMSSD is denoted as the root-mean-square of successive differences for *RR* intervals and is evaluated using the following formula:

$$\text{RMSSD} = \sqrt{\frac{1}{N-1}\sum_{i=1}^{N-1}(\Delta RR_i)^2}$$

The conservative approach for measuring RMSSD is on minimum record lengths of 5 min, but suggestions include measurement evaluation on ultrashort-term lengths of 10, 30, and 60 s (36) (Salahuddin et al., 2007; Baek et al., 2015; Esco and Flatt, 2014).

NN50 is another index measured using successive *RR* interval differences, which indicates the number of consecutive intervals having a variance of more than 50 ms. It quantifies the power owing to components having high frequency (HF). The index pNN50 for *RR* intervals signifies that proportion of values which differ by more than 50 ms when compared with the previous value and is given by the following expression:

$$\text{pNN50} = \frac{1}{N-1}\text{NN50} \times 100$$

Both NN50 and pNN50 indices require 2 min epoch. Some suggest ultrashort intervals of 60 s (Baek et al., 2015). The index pNN50 is found to have a close correlation with PNS activities, RMSSD, and the high frequency power (Umetani et al., 1998; Otzenberger et al., 1998). Even though the RMSSD is correlated with HF power, its effect on the respiration rate is yet to be explored further (Kleiger et al., 2005; Schipke et al., 1999; Pentillä et al., 2001). Low values of RMSSD may be indicative of fatal consequences in epilepsy patients (DeGiorgio et al., 2010).

Another time domain index Max−Min is the variance among the max and the min heart rate values through every respiratory cycle and requires at least a 2 min sequence.

Apart from the mentioned statistical measures, some geometrical measures can also be evaluated using the *RR*-interval histograms (Jovic and Bogunovic, 2011). One is the HRV-Index, a dimensionless measure, which can be evaluated by integrating the histogram of all *RR* intervals, duly divided by the height of the histogram. This is dependent on the bin-width chosen (recommended is 1/128 s) for evaluation and is given by the following expression:

$$\mathrm{HRV-Index} = \frac{N}{\max(\mathrm{Hist}RR-\mathrm{interval})}$$

Using the triangular interpolation, TINN is another index that can be measured, which represents the base-line width for a histogram presenting *RR* intervals and is given by the following expression:

$$\mathrm{TINN} = \frac{\mathrm{N.bin\ size}}{\max(\mathrm{Hist}\ RR-\mathrm{interval})} \times 2$$

Both HRV-Index and TINN reflect the total HRV and are impacted by lower frequency power.

6.2.2 Frequency-domain analysis

The frequency domain analysis of HRV requires understanding of the frequency bands in which the rhythmic oscillations of heart are divided into and is done through the spectral breakdown of the *RR* interval either with fast Fourier transform (FFT) which are simple to implement or autoregressive (AR) techniques that are comparatively complex models but can yield enhanced resolution and can be broken down into distinct spectral components (Marple, 1987; Tarvainen and Niskanen, 2012). ESC and NASPE have categorized them into four prime bands, viz., HF band of 0.15−0.4 Hz, low-frequency (LF) band of 0.04−0.15 Hz, very-low frequency (VLF) band of 0.003−0.04 Hz, and ULF range. Most commonly used frequency domain metrices attained from the PSD include absolute and relative figures of the HRV frequency bands, the peak frequencies, the LF/HF ratio, etc. as listed in Table 6−2. Power of the signal is related to the energy content confined in the frequency band. The absolute measures include peak frequency and power calculations VLF, LF, and HF bands. It also includes total power calculations which are denoted by the summation of entire energy component in the four categories of frequency bands ULF, VLF, LF, and HF for a 24-h segment and the three frequency bands VLF, LF, and HF for short-term segments. LF norm and HF norm measures the normalized LF and HF power, respectively, and is represented as the ratio of these frequencies w.r.t. total power. The LF to HF power ratio gives an estimate between SNS and PSNS activities under organized situations.

The spectral analysis based on FFT algorithm are evaluated by integrating the complete spectrum, whereas analysis performed using AR model techniques can be done by dividing

it in components. Band powers can be derived as powers of these components (Singh et al., 2018a,b).

HRV analysis is mostly performed on 5 min sequence length extracted from the 24-h recordings. It is reported that the HF components reveal the PSNS activities and LF components indicate the SNS impact. Irregularly sampled pattern of *RR* interval requires extra effort prior to analysis in frequency domain, as this uneven shape leads to generation of added harmonics in the spectrum. So, *RR* intervals are interpolated and evenly sampled signals are recovered before being analyzed in frequency domain.

The HRV frequency band details are presented subsequently.

6.2.2.1 Ultralow-frequency band

The ULF band falls below 0.003 Hz representing a rhythmic periodicity of 333 s, that is, 5.6 min and finds high correlation with the time domain index SDANN and can be assessed using 24-h long HRV recordings (Shaffer et al., 2014; Bigger et al., 1992; Kleiger et al., 2005). The natural circadian rhythm referring to a biological process which regulates the sleep cycle is the primary cause of ULF band other than the factors like body temperature, metabolic rate, hormones, etc. Influence of SNS and PSNS activities on ULF power is still being researched. Psychiatric ailments influence the circadian rhythm mainly during sleep cycle (Stampfer and Dimmitt, 2013).

6.2.2.2 Very-low-frequency band

The VLF band ranges between 0.003 and 0.04 Hz representing a rhythmic periodicity of 25−300 s presenting a better interpretation compared to LF and HF bands and is generally linked with adverse health conditions when assessed using 24-h long HRV recordings (Schmidt et al., 2005; Hadase et al., 2004; Tsuji et al., 1996; Kleiger et al., 2005). Low values of VLF power is understood to be having linkage to arrhythmic deaths, low testosterone levels, high inflammation, and post-traumatic stress disorders (Bigger et al., 1992; Shah et al., 2013; Lampert et al., 2008; Carney et al., 2007; Theorell et al., 2007). Researchers recommend that the VLF band is fundamentally produced by the heart and represents good health and wellbeing and its rhythmic amplitude and frequency patterns are influenced by the efferent sympathetic activities and physical activities (Berntson et al., 1997a,b; Bernardi et al., 1996). This frequency domain metric has a strong correlation with the time domain measure SDNN index which, as already indicated, denotes mean value of the standard deviation of *RR* intervals for the 5-min segment assessed out of the 24-h recording. VLF power has been recorded to increase in healthy people during the sleep, just before waking up (Huikuri et al., 1994; Singh et al., 2003).

6.2.2.3 Low-frequency band

The LF band range is between 0.04 and 0.15 Hz representing a rhythmic periodicity of 07−25 s, also referred to as the mid-frequency band reflects the baroreceptor activities of heart during rest and helps in maintaining the blood pressure to normal (McCraty and Shaffer, 2015a,b). Low frequency band is impacted by the SNS and PSNS activities producing

rhythms around 0.1 and 0.05 Hz, respectively. Low respiration rates and deep breaths tend to produce patterns in the LF power band (Ahmed et al., 1982; Lehrer et al., 2003; Tiller et al., 1996; Brown et al., 1993).

6.2.2.4 High-frequency band

The HF band range is between 0.15 and 0.4 Hz representing a rhythmic periodicity of 2.5−07 s, indicating the parasympathetic or vagal activity corresponding to respiratory sinus arrhythmia. In case of infants and children, the range varies from 0.24 to 1.04 Hz as they breathe faster than adults. The heart rate goes faster during inspiration as the vagal outflow is inhibited and slows down during expiration as the vagal flow is restored. HF power finds a close correlation with the RMSSD and pNN50 time domain metrices. The HF band-power has a tendency to go up through the night and goes down through the day (McCraty and Shaffer, 2015a,b). Low values of HF band power are indicative of anxiety, panic, and stress. The variation in vagal tone supports maintaining the cardiovascular health (Quintana et al., 2016; Eckberg and Eckberg, 1982; Thayer et al., 2010; McCraty and Shaffer, 2015a,b).

LF/HF ratio: this metric gives an estimate of the ratio between the LF and HF band power indicative of the ratio of SNS to PSNS activities and is generally assessed on 24 h data segment. The LF band power is primarily generated due to SNS activities whereas HF band power is the result of PSNS activities. Lower values of LF/HF ratio reveal dominance of parasympathetic activities, whereas higher value of LF/HF ratio indicates dominance of sympathetic activities. This ratio depends on the stress type and level. When exposed to physical stress, the LF component gets dominant while when under emotional stress the HF component gets dominant.

There exists a relationship between the time domain metrices and the frequency domain measures. While analyzing short-term stationary recordings, frequency domain events are known to be more revealing in providing physiological interpretations compared to the Time domain measures. However, analysis based on 24-h data segments finds close relation between both the domains. Diagnostic inferences drawn from spectral components based on 24-h recordings require extra efforts, so unless very specifically required, it is preferred to adopt the time domain approach. An approximate link between the frequency domain and time domain and methods when applied on 24-h ECG data segment is presented as follows:

- Time domain measures TINN, HRV Index, and SDNN correlate with frequency domain measure total power.
- Time domain measures RMSSD, SDSD, NN50 Count, and pNN50 correlate with frequency domain measure HF power.
- Time domain measure SDANN relates with frequency domain measure ULF power.

6.2.3 Nonlinear measurement analysis

The nonlinear measures help in assessing the random behavior of the time series, which arises due to the complexity involved in regulating the HRV and can be correlated with certain frequency and time domain measurements. Underlying health conditions impact the

nonlinear measurements. As reported, patients with postmyocardial infarction, have increased nonlinear HRV index that indicates high risk of mortality (Stein and Reddy, 2005). Various nonlinear metrices generally analyzed like Poincaré plot, S, SD1, SD2, SD1/SD2, sample entropy (SampEn), approximate entropy (ApEn), detrended-fluctuation analysis (DFA) $\alpha 1$ and DFA $\alpha 2$, etc. are listed in Table 6−3 (Brennan et al., 2001; Carrasco et al., 2001; Fusheng et al., 2001; Peng et al., 1995; Penzel et al., 2003; Richman and Moorman, 2000).

The simplest nonlinear method for analysis of HRV is the Poincaré plot which is the graphical illustration of relation amongst consecutive *RR* intervals leading to a scatter plot. The elliptical shape generated is oriented as per the line-of-identity. The total HRV is represented by the area of the ellipse and is denoted as *S*, which finds correlation with LF and HF band power, and also RMSSD time domain measures. The Poincaré plot analysis is unaffected by the deviation in the *RR* intervals, in contrast to the frequency domain measures (Behbahani et al., 2012). The measure SD1 gives the standard deviation for the points which are perpendicular to the line-of-identity while describing the short-term variation. SD1 is associated with the time domain measure SDSD as follows:

$$\mathrm{SD1}^2 = \frac{1}{2}\mathrm{SDSD}^2$$

The standard deviation of the points along the line-of-identity is known as SD2, which describes the concept of long-term variation and can be evaluated using the time domain measures as follows:

$$\mathrm{SD2}^2 = \frac{1}{2}\mathrm{SDSD}^2 = 2 \times \mathrm{SDNN}^2$$

Researchers find a correlation among the nonlinear measure SD1 and the time and frequency domain measures HR Max − Min, pNN50, RMSSD, SDNN, along with the LF and HF power bands, and also total power. SD2 finds correlation with LF power. The ratio of SD1/SD2 *finds* correlation with the LF/HF ratio (Zerr et al., 2015; Brennan et al., 2002; Guzik et al., 2007).

Approximate entropy (ApEn), the nonlinear measure, processes the complexity and complexity of a brief time series. High value of ApEn implies little likelihood of fluctuations in consecutive *RR* intervals (Beckers et al., 2001). The measure sample entropy (SampEn) provides a comparatively dependable assessment of signal regularity and complexity (Lake et al., 2002). Analysis of detrended fluctuation presents the relationships among successive *RR* intervals observed over diverse time series. This investigation gives slope $\alpha 1$, describing short-term fluctuations, while slope $\alpha 2$, describing long-term fluctuations.

HRV investigation established on nonlinear methodology brings forth significant facts about human physiology and presents grounds for assessment of death risk. Measures like scaling of H scaling exponent, Fourier spectra, and coarse graining spectral analysis are also used for nonlinear analysis. Technological progress and appropriate analysis using nonlinear methods are still required to be further explored before they can be ready for physiological and clinical applications.

6.2.3.1 Heart rate variability measurement and analysis platforms

HRV metrics are great signs of patient's health conditions. Numerous HRV analysis platforms and techniques are being established that offer a flexible and comprehensive open-source package along with graphical user interface and algorithm for R-peak detection and HRV parameterization. These software platforms find application in physiological and clinical research and are also used by physicians for drawing health−related inferences (McConnell et al., 2020). One such technologically advanced and user friendly platform is the Kubios HRV analysis software. It is a multifunctionality analysis platform supporting many data formats that offers, automated and adaptive QRS peak detection, artifact removal and optimized HRV analysis in frequency domain, time domain, and nonlinear techniques. The analysis report can be easily imported into tools like MS Excel, SPSS, Matlab MAT file or can even be saved as a PDF document. It is freely available for Linux and Windows operating systems (Tarvainen et al., 2014).

Researchers have benchmarked the HRV toolboxes based on MATLAB application software. Vest et al. have presented an open-source modular program developed in MATLAB for evaluating HRV. The developed software exhibits comparable performance results and comprises authenticated tools for executing preprocessing, artifact correction, and arrhythmia detection (Vest et al., 2017). HRVTool is another Open-Source MATLAB Toolbox available for HRV analysis developed by Marcus (2015, 2019).

The commonly used tools and techniques for HRV assessment of stationary *RR* intervals are the statistical and geometrical parameters, FFT, and AR models. However, there are situations where nonstationary HRV needs to be assessed like during the "tilt test" and during exercise. For such situations, a novel and freely available software SinusCor, is available that includes the conventional time and frequency domain metrices (Bartels et al., 2017).

Yet another platform named Cardiscope Analytics software employs BlueTooth enabled recorders to detect in real-time and display the ECG signal and the respiration. The HRV analysis from acquired biosignal is performed in real-time ensuring accuracy of recording by eliminating artifacts, ectopic beats, and arrhythmia. The platform offers continuous HRV analysis during Orthostasis (active stand) test and deep breathing manouevre, etc. automated ECG markers are employed for proper display and for calculation of HRV metrics and for future analysis (http://www.smartmedical.co.uk/products/categories/autonomic-function-testing-hrv/analysis-software/cardiscope-analytics-real-time).

The basic process involved in all these available platforms for HRV analysis is the detection of QRS peak out of the ECG signal which is being analyzed. The section below details various QRS peak detection algorithms.

6.3 QRS detection methods

HRV analysis aims at examining the sinus rhythm modified by the ANS, and so it becomes technically essential to detect the initiation of the SA node action potential. The same is achieved by identifying the QRS peaks from the ECG signal waveform and therefore forms the basis for calculating the *RR* interval for HRV characterization. Literature reports vast range of automated QRS

peak identification algorithm that incorporate several different techniques and analysis methods (Chen et al., 2020; Kohler et al., 2002; Hamilton and Tompkins, 1986a,b; Thakor et al., 1983). The QRS peak detection algorithms are categorized based on differentiation (Pan and Tompkins, 1985; Hamilton and Tompkins, 1986a,b; Yeh and Wang, 2008; Arzeno et al., 2008; Choi et al., 2012; Bae and Kwon, 2019), wavelet transforms (Li et al., 1995; Bahoura et al., 1997; Saxena et al., 2002; Legarreta et al., 2003; Martínez et al., 2004; Rizzi et al., 2009; Meraha et al., 2015; Yochum et al., 2016), Hilbert transforms (Benitez et al., 2001; Benítez et al., 2002; Zhang and Lian, 2009a,b; Yang and Zhang, 2018), mathematical morphology (Trahanias, 1993; Sun et al., 2005; Zhang and Lian, 2009a,b; Yazdani and Vesin, 2016), etc. QRS peak detection established on adaptive threshold techniques are also extensively explored in real-time as well (Christov, 2004; Chouhan and Mehta, 2008; Karimipour and Homaeinezhad, 2014; Ehab and Ali, 2019). Algorithms are also designed based on template matching (Dobbs et al., 1984) and artificial neural networks (Abibullaev and Seo, 2010). These QRS peak detection methods assist in deriving HRV measures but have the limitation of being tested on stored ECG from MIT/BIH database or is being simulated.

Pan and Tompkins initially established automated QRS peak detection techniques based on first-order derivatives, nonlinear transform techniques, and threshold methods, but could not achieve the desired accuracy. Li et al. were the first to explore wavelet transforms for automated peak detection. The wavelet based approach is time-consuming and pose difficulty in choosing the mother wavelet and scales to identify QRS peaks. Hilbert transforms based algorithm exhibit great accuracy and speed, but their implementation in real-time settings requires a very long memory. Detection of small and wide QRS peaks still requires to be studied. Thus an all-inclusive, power efficient, high speed, noise immune, less complex algorithm for QRS peak detection with good accuracy, applicable even in real-time and mobile scenarios is required to be designed.

We are aware that ECG signal can get distorted with artifacts like power-line interference, skin-electrode movement, electronic circuit components, baseline wander, high frequency T-wave components, etc. It is therefore absolutely essential that all QRS peak detection algorithms must have a preprocessing high-pass and low-pass filter stage prior to actual peak detection so that artifacts are suppressed. Filtered ECG signal are then utilized to detect peaks. Frequently deployed QRS peak recognition algorithms are based on differentiation methods, template-matching, and wavelets, which are deliberated in the ensuing sections.

6.3.1 Differentiation-based methods for QRS peak detection

Differentiation method sets the base for maximum number of the QRS peak recognition algorithms. The algorithm is established on first and second derivatives and involves elimination of noise as the first step, where the ECG signal is processed by a band-pass filter realized by cascading the high-pass and the low-pass filter. This is followed by differentiation to find high slopes, so that the QRS peaks can be easily distinguished from other ECG wave components. The signal samples are then squared using a nonlinear technique to convert the data segment positive prior to integration which is the next task to be executed. This is

implemented to identify the high frequency signal components denoting the QRS peak post-differentiation. The difference equation used as a differentiator to realize the high-pass filter is as follows:

$$y_1(n) = x(n+1) - x(n-1) \tag{6.1}$$

$$y_2(n) = x(n+2) - 2x(n) + x(n-2) \tag{6.2}$$

$x[n]$ is the input ECG signal and Eq. (6.1) gives the first derivative, which is generally incorporated. Eq. (6.2) computes the second derivative which is used in certain algorithms. A linear combination of the magnitudes of both derivatives is also deployed in certain cases as follows:

$$z(n) = 1.3\left|y_1(n)\right| + 1.1\left|y_2(n)\right| \tag{6.3}$$

The squared waveform generated is made to pass through a moving window integrator and decisions are arrived at based on the threshold value set. The threshold value is mostly dependent on the input ECG signal, so that easy adaption can be achieved as per signal characteristic variation. Decision rule box is implemented to detect the QRS peak in a manner such that the number of false positives can be minimized. These rules impose a constraint on the timing and on the feature signs or present secondary level of thresholds so that non-QRS peaks can be avoided.

6.3.2 Template matching methods for QRS peak detection

A QRS peak detection method established on template matching is also widely used. This procedure, consist of evaluating the cross correlation between the input ECG signal which is in alignment to a standard template of QRS peak. Cross correlation gives the degree of similarity between both the signals. The cross correlation factor evaluated is then maximized to distinguish the QRS peak. Alignment of ECG input signal with the template may be achieved by means of externally assigning the fiducial points on each signal. Another method involves finding continuous cross correlation between the input signal segment and the standard QRS template. On receiving a fresh signal data point, the previous data points from the segment are discarded. A cross correlation is then found among them, which have same set of signal points. Using this technique, the need to allocate fiducial points to the signal is eliminated, thus reducing the processing time. The standard template is essentially a window which travels upon the input ECG signal, step by step and helps in identifying the QRS peak.

There is another simpler template matching technique, rather than computing the cross correlation amongst the input ECG signal and the standard template, which involves extraction of a QRS template from the incoming ECG signal segment. This template becomes the base now for matching the input ECG signal where every point of the incoming ECG signal is subtracted from the equivalent point of the template, leading to a zero value. Minor absolute values that are detected suggest the position of the QRS peak.

6.3.3 Wavelets for QRS peak detection

Wavelets are also widely explored in detecting QRS peaks in an ECG signal. Wavelet transform of a signal $x(t)$ is as follows:

$$Wx(a,b) = \int_{-\infty}^{\infty} x(t)\Psi^*_{a,b}(t)dt \tag{6.4}$$

The mother wavelet function is represented by $\psi(t)$, while its complex conjugate is denoted by $\psi^*(t)$. Wavelet transforms gives a description in a time scale and uses a set of analyzing functions $\psi\ (a,\ b)$ for taking decisions in various frequency bands.

The analyzing functions, $\psi\ (a,\ b)$ can be found from $\psi\ (t)$ using the following equation:

$$\Psi_{a,b}(t) = \frac{1}{\sqrt{2}}\Psi\left(\frac{t-b}{a}\right) \tag{6.5}$$

where "a" represents the scaling parameter, while "b" denotes the transformation parameter. Appropriate selection of the parameters "a" and "b" decide the dyadic discrete WT realized deploying a dyadic filter bank whose filter coefficients are obtained from the wavelet function. Input to the filter bank is the digitized version of the ECG signal. Almost all wavelet-based QRS peak detection techniques are based on Mallat and Hwang's method where recognition of singularity and categorization is performed by means of local maxima of the wavelet coefficients. QRS peak is then identified by calculating the singularity degree, approximated by the decaying of the wavelet coefficients.

6.4 Real-time detection and analysis of heart rate variability

With the advancement in electronics, design, development, and commercialization of an enhanced and integrated scheme for the HRV detection in real-time and analysis of subtle variations using robust algorithms has become viable now. In general, such smart device incorporates a modular concept consisting of a module for ECG signal detection, a processing and filtering module, classification module, and finally a module for wireless communication. HRV metrics can then be obtained from the recordings (short-term and long-term) of the ECG signal (David Naranjo-Hernández et al., 2017). Compact and wireless ECG monitors designed based on sensor nodes have also being prototyped for real-time detection and analysis of HRV. TinyOS 2.0.x open-source operating system has been used to provide ECG data acquisition, computation, analysis and for wireless transmission of information in this application. The computer−based application utilizes the displaying and storing capacity of the PC for further analysis (Wong, 2009). Evaluation of HRV during exercise, on instant basis, to monitor minute and real-time changes in the HRV power spectrum is challenging needs very close monitoring. Shiraishi et al. have provided insights into real-time visualization into the changes in HRV while exercising and noticed a marked decline in the HF power band along with an extreme power spectrum swing (Shiraishi et al., 2018). Real-time monitoring of HRV

can bring about different insights in intensive care unit (ICU) setup and its importance is increasingly been felt over the years. Authors have prototyped a practical, noninvasive real-time HRV analysis set-up in the ICU using the MemCalc system. This enabled the physicians, especially for critical patents, to understand that under sedation, the machine-driven ventilation may reduce autonomic nervous function. This also assists them to draw many diagnostic inferences (Kasaoka et al., 2010). A continuous effort in this direction is being made for further improvement for real-time acquisition, as most of the HRV analysis algorithm deliberated still takes stored ECG database as the base.

In this context, an effort has been made in the present work to deploy a real-time ECG detection and HRV analysis system with the first stage as the data preprocessing module comprising of signal multistage amplification, band-pass filtering, artifact removal, power line hum reduction using analog notch filter, and digitization of the signal. The instrumentation includes surface Ag-AgCl electrodes to sense the ECG signal, cascaded amplifiers and filter module comprising buffer amplifiers, unity gain follower, right leg drive, DC-restoration circuit, feedback integrator, mono duplication interfacing jack, power management, and a computer. The CM*RR* set is to the order 86 dB and the gain is adjusted to 500 times. The right leg drive circuit used as the feedback body reference further improves the CM*RR*. The active integrator filter eliminates the interference picked during the acquisition process. The amplified and clean ECG signal is acquired on a Laptop through the single channel sound port and is viewed and processed on MATLAB based virtual oscilloscope for HRV analysis (Bansal et al., 2009, 2010; Bansal and Singh, 2014). The steps followed to acquire filtered single channel ECG data in MATLAB platform is as follows:

- create analog input object in MATLAB,
- add single channel,
- acquire ECG signal from the in-house instrumentation developed,
- set acquisition parameters,
- trigger immediate and record ECG data,
- set filter parameters and the band pass frequency range, and
- plot the ECG waveform.

This is followed by the second stage of learning module where initialization of a threshold value for QRS peak detection is done. After the learning phase is over, the algorithm designed is used to find the locations of the QRS peak and then the classification of the ECG waveform is performed. Normal *RR* interval is evaluated as the interval between QRS peaks of normal beats. Diagnostic inferences are then drawn from HRV analysis. The MATLAB functions used and the steps followed during the learning phase and classification stage are as follows:

- Set the threshold value for the acquired ECG signal.
- Detect QRS peak using the Function “peakdet” which detect peaks by finding the local maxima in the vector “V” using the MATLAB syntax.
  [MAXTAB, MINTAB] = peakdet (V, DELTA)

A point is said to be at a maximum peak if it has the maximal value, and was led by a value lesser by the variable DELTA.

- Plot the ECG waveform with identified QRS peaks.
- Find *RR* Interval between two adjacent peaks using the function "diff." This function evaluates the differences between neighboring elements of the variable "*X*" and estimated derivatives using the following syntax in MATLAB: $Y = \text{diff}(X)$.
  This assists in obtaining time domain HRV parameters.
- Finally evaluate HRV time domain metrics.

The present arrangement reliably locates the QRS peak marked with red stars in the ECG wave plot and computes the HRV time domain parameters in the real time. Fig. 6–3 presents the QRS peak detected in various subjects and Table 6–4 gives the heart rate, HRV time domain measures, Mean *RR*, RMSSD, SDNN, and SDNN Index for these subjects. These measures offer clinical data related to the changes in the sinus rhythm of the heart.

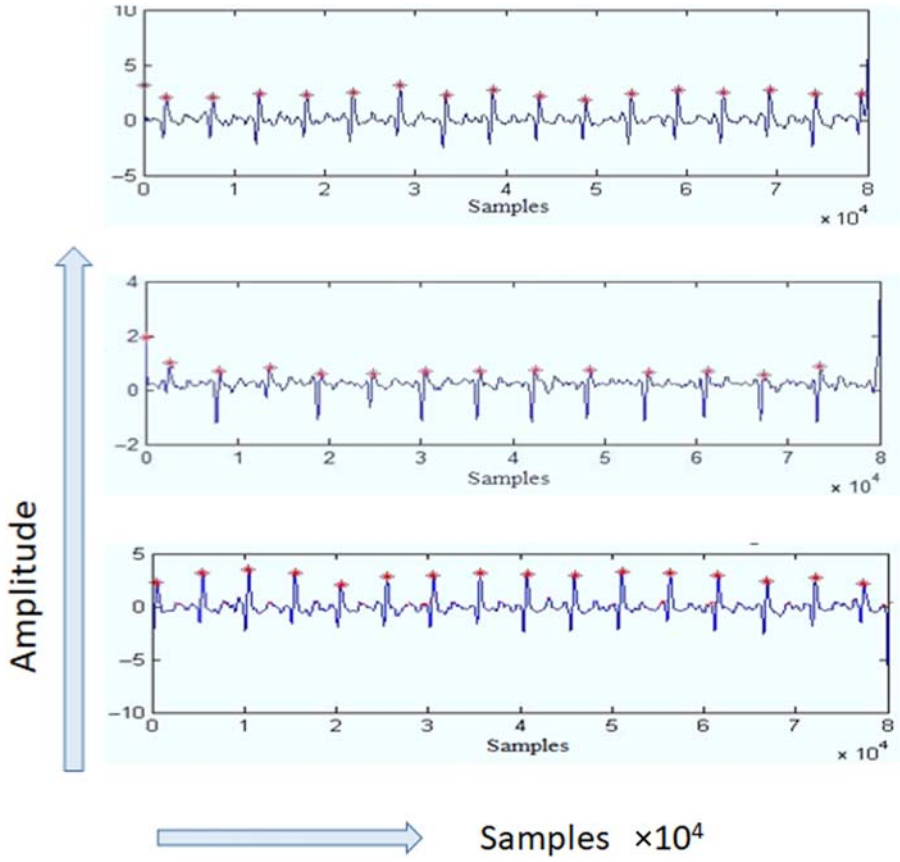

FIGURE 6–3 Peak detection and HRV parameterization in ECG signal for various subjects.

Table 6–4 Heart rate and HRV calculation from the real-time acquired ECG signal.

	Subject 1	Subject 2	Subject 3
Heart rate (bpm)	93.68	82.07	91.67
Mean *RR* (s)	0.6403	0.7343	0.6534
RMSSD	0.6403	0.7345	0.6540
SDNN	0.0069	0.0495	0.0263
SDNN index	0.0069	0.0495	0.0263

HRV, heart rate variability.

In ECG signal, amplitude and duration study of the QRS waves form the base for HRV analysis. It is therefore essential that precise *RR* intervals are calculated so that accurate and reliable physiological condition can be detected and inferred. As suggested by the literature, smaller standard deviation of the ECG *RR* intervals, points to lower HRV. More than 26 diverse arithmetic employments of *RR* intervals have been described to signify HRV (Sloan et al., 2005). The sampling frequency while acquisition should be at least 500 Hz to maintain accuracy so that the R-wave occurrence time estimate is around 1 ms (ESC and NASPE, 1996). The arrangement discussed is extended to simultaneously acquire two biosignals, viz., ECG and carotid pulsation and derive HRV parameters from them.

6.4.1 Dual channel system for real-time, simultaneous acquisition of ECG, and carotid pulse wave

Functional illustration for the dual-channel system designed for simultaneously acquiring ECG and carotid signal in real-time for HRV parameterization is depicted in Fig. 6—4. The set up consist of acquisition instrumentation for carotid pulse wave and the ECG signals as explained in earlier chapters and supplementary stereo input jack for dual channel interfacing with the computer.

The analog signal outputs obtained from the carotid pulse acquisition system and the ECG amplifier system is simultaneously fed into the stereo input port of a computer's sound card. Algorithm designed in MATLAB helps in visualizing and processing the concurrently acquired ECG signal data and carotid pulse data. Fig. 6—5 depicts the algorithm flow for online acquisition of dual channel inputs, FIR digital filtering, QRS peak detection, *RR* interval evaluation in ECG, peak to peak interval calculation in carotid pulse waveform, and time domain HRV parameterization in MATLAB.

The program generates a scope window for instantaneously displaying the real-time detected ECG signals and carotid pulse waves through the dual channel acquisition system developed. The band pass range of the digital filter is adjusted as 0.05—50 Hz to sufficiently cover both the ECG signal and carotid pulse wave spectrum. Peaks are marked for all the

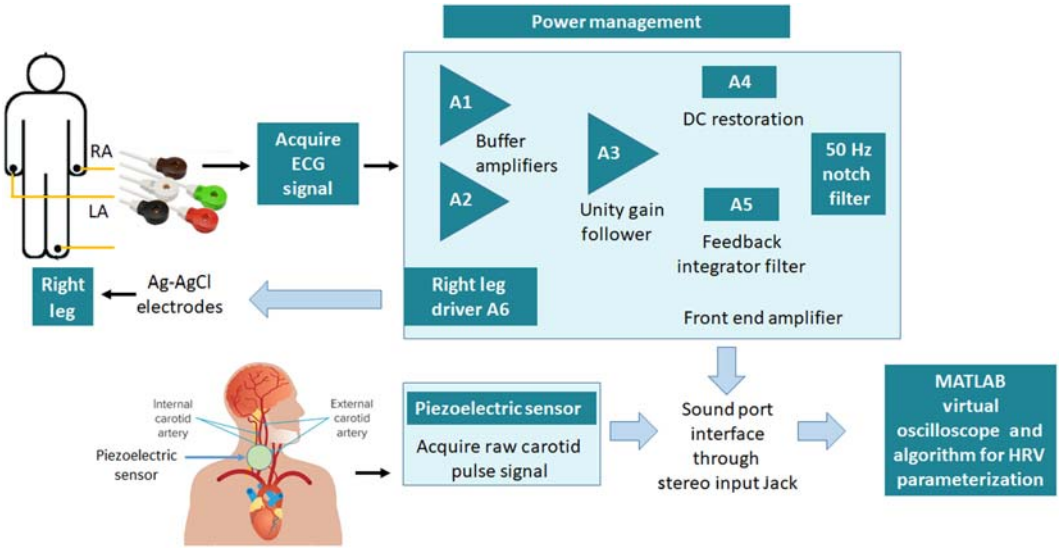

FIGURE 6–4 Functional illustration of dual-channel system for simultaneously acquiring ECG and carotid signal in real-time for HRV parameterization. HRV, heart rate variability.

maxima points identified in the ECG and carotid signal waveform after filtration based on the threshold set independently for both the biosignals and is plotted for further analysis. Intervals between two adjacent *RR* peaks are evaluated for ECG wave and peak to peak difference is calculated from the carotid pulse wave. Time domain HRV parameters are subsequently evaluated and analyzed.

Results obtained for various subjects displaying the simultaneously acquired ECG signal on channel 1 and carotid pulse wave on channel 2 with marked peaks are presented in Figs. 6−6 and 6−7. Table 6−5 gives the heart rate, HRV time domain measures—mean *RR*, RMSSD, SDNN, and SDNN Index for a set of male and female subjects evaluated both from ECG signal waveform and the carotid pulse wave. As can be visually verified from the results obtained, there subsists a direct relationship amongst the attained ECG signal and the carotid pulse data. The HRV time domain measures evaluated from both the real-time acquired biosignals also show negligible difference. An effort has been established through this experimentation to exploit the simple detection of carotid pulse wave which can form a base for evaluating HRV, as there is a direct correlation with ECG derived parameters.

While analyzing the time domain measures evaluated over small segments, it is noticed that the measure of SDNN and SDNN Index are similar as reported in the literature as well. The algorithm has the limitation of having a fixed threshold level for calculating the QRS peak, which can be improved by incorporating adaptive thresholding technique, where the

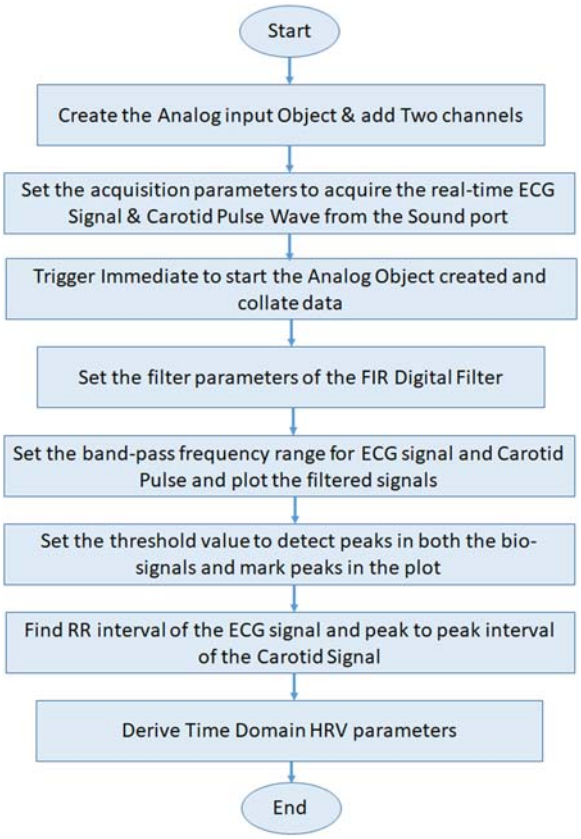

FIGURE 6–5 Algorithm flow for online dual channel acquisition, FIR digital filtering, QRS peak detection, peak to peak interval evaluation in carotid signal and HRV parameterization in MATLAB. HRV, heart rate variability.

output filtered signal is constantly improved to calculate the QRS peak. Numerous reports suggest a close relationship between emotional factors like anxiety and hostility with reduced level of HRV (Sloan et al., 2005). In healthy subjects, both SNS and PSNS tones vary during the day (Goldberger, 1999). As can be seen from the results obtained, HRV time domain measures Mean *RR*, and RMSSD have high values at lower heart rate values (Hazemi et al., 2002). HRV is found as sensitive and reactive to severe anxiety levels, cognitive tasks, complex decision making, etc. Heart rate measurement done while resting does not vary with growing age, but the HRV metrics show decline with age and is found to be highest during sleep. Physically active individuals have raised levels of HRV. It is observed that HRV analysis performed on randomly chosen ECG segment, are not well-defined statistical measures as it depends on the segment length. It is suggested that these evaluations must be performed on either short-term 5-min ECG segments or on 24 h long-term segments. Variation in body

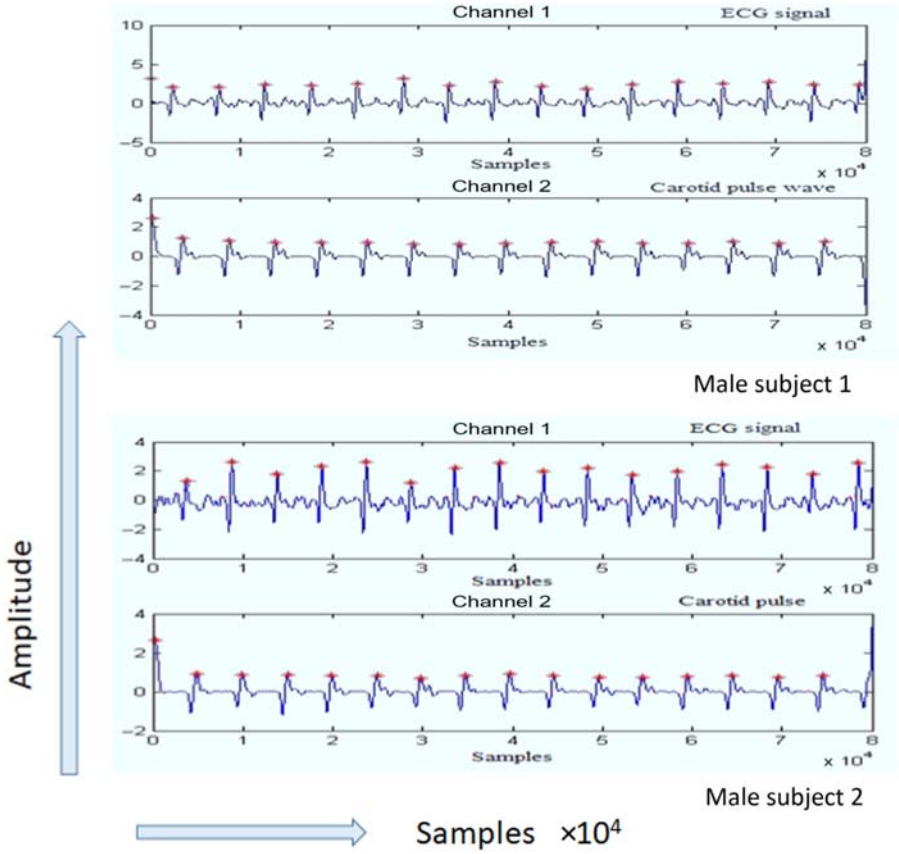

FIGURE 6–6 Results showing peak detected real-time concurrently detected ECG signal and carotid pulse waveform for male subjects.

posture, measurements done on tilt table, etc. affect the spectral measures of HRV. HRV analysis offers further insight into cardiopathological status, and thus supports physicians in getting quick diagnostic results.

Precise detection of QRS peaks, subsequent evaluation of *RR*-intervals and the variance among the intervals forms the basis for HRV analysis. Most of the algorithms proposed and deployed in the literature, utilize ECG signals as the base for HRV measurement and analysis. Physicians also find it comfortable to use ECG to draw health−related implications. Comparable explanations could not be established based on carotid pulse waves earlier. As can be seen, there is a close similarity in the HRV measures evaluated using ECG signal and the carotid pulse wave that were coherently acquired, so carotid pulse may be used for drawing similar diagnostic inferences.

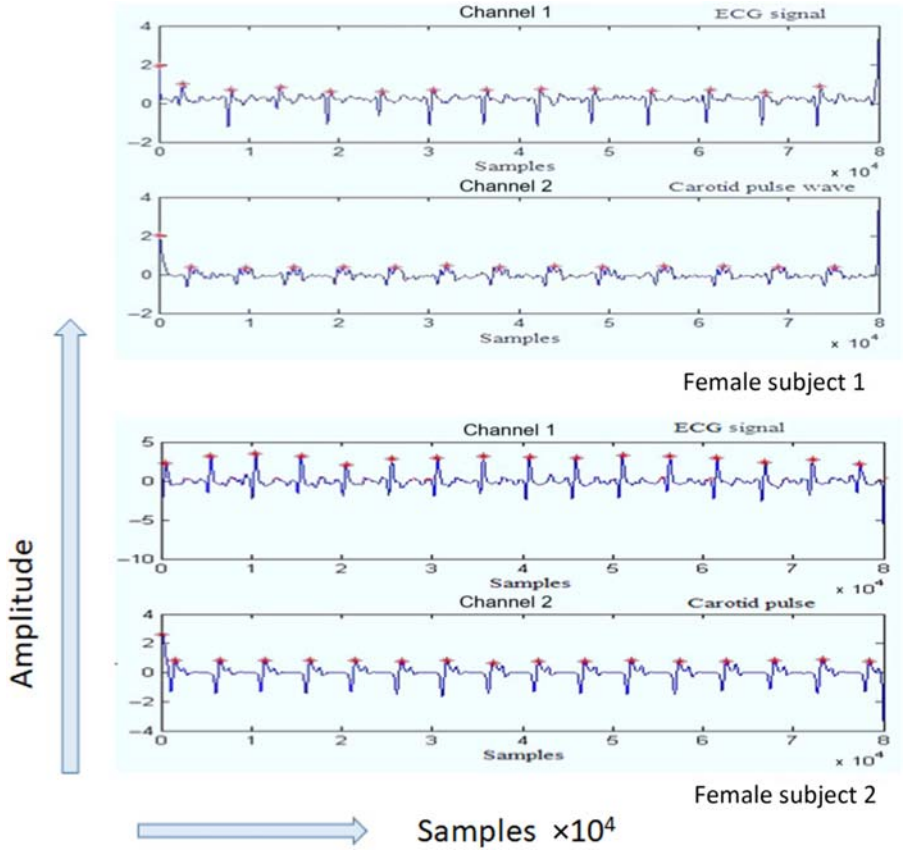

FIGURE 6–7 Results showing peak detected real-time concurrently detected ECG signal and carotid pulse waveform for female subjects.

Table 6–5 Heart rate and HRV time domain measures obtained from ECG signal and carotid pulse wave.

	Subject 1		Subject 2		Subject 3	
	ECG signal	**Carotid pulse**	**ECG signal**	**Carotid pulse**	**ECG signal**	**Carotid pulse**
Heart rate (bpm)	93.68	93.78	82.04	82.16	91.67	91.71
Mean *RR* (s)	0.6403	0.6401	0.7324	0.7304	0.6543	0.6540
RMSSD	0.6403	0.6402	0.7325	0.7317	0.6552	0.6544
SDNN	0.0067	0.0052	0.0495	0.0492	0.0271	0.0262
SDNN index	0.0067	0.0052	0.0495	0.0492	0.0271	0.0262

HRV, heart rate variability.

6.5 Conclusion

HRV analysis has gained popularity over the years as it permits easy means of inferring physiological conditions of an individual. HRV tracking can motivate the way one lives and thinks and can provide great insights into the behavioral impact on the nervous system and the functions of vital organs and body parts. HRV parameters are generally derived from the ECG signals. Compact, wireless, and commercially available ECG monitoring systems having multichannel data acquisition functionality and having in-built algorithm to calculate HRV parameters allow appreciated insight into human health conditions. However, there may be situations when deriving these inferences using ECG signal may not be feasible, for example, in remote locations or when at home. Under such circumstances it may be potentially useful to use carotid pulse waves to estimate HRV parameters as they have very close indices similar to those derived from the ECG wave. The system established here presents a close resemblance with HRV time domain measures obtained from simultaneously acquired ECG signal and carotid pulse wave detected from the real-time, noninvasive dual-channel detection system established and the algorithm made in MATLAB. As detection of carotid pulse waves involves much simpler instrumentation, which is compact, less cumbersome, requires minimum circuitry in comparison to ECG detection system, so can be an alternate to establish HRV measures.

As QRS peak detection sets the base for HRV parameterization, it is absolutely essential to have robust and reliable QRS peak detection algorithms. Virtually 99.5% sensitivity is achievable today for real-time QRS peak detection and is adequate from clinical perspectives, but higher accuracy is essential for research applications when impacted by noise interference. ECG signal analyzed offline based on standard available database gives improved performance. Modern advancements in soft computing techniques can further be useful for improvements in QRS peak detection algorithms.

To be able to appreciate and analyze various metrics of HRV to comprehend cardiac functioning, it is important to study them in time and frequency domain and using nonlinear techniques. The evaluation of HRV is progressively being utilized and standardized as it allows prediction of survival post heart attack. Though, the calculation of HRV involves expertise, the hardware and software setup involved is inexpensive and practical.

References

Abibullaev, B., Seo, H.D., 2010. A new QRS detection method using wavelets and artificial neural networks. J. Med. Syst. 35, 683–691.

Acharya, U.R., Joseph, K.P., Kannathal, N., Lim, C.M., Suri, J.S., 2006. Heart rate variability: a review. Med. Biol. Eng. Comput. 44 (12), 1031–1051.

Ahmed, A.K., Harness, J.B., Mearns, A.J., 1982. Respiratory control of heart rate. Eur. J. Appl. Physiol. 50, 95–104.

Arzeno, N.M., Deng, Z.D., Poon, C.S., 2008. Analysis of first-derivative based QRS detection algorithms. IEEE Trans. Biomed. Eng. 55, 478–484.

Baek, H.J., Cho, C.H., Cho, J., Woo, J.M., 2015. Reliability of ultra-short-term analysis as a surrogate of standard 5-min analysis of heart rate variability. Telemed. J. E Health 21, 404–414.

Bae, T.W., Kwon, K.K., 2019. Efficient real-time R and QRS detection method using a pair of derivative filters and max filter for portable ECG device. Appl. Sci. 9, 4128.

Bahoura, M., Hassani, M., Hubin, M., 1997. DSP implementation of wavelet transform for real time ECG wave forms detection and heart rate analysis. Comput. Methods Prog. Biomed. 52 (1), 35–44.

Bansal, D., Khan, M., Salhan, A.K., 2010. Wireless transmission of EMG signal and analysis of its correlation with simultaneously acquired carotid pulse wave using dual channel system. In: IEEE Second International Conference on Digital Library, eHealth, Telemedicine, and Social Medicine, St. Maarten, Netherlands Antilles, ETELEMED'10, pp. 125-129. Available from: https://doi.org/10.1109/eTELEMED.2010.24.

Bansal, D., Khan, M., Salhan, A.K., 2009. A computer based wireless system for online acquisition, monitoring and digital processing of ECG waveforms. Comput. Biol. Med. 39 (4), 361–367. 2009.

Bansal, D., Singh, V.R., 2014. Algorithm for online detection of HRV from coherent ECG and carotid pulse wave. Int. J. Biomed. Eng. Technol. 14 (4), 333–343.

Bartels, R., Neumamm, L., Peçanha, T., et al., 2017. SinusCor: an advanced tool for heart rate variability analysis. Biomed. Eng. Online 16, 110.

Beckers, F., Ramaekers, D., Aubert, A.E., 2001. Approximate entropy of heart rate variability: validation of methods and application in heart failure. Cardiovasc. Eng. 1, 177–182.

Behbahani, S., Dabanloo, N.J., Nasrabadi, A.M., 2012. Ictal heart rate variability assess-ment with focus on secondary generalized and complex partial epileptic seizures. Adv. Biores. 4, 50–58.

Benitez, D., Gaydecki, P., Zaidi, A., Fitzpatrick, A.P., 2001. The use of the Hilbert transform in ECG signal analysis. Comput. Biol. Med. 31, 399–406.

Benítez, D., Gaydecki, P., Zaidi, A., Fitzpatrick, A., 2000. A new QRS detection algorithm based on the Hilbert transform. In: Proceedings of the Computers in Cardiology 2000, Cambridge, MA, USA, 24–27 September 2002, pp. 379–382.

Bernardi, L., Valle, F., Coco, M., Calciati, A., Sleight, P., 1996. Physical activity influences heart rate variability and very-low-frequency components in Holter electrocardiograms. Cardiovasc. Res. 32 (2), 234–237.

Berntson, G.G., Bigger Jr., J.T., Eckberg, D.L., Grossman, P., Kaufmann, P.G., Malik, M., et al., 1997a. Heart rate variability: origins, methods, and interpretive caveats. Psychophysiology 34, 623–648.

Berntson, G.G., Bigger Jr, J.T., Eckberg, D.L., et al., 1997b. Heart rate variability: origins, methods, and interpretive caveats. Psychophysiology. 34 (6), 623–648.

Bigger Jr, J.T., Fleiss, J.L., Steinman, R.C., Rolnitzky, L.M., Kleiger, R.E., Rottman, J.N., 1992. Frequency domain measures of heart period variability and mortality after myocardial infarction. Circulation. 85 (1), 164–171.

Braune, H.J., Geisendörfer, U., 1995. Measurement of heart rate variations: influencing factors, normal values and diagnostic impact on diabetic autonomic neuropathy. Diabetes Res. Clin. Pract. 29 (3), 179–187.

Brennan, M., Palaniswami, M., Kamen, P., 2001. Do existing measures of Poincar_e plot geometry reect nonlinear features of heart rate variability. IEEE Trans. Biomed. Eng. 48 (11), 1342–1347.

Brennan, M., Palaniswami, M., Kamen, P., 2002. Poincaré plot interpretation using a physiological model of HRV based on a network of oscillators. Am. J. Physiol. Heart Circ. Physiol 283, H1873–H1886.

Brown, T.E., Beightol, L.A., Koh, J., Eckberg, D.L., 1993. Important influence of respiration on human R-R interval power spectra is largely ignored. J. Appl. Physiol. 75 (5), 2310–2317.

Buccelletti, E., Gilardi, E., Scaini, E., Galiuto, L., Persiani, R., Biondi, A., Basile, F., Gentiloni Silveri, N., 2009. Heart rate variability and myocardial infarction: systematic literature review and metanalysis. Eur. Rev. Med. Pharmacol. Sci. 13 (4), 299–307.

Campos, M., 2019. Heart rate variability: a new way to track well-being, Harvard Health Blog. October 22, 2019.

Carney, R.M., Freedland, K.E., Stein, P.K., et al., 2007. Heart rate variability and markers of inflammation and coagulation in depressed patients with coronary heart disease. J. Psychosom. Res. 62 (4), 463−467.

Carrasco, S., Caitan, M.J., Gonzalez, R., Yanez, O., 2001. Correlation among Poincare plot indexes and time and frequency domain measures of heart rate variability. J. Med. Eng. Technol. 25 (6), 240−248.

Chen, A., Zhang, Y., Zhang, M., Liu, W., Chang, S., Wang, H., et al., 2020. A real time QRS detection algorithm based on ET and PD controlled threshold strategy. Sensors (Basel) 20 (14), 4003.

Choi, C.C., Kim, Y.Y., Shin, K.K., 2012. A PD control-based QRS detection algorithm for wearable ECG applications. Conf. Proc. IEEE Eng. Med. Biol. Soc. 2012, 5638−5641.

Chouhan, V.S., Mehta, S.S., 2008. Detection of QRS complexes in 12-lead ECG using adaptive quantized threshold. IJCSNS Int. J. Comput. Sci. Netw. Security 8 (1), 155−163.

Christov, I.I., 2004. Real time electrocardiogram QRS detection using combined adaptive threshold. Biomed. Eng. Online 3, 28.

David Naranjo-Hernández, L.M., Roa, J., Reina-Tosina, G., Barbarov-Rostan, Galdámez-Cruz, O., 2017. Smart device for the determination of heart rate variability in real time. J. Sens. 2017, 11. Article ID 8910470.

DeGiorgio, C.M., Miller, P., Meymandi, S., Chin, A., Epps, J., Gordon, S., et al., 2010. RMSSD, a measure of vagus-mediated heart rate variability, is associated with risk factors for SUDEP: the SUDEP-7 inventory. Epilepsy Behav. 19 (78−81), 78−81.

Dobbs, S.E., Schmitt, N.M., Ozemek, H.S., 1984. QRS detection by template matching using real-time correlation on a microcomputer. J. Clin. Eng. 9 (3), 197−212.

Eckberg, D.L., Eckberg, M.J., 1982. Human sinus node responses to repetitive, ramped carotid baroreceptor stimuli. Am. J. Physiol. 242, H638−H644.

Ehab, A.R.H., Ali, S.H., 2019. Hilal Al-Libawy detection of electrocardiogram QRS complex based on modified adaptive threshold. Int. J. Electr. Comput. Eng. 9, 3512−3521.

Esco, M.R., Flatt, A.A., 2014. Ultra-short-term heart rate variability indexes at rest and post-exercise in athletes: evaluating the agreement with accepted recommen-dations. J. Sports Sci. Med. 13, 535−541.

Fusheng, Y., Bo, H., Qingyu, T., 2001. Approximate entropy and its application in biosignal analysis (Chapter 3) In: Akay, M. (Ed.), Nonlinear Biomedical Signal Processing: Dynamic Analysis and Modeling, II. IEEE Press, New York.

Goldberger, J.J., 1999. Sympatho vagal balance: how should we measure it? Am. J. Physiol. 276, H1273−H1280 (Heart Circ. Physiol. 4).

Grant, C.C., van Rensburg, D.C., Strydom, N., Viljoen, M., 2011. Importance of tacho-gram length and period of recording during noninvasive investigation of the autonomic nervous system. Ann. Noninvasive Electrocardiol. 16, 131−139.

Guzik, P., Piskorski, J., Krauze, T., Schneider, R., Wesseling, K.H., Wykretowicz, A., et al., 2007. Correlations between the Poincaré plot and conventional heart rate variability parameters assessed during paced breathing. J. Physiol. Sci. 57, 63−71.

Hadase, M., Azuma, A., Zen, K., et al., 2004. Very low frequency power of heart rate variability is a powerful predictor of clinical prognosis in patients with congestive heart failure. Circ. J. 68 (4), 343−347.

Hamilton, P.S., Tompkins, W.J., 1986a. Quantitative investigation of QRS detection rules using the MIT/BIH arrhythmia database. IEEE Trans. Biomed. Engg. BME-33 (12).

Hamilton, P.S., Tompkins, W.J., 1986b. Quantitative investigation of QRS detection rules using the MIT/BIH arrhythmia database. IEEE Trans. Biomed. Eng. 33, 1157−1165.

Hazemi, A.A., Ama, N.A., Syiamic, A., Qosti, R., Galil, K.A., 2002. Time domain analysis of heart rate variability in diabetic patients with and without autonomic neuropathy. Ann. Saudi Med. 22 (5−6), 400−402.

Huikuri, H.V., Niemela, M.J., Ojala, S., Rantala, A., Ikaheimo, M.J., Airaksinen, K.E., 1994. Circadian rhythms of frequency domain measures of heart rate variability in healthy subjects and patients with coronary artery disease. Effects of arousal and upright posture. Circulation 90 (1), 121–126.

Jovic, A., Bogunovic, N., 2011. Electrocardiogram analysis using a combination of statistical, geometric, and nonlinear heart rate variability features. Artif. Intell. Med. 51, 175–186.

Karimipour, A., Homaeinezhad, M.R., 2014. Real-time electrocardiogram P-QRS-T detection–delineation algorithm based on quality-supported analysis of characteristic templates. Comput. Biol. Med. 52, 153–165.

Kasaoka, S., Nakahara, T., Kawamura, Y., Tsuruta, R., Maekawa, T., 2010. Real-time monitoring of heart rate variability in critically ill patients. J. Crit. Care 25 (2), 313–316.

Kleiger, R.E., Miller, J.P., Bigger Jr, J.T., Moss, A.J., 1987. Decreased heart rate variability and its association with increased mortality after acute myocardial infarction. Am. J. Cardiol. 59, 256–262.

Kleiger, R.E., Stein, P.K., Bigger Jr., J.T., 2005. Heart rate variability: measurement and clinical utility. Ann. Noninvasive Electrocardiol. 10, 88–101.

Kohler, B.U., Hennig, C., Orglmeister, R., 2002. The principles of software QRS detection. IEEE Eng. Med. Biol. Mag. 21 (1), 42–57.

Kuusela, T., 2013. Methodological aspects of heart rate variability analysis. In: Kamath, M.V., Watanabe, M.A., Upton, A.R.M. (Eds.), Heart Rate Variability (HRV) Signal Analysis. CRC Press, Boca Raton, FL, pp. 9–42.

Lake, D.E., Richman, J.S., Griffin, M.P., Moorman, J.R., 2002. Sample entropy analysis of neonatal heart rate variability. Am. J. Physiol. Regul. Integr. Comp. Physiol. 283 (3), R789–R797.

Lampert, R., Bremner, J.D., Su, S., et al., 2008. Decreased heart rate variability is associated with higher levels of inflammation in middle-aged men. Am. Heart J. 156 (4), 759.e1–7.

Legarreta, I.R., Addison, P., Grubb, N., Clegg, G.R., Robertson, C., Fox, K., et al., 2003. R-wave detection using continuous wavelet modulus maxima. Computers in Cardiology. IEEE.

Lehrer, P.M., Vaschillo, E., Vaschillo, B., et al., 2003. Heart rate variability biofeedback increases baroreflex gain and peak expiratory flow. Psychosom. Med. 65 (5), 796–805.

Li, K., Rüdiger, H., Ziemssen, T., 2019. Spectral analysis of heart rate variability: time window matters. Front. Neurol. 10, 545.

Li, C., Zheng, C., Tai, C., 1995. Detection of ECG characteristic points using wavelet transforms. IEEE Trans. Biomed. Eng. 42, 21–28.

Malik, M., Bigger, J.T., Camm, A.J., Kleiger, R.E., Malliani, A., Moss, A.J., et al., 1996. Heart rate variability: standards of measurement, physiological interpretation, and clinical use. Eur. Heart J. 17 (3), 354–381.

Marcus, V., 2015. A robust, simple and reliable measure of heart rate variability using relative rr intervals. In: 2015 Computing in Cardiology Conference (CinC), IEEE, Nice, France, pp. 609–612.

Marcus, V., 2019. HRVTool – an Open-Source Matlab Toolbox for analyzing heart rate variability. In: 2019 Computing in Cardiology Conference (CinC), Computing in Cardiology, Singapore, pp. 1–4.

Marple, S.L., 1987. Digital Spectral Analysis. Prentice-Hall International, Englewood Cliffs, NJ.

Martínez, J.P., Almeida, R., Olmos, S., Rocha, A.P., Laguna, P., 2004. A wavelet-based ECG delineator: evaluation on standard databases. IEEE Trans. Biomed. Eng. 51, 570–581.

Martínez, C.A.G., Quintana, A.O., Vila, X.A., Touriño, M.J.L., Rodríguez-Liñares, L., Presedo, J.M.R., et al., 2017. Heart Rate Variability Analysis with the R Package RHRV, 157. Springer International Publishing, p. XVI, ISBN 978-3-319–65355-6.

McConnell, M., Schwerin, B., So, S., Richards, B., 2020. *RR*-APET—heart rate variability analysis software. Comput. Methods Prog. Biomed. 185, 105127.

McCraty, R., Shaffer, F., 2015a. Heart rate variability: new perspectives on physiological mechanisms, assessment of self-regulatory capacity, and health risk. Glob. Adv. Health Med. 4, 46–61.

McCraty, R., Shaffer, F., 2015b. Review heart rate variability: new perspectives on physiological mechanisms, assessment of self-regulatory capacity, and health risk. Glob. Adv. Health Med. 4 (1).

Meraha, M., Abdelmalika, T.A., Larbi, B.H., 2015. R-peaks detection based on stationary wavelet transform. Comput. Methods Prog. Biomed. 121, 149–160.

Otzenberger, H., Gronfier, C., Simon, C., Charloux, A., Ehrhart, J., Piquard, F., et al., 1998. Dynamic heart rate variability: a tool for exploring sympathovagal balance continuously during sleep in men. Am. J. Physiol. 275 (3 Pt 2), H946–H950.

Pan, J., Tompkins, W., 1985. A real-time QRS detection algorithm. IEEE Trans. Biomed. Eng. 32, 230–236.

Peng, C.-K., Havlin, S., Stanley, H.E., Goldberger, A.L., 1995. Quanti_cation of scaling exponents and crossover phenomena in nonstationary heartbeat time series. Chaos 5, 82–87.

Pentillä, J., Helminen, A., Jarti, T., Kuusela, T., Huikuri, H.V., Tulppo, M.P., et al., 2001. Time domain, geometrical and frequency domain analysis of cardiac vagal outflow: effects of various respiratory patterns. Clin. Phys. 21, 365–376.

Penzel, T., Kantelhardt, J.W., Grote, L., Peter, J.-H., Bunde, A., 2003. Comparison of detrended uctuation analysis and spectral analysis for heart rate variability in sleep and sleep apnea. IEEE Trans. Biomed. Eng. 50 (10), 1143–1151.

Quintana, D.S., Elstad, M., Kaufmann, T., Brandt, C.L., Haatveit, B., Haram, M., et al., 2016. Resting-state high-frequency heart rate variability is related to respiratory frequency in individuals with severe mental illness but not healthy controls. Sci. Rep. 6, 37212.

Richman, J.A., Moorman, J.R., 2000. Physiological time-series analysis using approximate entropy and sample entropy. Am. J. Physiol. 278, H2039–H2049.

Rizzi, M., Matteo, D.A., Castagnolo, B., 2009. High sensitivity & noise immune method to detect impedance cardiography characteristic points using wavelet transforms. J. Appl. Sci. 9, 1412–1421.

Salahuddin, L., Cho, J., Jeong, M.G., Kim, D., 2007. Ultra short term analysis of heart rate variability for monitoring mental stress in mobile settings. Conf. Proc. IEEE Eng. Med. Biol. Soc. 2007, 4656–4659.

Saxena, S.C., Kumar, V., Hamde, S.T., 2002. QRS detection using new wavelets. J. Med. Eng. Technol. 26 (1), 7–15 (9).

Schipke, J.D., Arnold, G., Pelzer, M., 1999. Effect of respiration rate on short-term heart rate variability. J. Clin. Basic. Cardiol. 2, 92–95.

Schmidt, H., Muller-Werdan, U., Hoffmann, T., et al., 2005. Autonomic dysfunction predicts mortality in patients with multiple organ dysfunction syndrome of different age groups. Crit. Care Med. 33 (9), 1994–2002.

Shaffer, F., Ginsberg, J.P., 2017. An. Overv. Heart Rate Variability Metr. Norms Front. Public. Health 5 (258), Article.

Shaffer, F., McCraty, R., Zerr, C.L., 2014. A healthy heart is not a metronome: an integrative review of the heart's anatomy and heart rate variability. Front. Psychol. 5, 1040.

Shah, A.J., Lampert, R., Goldberg, J., Veledar, E., Bremner, J.D., Vaccarino, V., 2013. Posttraumatic stress disorder and impaired autonomic modulation in male twins. Biol. Psychiatry 73 (11), 1103–1110.

Shiraishi, Y., Katsumata, Y., Sadahiro, T., Azuma, K., Akita, K., Isobe, S., et al., 2018. Real-time analysis of the heart rate variability during incremental exercise for the detection of the ventilatory threshold. J. Am. Heart Assoc. 7 (1).

Singh, R.B., Cornelissen, G., Weydahl, A., et al., 2003. Circadian heart rate and blood pressure variability considered for research and patient care. Int. J. Cardiol. 87 (1), 9–28. discussion 29–30.

Singh, N., Moneghetti, K.J., Christle, J.W., Hadley, D., Froelicher, V., Plews, D., 2018a. Heart rate variability: an old metric with new meaning in the era of using mhealth technologies for health and exercise training guidance. part two: prognosis and training. Arrhythm. Electrophysiol. Rev. 7 (4), 247–255.

Singh, N., Moneghetti, K.J., Christle, J.W., Hadley, D., Plews, D., Froelicher, V., 2018b. Heart Rate Variability: An Old Metric with New Meaning in the Era of using mHealth Technologies for Health and Exercise Training Guidance. Part One: Physiology and Methods. Arrhythmia Electrophysiol. Rev. 7 (3), 193–198.

Sloan, R.P., Huang, M.-H., Sidney, S., Liu, K., Williams, O.D., Seeman, T., 2005. Socioeconomic status and health: is parasympathetic nervous system activity an intervening mechanism? Int. J. Epidemiol. 34, 309–315.

Stampfer, H.G., Dimmitt, S.B., 2013. Variations in circadian heart rate in psychiatric disorders: theoretical and practical implications. Chronophysiol Ther. 3, 41–50.

Stein, P.K., Reddy, A., 2005. Non-linear heart rate variability and risk stratification in cardiovascular disease. Indian Pacing Electrophysiol. J. 5, 210–220.

Sun, Y., Chan, K.L., Krishnan, S.M., 2005. Characteristic wave detection in ECG signal using morphological transform. BMC Cardiovasc. Disord. 5, 28.

Tarvainen, M.P., Niskanen, J.-P., 2012. Kubios HRV version 2.1, USER'S GUIDEJuly 6 Biosignal Analysis and Medical Imaging Group (BSAMIG). Department of Applied Physics, University of Eastern Finland, Kuopio, Finland.

Tarvainen, M.P., Niskanen, J.P., Lipponen, J.A., Ranta-Aho, P.O., Karjalainen, P.A., 2014. Kubios HRV--heart rate variability analysis software. Comput. Methods Prog. Biomed. 113 (1), 210–220.

Task force of the European society of cardiology and the North American society of pacing and electrophysiology, 1996. Heart rate variability: standards of measurement, physiological interpretation, and clinical use. Circulation 93 (5), 1043–1065.

Thakor, N.V., Webster, J.G., Tompkins, W.J., 1983. Optimal QRS detector. Med. & Biol. Eng. & Comput. 21, 343–350.

Thayer, J.F., Yamamoto, S.S., Brosschot, J.F., 2010. The relationship of autonomic imbalance, heart rate variability and cardiovascular disease risk factors. Int. J. Cardiol. 141, 122–131.

The Framingham Heart Study, 1994. Reduced heart rate variability and mortality risk in an elderly cohort. Circulation .

Theorell, T., Liljeholm-Johansson, Y., Bjork, H., Ericson, M., 2007. Saliva testosterone and heart rate variability in the professional symphony orchestra after “public faintings” of an orchestra member. Psychoneuroendocrinology. 32 (6), 660–668.

Tiller, W.A., McCraty, R., Atkinson, M., 1996. Cardiac coherence: a new, noninvasive measure of autonomic nervous system order. Altern. Ther. Health Med. 2 (1), 52–65.

Trahanias, P., 1993. An approach to QRS complex detection using mathematical morphology. IEEE Trans. Biomed. Eng. 40, 201–205.

Tsuji, H., Larson, M.G., Venditti Jr, F.J., et al., 1996. Impact of reduced heart rate variability on risk for cardiac events. Framingham Heart Study. Circulation. 94 (11), 2850–2855.

Umetani, K., Singer, D.H., McCraty, R., Atkinson, M., 1998. Twenty-four hour time domain heart rate variability and heart rate: relations to age and gender over nine decades. J. Am. Coll. Cardiol. 31, 593–601.

Vest, A.N., Li, Q., Liu, C., Nemati, S., Shah, A., Clifford, G.D., 2017. Benchmarking heart rate variability toolboxes. J. Electrocardiol. 50 (6), 744–747.

Wong, K.-I., 2009. Real-time heart rate variability detection on sensor node. In: 2009 IEEE Sensors Applications Symposium, New Orleans, LA, 2009, pp. 184–187.

Yang, D., Zhang, Y., 2018. A real-time QRS detector based on low-pass differentiator and Hilbert transform. MATEC Web Conf. 175, 02008.

Yazdani, S., Vesin, J.M., 2016. Extraction of QRS fiducial points from the ECG using adaptive mathematical morphology. Digit. Signal. Process. 56, 100–109.

Yeh, Y.-C., Wang, W.-J., 2008. QRS complexes detection for ECG signal: the difference operation method. Comput. Methods Prog. Biomed. 91, 245–254.

Yochum, M., Renaud, C., Jacquir, S., 2016. Automatic detection of P, QRS and T patterns in 12 leads ECG signal based on CWT. Biomed. Signal. Process. Control. 25, 46–52.

Zerr, C., Kane, A., Vodopest, T., Allen, J., Hannan, J., Cangelosi, A., et al., 2015. The nonlinear index SD1 predicts diastolic blood pressure and HRV time and frequency domain measurements in healthy undergraduates [Abstract]. Appl. Psychophysiol. Biofeedb. 40, 134.

Zhang, F., Lian, Y., 2009a. Wavelet and Hilbert transforms based QRS complexes detection algorithm for wearable ECG devices in wireless body sensor networks. In: Proceedings of the IEEE Biomedical Circuits and Systems Conference, Beijing, China, 26–28 November 2009a, pp. 225–228.

Zhang, F., Lian, Y., 2009b. QRS detection based on multiscale mathematical morphology for wearable ECG devices in body area networks. IEEE Trans. Biomed. Circuits Syst. 3, 220–228.

This page intentionally left blank

7 Conclusion

7.1 Major contributions

Globalization and technological advancements have led to a change in the way people think, live, and interact in the present day. Even though the technology is upgrading by the day, the ever growing need for better systems are a good enough motivation to keep the research teams on the toes. This book presents an application driven, interdisciplinary, and experimental approach to bio-signal detection and processing. An attempt has been made to develop indigenously a credible bio-signal monitoring arrangement for recording and analyzing human physiological parameters, employing cost effective and versatile sensors, hardware−, and software−based signal conditioning. Personal Computer (PC)−based data acquisition is done using digital signal controllers (DSC), sound port−based simple interface, suitable amplifier, notch filter circuit, and MATLAB software for display and real-time processing. The book suggests solutions that could reduce response time to cure and provide home-health monitoring system designed for the medical environment. The system intends to reduce stress on the medical professionals by providing initial diagnosis and can be developed to make medical professionals free for other pressing purposes. The proposed system allows automated and continuous monitoring of vital signs and updated real-time information can be applied for preventive medical care as well. The book also covers simulation and modeling to interpret and detect abnormalities on the onset of a disease or abnormality through signal feature extraction and artifact removal, allows monitoring and storing of the health conditions in real-time, and performs objective analysis through algorithm development, thus reducing the subjectivity involved in manual and visual diagnosis and enhances reproducibility.

The contributions include experimental layout and development of computer−based instrumentation and software for acquisition, processing, and understanding of human electrocardiogram (ECG), electromyogram (EMG), carotid pulse wave, and heart rate variability (HRV). Contribution made toward detection, processing, and analysis of each physiological parameter is detailed in the subsequent sections.

7.1.1 Detection and analysis of carotid pulse wave

- An indigenous computer−based system has been deliberated and established to detect the human carotid artery pulsation. The arrangement has the capability of easy and direct interface through the sound port of the PC and requires no proprietary data acquisition unit (DAQ) or analog to digital converter (ADC) units for acquisition.

Real-Time Data Acquisition in Human Physiology. DOI: https://doi.org/10.1016/B978-0-12-822118-1.00007-2
© 2021 Elsevier Inc. All rights reserved.

- Carotid pulse wave is extracted and analyzed under different body postures using a noninvasive and commercially available piezoelectric transducer extracted from a buzzer. The signal so acquired is examined on a virtual oscilloscope which is freely downloadable and simple to use.
- The property of a piezoelectric sensor having lead zirconate titanate ceramic disk is successfully exploited to pick microlevel vibrations from the carotid artery when placed suitably on the neck after palpating without additional electronic circuitry or preamplification. The transducer is very compact, light in weight, rugged, and provides a very stable output. Other methods using strain gage transducer need preamplification to measure the carotid data, while fluid volume displacement method gives erroneous results as it picks up adjacent signals due to its bigger size.
- A functional model has been implemented in Simulink application software of MathWorks to filter and acquire real-time carotid pulse wave using its integral library.

7.1.2 Detection and analysis of electromyogram signal

- An amplifier system has been developed using Texas Instruments' TL084C Operational Amplifier to pick human EMG signal under various contraction levels in bicep muscles using a standard Ag-AgCl sensor. A cascaded amplifier including DC restoration circuit, analog filters, and a circuit for right leg drive constitutes the front end of the acquisition process.
- Reusable sensor Ag-AgCl is highly recommended for use to detect the ECG and EMG signal from the body surface as it is electrochemically stable, has high CMRR ratio, is able to sense very low amplitude signals in mV range even in a noisy environment, and has comparatively small half-cell potential resulting in minimum offset. Hydrogen electrodes have comparable half-cell potential but are avoided in this work owing to their gaseous nature. Some other electrodes which give accurate measurements but are invasive have been avoided as they are unrealistic and highly skilled clinicians are required to operate. Thus signal detection using the Ag-AgCl sensor enabled easy and relatively accurate measurement which could be translated into suitable signal processing and analysis.
- A virtual oscilloscope coupled with algorithm for digital filtration in MATLAB has been deployed to detect and analyze EMG signal in real time.
- The dual channel system in a home−based computer set-up was further explored to concurrently detect EMG and carotid wave signal so as to study the outcome of rectus abdominal contractions of the muscle on the carotid pulsation contour.
- To facilitate simultaneous and time coherent acquisition of carotid pulse and EMG signal under pressure change in rectal abdominal region and related variations in carotid wave form, a hardware channel capable to acquire dual signals is synchronized with an algorithm developed in MATLAB.
- MATLAB−based algorithm has been generated for noise reduction using digital zero phase band pass filtering techniques and feature extraction techniques have been incorporated to infer diagnostic features in real-time.

7.1.3 Detection and analysis of electrocardiogram signal and heart rate variability

- The concept established was progressed further for detection and automated analysis of ECG signals. An audio processing kit developed by Microchip—dsPIC—33F—DSC, has been explored for this purpose. An additional algorithm is also made in MATLAB so that real-time automated analysis of filtered ECG signal can be realized. The twin channel arrangement explained above is utilized to acquire carotid pulse and ECG signal simultaneously so as to compute parameters related to HRV in real time.
- The twin channel system developed depicts raised amplitude in carotid pulse wave with increased rectus abdominis pressure and is in sync with time-domain HRV data which is a resultant from ECG data and carotid pulse signal. The analysis clearly indicates that under critical situations, where ECG measurement is not feasible and affordable, Carotid pulse information can be a suitable alternate for HRV analysis and interpretation, as there was negligible difference. The purpose is to create an indigenous, cost-effective, user friendly solution to real-time acquisition, processing, and monitoring of human physiology which can directly benefit the common people.
- MATLAB algorithm created for online parameterization allows QRS peak detection, RR interval calculation, heart-rate, and power-spectral-density (PSD) evaluation of ECG waveform.
- HRV statistics in time domain that were analyzed are the average heart-rate, mean RR interval, SD-index, etc.
- A stand-alone, platform−independent executable file for the algorithm has been developed in MATLAB for deployment in future applications.
- Recent front end amplifier systems designed with the best of technology used in biomedical applications have high CMRR but still show stains of 50/60 Hz power line interference. In this work, various 50 Hz notch filter design concepts were explored in P-Spice to compare and evaluate their performance. Two filter designs which produced a sharp notch instead of eliminating a frequency band, gave decent notch-depth and required minimum number of high precision components were selected for hardware implementation. Theoretical and practical frequency response curves showed variation because of tolerance in real world precision components. Output of the filter which closely matched the theoretical result was selected and used with the amplifier system to eliminate the effect of power line hum from the ECG and EMG signal.
- DSC has been used to enhance features of acquired human physiology and to establish a real time embedded solution to biomedical instrumentation.
- Thus a proof of concept of a PC−based twin channel acquisition system for recognition of multiple physiological parameters that are coherent in time for comparison and analysis has been established.

7.2 Conclusion

The arrangement established comprises of development of a user-friendly, compacted, transportable, and economic real-time data detection system to acquire and analyze the human physiological parameters such as ECG signal, EMG signal, and carotid pulsation. The DAQ unit developed includes versatile medical sensors, on board signal conditioning and simple interfacing with computer for viewing and analysis. Processing powers of DSC are also explored to successfully acquire and analyze the signal. The book also extensively covers the clinical aspects of the physiological signals, DSP theories, and LabVIEW− and MATLAB−based software applications. Feature extraction methods are realized on the real-time detected bio-signal and inferences are drawn for diagnosis and therapeutics. The set-up developed is particularly beneficial for continuous monitoring of physiological signals in a home environment, where acquisition and processing are cumbersome and prone to noise. In addition, the bio-signal analysis software has been developed with MATLAB which has finally been compiled to a stand-alone Windows application and hence can be openly used by clinicians and researchers.

Commonly used physiological parameter detection units are proprietary, platform−dependent dedicated instruments, and are not truly cost effective. Recently PC−based portable data acquisition systems are being widely utilized in biomedical applications. The front end of constructed single channel PC−based system developed using TL084C instrumentation amplifier is successful in acquiring ECG and EMG signals. To prevent the single-stage amplifier from saturating, a cascade amplifier organization was developed including a dc restoration circuit to eliminate DC offset. Right-leg drive circuit and active filters were added to improve CMRR so as to obtain a better pickup. The amplified and filtered bio-signals were interfaced with the PC through the sound port. Medical monitoring systems are commonly linked to a computer through parallel port, serial port (RS232), and USB which require proprietary DAQ units and ADC in addition. The interface in this work is via a common communication port, that is, the sound port and the amplifier system developed are compatible to commonly available computers and the output can be viewed and further processed on a virtual oscilloscope. The proposed system is not cumbersome, is platform independent, and relatively cost effective.

Microcontrollers are primarily used to handle data control in biomedical applications which is now gradually giving space to DSP−based controls. DSC that are combination of DSP processors and Micro controllers are upgrading the existing system by allowing low power requirement, improved effectiveness and reliability, large memory, quick response, and compact size. Proprietary DSC solutions are being used for bio-signal processing but with the limitation of additional DAQ boards and ADC units. Microchip dsPIC kit largely used for audio signal processing has been innovatively employed in this work for acquiring bio-signals. It has on board ADC module and in circuit debugging facilities. This kit directly draws power from the computer through USB interface and is also compatible to existing wireless modules. It proves to be a low cost yet effective integrated hardware and software technique for real-time processing of bio-signals. The output of the kit was directly interfaced to the computer's sound port for viewing and analyzing ECG signals. The results obtained

can finally be embedded on to the dsPIC single chip to give a compact solution capable of giving automated analysis of other human physiological parameters in real time.

Recently computer simulations and model creation are being widely utilized in understanding biological signals as they provide a lucid and easy method to test and verify the human physiology. The challenge lies in online acquisition and analysis of the inputs while the customary simulation software is usually tested on stored database, artificially created or assumed inputs. In this work, MATLAB and Simulink have been used to acquire real-time human carotid signals with ease. The model created in Simulink was used to process and filter this real-time bio-signal using various software digital signal processing techniques such as FIR filters and IIR notch filters. The model also gives spectral domain analysis of the real-time acquired signal. The results obtained are satisfactory and provide the flexibility of being used with different proprietary DAQ boards. The aim of proposed virtual instrument in Simulink model was to utilize the knowledge of DSP in removing interference from acquired physiological parameters.

Computer−based display software are an integrated part of the proprietary DAQ units available that enable viewing and processing of the acquired signal. It is however necessary to install the driver software which is an integral part of the data acquisition unit and thus the entire system becomes expensive. They do not provide automated analysis and are also not compatible to general purpose hardware. MATLAB however provides an easy interface with computer and features interactive support, graphical output, easy code generation, and compatibility of real-time collected bio-signal. Script files developed in MATLAB along with in built library functions enabled sound port−based easy acquisition, online filtration of ECG, EMG, and carotid pulse wave. Digital filters designed is nearly unaffected by the noise interference. Further algorithm was developed to extract features such as QRS peak, RR interval, heart rate, etc. from an ECG signal in real time. Spectral analysis of ECG signal was also done by calculating the PSD which gives additional information about human physiology in real time. However, existing feature extraction algorithms mostly have been tested off-line on stored, standard ECG data base.

It is rather exciting to examine the correlation between simultaneously acquired human physiological signals under comparable physical and mental state of a subject. The learning can reveal significant inferences as there could be circumstances like when a human body is under shock or trauma, where it is practically impossible to detect the targeted human physiological signal using standard methods and procedures. Therefore a proof of concept of a dual channel monitoring and recording system has been established in this work, where ECG and carotid pulse wave could be coherently detected to derive and correlate HRV time domain parameters. Algorithm established using MATLAB application software permitted time coherent acquisition of both the signals through sound port of the PC. Algorithm for peak detection and RR interval calculation enabled time domain derivation of HRV parameters from ECG and carotid pulsation. The HRV information evaluated from both the readings exhibit similar results, hence HRV derivation from carotid pulsation can be potentially used, as it is much simpler to detect carotid wave compared to detection of ECG signal. This is a very important development considering the fact that the physicians and clinicians have

been typically using ECG as the prime parameter for HRV analysis. The chief purpose of measuring and analyzing HRV stems from its capability to forecast survival after a heart stroke. The dual channel system was further explored to concurrently detect EMG signal and carotid pulsation so as to study the outcome of rectus abdominal contractions of muscle on the carotid pulsation contour.

It also successfully acquires EMG under different levels of bicep and rectal muscle contractions after digital filtration. Developed hardware 50 Hz notch filter along with amplifier system gave improved ECG output. DSC−based ECG acquisition system provided a platform for automated analysis of the signal. Interactive and user friendly environment of MATLAB helped in developing programs to acquire, store, and process the bio-signals for better viewing, dual channel applications, and feature extraction. This demonstrates the capability of the MATLAB program and removes the necessity of supplementary ADC for computer interface. Though there have been numerous research determinations in the field of detection, monitoring and analysis of human physiological parameters, wireless transmission, and signal feature extraction, most of them stay theoretical at best. This work marks an effort to offer an answer that is more realizable and would directly benefit the common mass and the health care providers (Bansal et al., 2009a,b,c,d, 2010; Bansal, 2012, 2013; Bansal and Singh, 2014; Singh and Bansal, 2014; Bhogeshwar et al., 2014; Mahajan and Bansal, 2014, 2015a,b; Bhogeshwar et al., 2015; Naik et al., 2014).

Currently, few researchers take active interest in developing enhanced and reliable hardware− and software−based techniques for detecting and continuous monitoring of human physiological signals. Considering the medical content of the targeted applications and human life at stake, the absence of reliable techniques in existing systems, call for further improvements. With the shrinkage in available band width and extensive use of wireless technologies for communication, the security, and reliability factor in noisy environment for transport of bio-signals must be researched. Modern advancements in nanotechnologies leading to flexible, reliable, and power efficient systems are a good enough motivation to improve the biomedical applications. By designing miniature-size devices with milliwatt power requirements, microelectronics can pave the way for new generations of systems featuring a multitude of functions for addressing number of medical problems. Smart sensors with on-board signal processing capabilities need to be further explored and made cost effective for general use.

In software domain, almost 99.5% sensitivities are possible today for detection and automated analysis of bio-signals and are sufficient for clinical applications, but higher accuracy is still required in case of noise interference. Biological signals especially ECG, are generally analyzed offline and are tested on standard database. However, recent advances in soft computing techniques can be applied to achieve improvement in analyzing other human physiological signals as well. The hardware and software arrangement discussed in this work can further be explored to detect EEG signals. Separately, an appropriate data format requires to be established for recording and processing these physiological signals so that they are compatible with many hardware and software available. The section below provides future direction of this domain.

7.3 Future directions

It is a no brainer that cardiovascular diseases (CVDs) account for more deaths than other ailments globally. The causes include genetic background, lifestyle problems, ignorance to appreciate symptoms, poverty, lack of medical treatment, to name a few. These predicaments call for greater efforts to prevent, diagnose, monitor, and treat such life-threatening diseases. CVD is sometimes revealed by ECG as it could indicate cardiac abnormalities even when it is not very critical. The ECG which traditionally requires trained medical staff and hospital environment is seeing paradigm shift owing to emergence of better system technologies, advancements in electronics, and sensors. The development in algorithms leading to artificial intelligence (AI)−based solutions, Internet of things (IoT), 5th generation mobile and communication networks, advancements in microelectronics, and e-textiles and successful implementation of these technologies at commercial scale for varied applications, holds the promise to horizontally deploy and disrupt the present health monitoring methodologies.

In this section, we shall discuss some recent developments at the subsystem and system level to invigorate the reader to dive deeper in the relevant area of interest around diagnosis and monitoring of CVD. Cardiac biomarkers have the capability to pre-empt early diagnosis of underlying conditions especially in case of known genetic history for cardiac diseases. The recent work on cardiac biomarkers has shown the reproducible nature, etiological specificity and safety across multiple populations. The specific analysis of the cardiac biomarkers was not possible earlier due to extremely low concentration (in range of ng mL/L to pg mL/L) against body fluid proteins like globulin (in range of g mL/L). Sensors with improved sensitivities involving nanomaterials leading to appreciable electron transfers, and reduced noise have dawned a new era in biomarker identification. Cardiac sensors using graphene and graphene oxide have detected cardiac troponin I (cTnI) in blood samples of humans in very low concentrations (up to 0.1 pg mL/L) and hold promise for saliva screening also for biomarkers. While troponin I remains the commonly identified biomarker, B-type natriuretic peptide, and N-terminal pro-B-type natriuretic peptide are other identified cardiovascular biomarkers. Biosensors for biomarker detection are subcutaneously implanted for real-time benefits and to avoid repeated blood drawing. The downside is infection risk, abnormal esthetics, and limited life spans. The present solution thought process spans around vascular implants, skin patches for sweat−based biosensors, or saliva monitoring techniques. More work is required to enhance the viability of this approach (Szunerits et al., 2019).

While metals like silver and copper are used in bio-signal transduction owing to various properties explained in Chapter 2, PC−based Data Acquisition, the diagnosis trend is shifting more toward health monitoring through wearable systems. Such monitoring systems exploit flexible electronics necessitating conductive, light weight, inexpensive, and biocompatible materials. Graphene−based ingredients have been found to be suitable for such applications as they are capable of being fabricated using photo thermal techniques where porous nanographene is deposited on polymide substrates which are inherently flexible. Graphene has been deposited through chemical vapor method on the conventional Ag−based electrode.

The concept framed inside the IOT paradigm, paves way for an inexpensive, reliable, and stable solution to available electrodes suitable for smart and wearable devices. Other graphene−based electrodes have also been suggested. This family of electrodes is appropriate for long-term usage, as no conductive gels or adhesives are required and are hence categorized as "dry" electrodes. There are expectations around small size, low power consumption, and similar or better signal transduction capabilities for dry electrodes. Ongoing research is dwelling on the delicate compromise between the bio-signal quality and processing algorithms optimization so as to attain accurate results (Romero et al., 2019; Majumder et al., 2017).

As stated earlier, physiological parameters monitoring systems need to consider requirements around preventive measures, timely diagnosis (in case of clinical symptoms signaling direct correlations, indicative comorbidities, or past family history), and patient care or monitoring after an episode to improve the overall quality of life for the patients. Modern and smart health care systems with advancements in microelectronics and other technologies can radically transform the outcomes and prognosis. Continuous heart monitoring through radar cardiography (RCG), insertable cardiac monitors (ICM), technologies using AI, Communication architecture improvements with advent of 5G technologies, and ECG steganography to enhance privacy are some of the upcoming techniques in this area.

Holter ECG monitoring facilitates 24 h continuous monitoring with the provision to start the recording if the patient is experiencing symptoms and can lead to missed diagnosis. It could cause skin irritation and the equipment needs to be prevented from getting wet. Heart ailments are on the rise due to sedentary life style, typical eating habits, depressions and use of tobacco. Photo-plethysmography or PPG−based green LED sensors are part of wearables like head phones and smart watches which measure the reflected light intensity through the tissue referring to the physiological information like heart beat pulse, etc. While the heart beats can be quantified, electrical activity cannot be measured by these sensors. The next generation Apple watches from series 4 onward can indicate ECG wave forms and heart rate in the ECG App while indicating any arrythmia by using advanced algorithms based on machine learning. Bluetooth ECG sensors are attached close to the heart on chest to wirelessly transmit ECG signals to enabled devices. RCG holds promise as an alternate for continuous monitoring of physiological parameters which considers heart beat monitoring at close vicinity in a contact-free manner. The RCG sensing mechanism banks on an impulse−based sensor with multiple antennas. As the antennas pickup both the heart beat and respiratory signals, the heart beat signals need to be isolated and the heart beat waveform needs to be reconstructed. This waveform closely mimics the ECG reference signal and is capable of storing the heartbeat rhythm details. Advanced radar systems including impulse radars and continuous wave (frequency modulated) radars (Rong and Bliss, 2019; Thijs et al., 2005).

ICM or implantable loop recorder are found suitable in the management of atrial fibrillation (AF) especially following a cryptogenic stroke, palpitations, and unexplained syncope. AF can lead to further brain strokes and can lead to permanent and uncurable disabilities in addition to fatalities. The normal investigations and course of action after a cryptogenic stroke include ECG, Holter monitoring, computed tomography scans, and magnetic resonance imaging and laboratory investigations for blood clotting disorders. The treatment also

favors administration of blood anticoagulating agents under proper monitoring. ICM can hugely assist in monitoring such patients with unexplained syncope and cryptogenic stroke as against conventional monitoring methods as they have intermittent scope for measurements. ICM are placed subcutaneously appropriately in the rib locations corresponding to V2−V3 lead positions of ECG. The ICM developed now have recording and wireless transmission features. ICM while weighing a few grams, the associated miniature batteries can last up to 3 years. The entire mechanism is coupled with algorithms for the detection of AF and p-wave detection. The cost of device and the minor surgical procedure is still high and needs to be optimized for higher commercial usage. There are reports of false positives due to motion artifacts and ectopic beats requiring trained physician's support for analysis while monitoring. The benefits will multiply in prevention of further complications if the miniaturization is maintained with battery/power management and mature wireless transmission protocols. The implant size and the placement location in the body are interrelated in the sense that the power requirements, design of the transducer and the carrier frequency are dependent on both of them. With potential applications also in sports and medicine, the ICM need to be made reliable to sustain the prolonged service expectations. Quasi permanent wirelessly rechargeable batteries or surgical replacement of batteries at end of life need to be considered while looking at reliability, safety, patient comfort, and cost issues. Power consumption also impacts the life span and transmission range of the implants. The wireless power charging deploys mechanisms like near-field transmission systems where power is transmitted over small distances by magnetic fields or electric fields created by inductive coupling (in wire coils) or capacitive coupling (in metal electrodes), respectively. A suitable circuit to acquire and amplify the microfine ECG signals using a band-pass filter with overall low power consumption and noise isolation is necessary. Overall, the insert material needs to be biocompatible (like titanium) and ergonomically designed not to cause discomfort after placement in human body. The sensor bodies are coated with suitable adhesives or medical epoxy so as it should not absorb electric current/potential generated by the heart muscles. The insert should conduct internally and needs to be airtight. Timely diagnosis and continuous health monitoring using biomedical implants can benefit patients and minimize emergency situations (Lee, 2016; Giancaterino et al., 2018; Sakhi et al., 2019; Tomson and Passman, 2017).

The wireless communication systems suffer from interference, latency, and band-width limitations. Many severe conditions say, after valve replacement, implants, patients under trauma, etc., require continuous monitoring and need early mobilization to prevent development of further comorbidities. Such patients require telemetric monitoring while under medical observations and limited movement stage. While standalone ECG or physiological parameter monitoring in intensive care units may require limited bandwidth, safe transmission of these signals need baud rates ranging from 3.6 to 20 kbps for each patient. Bandwidth requirement depends on the signal size, encryption protocols, and the noise in the communication channel. Security, privacy, and data protection immediately comes to play when transmission of information is done over shared networks. 5G or 5th generation mobile technologies have features like software−defined networks and network function

virtualization which can help to individualize the diagnostics. Like other applications 5G technology has the ability to provide security by design features and healthcare can hugely benefit from advancements in 5G technology. 5G has features to significantly reduce latency, enable high upload and download speeds, as it has transfer rates up to 20 gbps and is 10−100 times faster than 4G technology. 5G supports Edge cloud technology, wherein the computing assets and storage work in tandem, interconnected in scalable, secure, real-time, and application aware network. Telemetric monitoring of patients using 5G technology can get substantially enhanced due to faster response to geofencing and GPS technology when compared with WLAN−based monitoring. 5G can also support individual and precision medicine, improving patient satisfaction and quality of service. The technology is suited for large health care centers for real-time monitoring for ailments including cardiac monitoring (Thuemmler et al., 2018; Network, 2020).

AI has applications across industries in marketing, banking, agriculture, gaming, space exploration, chatbots, autonomous vehicles, and even in healthcare. AI has been used in prevention of heart strokes. Asymptomatic left ventricular dysfunction (AVLD) effects populations around the globe and is detected after ischemic attacks or even sometimes during medical check-ups related to high blood pressure or other age−specific routine monitoring. The diagnosis is made by jointly analyzing 12-lead ECG output and echocardiogram data. A lower left ventricle ejection fraction (<35%) often points out to AVLD. However, AI has facilitated to deploy algorithms on ECG data alone to point out AVLD and also identify high-risk patients. A study by Mayo clinic on 44,959 patients, the ECG data and the corresponding ejection fraction has been used to train a visual ECG model using deep learning techniques, also called convolutional neural network for the detection of AVLD. The trained model has been further tested on 52,870 patients which returned more than 85% sensitivity, specificity, and accuracy. The patients under observation which returned a positive screening result but were without ventricular dysfunction, stood four times risk to develop AVLD in future (next 5 years). It signified the capability of the algorithm to identify early and subclinical abnormalities in ECG pattern which is beyond the human abilities. Here AI has been successfully applied to ECG as a powerful tool to screen AVLD resulting in low-cost, swift, and ubiquitous solution. The usual medical treatment protocols are followed once AVLD is diagnosed. AI has applications in pathology, identification of mammographic lesions, etc. The AI neural network developed was found accurate applicable across age and sex. The potential of horizontal deployment of the concept in medical field holds a huge potential for the future (Attia et al., 2019; Salazar-Licea et al., 2017).

E-healthcare systems must honor ethical, legal, patient, and data privacy mandates while handling patient data physically or remotely. Steganography techniques have found application in ECG signal transmission to provide point-of-care patient monitoring using singular value decomposition (SVD) and discrete wavelet transform (DWT). Other physiological parameters, such as blood glucose, blood pressure, temperature, etc., can also be transmitted and could be helpful in emergencies. Data encryption alone is not sufficient as expert hackers can decrypt the data. Also, encryption increases the size and requires huge computational and storage assets. Steganography stores and hides the important data with insensitive information without significant increase in size of overall cover. ECG data is coupled with

other physiological information and biometric information of the patient. The patient data is converted in to ASCII values and then into binary data which is called "watermark." The data is camouflaged by DWT coupled with standard MIT-BIH arrhythmia database and converted into a 2-D image. SVD is then used on the image to decompose and embed the converted data. Inverse DWT reconstructs the image back to original state. Least significant bit algorithm has also been used in some cases along with DWT. The same methodology is also feasible for EEG and EMG signals. The above steganography techniques preserve the physiological signals with minimum distortions. All these developments are very much desired as we move higher on the technology platforms with higher patient expectations and quantum increase desirable in quality of services (Meghani and Subbiah, 2016; Yang et al., 2019). The softer challenges would definitely require quicker adaptations and involvement from the health care fraternity benefitting from the rapid strides in technological advancements in lines with the acceptance of robot assisted intricate surgical procedures. Medicine and technology will have to work in tandem like never before to take benefit and to reach where it really matters.

References

Attia, Z.I., Kapa, S., Lopez-Jimenez, F., et al., 2019. Screening for cardiac contractile dysfunction using an artificial intelligence—enabled electrocardiogram. Nat. Med. 25, 70—74.

Bansal, D., 2012. Potential of piezo-electric sensors in bio-signal acquisition. Int. Sens. Transducers J. 136 (1), 147—157.

Bansal, D., 2013. Design of 50 Hz notch filter circuits for better detection of online ECG. Int. J. Biomed. Eng. Technol. 13 (1), 30—48.

Bansal, D., Singh, V.R., 2014. Algorithm for online detection of HRV from coherent ECG and carotid pulse wave. Int. J. Biomed. Eng. Technol. 14 (4), 333—343.

Bansal, D., Khan, M., Salhan, A.K., 2009a. A computer based wireless system for online acquisition, monitoring and digital processing of ECG waveforms. J. Comput. Biol. Med. 39 (4), 361—367.

Bansal, D., Khan, M., Salhan, A.K., 2009b. Real time acquisition and PC to PC wireless transmission of human carotid pulse waveform. Int. J. Comput. Biol. Med. 39 (10), 915—920.

Bansal, D., Khan, M., Salhan, A.K., 2009c. A real time embedded set up based on digital signal controller for detection of bio-signals using sensors. Sens. Transducers J. 105 (6), 26—32.

Bansal, D., Khan, M., Salhan, A.K., 2009. A review of measurement and analysis of heart rate variability. In: International Conference on Computer and Automation Engineering (ICCAE 2009), Bangkok, Thailand, March 8—10, 2009, pp. 243—246.

Bansal, D., Khan, M., Salhan, A.K., 2010. Wireless transmission of EMG signal and analysis of its correlation with simultaneously acquired carotid pulse wave using dual channel system. 2nd Int. Conference on eHealth, Telemedicine, and Social Medicine, 2010, pp. 125—129.

Bhogeshwar, S.S., Soni, M.K., Bansal, D., 2014. To verify and compare denoising of ECG signal using various denoising algorithms of IIR and FIR filters. Int. J. Biomed. Eng. Technol. 16 (3), 244—267.

Bhogeshwar, S.S., Soni, M.K., Bansal, D., 2015. Circuit system analysis for real-time acquisition of bio-signals. Int. J. Biomed. Eng. Technol. 18 (3), 272—288.

Giancaterino, S., Lupercio, F., Nishimura, M., Hsu, J.C., 2018. Current and future use of insertable cardiac monitors. JACC Clin. Electrophysiol. 4 (11), 1383—1396.

Lee, J.-H., 2016. Miniaturized human insertable cardiac monitoring system with wireless power transmission technique. J. Sens. 7.

Mahajan, R., Bansal, D., 2015a. Automated cardiac state diagnosis from hybrid features of ECG using neural network classifier. Int. J. Biomed. Eng. Technol. 17 (3), 209–231.

Mahajan, R., Bansal, D., 2014. Hybrid ECG signal compression system: a step towards efficient tele-cardiology. In: 2014 International Conference on Optimization, Reliabilty, and Information Technology (ICROIT), February 6–8, 2014, pp. 437–442. Print ISBN: 978-1-4799-3958-9.

Mahajan, R., Bansal, D., 2015b. Identification of heart beat abnormality using heart rate and power spectral analysis of ECG. In: IEEE Conference on Soft Computing Techniques and Implementations, October 8–10, 2015.

Majumder, S., Mondal, T., Deen, M.J., 2017. Wearable sensors for remote health monitoring. Sensors 17, 1–45.

Meghani, D., Subbiah, G., 2016. ECG steganography to secure patient data in an E-Healthcare System, pp. 66–70. Available from: https://doi.org/10.1145/2909067.2909078.

Naik, S., Soni, M.K., Bansal, D., 2014. Design of Simulink Model to denoise ECG signal using various IIR and FIR filters. In: 2014 International Conference on Optimization, Reliabilty, and Information Technology, February 6–8, 2014, pp. 477–483.

Network, 2020. Mission Critical Communications. <https://www.gsma.com/futurenetworks/wp-content/uploads/2017/03/Network_2020_Mission_critical_communications.pdf>.

Romero, F.J., Castillo, E., Rivadeneyra, A., et al., 2019. Inexpensive and flexible nanographene-based electrodes for ubiquitous electrocardiogram monitoring. npj Flex. Electron. 3, 12.

Rong, Y., Bliss, D.W., 2019. Is radar cardiography (RCG) possible? In: 2019 IEEE Radar Conference (RadarConf), Boston, MA, USA, 2019, pp. 1–6.

Sakhi, R., Damj, T., Szili-Torok, T., Yap, S.C., 2019. Insertable cardiac monitors: current indications and devices. Expert. Rev. Med. Dev 16 (1), 45–55.

Salazar-Licea, L.A., Pedraza-Ortega, J.C., Pastrana-Palma, A., Aceves-Fernandez, M.A., 2017. Location of mammograms ROI's and reduction of false-positive. Comput. Methods Prog. Biomed. 143, 97–111.

Singh, S., Bansal, D., 2014. Design and development of BCI for online acquisition, monitoring and digital processing of EEG waveforms. Int. J. Biomed. Eng. Technol. 16 (4), 359–373.

Szunerits, S., Mishyn, V., Grabowska, I., Boukherroub, R., 2019. Electrochemical cardiovascular platforms: Current state of the art and beyond. Biosens. Bioelectron. 131, 287–298.

Thijs, J.A., Muehlsteff, J., Such, O., Pinter, R., Elfring, R., Igney, C.H., 2005. A comparison of continuous wave Doppler radar to impedance cardiography for analysis of mechanical heart activity. Conf. Proc. IEEE Eng. Med. Biol. Soc. 2005, 3482–3485.

Thuemmler, C., Rolffs, C., Bollmann, A., Hindricks, G., Buchanan, W., 2018. Requirements for 5G based telemetric cardiac monitoring. In: 2018 14th International Conference on Wireless and Mobile Computing, Networking and Communications (WiMob), Limassol, 2018, pp. 1–4.

Tomson, T.T., Passman, R., 2017. Current and emerging uses of insertable cardiac monitors: evaluation of syncope and monitoring for atrial fibrillation. Cardiol. Rev. 25 (1), 22–29.

Yang, C.Y., Cheng, L.T., Wang, W.F., 2019. Effective reversible data hiding in electrocardiogram based on fast discrete cosine transform. In: Arai, K., Bhatia, R., Kapoor, S. (Eds.), Proceedings of the Future Technologies Conference (FTC) 2018. FTC 2018. Advances in Intelligent Systems and Computing, vol. 880. Springer, Cham.

Index

Note: Page numbers followed by "*f*" and "*t*" refer to figures and tables, respectively.

A

Acoustic sensors-based hearing aids, 30
ADC. *See* Analog-to-digital converters (ADC)
Affinity biosensors, 36
AI. *See* Artificial intelligence (AI)
Amperometry, 37
Analog-to-digital converters (ADC), 10
ANS. *See* Autonomic nervous system (ANS)
Aptasensors or nucleic acid bioreceptors, 36
Arterial Catheter method, 60
Artificial intelligence (AI), 14
Autonomic nervous system (ANS), 145–146, 146*f*

B

Biomedical data acquisition, 8–12, 9*f*
  challenges to, 15–16
Biomedical instruments, classification of, 8*f*
Biomedical signal processing, 2–3
Biosensors, 35–38
  aptasensors or nucleic acid bioreceptors, 36
  electrochemical transducers, 37
  enzymatic biosensors, 35–36
  living biosensors or microbial sensors, 36–37
  mass-based detection methods, 38
  optical transducers, 37–38
Bio-signals, 7–9
  data transmission, 12
  processing, 8–12, 9*f*
Bladder temperature measurement, 31–32
Blood flow measurement, using Doppler sonography, 27–28
Blood gases, sensors for, 32–35
Bulk micromachining, 43
Butterworth filter, 50–51, 50*f*

C

Carotid Artery Stenosis (CAS), 60, 62
Carotid pulse waves, real-time detection and processing of, 58*f*, 175–176
  algorithm, 78–79, 79*f*
  clinical significance, 58–60, 59*f*
  digital filter designs, 67–72
    finite impulse response filter design, 68–70, 69*f*, 70*f*
    infinite impulse response filter design, 70–72, 71*f*, 72*f*
  experimental arrangement, 62–67, 63*f*
    acquisition protocol and results, 66–67, 67*f*, 68*f*, 69*t*
    piezoelectric sensor, 63–66, 65*f*
  investigation, 60–62
  simulated model, 72–77
    filter design and analysis tool, 73
    Simulink model, 73–77, 74*f*, 75*f*, 77*f*, 78*f*
CAS. *See* Carotid Artery Stenosis (CAS)
Chemical sensors, 32–35
  for pH and blood gases, 32–35
Conductometry, 37
Crystal resonators, 30–31

D

Data acquisition system hardware, 45–52
  Butterworth filter, 50–51, 50*f*
  filtering subsystem, 49–50, 49*f*
  front end of, 46–49
    common-mode rejection ratio, 47
    electrode polarization, 47–49, 48*f*
    frequency response, 46–47, 46*f*
    gain, 46
    input impedance, 47
    noise and drift, 47
    recovery time, 47
Data acquisition systems market, 53
Data acquisition system software, 10–11, 52–53
Database, 11–12

Digital filter designs, 67–72
finite impulse response filter design, 68–70, 69*f*, 70*f*
infinite impulse response filter design, 70–72, 71*f*, 72*f*
Digital signal controller-based electrocardiogram acquisition system, 135–140
acquisition protocol and results, 136–140, 137*f*, 139*f*
Digital Signal Processing, 2
Digital Storage Oscilloscope, 60
Disaster management, 15
Doppler sonography, blood flow measurement using, 27–28

E

Electrocardiogram signal, real-time detection and processing of, 112*f*, 130*f*, 131*f*, 132*f*, 177
digital signal controller-based electrocardiogram acquisition system, 135–140
acquisition protocol and results, 136–140, 137*f*, 139*f*
feature extraction, online algorithm for, 131–135, 133*f*, 134*f*
lead placement, 114–116, 115*f*
measurement, investigation of, 116–118, 117*f*
notch filter designs for reducing PLI in electrocardiogram signals, 123–130, 123*f*
computer simulation, 125–130, 127*f*, 128*f*, 129*f*, 129*t*
recent trends, 118–122
waveform interpretation, 111–114
Electrocardiography (ECG) electrodes, 40
Electrochemical transducers, 37
standalone MATLAB code, 103–105, 104*f*
Electroencephalogram (EEG) electrodes, 40–41
Electromyography signal, real-time detection and processing of, 84*f*, 176
application areas, 85–87, 85*f*
data processing, 88–93
dual channel mode, 99–103, 100*f*, 101*f*, 102*f*, 103*f*
standalone MATLAB code, 103–105, 104*f*
measurement, investigation of, 87–88
single channel mode, 93–99, 94*f*
acquisition protocol and results, 98–99, 99*f*, 100*f*
digital filter for online processing, 96–98, 97*f*
front-end amplifier and interface unit, 95–96
silver–silver chloride surface electrodes, 93–95
Electropotential sensors, 38–41
ECG electrodes, 40
EEG electrodes, 40–41
EMG electrodes, 40
EMG electrodes, 40
Enzymatic biosensors, 35–36
Esophageal temperature measurement, 31–32

F

Fiber optic monitoring system, 34
Filtering subsystem, 49–50, 49*f*
Finite impulse response (FIR) filter design, 68–70, 69*f*, 70*f*
FIR. *See* Finite impulse response (FIR) filter design

G

Glass mercury thermometer, 31

H

Heart rate variability, measurement and analysis of, 161*f*, 162*t*, 177
basic block diagram, 147–148, 147*f*
dual channel system, 162–166, 163*f*, 164*f*, 165*f*, 166*f*, 166*t*
metrics and norms, 148–156
frequency-domain analysis, 149*t*, 152–154
nonlinear measurement analysis, 149*t*, 154–156
time-domain analysis, 148*t*, 149–152
platforms, 156
QRS detection methods, 156–159
differentiation-based methods, for QRS peak detection, 157–158
template matching methods, for QRS peak detection, 158
wavelets for QRS peak detection, 159
Hemodynamic invasive blood pressure sensors, 28

I
IIR. *See* Infinite impulse response (IIR) filter design
Immunosensors, 36
Indwelling probes, 31
Infinite impulse response (IIR) filter design, 70–72, 71*f*, 72*f*
Interface units, 51–52
Internal ocular pressure (IOP) measurement, 29–30
IOP. *See* Internal ocular pressure (IOP)
IoT sensors, 42

L
LabVIEW, 52
Living biosensors or microbial sensors, 36–37

M
Magnetic sensors, 32
Mass-based detection methods, 38
MATLAB, 17–18, 52–53
  carotid pulse waves, detection and processing of, 67–68, 73
  electromyography signal, real-time detection and processing of, 103–105, 104*f*
MDG. *See* Millennium Development Goal (MDG)
Measurand (bio-signals), 9
Mechanical sensors, 26–28
  blood flow measurement, using Doppler sonography, 27–28
  hemodynamic invasive blood pressure sensors, 28
MEMS sensors, 43–44
Millennium Development Goal (MDG), 1
MIT-BIH Arrhythmia database, 11–12
Modeling, 12

N
NEMS sensors, 44
Notch filter designs, for reducing PLI in electrocardiogram signals, 123–130, 123*f*
  computer simulation, 125–130, 127*f*, 128*f*, 129*f*, 129*t*

O
Optical image sensors, 43
Optical transducers, 37–38

P
Personal Computer (PC)-based data acquisition systems, 23*f*
  hardware, 45–52
    Butterworth filter, 50–51, 50*f*
    filtering subsystem, 49–50, 49*f*
    front end of, 46–49
    interface units, 51–52
  market, 53
  sensors. *See* Sensors
  software, 52–53
  transducers, 23–41
    optical transducers, 37–38
Photon detectors, 31
pH sensors, 32–35
Physical sensors, 24–32
  magnetic sensors, 32
  mechanical sensors, 26–28
    blood flow measurement, using Doppler sonography, 27–28
    hemodynamic invasive blood pressure sensors, 28
  radiation sensors, 24–25
  spirometry, 27–28
  thermal sensors, 30–32
  ultrasonic pressure transducer module, 28–30
    acoustic sensors-based hearing aids, 30
    internal ocular pressure measurement, 29–30
    piezo sensors, for pressure pulses, 29
PhysioNet, 11
Piezoelectric sensor, 63–66, 65*f*
Piezo sensors, for pressure pulses, 29
Pneumotachometer, 28
pollution sensors, 42–43
Potentiometry, 37
Power line interference (PLI)
  in electrocardiogram signals, notch filter designs for reducing, 123–130, 123*f*
    computer simulation, 125–130, 127*f*, 128*f*, 129*f*, 129*t*

Pressure sensors, 27
Pressure Transducer Module (PTM), 28
  ultrasonic, 28–30
  Vortex-Shedding, 29
PTM. *See* Pressure Transducer Module (PTM)

Q
QRS peak detection methods, 156–159
  differentiation-based methods, 157–158
  template matching methods, 158
  wavelets for, 159

R
Radiation sensors, 24–25
Rectal temperature probes, 31–32
RFID sensors, 42

S
Savitzky Golay filters, 60
SDGs. *See* Sustainable Development Goals (SDGs)
Sensors, 23–41
  biosensors, 35–38
    aptasensors or nucleic acid bioreceptors, 36
    enzymatic biosensors, 35–36
    living biosensors or microbial sensors, 36–37
    optical transducers, 37–38
  chemical sensors, 32–35
    for pH and blood gases, 32–35
  electropotential sensors, 38–41
    ECG electrodes, 40
    EEG electrodes, 40–41
    EMG electrodes, 40
  market research and latest developments, 41–45
    IoT sensors, 42
    MEMS sensors, 43–44
    NEMS sensors, 44
    optical image sensors, 43
    pollution sensors, 42–43
    RFID sensors, 42
    wearable sensors, 42
  materials, 44–45
  physical sensors, 24–32
    magnetic sensors, 32
    mechanical sensors, 26–28
    radiation sensors, 24–25
    spirometry, 27–28
    thermal sensors, 30–32
    ultrasonic pressure transducer module, 28–30
Signal conditioning, 10
Signals, 5–7
Silver–silver chloride surface electrodes, 93–95
Simulation, 12
Simulink
  carotid pulse waves, detection and processing of, 67–68, 72–77, 74*f*, 75*f*, 77*f*, 78*f*
SphygmoCor applanation tonometry, 61
Spinal surgery, 13–14
Spirometry, 27–28
Surface micromachining, 43
Sustainable Development Goals (SDGs), 1
  SDG3, 1

T
Technical overview, 5–16
Thermal detectors, 31
Thermal sensors, 30–32
Thermistors, 30–31
Thermocouples, 30–31
Transducers, 9–10, 23–41
Tympanic thermometer, 31

U
Ultrasonic pressure transducer module, 28–30
  acoustic sensors-based hearing aids, 30
  internal ocular pressure measurement, 29–30
  piezo sensors, for pressure pulses, 29
US Preventive Services Task Force, 60

V
Vortex-Shedding PTM, 29

W
Wearable sensors, 42
Wearable technology, 13
WHO. *See* World Health Organization (WHO)
World Health Organization (WHO), 1

REAL-TIME DATA ACQUISITION IN HUMAN PHYSIOLOGY

Real-Time Acquisition, Processing, and Interpretation—A MATLAB-Based Approach

Dipali Bansal

Real-Time Data Acquisition in Human Physiology focuses on the design and development of a computer-based system to detect and digitally process human ECG, EMG, and carotid pulse waveforms in real time. The indigenous system developed and described in this book allows for an easy-to-interface, simple hardware arrangement for bio-signal detection. The computational functionality of MATLAB is verified for viewing, digital filtration, and feature extraction of acquired bio-signals.

This book demonstrates a method of providing a relatively cost-effective solution to human physiology real-time monitoring, processing, and interpretation that is more realizable and would directly benefit a larger population of patients.

Key Features

- Presents an application-driven, interdisciplinary, and experimental approach to bio-signal processing with a focus on acquiring, processing, and understanding human ECG, EMG, carotid pulse data and HRV.
- Covers instrumentation and digital signal processing techniques useful for detecting and interpreting human physiology in real time, including experimental layout and methodology in an easy-to-understand manner.
- Discusses development of a computer-based system that is capable of direct interface through the sound port of a PC and does not require proprietary DAQ units and ADC units.
- Covers a MATLAB-based algorithm for online noise reduction, features extraction techniques, and infers diagnostic features in real time.
- Provides proof of concept of a PC-based twin channel acquisition system for the recognition of multiple physiological parameters.
- Establishes the use of Digital Signal Controller to enhance features of acquired human physiology.
- Presents the use of carotid pulse waveforms for HRV analysis in critical situations using a very simple hardware/software arrangement.

About the Author

Dr. Dipali Bansal is the Dean of Engineering at Graphic Era (Deemed to be University), Dehradun, India. She is part of a curiosity-driven research group working in the field of bio-signal processing that brings together experimental and theoretical techniques and approaches in acquiring and analyzing human physiological parameters, namely ECG, EMG, EEG signals, using professional tools like MATLAB and LabVIEW. She got her Bachelor's degree from BIT Sindri and obtained a PhD in Bio-signal Processing from Jamia Millia Islamia Central University, New Delhi, India. In more than two decades of her professional career, she has honed her skills as an academician, a researcher, and also as an administrator.

ELSEVIER

ACADEMIC PRESS

An imprint of Elsevier

elsevier.com/books-and-journals

ISBN 978-0-12-822118-1

9 780128 221181